



November 28, 2011

Mr Keith McConnell, Deputy Director  
Decommissioning and Uranium Recovery Licensing Directorate  
US Nuclear Regulatory Commission  
C/o Document Control Desk  
Two White Flint North  
11545 Rockville Pike  
Mail Stop T-8F5  
Rockville, Maryland 20855-2738

Dear Mr McConnell:

Under cover of this letter we submit the following documents for your consideration:

- "An Alternate Concentration Limit Proposal for the Ground Water Resources at the Bear Creek Uranium Mill"
- "A Comprehensive Risk Assessment for the Predicted Concentrations of Nickel, Radium and Uranium at the Bear Creek Uranium Company Site"
- "Re-evaluation of Metals Transport at Bear Creek Uranium, Converse County, Wyoming"

This work was performed at the request of the Nuclear Regulatory Commission (NRC) in a letter dated November 30, 2010. A new model was developed which incorporated a new modeling procedure and 13 additional years of sampling data. The new model and consequent documents lead us to the following conclusions:

- The predictive modeling of the ground water and associated risk assessment shows that there is no unacceptable risk to the public from the Bear Creek site.
- There is no history of this upper zone of the Wasatch formation being used for a domestic or livestock water supply in this region of the Powder River Basin in Wyoming. All of the regional livestock wells are completed to depths of 300 to 500 feet in an aquifer separated from the N-sand by an aquitard hundreds of feet thick. The two nearest wells, Manning B.C. 18 (drilled 1983) and Hardy No. 4 (drilled 1947), located north of the POEs are completed at depths of 432 ft. and 443 ft. respectively and showed no water present in the N-sand in the well logs. There is no known past or current use of this shallow aquifer and no surface expression or communication with lower aquifers or surface water in the area.
- The boreholes drilled by S.M. Stoller in 1997 along Lang Draw north of MW-14 did not encounter significant water. Only boreholes near MW-108 in Lang Draw were found to contain wet sands. Stoller's report stated that *"it is very unlikely that the alluvium will produce enough water to satisfy the NRC definition of an aquifer"*. Water sampling in both monitor wells MW-108 and MW-109 over the past 13 years show yields are <0.01 gallons per minute which supports this conclusion.

**AN ALTERNATE CONCENTRATION LIMIT PROPOSAL**  
**FOR THE GROUND WATER RESOURCES**  
**AT THE**  
**BEAR CREEK URANIUM MILL**



## **Table of Contents**

### **Executive Summary**

**1.0 Background Information/Chronological sequence of events**

**2.0 Model Review Summary/In-house Data Review**

**3.0 Hazard Evaluation.**

**4.0 Proposed Action**

### **References**

### **Appendix: Risk Assessment**

## **Executive Summary**

This application for alternate concentration limits (ACL) is being submitted in response to the Nuclear Regulatory Commission's (NRC) letter to Anadarko Petroleum Corporation (APC) dated November 30, 2010 requesting that a new risk-based ACL application be submitted incorporating the ground water data collected over the 13 years since the original ACL application.

APC embarked on parallel paths to study and evaluate the discrepancy between the predicted concentrations of uranium at MW-14 and the observed results.

First, TetraTech GEO the consulting firm that had done the ground water modeling for the 1997 ACL application was retained to re-evaluate the previous model results utilizing the ground water monitoring data collected during the past 13 years. The re-evaluation of the transport model is attached under separate cover.

Secondly, an in-house review of the corrective action program, ground water monitoring data, well completion data and operating conditions observed at the Bear Creek Uranium Company (BCUC) site was conducted by APC personnel.

It is APC's consensus that the anomaly noted in NRC's review and subsequent letter is a singular event created by the early time-frame seepage under the tailings dam, subsequent ponding of low pH water behind the catchment basin dam located about 600 feet below the tailings dam and use of recovery wells located downstream of the tailings area in Lang Draw. By extending the POE for each drainage plume to the property boundary located just north of wells MW-109 and MW-111 and utilizing currently measured water quality data at those points for estimating peak concentrations of contaminants, it would not require a change to the ACLs, which have never been exceeded, nor would this increase risk to the general public.

## 1.0 Background Information/Chronological Sequence of Events

### Background Information

BCUC, originally a partnership of Rocky Mountain Energy (RME) and Mono Power Company and now operated by RME's successor, APC, began its tailings basin/mill operation in August of 1977 under United States Nuclear Regulatory Commission (NRC) Source Materials License No. SUA-1310. The milling process consisted of sulfuric acid leach, sodium chlorate oxidant, and liquid ion exchange extraction and concentration. Approximately 4.7 million tons of tailings were discharged into the tailings basin as a slurry. This above grade disposal was done in compliance with 10 CFR Part 40 Criterion 3 requirements and approved by the NRC. The January 1996 revised version of the CFR is referenced here and in the remainder of this summary. The mill and solvent extraction buildings were decommissioned in 1988.

The tailings facility, installed in 1977 in a local drainage known as Lang Draw, consisted of a keyed, zone-fill dam and an integral, compacted soil-lined basin. Basin soils were reworked where necessary to meet a  $1 \times 10^{-6}$  cm/sec permeability requirement. Subsequent portions of the basin were lined to a permeability of  $1 \times 10^{-7}$  cm/sec as the dam was raised to increase tailings capacity. The dam and clay liner were designed to meet or exceed all performance criteria established by the NRC in accordance with 10 CFR Part 40 Criterion 5A. Despite use of these "state of the art" dam and liner construction techniques, BCUC anticipated that some seepage would occur and constructed a seepage catchment structure below the tailings dam to intercept the anticipated seepage and pump it back to the tailings basin. The potential impacts of this anticipated seepage were discussed in BCUC's permit and license applications and in the Final Environmental Impact Statement (FEIS) dated June 1977 and are on file with NRC.

Surface seepage was first observed at the downstream toe of the tailings dam in early 1978. Several wells were developed to determine groundwater contamination potential. Elevated chloride levels, a common seepage indicator, were observed and as a result more wells were developed to expand the monitoring network. This action complies with the requirements established in 10 CFR Part 40 Criterion 7A. Additionally, wells were completed as recovery wells and seepage recovery began in October of 1979 with the operation of pump back wells MW-7, MW-12, and MW-13. This action was in keeping with the requirements of 10 CFR Part 40 Criterion 5D. The aforementioned actions were taken voluntarily by BCUC well in advance of any NRC mandates. The corrective action taken is described in detail in Attachment 1 of the original submittal to NRC titled *Union Pacific Resources Group, Inc. Bear Creek*

*Uranium Company Alternate Concentration Limit (ACL) Application* dated February 28, 1997

On May 7, 1985 the NRC issued License Amendment No. 6 requiring the implementation of a groundwater detection monitoring program with MW-12 as the point of compliance (POC) well and MW-9 as the background well. This was in compliance with the requirements of 10 CFR Part 40 Criterion 7A. Indicator parameters were designated as Arsenic, Selenium and pH. It was not until 1985 that the NRC formally shifted its attention to the "first underlying aquifer" or N-sand formation. Wells MW-12 and MW-9 are both alluvial N-sand wells. It should be noted that pre-milling groundwater data was focused on the ore sand.

Threshold values were established at 0.005 mg/L and 0.001 mg/L for As and Se respectively. A threshold value of 6.8 s.u. was picked for pH. These values were designated in License Condition 47E issued in Amendment No. 15 September 10, 1987.

The NRC was notified on October 19, 1987 that pH and selenium threshold values had been exceeded at MW-12 and in 1989 a corrective action plan (CAP) and monitoring program were submitted by BCUC and approved by the NRC. This action was required by 10 CFR Part 40 Criterion 7A.

Groundwater protection standards were established by the NRC, in accordance with 10 CFR Part 40 Criterion 5D and 13, and implemented by Amendment No. 10, issued on September 12 1990, to BCUCs Source Materials License SUA-1310.

MW-74 was designated, by the NRC, as the POC well in the direction of the northern flow path in January of 1992. This is in compliance with 10 CFR Part 40 Criterion 7A.

In February of 1992, the NRC approved the BCUC tailings reclamation plan. This follows 10 CFR part 40 Criterion 6 requirements.

An application for alternate concentration limits (ACLs) was submitted on February 28, 1997 in accordance with 10 CFR Part 40, Appendix A, Criterion 5B(5), which states that at the point of compliance, the concentration of a hazardous constituent must not exceed the NRC approved background concentration, the Table 5C value or an alternate concentration limit established by the NRC. At that time, all concentrations of hazardous constituents, with the exception of uranium, met the license established background values as measured at the point of compliance locations. However, modeling data, included in Attachment 2 of the 1997 ACL

application, suggested that the low pH plume would eventually reach the POCs before it was completely neutralized and would result in elevated levels of U-nat, Ra-226 and nickel.

A corrective action program (CAP), found in Attachment 1 of the 1997 ACL application, was implemented in response to elevated levels of hazardous constituents found to exist at the NRC approved background location. The up-gradient edge of the tailings impoundment coincides with the near surface formations which could encounter tailings seepage, locally known as the alluvium and the N-sand. Due to this, the NRC selected well MW-9, which resides in a down-gradient setting, as a representative background location. Background values of representative hazardous constituents were derived from this well during a time that the pH was neutral and total dissolved solids concentrations were low.

The CAP was operational for over ten years. During that time, the program recovered 301,000,000 gallons of seepage waters, containing 6.5 tons of heavy metals as well as 9,993 tons of sulfate and chloride. These waters plus an additional 165,000,000 gallons of tailings solution were lost to the atmosphere, by way of an enhanced evaporation system. In total, the system was responsible for the treatment and evaporation loss of 466,000,000 gallons of tailings solution. These efforts resulted in dewatering of the tailings and adjoining formations, to levels consistent with the pre-milling groundwater gradient. Based upon the ground-water quality measured at that time, the resulting water levels, and the mass of constituents that were recovered, it was concluded that concentrations of hazardous constituents were "as low as reasonably achievable" (ALARA), considering the practicable corrective actions. The ALARA evaluation is found in Attachment 3 of the 1997 ACL application. The CAP was discontinued in 1996 in accordance with NRC License Amendment No. 39 in order to facilitate final reclamation of the tailings area. Monitoring of the remaining wells was conducted annually from that time on.

Although the corrective action program was successful in removing hazardous constituents and re-establishing the pre-milling water levels, predictive modeling suggested that within 40 to 60 years following termination of the CAP, the values of nickel, radium 226+228 (radium), and uranium would eventually increase to levels that would be in excess of the background concentrations at the POC locations. The modifications in water quality would accompany a slowly advancing acid front that would pass the POC and reach the point of exposure (POE) over the next 80 to 400 years. The rate at which the water quality would be modified would be dependent upon the individual constituent and the preferential flow path that is selected. The ground water modeling summary referenced in this paragraph is included in Attachment 2 of the 1997 ACL application.

It was also determined that additional corrective actions would have little or no effect on the eventual movement of the acid front. The CAP was successful in decreasing the areal extent of the seepage plume to within the tailings impoundment area. The CAP also reduced the saturated thickness of the alluvium, the N-sand, and the tailings making the recovery of additional acidic solutions technically challenging and expensive. Consequently ACLs that are protective of human health and the environment were proposed for nickel, radium, and uranium.

To determine the potential for hazardous constituent transport the seepage recovery wells were temporarily shut down from September 1994 to January of 1995. The ground-water level response was monitored and used as the basis for a transport assessment. Additionally, geochemical data were collected by coring the alluvium and the N-sand which are the formations that have encountered tailings seepage. These cores were analyzed for their attenuation capacity. Following the development of these data, the amount of alluvium and N-sand attenuation capacity were simulated to encounter the remaining acidic seepage from the tailings and underlying formation. The simulation indicated that the acid front would carry nickel, radium, and uranium beyond the POCs. Significant attenuation would occur between the POCs and the points of potential exposure (POEs). It was predicted that the attenuation would be sufficient to reduce the concentrations of nickel, radium, and uranium to levels that would be protective human health and the environment.

Predictive modeling indicated that the maximum concentration of nickel, radium, and uranium, at the POC locations, would be 3.8 mg/l, 46 pCi/l, and 2038 pCi/l, respectively through the flow paths. Similarly, maximum concentrations of nickel, radium, and uranium at the POEs, would be 0.055 mg/l, 13 pCi/l, and 45 pCi/l respectively. Background concentrations for these constituents, defined at MW-9, were 0.05 mg/l Ni, 9.7 pCi/l Ra-226, and 98.7 pCi/l U-nat. It should be noted that the ACLs at the POCs have not been exceeded to date.

The modeling predicted times to reach peak concentrations at the POC locations would range from 40 to 60 years following termination the CAP. Attenuation beyond these locations would slow the movement of constituents. Consequently, following termination of the CAP, peak concentrations at the POE locations would be seen from 260 to 400 years for nickel, 80 to 100 years for radium, and 80 to 130 years for uranium, dependent upon which of the two preferential flow paths was selected. The predictive modeling was terminated following the 400 year point. This period of time was sufficient to simulate the arrival of the peak concentrations of nickel, radium, and uranium. Radium and uranium arrive and decline to background concentrations prior to the arrival of the nickel plume.

To determine the risk associated with water use having these concentrations of hazardous constituents potential use locations were defined and the POEs were determined. The POE was the down-gradient edge of the land mass that contains the reclaimed tailings as well as the area that contains the buried mill debris. Consequently, it represented the minimal land area necessary to assure long-term control of the reclaimed by product materials. This land mass generally coincided with the original restricted area boundary, does not utilize the "distant POE" concept, and is the area that was determined to accompany an amendment application for a general license. Two POE locations, MW-14 and MW-74, were defined for the Bear Creek site. The POE locations are within the Northern and Lang Draw flow paths. The Union Pacific Resources(UPR) Group Bear Creek Uranium Company Amendment request(AR 1996) to SUA-1310; Docket No. 40-8452, submitted to NRC May 30, 1996, requested that the POEs be located at the furthest point of the property owned by UPR, now Anadarko. The NRC, did not approve that request due to trying to keep the land transfer required by UMTRCA to a small area. The land transfer to the Department of Energy (DOE) ultimately became much larger, for DOE's ease of land management, and now includes the POEs currently being requested. The 1996 document also contains a map of the proposed locations of the POEs, a model summary of hydrogeologic and chemical transport analysis which was conducted by GeoTrans in March of 1995, and maps showing the environmental sample locations and tailings area well locations.

There are no records of past water use associated with the alluvium and the N-sand, which are the formations encountering tailings seepage at the Bear Creek site. This is due to there being little water in these formations prior to the milling operation as well as the limited extent of these formations. Similarly, there is no present or predicted future use of the limited amount of water that now resides in these formations. Groundwater development in the region has been limited to stock watering by windmills. These wells are developed to depths of 400 to 500 feet which have a more reliable source of water with better well yield and water quality.

An exposure assessment indicated that there was no present or predicted future water use associated with the formations that have encountered tailings seepage. Similarly, the water residing in the alluvium and the N-sand is not hydraulically connected to any surface water resource. This is due to the limited extent of the alluvium and the N-sand as well as the lack of surface water resources in the area of the mill.

It is questionable if the alluvium can be considered an aquifer because of low well yield. However, for the purpose of compliance with EPA guidelines for ACL



applications, the original proposal for ACLs assumed that these near surface formations would experience some future use. Although the use of the water in the near surface alluvium and the hydraulically connected N-sand is not predicted to occur, the risk associated with use of this water would be essentially the same as the risk associated with use of water having background hazardous constituent concentrations. Furthermore, the alluvium and the N-sand have no source of recharge other than the minimal amount of precipitation that falls on these formations, which is rapidly consumed by vegetation. All considerations indicate that the proposed alternate concentration limits were associated with a CAP that had reduced levels of hazardous constituents to levels that were as low as reasonably achievable. Assuming this, the resulting water quality, as measured at the POE location, would afford the same protection to human health and the environment as the background water quality. This approach was consistent with 10 CFR Part 40, Appendix A, Criterion 5B (6), which states that "Conceptually, background concentrations pose no incremental hazards..."

As referenced in AR 1996 and based upon NRC Inspection Report 40-8452/94-01 dated July 15, 1995, confirming that "... all 26 settlement monuments had reached 90 percent of the final settlement rate (T-90). ... Now that the T-90 has been met, the final radon barrier can be placed with NRC approval", BCUC began final reclamation of the tailings area and began plug and abandonment procedures of all wells in advance of reclaiming and placement of cover material in the tailings area. The nine wells that remain at this time are the ones required by license conditions for monitoring down gradient seepage of contaminated solution.

The tailings area reclamation was completed in 1999. By letter dated March 16, 2000, BCUC submitted the *Bear Creek Uranium Tailings Reclamation Report* to document the completion of reclamation of the tailings disposal cell at the Bear Creek site. A follow up inspection of the completed reclamation construction activities at Bear Creek was conducted by NRC on July 19, 2000 and their conclusion was that the reclamation of the Bear Creek disposal cell was performed in accordance with the requirements of 10 CFR Part 40, Appendix A, and the BCUC *Tailings Reclamation Plan* as specified in License Condition 44, (ref. USNRC letter dated July 3, 2001 to Mr. Ernie Scott, Anadarko Petroleum Corporation).

From 2001 until 2011, the water sampling was conducted annually by contract personnel and an annual report of the data collected was submitted to the NRC by Anadarko personnel.

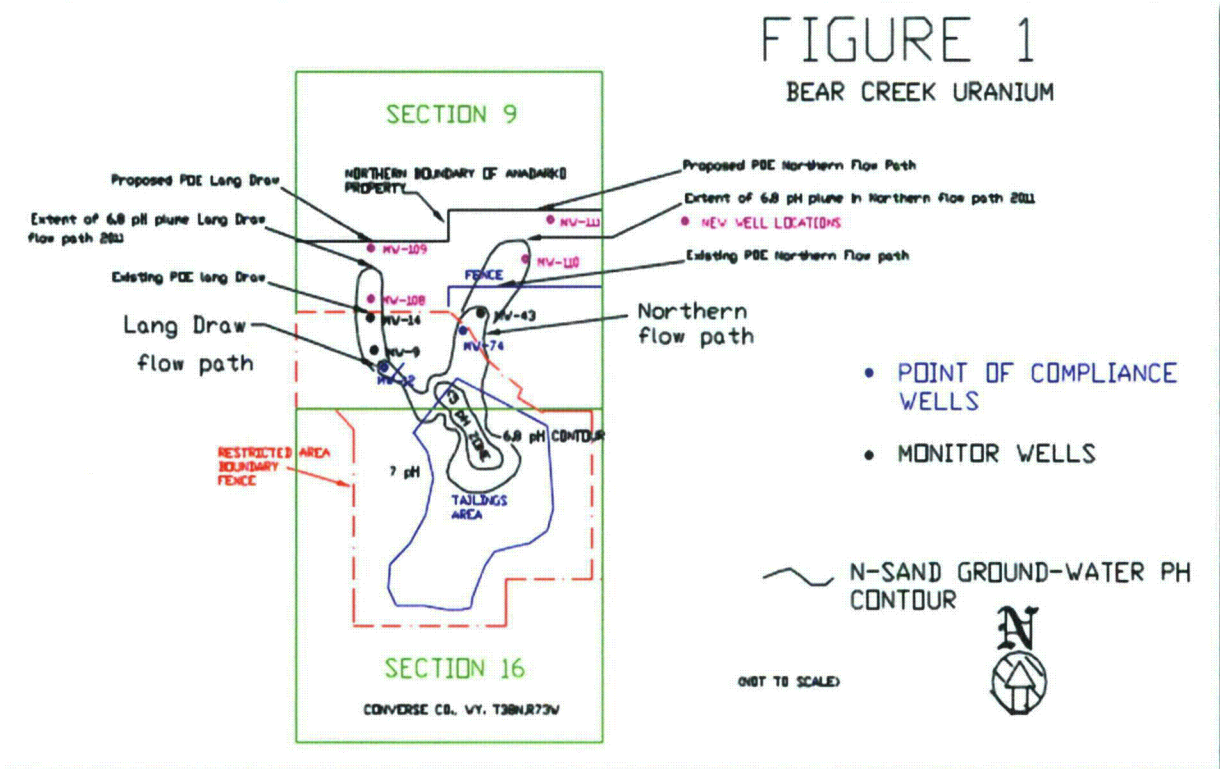
In 2010, in preparation for License termination, NRC reviewed the groundwater data received from the BCUC facility, they found that uranium concentrations had



exceeded the predicted concentration at well MW-14 by more than ten times and requested that a new risk-based ACL be submitted. Although the value predicted by the modeling had been exceeded, at no time did the uranium concentrations exceed the approved ACLs.

TetraTech Geo the consulting firm that had done the ground water modeling for the 1997 ACL application was retained to re-evaluate the previous model results based upon the ground water monitoring data collected during the past 13 years.

In-house evaluation of historical ground water data, operational events, tailings dam construction, well completion and well log data was conducted to assist in this task. Figure 1 shows the general location of the site boundaries and wells.



## **Chronological Sequence of Events**

Although the CAP was not officially implemented until 1989, other tailings management practices were successful in minimizing the seepage that was encountered at the seepage collection dam and at the downstream monitor wells. Similarly, tailings management practices implemented prior to the CAP were successful in limiting the amount of tailings seepage. Additional action and changes implemented during the time frame from 1982 to 2000 that impacted the project are presented here in chronological order. The impact of these changes can be observed in the attached graphs of static water levels and chemical parameters measured in the down gradient monitor wells.

**1980 & 1984** Two dam raises were completed and the addition of wings to the east and west portion of the tailings dam allowing increase mill through-put to 2000 tpd.

**1985-1989** Utilize monitor/recovery wells in the seepage control basin to pump accumulated seepage to the mill and/or tailings pond. The seepage rate measured at the toe of the dam was 17 gpm in 1985 and decreased to <0.5 gpm in 1988 with no measurable seepage in 1989. It should be noted that the recovery well casings located in the catchment basin were slotted from top to bottom and at times some were under seepage water. This had an impact at down gradient monitor wells.

**1986** Mill shut down. Recovery wells and enhanced evaporation system operational.

**1988** Placement of interim cover to prevent blowing tailings and construction of the Number 1 clay lined evaporation pond.

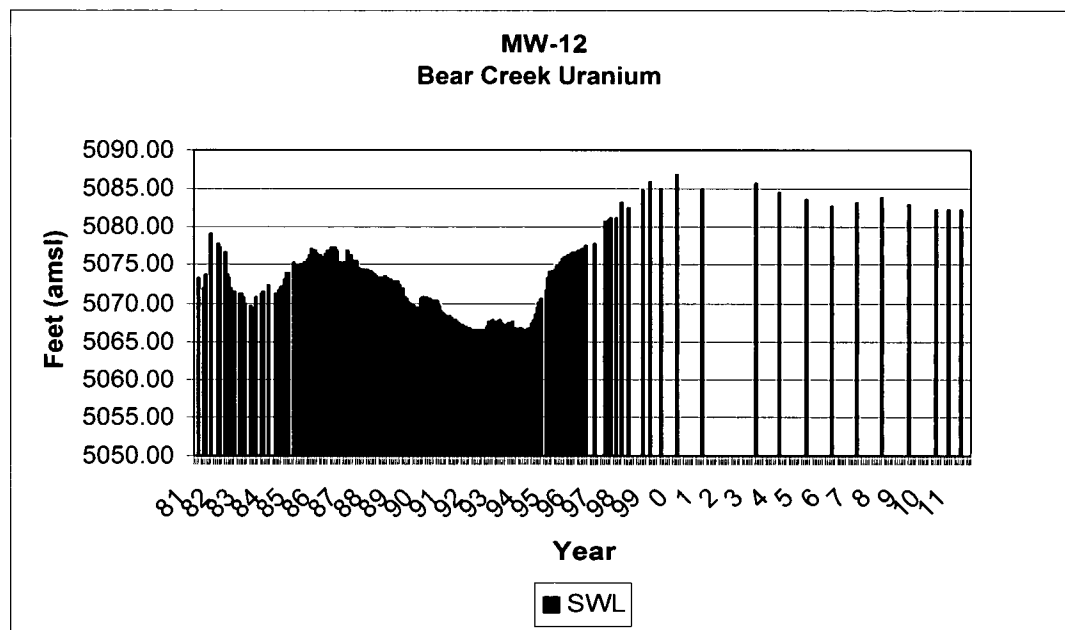
**1990** Placement of more interim cover to prevent blowing tailings. Construction of the Number 2 clay lined evaporation pond. Start construction of the Number 3 clay lined evaporation pond.

**1991** Complete construction of the Number 3 evaporation pond. Shut down enhanced evaporation system and direct all water from the recovery well system to the clay lined ponds. All surface areas were then covered with enough clay to prevent further recycling of tailings solution back into the tails sands and prevent windblown tailings.

**1992-1994** Shut off down gradient seepage recovery wells to prevent pulling contaminated solution away from the tailings pond.

**1994** In September of 1994, GeoTrans consultants shut down all recovery wells for 102 days to compare model determined final static water level (SWL) recovery levels against measured levels. GeoTrans predicted 12 foot recovery in SWL at MW-12 with no potential for mounding when the system was shut down for final reclamation of the tailings area. (Hydrogeological and Geochemical Transport Analysis, UPR BCU Mill Tailings Impoundment, GeoTrans, Inc., March 7, 1995).

Measurements of the SWL at MW-12 conducted after reclamation of the tailings area actually show a recovery of almost 22 feet as shown in the graph below.



**1996** The recovery well system was shut down for final reclamation of the tailings area. (License Amendment Request dated May 30, 1996, NRC License Amendment No. 39)

**1997-1999** Plugged and abandoned all wells not necessary for monitoring of the BCUC mill tailings area site and mining areas. (License Amendment Request dated May 30, 1996; License Amendment No. 45 1996; Report to the Wyoming State Engineer's Office 1999)

**1997-1999** Placement of over one million tons of cover material in the tailings area between the ridge line and the tailings dam. This material was placed after the modeling was completed and report submitted with the 1997 ACL application.

**2000-2011** Annual water sampling conducted in compliance with Source Materials License SUA-1310 Condition 47, annual survey of land use within two kilometers of the site and reporting as required by License Condition 21, Department of Energy (DOE) site visits and collection of water samples, additional engineering surveys required by DOE for site access, weed control as required.

## **2.0 Model Review Summary/In-House Data Review**

### **Model Review Summary**

In compliance with NRCs requests that a new risk-based ACL application be submitted incorporating the ground water data collected over the 13 years since the original ACL application, Anadarko contracted with TetraTech GEO (formerly GeoTrans) to complete a new predictive transport model. The transport model is attached under separate cover. The new model has two significant advantages over the 1995 model. First, data are available regarding the transport of uranium and other constituents along Lang Draw and the Northern Pathway for use in calibration of the model. The 1995 model was performed in a predictive mode, without information on transport rates at the site. Second, modeling technology has improved allowing direct incorporation of the chemical reactions into the transport model. Separate models were constructed for Lang Draw and for the Northern Pathway.

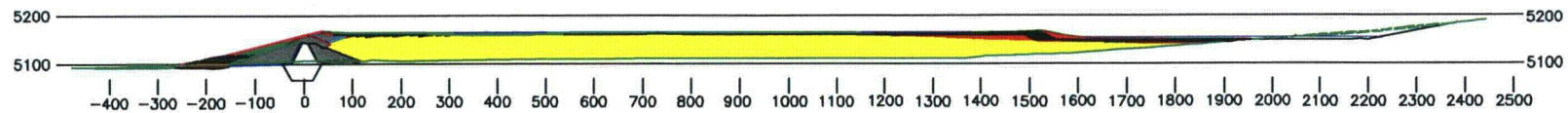
As noted by NRC, the 1995 model under predicted the U concentrations that would reach MW-14. The 1995 model in BIO1D used the observed concentrations as the modeling initial conditions down-gradient from the low pH part of the plume. For the upstream boundary condition, the model used the observed uranium concentration at the downstream edge of the pH front, 92 pCi/L. The assumption that was made was that this concentration was a good estimate of future uranium concentrations. As observed in Figure 10B of the attached 2011 model, MW-12 had a uranium concentration of approximately 110 pCi/L in 1994, while MW-9 had a concentration of around 80 pCi/L. Because the modeling was only addressing transport down gradient of the pH front, these values appeared to be reasonable, based on the measurements at that time.

What the modelers did not consider was the effect of dilution during the recovery pumping on the observed concentrations. The recovery pumping was causing steeper gradients west of Lang Draw than present after the pumping was stopped. The steeper gradients produced more water moving into the Lang Draw area than would occur after pumping stopped and water levels recovered. When pumping stopped, the dilution provided by this lateral inflow decreased. This water probably assisted in the neutralization of the acidic plume. The net result was that after water levels recovered, the uranium concentrations increased. Because the 1995 model used an up-gradient boundary condition that was based on concentrations that were “artificially” low because of the recovery well pumping. It is the modeler’s contention that this underestimated the peak concentrations that were to develop.

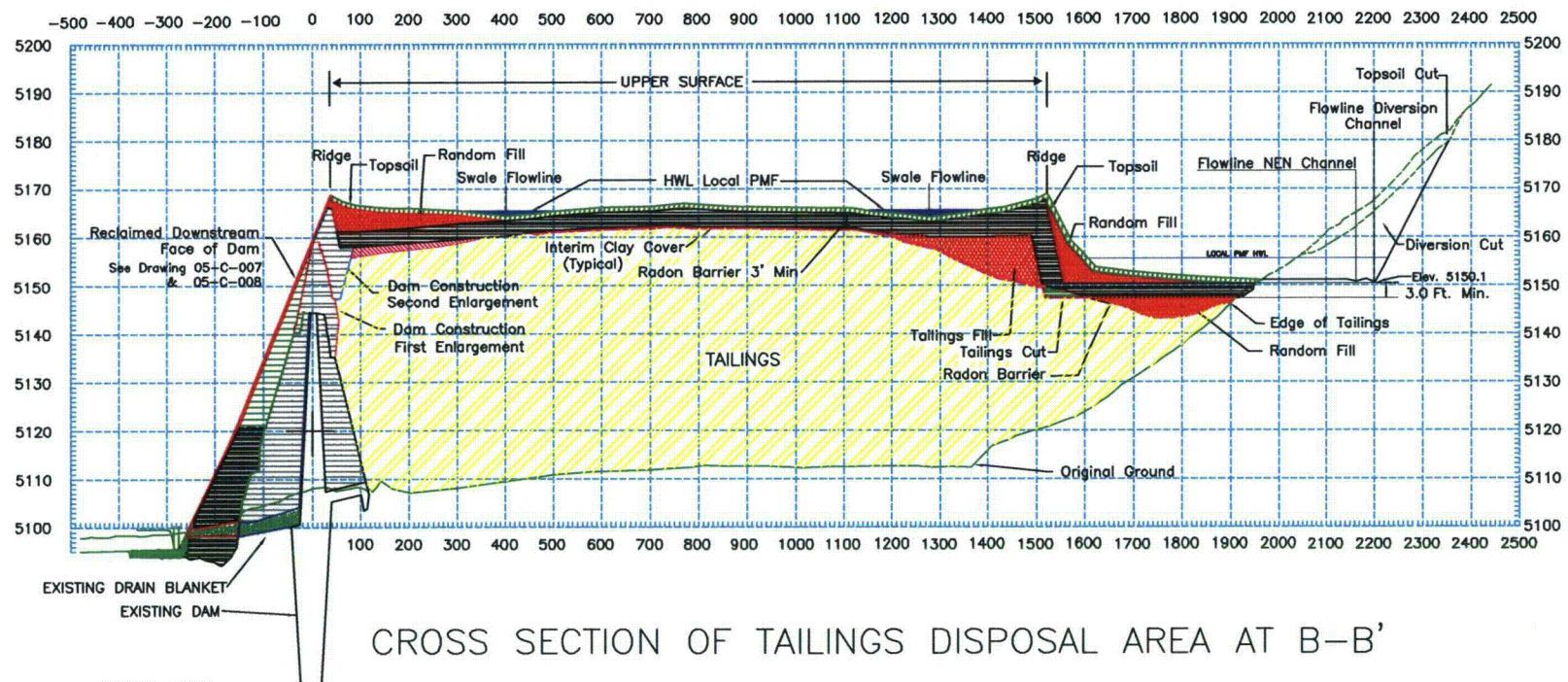
### **In-House Data Review**

The early time-frame seepage from the tailings dam is estimated to have been a major factor that would have influenced the higher than expected uranium values predicted at MW-14 in the first model. A drawing of the tailings dam cross section showing dam raises, drain blanket, and core trench is shown as Figure 2. Figure 3 shows a general cross section of the tailings area.





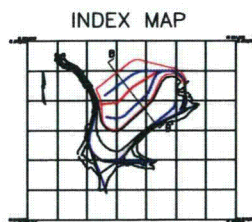
TRUE SCALE CROSS SECTION OF TAILINGS DISPOSAL AREA  
AT B-B'



CROSS SECTION OF TAILINGS DISPOSAL AREA AT B-B'

VERTICAL EXAGGERATION 10:1

All measurements in feet



NOTE: Cross section B-B' crosses channel flowline at Sta 66+46.52  
tailings North Fork swale at Sta 25+10.52, tailings South Fork swale  
at Sta. 124+30.79

Revisions				Issue	Date	ANADARKO PETROLEUM CORP.
No.	By	Checked/Approved	Date	Revised By	Date	
1	AW	AW	11/91	Revised	11/91	
2	AW	AW	3/92	Revised	3/92	
3	AW	AW	3/92	Revised	3/92	
						BEAR CREEK URANIUM
						TAILINGS DISPOSAL AREA
						CROSS SECTION OF TAILINGS
						AREA AT B-B'
						File/Dwg.No. 05-C-010

Figure 2

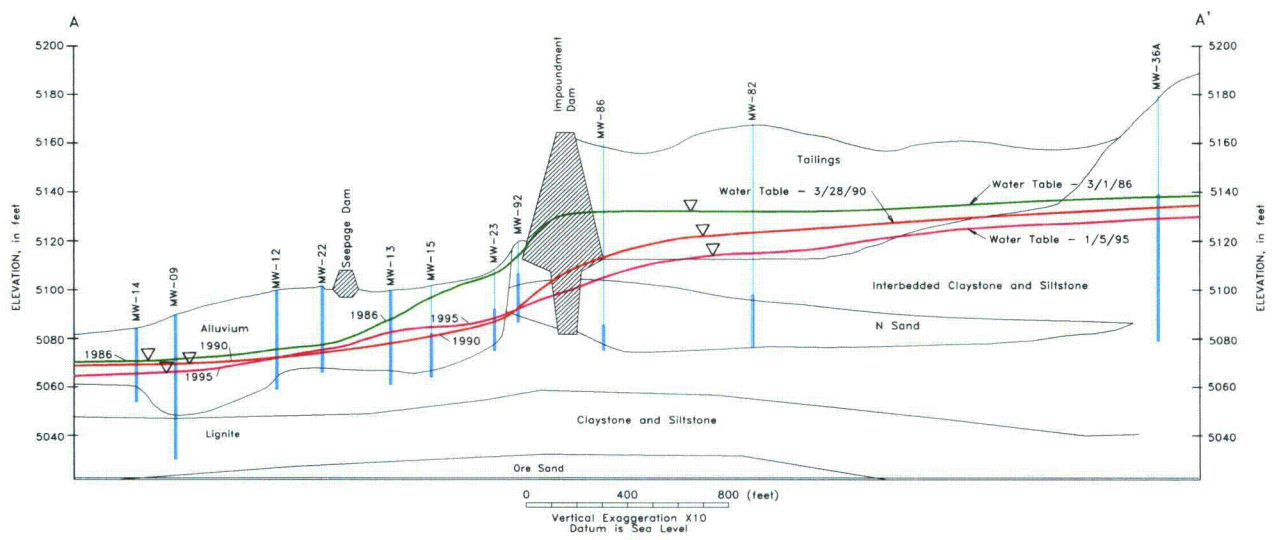


Figure 3 . N Sand/alluvium potentiometric-surface elevations for 1986, 1990, and 1995 along geologic section A-A'.

As referenced in the Background Information, seepage was first noticed at the toe of the dam in 1978. Three wells were drilled to monitor groundwater down gradient from the tailings dam. The wells were designated MW-7 (completed Oct. 1980), MW-12 (completed Feb. 1981) and MW-13 (completed Feb 1981). The wells were also used as recovery/pump-back wells, with MW-12 only used for a short period of time. MW-7 and MW-12 were located down gradient from the catchment basin (a map of the N-sand well locations is provided for reference at the end of this section). MW-12 was to later become the point of compliance well. Several wells were drilled and cased in the catchment basin to be used for monitoring and/or recovery wells. The well casings were perforated from top to bottom. As the rate of seepage increased, MW-37 (completed Oct. 1981), which was located in the low spot in the catchment basin near the catchment basin dam, became the major recovery well along with MW-7, MW-13, MW-38, MW-39 and MW-22 located in the Lang Draw flow path. Low pH solution recovered from these wells was pumped to a sump and from there pumped back to the tailings basin. During the time frame of 1978 through 1985 the amount of seepage recovered in the catchment basin and pumped back to the tailings pond was estimated to be 75 million gallons. In 1984 a weir was installed near the toe of the tailings dam and used to more accurately measure seepage flow. Measured flows were 17 and 14 gallons per minute during 1985 and 1986 respectively. During the early use of the pump-back system in the catchment basin improper operation combined with periodic power failures of the system would temporarily allow ponding of seepage water in the catchment basin. The wells with perforated casing from top to bottom became conduits for the low pH solution to enter the groundwater. The only thing that held this solution in check, i.e. from not reporting to down gradient monitor wells, was the continued use of the recovery well system combined with the drawdown impact from tailings basin recovery wells. The catchment basin recovery wells were pumped until 1994. When the tailings dewatering system was shut down in 1996, the overall hydraulic gradient in the tailings basin increased and the solution previously held in check in the catchment basin was then free to migrate down gradient. (see MW-13, MW-12 and MW-14 U-nat graphs note peak concentration difference and the well locations on the N-sand well location map and Figure 3)



**THIS PAGE IS AN  
OVERSIZED DRAWING OR  
FIGURE,**

**THAT CAN BE VIEWED AT THE  
RECORD TITLED:**

**DRAWING NO.:**

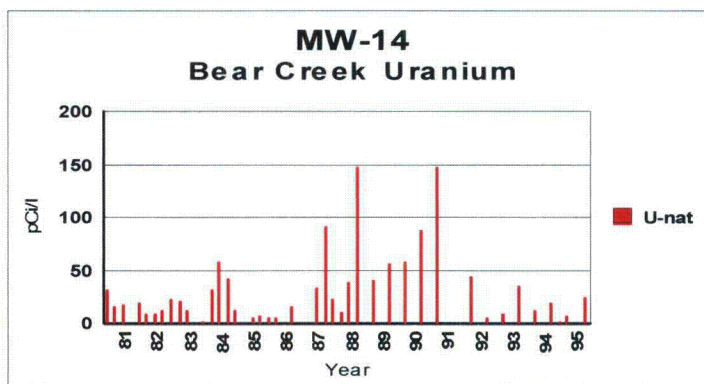
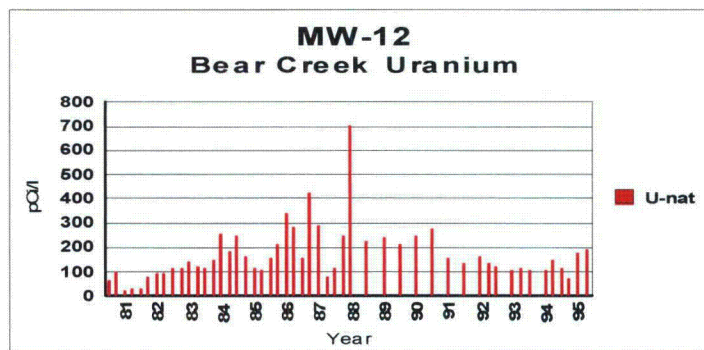
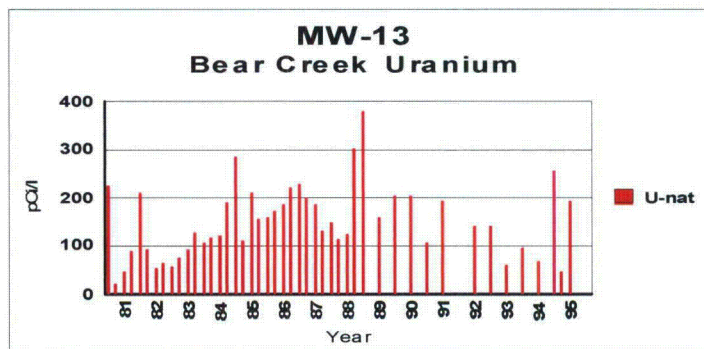
**N-Sand-W-ph-contr.dwg,  
“BEAR CREEK URANIUM  
TAILINGS DISPOSAL BASIN**

**N-SAND  
WELL LOCATIONS  
WITH Ph CONTOURS”**

**WITHIN THIS PACKAGE... OR,  
BY SEARCHING USING THE  
DOCUMENT/REPORT  
DRAWING NO.**

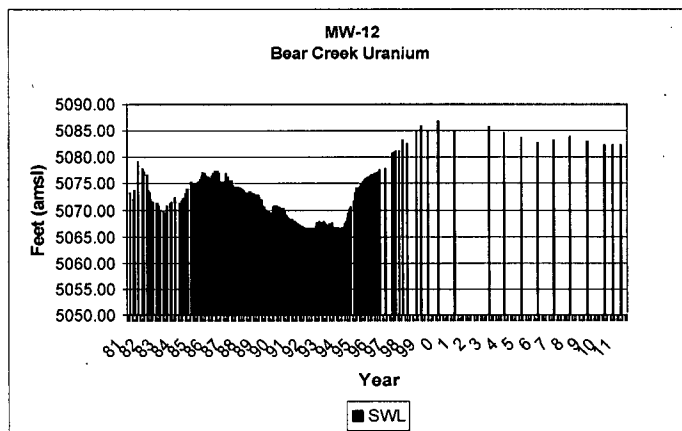
**N-Sand-W-ph-contr.dwg**

**D-01**

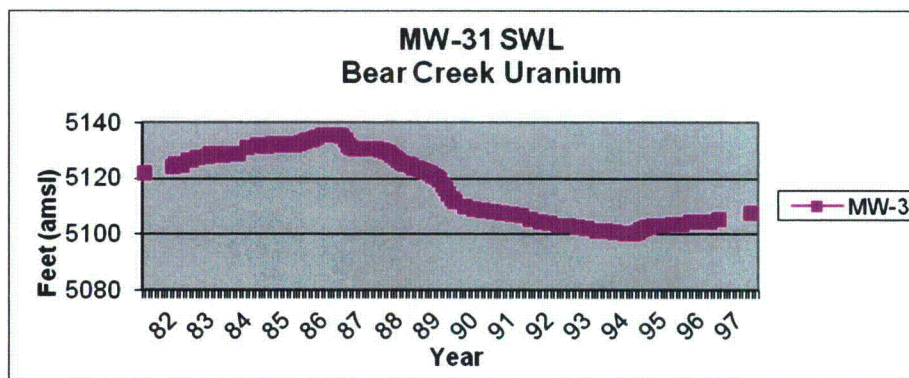
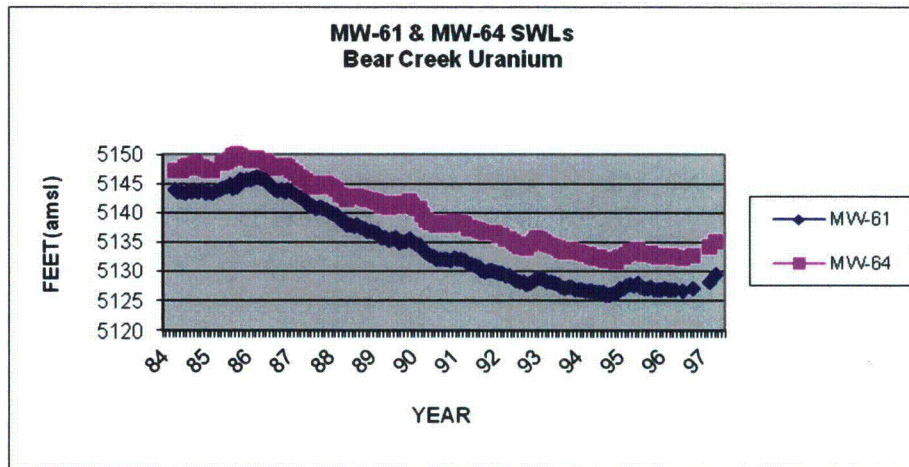


Uranium measured at MW-14 shows similar peaks with high concentrations over three times higher than the 45 pCi/l predicted level at the Lang Draw POE in the 1997 ACL model.

Use of these recovery wells in the catchment basin would also explain the artificially reduced water levels measured in the catchment basin monitor wells during operation of the mill until 1994 when the catchment basin recovery wells were temporarily shut down (i.e. the predicted water level recovery at MW-12 was 12 feet after recovery wells were shut off). In 1996 the tailings basin recovery wells were shut down and the water levels in the catchment basin monitor wells recovered to higher levels than what were seen in these wells during operation of the mill at peak levels.



Another event that was not considered in the model was the impact of fresh water dilution on the low pH solution located beneath the tailings in the N-sand. The neutralization impact could have been under estimated. Draw down data from wells MW-61 and MW-64 located 1000 to 1200 feet west of the tailings recovery wells and MW-31 located ~1000 feet east of the tailings recovery wells indicate a cone of depression a half mile in diameter lateral to the tailings basin.



These three wells had good well yields >5 gallons per minute, 7.0-7.2 pH, ~1000 mg/l TDS, ~500 mg/l SO<sub>4</sub>, ~15 mg/l Cl, 25 pCi/l U-nat. It should be noted that even these wells would not meet Wyoming Class 1 or 2 water standards because of TDS and Sulfate levels. The estimated gradient, using wells MW-61 to MW-86, was 0.017 ft/ft from southwest to northeast. This is about a 20% increase in gradient compared with the MW-36a to MW-86 south to north gradient of 0.014 ft/ft used in both models. Conservative estimates, or not including the impact from the recovery wells, enhanced evaporation, clay cover over exposed tailings, clay lined evaporation ponds (preventing recirculation of recovered solution) and potential for dilution may have overestimated the remaining volume of <5 pH solution in the tailings area.

The static water level graphs show the extent of the actual down gradient drawdown in these wells.

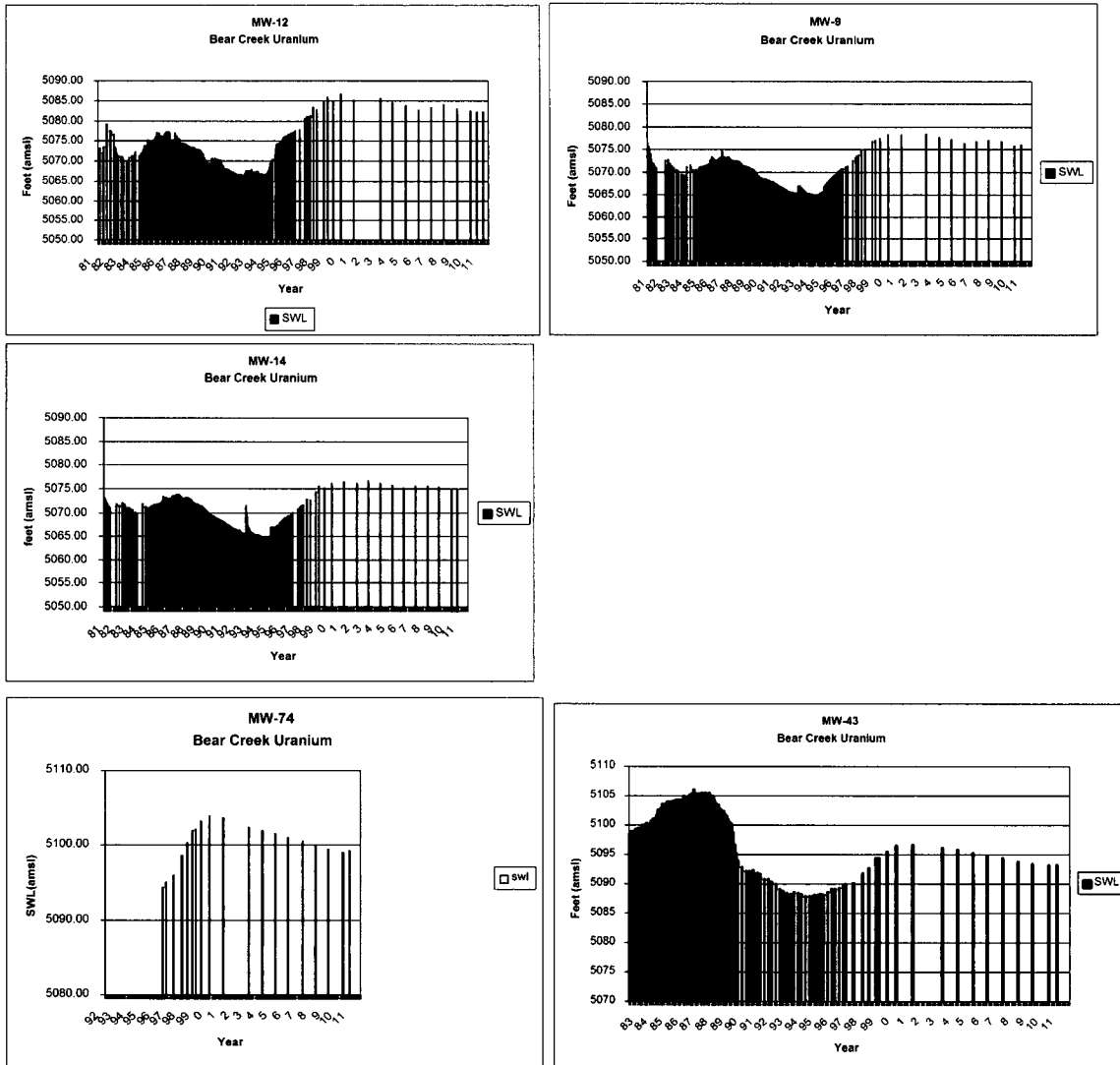


Figure 4 was constructed to see if solution contained in the slimes at the bottom of the tailings sand would follow the declining level of solution in the N-sand or stay bound in the slimes as predicted, i.e. pumping in the slimes area was estimated by bench testing, to get to a point of diminishing returns (about 30% saturation) and would not readily seep out or be pumped out of the tailings sand. Static water levels measured across the tailings basin (see Figure 4) shows visible separation between the bottom of the saturated zone of the tailings sand and top of the saturated zone of the N-sand. A pH of greater than 6.2 was measured at MW-107 in 1994 (Attachment 1, Section 2.a operational year 1994 of UPR Group, Inc. Alternate Concentration Limit Application Feb 28, 1997) indicating that substantial neutralization was

taking place in the N-sand beneath the low pH solution in the tails sand. MW-107 was completed in the N-sand about midway between TS-2 and TS-4 (see Figure 4) and directly in line with flow to the toe of the dam and down Lang Draw. MW-85, also an N-sand well, had a pH of 7. Two other wells, MW-106 and MW-105, were completed in 1994 and were used as N-sand recovery wells as their pH values were 5.6. They were located near the north east section of the dam. Comparing this graph to the attached N-sand Well Location map gives a better perspective to what was happening beneath the saturated zone of the tailings sand. Figure 2 is a cross section looking from north to south through the dam and includes the approximate location of the cut off trench superimposed. The cutoff trench keeps water contained in the west part of the basin as it (the cutoff trench) was completed about 5 feet into the claystone located below the N-sand. This helped create a somewhat confined large source of 7 pH solution that was drawn toward the cone of depression created by the N-sand recovery wells in the tailings basin. Using the N-sand well location map and Figure 3 puts Figure 4 in three dimensional perspective. The main objective of Figure 4 is to show the hydraulic gradient from southwest to northeast and point out the failure of the cut off trench in the northeast section to get below the N-sand into the claystone. It also shows the potential for overestimating the volumes of low pH solution used in the original 1997 ACL Application model (see 1997 ACL App., Attachment 2, Figure. 3-1)



Figure 4  
E/W CROSS SECTION THROUGH DAM/TAILINGS

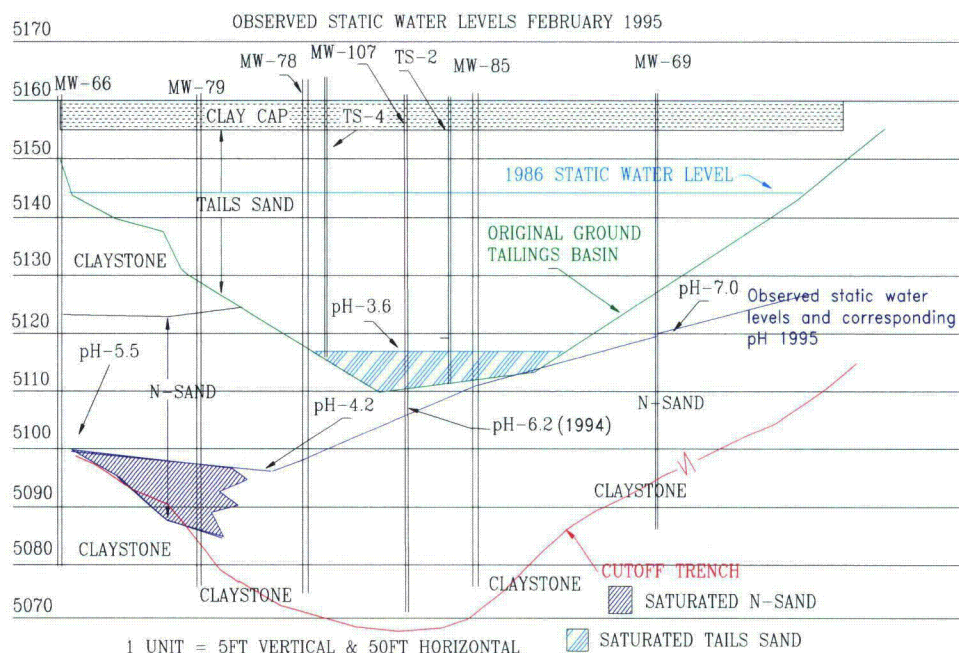


Figure 4 shows where low pH solution was able to seep through and can be seen in well MW-77 (see the N-sand Well Location map in map pocket). When the static water level in the N-sand goes below ~5085 feet, which was defined as the bottom of the N-sand in the northeast corner of the tailings dam, the seepage to the Northern flow path may subside.

The highest potential for seepage from the tailings to the N-sand was estimated to be in the up-gradient, southern, extent of the tailings impoundment where the sand begins to outcrop. The area was graded and lined with clay prior to the dam raise in 1980. By 1996, the low pH solution was located well within the confines of the tailings dam.

In 1991 all of the recovered low pH solution was pumped to clay lined ponds and all of the tails sands were covered with clay material so there was no potential for recirculation of low pH solution back to the tailings sand during the last 5 years of

dewatering of the tailings and N-sand. An estimated 100 million gallons of low pH solution was recovered and evaporated during that time frame.

The table below contains the background concentrations, and predicted breakthrough maximum concentrations (PBMC) for uranium, radium, and nickel as shown in Figures 18A., 18E.,18F., 21A.,21E.,and 21F of the 2011 model for the Lang Draw flow path and the Northern flow path Also included in the table are the results predicted in the 1997 ACL model.

Hazardous constituent	Lang Draw PBMC	Lang Draw year of PBMC	Northern flow path PBMC	Northern flow path year of PBMC	Background concentrations
Uranium 2011 model	*460 pCi/l	2015	75 pCi/l	2032	98.7 pCi/l
Radium 2011 model	2.1 pCi/l	2015	5.8 pCi/l	2040	9.7 pCi/l
Nickel 2011 model	0.032 mg/l	2015	0.034 mg/l	2039	0.05 mg/l
Uranium 1997 ACL model	45 pCi/l	2075	45 pCi/l	2125	98.7 pCi/l
Radium 1997 ACL model	13 pCi/l	2075	10 pCi/l	2095	9.7 pCi/l
Nickel 1997 ACL model	0.053 mg/l	2255	0.055 mg/l	2395	0.05 mg/l

\* 2011 model for uranium in Lang Draw does not match any measured data for MW-109, MW-108 or MW-9 (see Figure 18A. Predicted Breakthrough of Uranium Lang Draw, *Re-Evaluation of Metals Transport At Bear Creek Uranium October 2011*)

The 2011 model predicted levels of radium and nickel are less than background in both flow paths and compare well with predicted levels of radium and nickel in the 1997 ACL model. The 2011 model predicted uranium in the Northern flow path to be about 67% higher, still less than background concentrations, than the predicted levels in the 1997 model; however, uranium in the 2011 model for the Lang Draw flow path POE is predicted to be almost 11 times higher, in year ~2015, than what was predicted in the 1997 ACL model. The uranium value measured at MW-109 in 2011 was 60 pCi/l compared to the 2011 model predicted value of ~325 pCi/l. MW-108 and MW-9 show comparable results, 3 to 12 times higher respectively, in predicted versus measured results for uranium.

For a uranium risk assessment calculation at the Lang Draw POE the average value under the curve (see Figure 18A of the 2011 model) of 166 pCi/l for uranium, converted to U238, at MW-109 was used. The calculated risk was 3.8E-4 for a chronic exposure over a 75 year time frame versus 2.3E-4 for the background



concentration. The combined (U238+D and Ra-226+D) radiological cancer risk for the POE on Lang Draw is  $4.2\text{E-}4$  while the combined risk for the same background parameters is  $4.3\text{E-}4$ . All parameters, other than uranium at the Lang Draw POE, for both flow paths were predicted to be less than background in the 2011 model at the extended POEs.

Water sampling in both monitor wells MW-108 and MW-109 takes three days to obtain a sample after two casing volumes have been pumped. Measured static water levels prior to pumping took at least 24 hours to recover before another casing volume could be pumped. The 5 inch well bore holds 1 gallon per foot and static water levels indicated 13 to 15 gallons of water in the wells. The estimated well yields on wells MW-108 and MW-109 are  $<0.01$  gallons per minute.

### **3.0 Hazard Evaluation**

The physical setting of the former mill site and the reclaimed tailings is located in a remote semi-arid section of central Wyoming. Annual precipitation measured over twenty years on site averaged 10 inches. The land use is limited to open range used for grazing cattle and sheep. The ranches that encompass the Bear Creek project are each generally thousands of acres or more in size and have been in existence for almost a hundred years. They are now in their third and fourth generation of family operation with no change in the land use scenario. The nearest ranch headquarters is located 4 miles from the project. When homesteads were claimed, the ranch house was normally built close to an artesian spring with good water quality as most "streams," i.e., forks of Bear Creek and the Dry Fork of the Cheyenne River, in the region are intermittent. The towns and cities throughout Wyoming are typically found along the major water ways which are located nearly 50 miles away from the Bear Creek site in any direction.

The ranchers are adamantly opposed to man camps and people living on site within their property boundaries. There is no reason to believe that the land use will change.

The first shallow potential aquifer within 40 feet of the original ground surface below the tailings impoundment has been referred to as the N-sand. The low pH tailings solution that has seeped into this formation travels in a north to northeast direction. There is no history of this upper zone of the Wasatch formation being used for a domestic or livestock water supply in this region of the Powder River Basin in Wyoming. All of the regional livestock wells are completed to depths of 300 to 500 feet in an aquifer that is separated from the N-sand by an aquitard hundreds of feet thick. Water quality is generally influenced by the presence or absence of

mineralized zones and stringers of lignite/coal which are scattered throughout the Wasatch formation in the Powder River Basin. Wells completed into water bearing formations containing lignite or coal are generally marginal for livestock use in this area due to high dissolved solids, Sulfate and Selenium.

The estimated well yield for monitor wells MW-108 and MW-109 are <0.01 gallons per minute which would not be sufficient for daily residential or livestock use. There are several existing stock water wells completed to 430 to 515 foot depths, in which the water bearing formations are separated from the N-sand by hundreds of feet of claystone, located within a mile or less of the proposed POE locations on Lang Draw and the Northern flow path. These wells provide water at 2-3 gallons per minute and the water is utilized for livestock. All three are windmill driven and have been sampled in the past for groundwater parameters. The wells GW-8, GW-10 and GW-15 are located <1/2 mile south-west of the POE on Lang Draw, <1 mile north of both Lang Draw and the Northern flow path, and ~ 1 mile north-west of the Lang Draw flow path POE respectively. Water samples were collected on these wells and reported to the Wyoming Department of Environmental Quality in required annual reports during operation of the mine.

With the mine, mill and tailings sites having been totally reclaimed and re-vegetated the only potential exposure pathway is from drinking water and ingestion of irrigated garden products contaminated by utilizing the water from this shallow formation. There is no potential for airborne inhalation or external exposure increase above background. There has not been in the past and there is no expected use of this water now or in the future.

Several options were considered to meet the as low as reasonably achievable demonstration (ALARA) in 1997 prior to final reclamation of the tailings area (Letter to J.J. Holonich USNRC dated May 13, 1997). Continue to pump and evaporate, passive reactive barriers (one in each plume), pump and treat with reverse osmosis and reinjection, and fresh water injection were considered. All were cost prohibitive at that time and would be even more so now that the site is reclaimed.

A conservative risk analysis was performed and submitted with the 1997 ACL application. The calculated risk to human health at that time for all of the hazardous constituents were in the E-4 range for predicted and background levels of radioactive contamination of groundwater at the POEs. Uranium in the Lang Draw flow path is the only parameter that is estimated in the 2011 model to exceed the level predicted in the 1997 model. It is still within the E-4 risk range. As previously stated, the predicted uranium value in the 2011 model is at least 5 times higher than the measured levels of uranium in the MW-109 monitor well in the same time frame.

The only potential exposure pathway to be considered is from intake of contaminated groundwater as there is no potential for airborne or external exposure since the site is completely reclaimed.

In 1997, boreholes were drilled by S.M. Stoller north of the POEs located near MW-14 (Lang Draw) and MW-111 (Northern flow path) and south of the Anadarko property boundary. Significant water was not encountered in any of the boreholes along Lang Draw at the time of drilling. Only boreholes near MW-108 in Lang Draw were found to contain wet sands. It was Stoller's opinion that "it is very unlikely that the alluvium will produce enough water to satisfy the NRC definition of an aquifer". Two wells, drilled north of the proposed POEs (MW-109 and MW-111), designated Manning B.C.18 (GW-18, Permit NO. U.W. 64632 completed Aug. 1983) and Hardy No. 4 (U.W. Well permit No.1365 drilled 1947), which were completed to depths of 432 feet and 443 feet respectively, show no water present in the N-sand in the well logs. Both wells are located north of the POEs in Section 9, T 38N, R 73 W. (source on internet "State of Wyoming, State Engineer's Office, Water Rights Data Base, Search by Well Location, ground water information only").

The lithologies encountered north of the Bear Creek Tailings Facility are typical of sediments deposited in a fluvial environment. These deposits are characterized by interbedded sand, silt, and clay units which vary in thickness due to different modes of deposition. The geometry of the stream, at the time of deposition, controlled these facies changes (increasing silt and clay) where sands are typical of stream channel deposits and silts and clays are typical of over-bank deposition. The fining and thinning of the N-sand controls groundwater movement through the study area. Facies changes in boreholes located between Lang Draw and the Northern flow path restricts groundwater flow and separates the study area into two different groundwater flow environments. It is suspected that the facies changes are reflected in the current division of plume migration evident near the tailings facility and may retard flow to the southeast in the Northern flow path. (Stoller 1997).

The water in the Northern flow path is not predicted, in the 2011 model, to exceed background concentrations for the hazardous constituents of interest. Criterion 5B(5) of Appendix A states that conceptually, background concentrations "...pose no incremental hazards..."

There is no known past or current use of this shallow aquifer and no surface expression or communication with lower aquifers or surface water in the area. The remedial action costs are high in relation to the long term benefit. The mine, mill site, tailings area, and five miles of access road were reclaimed and revegetated over ten years ago. All additional monitor wells and piezometer wells were plugged and

abandoned ahead of the reclamation sequence. There is also no likelihood of buildings or structures being placed in the area. The groundwater in this shallow formation should qualify for supplemental standards according to criterion cited in EPA 40 CFR 192.21(b).

The following information was taken from the Department of Energy *Site Observational Work Plan For the UMTRA Project Site At Spook, Wyoming* which is located on the Dry Fork of the Cheyenne River about 2 miles south of the Bear Creek Uranium site. The State of Wyoming held title to the surface area over the disposal cell at the Spook site.

Regional background water quality data from sandstones in the Wasatch Formation were collected by Rocky Mountain Energy (RME) from 22 domestic wells and monitor wells during the period between 1974 and 1977. The data were collected as part of a mining permit application for the RME Bear Creek Project. The regional data demonstrate that ground water from the altered sandstones has uranium and selenium concentrations generally greater than those in the unaltered sandstones and that the altered sandstones contain ground water with ambient uranium and selenium concentrations in excess of the MCLs for UMTRA Project sites.

The Spook work plan concluded that there is no apparent risk to human health and the environment because there are no known exposure pathways for contaminated ground water from the uppermost aquifer to lower aquifers or the surface. No one is using the ground water from this aquifer for any purpose and there is no discharge of ground water from the uppermost aquifer to the surface or to surface water. A baseline risk assessment of site-related contamination was not performed for the Spook site because of the lack of exposure pathways for the uppermost aquifer and because of the naturally contaminated nature of background water from that aquifer.

The rationale being that "ground water in the uppermost aquifer (also the zone of contamination) being classified as limited use, which allows the application of supplemental standards. No one is using or is projected to use the ground water from this aquifer for any purpose; there is no discharge of ground water from the uppermost aquifer to deeper aquifers used for domestic and agricultural purposes or to the surface or to surface water."

#### **4.0 Proposed Action**

The recalibrated ground water model predicts that the currently approved ACLs will not be exceeded and the risk assessment confirms there is no unacceptable risk to the public. Therefore, there is no need to change the ACLs.

## References:

*Final Environmental Statement related to operation of Bear Creek Project (FEIS), NUREG-0129 Docket No. 40-8452 June 1977*

Staff Technical Position, *Alternate Concentration Limits for Title II Uranium Mills, Standard Format and Content Guide, and Standard Review Plan for Alternate Concentration limit Applications*, January 1996.

Union Pacific Resources Group, Bear Creek Uranium Company, *Amendment Request to SUA-1310; Docket No. 40-8452, May 30, 1996*

Union Pacific Resources Group, Inc., Bear Creek Uranium Company, *Alternate Concentration Limit Application, February 28, 1997*

Union Pacific Resources Letter dated May 13, 1997 to Joseph J. Holonich, Chief USNRC, Attn: Charlotte Abrams, containing *additional information relating to Section 3.5 of Bear Creek Uranium Company's Alternate Concentration Limit Application.*

Union Pacific Resources, Bear Creek Uranium Mill Tailings Impoundment, *Hydrogeologic and Geochemical Transport Analysis*, GeoTrans Project #8386-000, March 7, 1995

*Fate and Transport Modeling Analysis of Tailings Water Constituents, Bear Creek Uranium Mill Site, Converse County Wyoming*, HSI GEOTRANS, June 30, 1998

*2011 Edition of the Drinking Water Standards and Health Advisories*, EPA 820-R-11-002, Office of Water, U.S. Environmental Protection Agency, Washington, DC

*Code of Federal Regulations (CFR), Energy, 10 Parts 0 to 50*, Revised as of January 1, 1996.

Wyoming Department of Environmental Quality, *Water Quality Rules and Regulations, Chapter 8*, Adoption Date: March 16, 2005.

*EPA Risk Assessment Guidance for Superfund, Vol. 1 Human Health Evaluation Manual (Part A and B)*, Environmental Protection Agency (EPA), 1989 (RAGS)

*EPA Integrated Risk information System (IRIS)*, U.S. Environmental Protection Agency, New Assessments and Reviews, 2011

*EPA Cancer Risk Coefficients for Environmental Exposure to Radionuclides*, Federal Guidance Report No. 13, Sept. 1999

*EPA Radionuclide Table: Radionuclide Carcinogenicity Slope Factors*, Federal Guidance Report No. 13, Morbidity Risk Coefficients in units of picocuries, U.S. Environmental Protection Agency, April 16, 2001

*EPA Limiting Values of Radionuclide Intake and Air Concentration and Dose Conversion Factors for Inhalation, Submersion, and Ingestion, Table 2.2*, U.S. Environmental Protection Agency, Federal Guidance Report No. 11, 1988

*Delineation of N-sand and Lang Draw Alluvium - Bear Creek Uranium* S.M. Stoller Corporation, April 7, 1997

*Site Observational Work Plan For The UMTRA Project Site At Spook, Wyoming* Prepared by the U.S. Department of Energy Albuquerque, New Mexico May 1995 DOE/AL/62350-156 Rev. Oc.1

*Re-Evaluation of Metals Transport at Bear Creek Uranium, Converse County Wyoming* prepared by Tetra Tech Geo, Louisville, Colorado, October 13, 2011

*RESRAD 2.6* Release date July 7, 2010, Argonne National Laboratories

A COMPREHENSIVE RISK ASSESSMENT  
FOR THE  
PREDICTED CONCENTRATIONS  
OF  
NICKEL, RADIUM AND URANIUM  
AT THE  
BEAR CREEK URANIUM COMPANY SITE



## **TABLE OF CONTENTS**

### **EXECUTIVE SUMMARY**

#### **1.0 HUMAN HEALTH EVALUATION**

- 1.1 Introduction
- 1.2 Selection of Contaminants for Risk Evaluation Toxicity
- 1.3 Toxicity Information for Noncarcinogenic and Carcinogenic Effects
- 1.4 Dose Conversion Factors and Exposure Pathways
- 1.5 Ground Water Concentrations
- 1.6 Future Land Use
- 1.7 Quantification of Potential Risk
- 1.8 Risk Characterization
- 1.9 Uncertainties in the Characterization of Risk

#### **2.0 CONCLUSIONS**

##### **LIST OF TABLES**

- Table 1.3.1 Toxicity Values for Hazardous Constituents
- Table 1.5.1 Hazardous Constituents Concentrations at the POE Locations
- Table 1.6.1 Potentially Exposed Populations and Exposure Routes
- Table 1.7.1 Radionuclides Expressed in Terms of Effective Dose
- Table 1.8.1 Lifetime Intake of Hazardous Chemicals
- Table 1.8.2 Carcinogenic Risks to Residents
- Table 1.8.3 Noncarcinogenic Hazard Quotients for Residents
- Table 1.8.4 Total Radionuclide Risk of Developing Cancer for Residents
- Table 1.8.5 Total Nickel Hazard Quotient for Residents

## EXECUTIVE SUMMARY

This assessment of risk is being prepared in support of a request from the Nuclear Regulatory Commission for a risk-based alternate concentration limit (ACL). The measured level of uranium at the point of exposure (POE) down Lang Draw has exceeded the 1997 ACL submittal prediction by a factor of 10. Although the value predicted by the modeling had been exceeded, at no time did the uranium concentrations exceed the approved ACL's.

To determine the risk associated with water use with the predicted maximum concentrations of nickel, radium, and uranium, a residential use scenario was assumed to exist. There is no current use of the affected water resource and none is expected at this site.

Environmental Protection Agency (EPA) Federal Guidance Report (FGR) No. 13 Morbidity Risk Coefficients, in Units of Picocuries were used to determine radionuclide carcinogenicity risks for Uranium and Radium concentrations in drinking water based upon chronic intake over a 75 year life time. Nickel is not currently listed as a contaminate in drinking water by either the State of Wyoming, which defaults to the National Primary Drinking Water Standard, or the EPA Primary Drinking Water Standards which remanded Ni from drinking water standards in 1996. Prior to 1996, the Maximum Concentration Limit (MCL) for Ni in drinking water was listed as 0.1 mg/l with an oral reference dose (RFD) of 0.02 (mg/kg/day). The current, January 2011, EPA lifetime health advisory (LHA) MCL for Ni is listed as 0.1 mg/l. A lifetime HA is defined as: "The concentration of a chemical in drinking water that is not expected to cause any adverse non-carcinogenic effect for a lifetime exposure. The lifetime HA is based on exposure of a 70kg adult consuming two liters of water per day." Nickel was not listed in Table 5c of the Nuclear Regulatory Commission regulations contained in 10 CFR Part 20 for hazardous constituents in drinking water and was based on the EPA national drinking water standards listing prior to 1996. For purposes of determination of relative risk from Ni in groundwater, the EPA's remanded standard was used along with an oral reference dose for soluble Nickel from studies that were conducted and reported on EPA's Integrate Risk Information System (IRIS) web site. The most recent model completed in October of 2011 has predicted nickel and Uranium concentrations to be below background at the points of exposure down Lang Draw and in the Northern flow path.

The carcinogenic risks for individual radionuclide constituents were assessed. The risk associated with radium and uranium was found to be within a reasonable range of E-4. The risk associated with nickel was found to be acceptable because all expected levels of Ni were less than previously remanded EPA standard of 0.1 mg/L

MCL and an oral RFD for soluble nickel. To determine the relative incremental increase in risk due to the reclaimed mill tailings, the risk associated with consumption of water having background concentrations of nickel, radium, and uranium was calculated and compared to the predetermined background levels, the EPA recommended MCL for each constituent and the expected concentration for each constituent at the point of exposure. The assessment of total risk associated with the background conditions indicated that nickel concentrations were within acceptable limits, while radium and uranium were on the order of E-4. The summation of the predicted concentrations of nickel, radium, and uranium did not change the risk order of magnitude.

The exposure assessment indicated that there is no exposed population and it is reasonable to assume that there will be no future exposed populations. However to support the calculation of risk, a hypothetical population was assumed to exist. This scenario demonstrated that the total risk associated with the utilization of background water was within the order of magnitude for the risk associated with the predicted water quality and MCL's for uranium and radium.

## **1.0 HUMAN HEALTH EVALUATION**

### **1.1 Introduction**

This document evaluates the potential risks to human health associated with groundwater water use at the POE locations in the Northern and Lang Draw flow paths. The risk assessment is based on the United States Environmental Protection Agency's (EPA) Risk Assessment Guidance for Superfund, Vol.1 Human Health Evaluation Manual (Part A and B) 1989 (RAGS), the EPA Integrated Risk Information System (IRIS), EPA Cancer Risk Coefficients for Environmental Exposure to Radionuclides, Federal Guidance Report No. 13, the Radionuclide Table: Radionuclide Carcinogenicity Slope Factors Federal Guidance Report No.13 Morbidity Risk Coefficients, and the Federal Guidance Report Number 11: Limiting Values of Radionuclide Intake and Air Concentration and Dose Conversion Factors for Inhalation, Submersion, and Ingestion, Table 2.2., EPA 2011 Edition of the Drinking Water Standards and Health Advisories

### **1.2 Selection of Hazardous Constituents for Risk Evaluation**

Predictive modeling associated with information collected from monitoring of the corrective action program (CAP) was utilized to determine the parameters for risk evaluation. This predictive modeling indicated that nickel, radium, and uranium



would require alternate concentration limits and an evaluation of risk at the point of exposure (POE) locations.

The modeling information indicated that although other hazardous constituents are present in the water found in the Northern and Lang Draw flow paths, the concentrations are below the license-established standards. Evaluation of past concentrations and current concentrations indicate that, in the near term, they will remain below the license-established standards and eventually diminish to below these concentrations.

### **1.3 Toxicity Information for Non-carcinogenic and Carcinogenic Effects**

The only carcinogenetic toxicity information found for Nickel was from air intake. There is no source for airborne Nickel at the Bear Creek site. Due to the fact that Nickel was removed from EPA Primary Drinking Water Standards in 1995, a comparison was made to the maximum concentration level (MCL) listed prior to that time and the oral RFD listed in IRIS in an attempt to show relative risk for ingested nickel. Exposures were assumed to be chronic over a 75 year life span. The primary health effect associated with Radium and Uranium is from radioisotope exposure and the resulting potential for cancer although it is commonly accepted that the primary health effect of Uranium ingestion is chemical toxicity to the kidney.

The EPA assumes that there is essentially no level of exposure to a chemical that does not pose a finite possibility, no matter how small, of generating a carcinogenic response. In evaluating carcinogenic effects, no threshold value can be assumed. The EPA uses a two part evaluation in which the substance is first assigned a weight of evidence classification defined by the EPA as a plausible upper-bound estimate of the probability of a response per unit intake of a chemical over a lifetime. Following this, a slope factor is calculated. This value is multiplied by the chronic daily intake of the chemical to produce an estimate of probability of an individual developing cancer due to exposure to that chemical.

Exposure to radioisotopes requires that the slope factor is multiplied by the chronic daily intake over the life span of the individual. These calculations were carried out for Nickel, Radium and Uranium. Slope factors and weight-of-evidence classifications for these constituents are included in Table 1.3.1.

**Table 1.3.1 Toxicity Values for Hazardous Constituents**

<b>Hazardous Constituent</b>	<b>Uranium-238+D</b>	<b>Radium-226+D</b>	<b>Radium-228</b>	<b>Nickel</b>
Oral Slope Factor	8.71E-11 (risk/pCi)	3.86E-10 (risk/pCi)	1.04E-9 (risk/pCi)	8.4E-1 (mg/kg-day)-1
Weight of Evidence	Carcinogen per EPA	Carcinogen per EPA	Carcinogen per EPA	non-stochastic
Chronic Oral RfD (mg/kg-day)	None	None	None	2E-2
Uncertainty Factor	None	None	None	300
Reference	FGR No.13	FGR No. 13	FGR No. 13	EPA lifetime HA 2011
Target Organ System	Skeletal system	Skeletal system	Skeletal system	Whole body, major organs

There are inherent uncertainties in the toxicity data used to assess risk in this and any other evaluation. For instance, using dose-response information from effects observed at high doses to predict the health effects that may occur following exposure to the low levels of hazardous constituent Concentrations introduces uncertainties. Similarly, using animal studies to predict human response and the use of short-term studies to predict the effects of a lifetime exposure add to the uncertainties.

Experimental studies of animal populations coupled with studies of healthy human populations are used to predict the response likely to be observed in a population consisting of individuals with a wide range of sensitivities.

Uncertainty factors which may overestimate potential risk, and are used to calculate risk, are presented along with toxicity values in Table 1.3.1. These values give an indication of the confidence in experimental data used to determine the associated risk. The greater the uncertainty factor, the greater the uncertainty associated with the experimental data.

## **1.4 Exposure Pathways**

This assessment considered risk to future populations at a POE in the Northern flow path and a POE in the Lang Draw flow path. Ground water within the range for Nickel, Radium, and Uranium concentrations predicted to be present at these points were assumed to be utilized by humans. The exposure matrix assumed that water at the POEs would be a drinking water source and would nourish consumable food products.

Intake of hazardous constituents as a result of exposure to contaminated soils was not considered, as there are no contaminated soils at the BCUC site because the site has been reclaimed. Similarly, dermal and inhalation exposure were not considered a probable exposure pathway and not included in the assessment.

## **1.5 Ground Water Concentrations**

The concentrations of nickel, radium, and uranium that are predicted to occur in the Northern and Lang Draw flow paths were used in this risk assessment. The POE locations are established at the down gradient edge of the land mass that will accompany an amendment application for a general license. Consequently, this land mass is the minimal amount of land that is necessary to assure long term control of the reclaimed byproduct materials. Additional information on the predictive modeling is contained in the modeling summary.

The values for nickel, radium, and uranium that were utilized were predicted to reach their maximums at times in the future varying from 18 to 44 years, from the time that the CAP was terminated. Information for the concentrations of hazardous constituents and the years to attain these concentrations are shown in Table 1.5.1.



**Table 1.5.1 Hazardous Constituent Concentrations at the POE Locations**

Hazardous Constituent	Lang Draw Max. Conc.	Lang Draw Year of Max. Conc.	Northern Flow Path Max. Conc.	Northern Flow Path Year of Max. Conc.	EPA MCL @ POE	Background Standard
Nickel	0.032 mg/l	2015	0.034 mg/l	2039	0.10 mg/l	0.05 mg/l
Ra-226 + Ra-228	2.1 pCi/l	2015	5.8 pCi/l	2040	5 pCi/l	9.7 pCi/l
Uranium	166 pCi/l*	2015	75.0 pCi/l	2032	20 pCi/l	98.7 pCi/l

\* The value for uranium was the average of the model projected curve which is used as the chronic exposure for 75 years.

The values for nickel, radium, and uranium shown in Table 1.5.1 represent the levels that risk was assessed for and represent the entire range of hazardous constituents that are predicted to occur. The risk for nickel was assessed for the background concentration of 0.050 mg/l as well as the predicted maximum concentrations of: 0.034 mg/l and 0.032 mg/l; 0.10 mg/l, which was the previous MCL; and the listed RFD to demonstrate the relative incremental risk associated with these concentrations in nickel. Similarly, the background concentrations of radium and uranium, the recommended MCL concentrations, and the predicted concentrations at the POE's were assessed for relative risk. The entire range of values was evaluated in the Northern and Lang Draw flow paths.

## **1.6 Future Land Use**

Although no exposed populations currently exist within four miles of the BCUC site and none are predicted to be in the area in the future, residential land use was considered in the risk assessment. Lesser exposure scenarios would have resulted in no exposed populations. Although this is the likely scenario it is inconsistent with the ACL guidance document. Exposure pathways considered for future populations include ingestion of contaminated ground water and consumption of vegetables using contaminated ground water for irrigation. Table 1.6.1 summarizes the potential for exposure to future residents across the routes of exposure.

**Table 1.6.1 Potentially Exposed Populations and Exposure Routes**

Potentially Exposed Population	Exposure Route, Medium, and Exposure Point	Pathway Selected for Evaluation?	Reason for Selection or Exclusion
Residential	Ingestion of contaminated ground water	Yes	Wells developed in the alluvium and the N-sand
Residential	Ingestion of home-grown vegetables	Yes	The site and the surrounding area is in a rural location, increasing the potential for home gardening. The only source of irrigation water is wells developed in the alluvium and the N-sand.
NA	Dermal absorption through bathing	No	According to the EPA, dermal uptake of radionuclides and metals is generally not an important route of uptake (EPA RAGS, 1989).
NA	Inhalation of contaminated dust	No	The soil at the BCUC site is not contaminated. The site has been reclaimed.
NA	Dermal contact with contaminated soil	No	The soil at the BCUC site is not contaminated.
NA	Inhalation of airborne (vapor phase) chemicals	No	There are no volatile hazardous constituents at the BCUC site.
NA	Ingestion of contaminated soils	No	The soil at the BCUC site is not contaminated. The site has been reclaimed

### 1.7 Quantification of Potential Risk

The quantification of risk for nickel utilized standard EPA equations and the methodology as discussed in RAGS, 1989 and HEAST tables. Included in this subsection are explanations of the calculations which were performed for each pathway. The equations that were utilized are shown below. EPA FGR No. 13 was used for radionuclides.



Intake of nickel by ingestion of ground water was calculated by using the following equation:

$$\text{Intake (mg/kg-day)} = \frac{\text{CW} \times \text{IR} \times \text{EF} \times \text{ED}}{\text{BW} \times \text{AT}}$$

Where: CW = Nickel concentration in ground water (mg/l)

IR = Ingestion Rate (liters/day)

EF = Exposure Frequency (days/year)

ED = Exposure Duration (years)

BW = Body Weight (kg)

AT = Average Time (days)

Intake of Nickel due to ingestion of home grown produce irrigated with contaminated ground water was calculated by using the following equation:

$$\text{Intake (mg/kg-day)} = \frac{\text{CW} \times \text{IR} \times \text{FI} \times \text{EF} \times \text{ED}}{\text{BW} \times \text{AT}}$$

Where: CW = Nickel concentration in ground water (mg/kg)

IR = Ingestion Rate (kg/meal)

FI = Fraction ingested from Contaminated Source (unitless)

EF = Exposure Frequency (days/year)

ED = Exposure Duration (years)

BW = Body Weight (kg)

AT = Average Time (days)

For calculation of ingestion of radionuclides, average time (AT) and body weight (BW) were deleted and the resulting intake was multiplied by the dose conversion factor (DCF) in mrem/pCi. The units of intake are therefore discussed in terms of effective dose and expressed as fractions of radiation equivalent man (mrem) over a 75 year time frame and are shown in Table 1.7.1

**Table 1.7.1 Radionuclides Expressed in Terms of Effective Dose**

Hazardous Constituent	Ingestion of groundwater		Ingestion of home grown plants		Ingestion of groundwater	
	Lang Draw flow path	Northern flow path	Lang Draw flow path	Northern flow path	Background	MCL
U-238+D (mrem)	1192	540	2.9	1.4	710	147
Ra-226+D (mrem)	155	422	0.4	1.1	706	364

## 1.8 Risk Characterization

The carcinogenic and non-carcinogenic risk associated with exposure to Nickel, Radium, and Uranium under the residential future land use scenario serve as the characterization for this assessment. Although there is no current indication that the ground water in the Northern flow path and the Lang Draw flow path will be utilized under a residential scenario, this type of use was assumed to take place. This use scenario incorporates the most conservative exposure values; i.e., length of residence, and duration of exposure.

If exposure to Nickel, Radium, and Uranium under this land use scenario demonstrates no significant increase in risk of development of cancer and non-cancer illnesses, then it will be assumed to be the case for all other land use scenarios.

A lifetime exposure of 75 years was used for the calculations. FGR 13 risk coefficients for ingestion of radionuclides in tap water or food are expressed as the probability of radiogenetic cancer morbidity per unit intake, where the intake is averaged over all ages and both genders. The exposure pathways under the residential land use scenario include the ingestion of contaminated ground water and the ingestion of home grown produce irrigated with contaminated ground water. The lifetime intake of potentially hazardous chemicals by residents is summarized in Table 1.8.1

**Table 1.8.1 Lifetime Intake of Hazardous Chemicals**

Hazardous constituent	Ingestion of groundwater		Ingestion of home grown plants		Ingestion of groundwater	
	Lang Draw flow path	Northern flow path	Lang Draw flow path	Northern flow path	background	MCL
U-238 (pCi)	4.4E+6	2.0E+6	11.0E+3	5.0E+3	2.64E+6	0.5E+6
Ra-226 (pCi)	1.24E+5	3.2E+5	3.0E+2	8.0E+2	5.31E+5	2.74E+5
Nickel (mg/kg-day)	1.51E-3	1.57E-3	7.6E-5	7.8E-5	1.4E-3	2.9E-3

The potential risk for residents from the predicted nickel concentrations in the groundwater, is provided by the product of the slope factor and the intake. The potential risk to residents to develop cancer from radium and uranium is determined by the product of the estimated ingested activity in pCi and the slope factor (risk/pCi). The potential risk for residents to develop cancer due to exposure to site contaminants is summarized in Table 1.8.2.

**Table 1.8.2 Carcinogenic Risks to Residents**

Pathway	Hazardous constituent	Resident Risk (unitless)		background	MCL
		Lang Draw flow path	Northern flow path		
Ingestion of groundwater	U-238+D	3.8E-4	1.0E-4	2.3E-4	0.4E-4
Ingestion of groundwater	Ra-226+D	0.4E-4	1.2E-4	2.0E-4	1.0E-4
Ingestion of groundwater	Ni	1.26E-3	1.34E-3	1.18E-3	2.4E-3
Ingestion of home grown produce	U-238+D	9.5E-7	2.6E-7	4.0E-7	1.0E-7
Ingestion of home grown produce	Ra-226+D	1.0E-7	3.0E-7	5.01E-7	2.6E-7
Ingestion of home grown produce	Ni	6.0E-5	6.7E-5	5.9E-6	1.2E-4

Hazard quotients (HQ) for nickel measured at the background well and the POEs are summarized in Table 1.8.3. A Hazard quotient is defined as the ratio of a substance exposure level over a specified time period to a reference dose for that substance derived from a similar exposure period. The ratios are expected to be less than unity (1) for risk to non-stochastic effects.

**Table 1.8.3 Non-carcinogenic Hazard Quotients For Residents**

Pathway	Hazardous constituent	Background	Residents HQ (unitless)	
			Lang Draw flow path	Northern flow path
Ingestion of groundwater based on RFD	Ni	7.1E-2	7.6E-2	7.8E-2
Ingestion of food based on RFD	Ni	3.6E-3	6.5E-3	3.8E-3
Ingestion of ground water based on MCL	Ni	5.0E-1	5.2E-1	5.5E-1
Ingestion of food based on MCL	Ni	2.5E-2	2.6E-2	2.7E-2

An overall assessment of the risk of developing cancer or a non-cancer illness due to exposure to nickel, radium, and uranium was conducted. The assessment utilized the residential land use scenario and combined risks and HQs across all pathways. Summing the risks and HQs over all pathways produces a very conservative representation of the risks.

In order for the estimated cancer risk to fall within EPA guidelines for acceptable risk, the risk from an individual chemical should be less than 1E-6, and the combined cancer risk across all pathways from all chemicals should be less than 1E-4. This differs from the ACL guidance, which allows a 1E-4 risk for any individual constituent.

According to the same EPA guidelines, the risk for contracting a non cancer illness, described by the HQ from an individual chemical and combined for all chemicals across all pathways, should be less than one.

The total risk for residents to develop cancer across an individual pathway is summarized in Table 1.8.4.

**Table 1.8.4 Total Radionuclide Risk of Developing Cancer for Residents**

Pathway	Risk (unitless)			
	Lang Draw flow path	Northern flow path	Background	MCL
<b>Total Risk</b>	4.2E-4	2.2E-4	4.3E-4	1.4E-4

The HQ is obtained by dividing the intake of nickel (units of mg/kg-day) by the RfD for nickel (units of mg/kg-day) and measured levels of Ni in mg/l divided by the lifetime HA MCL. A summary of chronic HQs across each exposure pathway is given in Table 1.8.5.

**Table 1.8.5 Total Nickel Hazard Quotient for Residents**

Pathway	HQ (Unitless)		
	Lang Draw flow path	Northern flow path	Background
<b>Ni HQ RFD-based</b>	8.2E-2	8.2E-2	7.5E-2
<b>Ni HQ MCL-based</b>	5.4E-1	7.8E-1	5.2E-1

The overall risk for individuals residing at the POE locations to develop cancer is within the range of the 1E-4 required by Alternate Concentration Limits for Title II Uranium Mills (ACL) guidance. Including nickel for the potential carcinogenic risk does not appear to be warranted as there is no data to support cancer risk to humans and currently no listed MCL for nickel in the EPA primary or secondary drinking water standards. Nickel concentrations are less than the MCL and the MCL calculated risk is 2.4E-3. Including this in the summation skews the overall risk evaluation.

The calculations indicate that all hazard quotients for nickel are within recommended levels. Therefore, they are not a contributor to the overall risk. The driving factor for risk is the predicted development of cancer due to the presence of radionuclides in the ground water in the Northern and Lang Draw flow paths.



## **1.9 Uncertainties in the Characterization of Risk**

There are many uncertainties inherent in calculating the risk of developing cancer and non-cancer illnesses due to exposure to Nickel, Radium, and Uranium. Included are the site specific uncertainty factors associated with characterizing the physical setting, and determining the fate and transport, as well as toxicity.

The concentrations of Nickel, Radium, and Uranium that are currently in the background water, as well as the concentrations of those constituents predicted to occur at the POE locations, were utilized in the risk assessment.

Utilizing the ground water model introduces levels of uncertainty in the data, particularly extending the time frame of the model to over a hundred years.

Significant site data gaps occur when site specific data is unavailable or unknown. This specifically occurs when estimating the exposure to future populations. For example, when estimating what the exposure to a future resident will be, there are no current residents upon which to base the estimates of exposure parameters; therefore, the EPA recommended values have been used to estimate exposure to residents. When several options are available, the most conservative value was utilized.

A certain amount of uncertainty exists with the slope values and reference doses that were used in the calculation of risk. These values were obtained from EPA sources. The references acknowledge the uncertainty associated with the lack of human or animal data and the extrapolation that is necessary. The uncertainty factors generally overestimate the calculated risk.

## **2.0 Conclusions**

The EPA RAGS methodology, HEAST tables, and EPA January 2011 Edition of the Drinking Water Standards and Health Advisories were implemented in the risk assessment for nickel. The Federal Guidance Report No. 13 was used to estimate risk and dose for radionuclides. The objective of this procedure was to assess the degree of risk associated with the possibility of future residential land use at the POE locations.

The assessment assumed that the maximum predicted concentrations would be realized at the POE locations. The exposure routes included ingestion of contaminated ground water and ingestion of home grown vegetables or produce irrigated with contaminated ground water.

Under a residential land use scenario, the overall risk across all pathways for residents to develop cancer was evaluated at the POE locations. The risk is within the  $1\text{E-}4$  order of magnitude for cumulative pathways for radionuclides.

Although the nickel calculated risk were higher than those observed in the radionuclide constituents, they were within the same order of magnitude as the hazard quotients for nickel found in the background well and less than the risk for the remanded EPA MCL for nickel.

The predicted concentrations of uranium and radium in the ground water will cause a minimal increase in the acceptable risk of cancer to future residents from the ingestion of ground water. Risks of developing cancer from ingesting ground water and eating produce irrigated with water containing uranium are  $2.2\text{E-}4$  and  $4.2\text{E-}4$  in the Northern flow path and the Lang Draw flow path respectively. These risks are within acceptable ACL guidance levels.

The exposure estimates for the exposure pathways were determined by using the most conservative values recommended by the EPA. They represent the worst case scenario and overestimate the potential exposure, i.e. the nickel drinking water equivalent level of  $0.7\text{ mg/l}$  listed in EPA's 2011 Edition of the Drinking Water Standards and Health Advisories which is defined as: "A lifetime exposure concentration protective of adverse, non-cancer health effect, which assumes that all of the exposure to a contaminant is from drinking water." That level is seven times higher than the one used here to estimate potential risk from nickel.

- DOE's Title I Spook site is located on the Dry Fork of the Cheyenne River about 2 miles south of the Bear Creek Uranium site. The Spook work plan concluded that groundwater monitoring was not required because there is no apparent risk to human health and the environment because there are no known exposure pathways for contaminated ground water from the uppermost aquifer to lower aquifers or the surface. No one is using the ground water from this aquifer for any purpose and there is no discharge of ground water from the uppermost aquifer to the surface or to surface water. This conclusion is also true for the Bear Creek site. The groundwater in this shallow formation should qualify for supplemental standards according to criterion cited in EPA 40 CFR 192.21.

By this letter we formally request that NRC amend Bear Creek's Source Material License No. SUA-1310 to delete License Condition 47 and proceed with termination of the license and transfer of the General License to DOE.

Should you have any questions or comments, please contact me.

Sincerely



Harry Nagel  
Manager Minerals  
832.636.2732  
harry.nagel@anadarko.com



**RE-EVALUATION OF METALS TRANSPORT AT BEAR CREEK URANIUM  
CONVERSE COUNTY, WYOMING**

October 13, 2011

***Prepared for:***

Anadarko Petroleum Corporation  
1201 Lake Robbins Drive  
The Woodlands, Texas 77380

Attention: Harry Nagel

***Prepared by:***

Tetra Tech GEO  
363 Centennial Parkway, Suite 210  
Louisville, Colorado 80027



**TETRA TECH GEO**

## TABLE OF CONTENTS

1.0 Introduction.....	1
1.1 Objectives and Approach.....	2
1.2 Site Description.....	3
2.0 Groundwater System.....	3
2.1 Geology of the Site .....	3
2.2 Site Hydrogeology .....	4
2.2.1 Groundwater Flow Paths.....	4
2.2.2 Temporal changes in water levels.....	4
2.3 Groundwater Chemistry.....	5
2.3.1 Uranium .....	6
2.3.2 Sulfate .....	7
2.3.3 Chloride.....	7
2.3.4 pH.....	8
2.3.5 Radium.....	8
2.3.6 Nickel.....	9
2.4 Site Geochemistry.....	9
2.4.1 Geochemical speciation results.....	9
3.0 Updated predictive transport modeling.....	11
3.1 Model construction and calibration .....	12
3.2 Model Results .....	13
3.2.1 Lang Draw .....	13
3.2.2 Northern Pathway .....	16
4.0 Conclusions.....	18
5.0 References.....	19

## FIGURES

Figure 1	Location of the Bear Creek, Wyoming Disposal Site, Converse County
Figure 2	Aerial Photograph of the Disposal Site
Figure 3	Saturated Thickness of the N sand, June 1986
Figure 4	Saturated Thickness of the N sand, March 1996
Figure 5	Saturated Thickness of the N sand, February 2011
Figure 6	Water Level Elevations, June 1986
Figure 7	Water Level Elevations, June 1986
Figure 8	Water Level Elevations, June 1986
Figure 9	Measured Water Level Elevations, 1981 to 2011
Figure 10	A. Distribution of Uranium Concentrations, February 2011 B. Temporal Changes in Uranium Concentrations, Lang Draw C. Temporal Changes in Uranium Concentrations, Northern Pathway
Figure 11	A. Distribution of Sulfate Concentrations, February 2011 B. Temporal Changes in Sulfate Concentrations, Lang Draw C. Temporal Changes in Sulfate Concentrations, Northern Pathway
Figure 12	A. Distribution of Chloride Concentrations, February 2011 B. Temporal Changes in Chloride Concentrations, Lang Draw

- Figure 13 C. Temporal Changes in Chloride Concentrations, Northern Pathway  
A. Distribution of pH, February 2011  
B. Temporal Changes in pH, Lang Draw  
C. Temporal Changes in pH, Northern Pathway
- Figure 14 A. Distribution of Radium Concentrations, February 2011  
B. Temporal Changes in Radium Concentrations, Lang Draw  
C. Temporal Changes in Radium Concentrations, Northern Pathway
- Figure 15 A. Distribution of Nickel Concentrations, February 2011  
B. Temporal Changes in Nickel Concentrations, Lang Draw  
C. Temporal Changes in Nickel Concentrations, Northern Pathway
- Figure 16 Simulated initial values along Lang Draw  
A. Uranium  
B. Sulfate  
C. Chloride  
D. pH  
E. Radium  
F. Nickel
- Figure 17 Simulated breakthrough along Lang Draw  
A. Uranium  
B. Sulfate  
C. Chloride  
D. pH  
E. Radium  
F. Nickel
- Figure 18 Predicted breakthrough along Lang Draw  
A. Uranium  
B. Sulfate  
C. Chloride  
D. pH  
E. Radium  
F. Nickel
- Figure 19 Simulated initial values along Northern Pathway  
A. Uranium  
B. Sulfate  
C. Chloride  
D. pH  
E. Radium  
F. Nickel
- Figure 20 Simulated breakthrough along Northern Pathway  
A. Uranium  
B. Sulfate  
C. Chloride  
D. pH  
E. Radium  
F. Nickel
- Figure 21 Predicted breakthrough along Northern Pathway  
A. Uranium  
B. Sulfate

C. Chloride  
D. pH  
E. Radium  
F. Nickel

## **TABLES**

Table 1	Results of monitoring wells samples, February 10 through February 12, 2011
Table 2	Saturation indices for water samples on Lang Draw Flow path, 2011
Table 3	Saturation indices for water samples on Northern Pathway, 2011

## **ATTACHMENTS**

- I. Temporal plots of chemical parameters measured in monitoring wells
- II. Input PHREEQC data set for Lang Draw
- III. Input PHREEQC data set for Northern Pathway
- IV. Modifications to the Thermodynamic Database for Uranium and Radium

# **Re-evaluation of Metals Transport at Bear Creek Uranium Converse County, Wyoming**

## **1.0 Introduction**

The former Bear Creek Uranium Mine and milling operations are located in Converse County, Wyoming (Figure 1). Tailings were placed in an impoundment formed by a dam constructed across Lang Draw, west of the former mill. The milling operation was shut down in 1986, beginning a period of reclamation for the tailings impoundment.

A groundwater recovery system was operated beneath and downgradient of the tailings impoundment. Recovered water was pumped into the impoundment and allowed to evaporate. Later evaporation occurred within clay-lined impoundments, which had been constructed on top of the tailings.

In 1995, GeoTrans, Inc. (now called Tetra Tech GEO) performed a geochemical evaluation (GeoTrans, Inc., 1995) of the future transport of uranium, radium, and nickel, based on chemical conditions that existed at that time. An important consideration at that time was prediction of the neutralization of acidic water found beneath and a short distance downgradient of the tailings impoundment as the water moved downgradient through alluvium and rock that contained calcite. Measurements of the acidity of the water and the neutralization capacity of the alluvium and rock were made, and calculations indicated that the movement of low pH water would be slower than the movement of the water because of the neutralization reactions. For Lang Draw, the 1995 study estimated that the retardation factor of the pH front would be approximately 10 for the area upgradient of the seepage control dam, and approximately 15 for the area downgradient of it. The study also found that the concentrations of metals As, Be, Cd, Cl, Th, and Ra all decreased sharply as the pH increased above approximately 4.5, as did the concentrations of Fe and Al. This behavior was interpreted as being indicative of coprecipitation of the former list of metals with iron and aluminum hydroxides. During the 1995 modeling effort, GeoTrans used MINTEQA2 (Allison et al, 1991) to perform the geochemical speciation modeling to estimate retardation coefficients of uranium and nickel, and other laboratory measurements for Ra and Th. These values indicated that the metals would move more quickly than the pH front, and therefore one-dimensional transport models using linear sorption theory were prepared to predict future movement. Predictions of peak uranium concentrations at the property line at that time (near MW-14) were between approximately 50 and 70 pCi/L, depending on the amount of dilution from convergent flow into Lang Draw, with the peak occurring approximately 80 years after 1995, or in 2075. Nickel was estimated to travel more slowly, with the peak concentration ranging between approximately 0.05 and 0.85 mg/L in about 2250. These modeling predictions were used in an application to set Alternate Concentrations Limits (ACLs) in 1997. The ACLs for U, Ra, and Ni were set at 2038 pCi/L, 46 pCi/L, and 3.8 mg/L, respectively, with the points of compliance established at MW-12 for Lang Draw and MW-74 for the northern flow path. These ACLs were based on the model results indicating that concentrations at the point of exposure wells for U, Ra, and Ni would be 45 pCi/L, 13 pCi/L, and 0.55 mg/L, respectively.

In the interim, the recovery well system was shut down in 1996, and all wells not to be used for monitoring were plugged and abandoned. A cover was placed over the tailings, and additional grading was performed to control surface-water flow.

Five wells along Lang Draw (MW-12, MW-9, MW-14, MW-108, and MW-109), and 4 wells along the “northern pathway” (MW-74, MW-43, MW-110, and MW-111) have been monitored. No other monitoring wells exist for monitoring.

In reviewing the monitoring data in preparation to the transfer of the site to the DOE for long-term care and surveillance, the NRC recently compared the monitoring data with the predictions from the modeling work done in 1995, and noticed that uranium concentrations in MW-14 had reached values of 520 pCi/L. As a result, the NRC requested that Anadarko Petroleum Corporation, current owner of Bear Creek Uranium, submit a revised ACL application. Anadarko has requested that Tetra Tech GEO, using the newer information collected since the cessation of the recovery well pumping, reevaluate the transport of the radionuclides and metals in support of a new ACL application.

### ***1.1 Objectives and Approach***

This re-evaluation of transport is being done to improve the prediction capability of the transport modeling, using information collected over the sixteen-year period since the last predictions were made. This work involves several steps:

- a) Collect additional water samples from available monitoring points for analysis of parameters important to understanding geochemical controls on metals transport. The standard suite of analytes includes the trace metals and radionuclides of interest, and limited geochemical parameters (sulfate, chloride, and pH). The additional sampling added other parameters such as major anions and cations, iron, manganese, phosphate, and silica.
- b) Evaluate water-level data to determine if flow directions have changed significantly from when the recovery wells were still pumping and the tailings were draining more rapidly than today.
- c) Evaluate the areal distribution of and the temporal changes in water chemistry parameters, to understand if there are changes in water chemistry that affect the transport of the radionuclides and metals.
- d) Perform geochemical speciation modeling, to determine whether there are changes in chemical behavior that have occurred over the last sixteen years.
- e) Re-evaluate the transport modeling that was done in 1995 to develop an understanding of why it underpredicted the transport of uranium.
- f) Develop an improved transport model calibrated against more recent information, and predict future movement of the parameters of interest. The model that was used is PHREEQC (Parkhurst and Appelo, 1999), which has the capability of performing one-dimensional transport calculations considering the chemistry of the water in the system and the chemical reactions that occur in the water and between the water and the soil and rock.

## ***1.2 Site Description***

As shown on Figure 2, the site currently consists of the following major features:

- A tailings impoundment with a riprap-armored tailings embankment (dam) on the northwest (downgradient) side;
- Diversion channels to direct runoff around the tailings impoundment; and
- A smaller dam for seepage control located in Lang Draw about 600 feet northwest of the main dam.

The site is about 8500 feet from north to south, with the tailings impoundment approximately in the center. Thus, the downgradient (northern) site boundary is between 2600 and 2900 feet from the tailings impoundment. The former uranium mine is located about 850 feet east of the tailings impoundment but is not considered to be part of the site.

Surface drainage is generally toward the north. Lang Draw emerges from the base of the impoundment and heads north to the property boundary, and an unnamed draw begins northeast of the impoundment and heads northwest toward the property boundary. These two draws continue off the property and ultimately join some distance north of the property boundary.

## **2.0 Groundwater System**

Information about the groundwater system consists of observations of the geology, hydrogeology, and geochemistry observed at the site. Much of the basic information used during the current model update was presented in the previous modeling report, and only the most relevant portions are repeated below. Since the modeling report was generated in 1995, a number of water level and groundwater quality data collection events have occurred. Trends will be discussed where appropriate, and the most recent data set (collected in February 2011) will be presented.

### ***2.1 Geology of the Site***

The tailings basin is underlain by sandstone, shales, and lignites of the Wasatch Formation. The uppermost sandstones have been named the K and N sands. The depositional environment appears to have been one of rivers carrying fine- to coarse-grained materials in a coastal or deltaic plain setting. The numerous shale deposits indicate that the river gradient was low. The massive thickness of the K sand suggests that it may have been deposited by a meandering river of moderate size. The underlying N sand is less consistent and of variable thickness. Drill hole information shows that it changes from a small channel sand into several sands splaying out into an overbank environment. Laterally continuous lignites and coals are present, and further suggest a meandering river through a low gradient wet overbank environment.

The K and N sands crop out within and underlie the tailings basin. The K sand is the upper sandstone and is exposed at the surface and on the sides of Lang Draw. In some places, the K sand has been eroded away. Within Lang Draw, the K sand has been eroded and replaced by up to 20 to 40 feet of alluvial sand, silt, and clay deposits. The K sand is separated from the N sand by a claystone that varies in thickness between 5 and 50 feet. The N sand tends to be thicker to the northeast near the unnamed draw than toward Lang Draw (S.M. Stoller, 1997) and dips to the



east north east. The N sand outcrops in Lang Draw north of MW-108, and in the unnamed draw about 500 feet northwest of MW-111.

## **2.2 Site Hydrogeology**

The site hydrogeology will be discussed in two parts: groundwater flow paths and individual well hydrographs showing changes over time.

### **2.2.1 Groundwater Flow Paths**

The primary focus of this report is on flow occurring in the N sand, since that is the permeable unit in which groundwater contamination has been found to occur. Saturated thickness maps have been prepared for the N sand based on the June 1986, March 1996, and February 2011 groundwater elevation data sets. These maps are provided as Figures 3 to 5. In addition, Figures 6 to 8 illustrate the potentiometric surface maps from the same time frames. The potentiometric surface and saturated thickness maps illustrate the two groundwater flow paths present at the site: the Lang Draw and Northern flow paths.

Water level data have consistently indicated a convergence of flow toward Lang Draw. The N sand is normally unsaturated on the east side of Lang Draw (see Figures 3 to 5), creating an area of decreased permeability. Coupled with the higher permeability of the alluvial sediments, there is a tendency for groundwater contour lines to indicate a strong flow component toward Lang Draw. East of Lang Draw (for example, near MW-74), flow appears to be toward the unnamed draw. Water-level data collected prior to installation of the groundwater recovery well system showed a flow pattern whereby groundwater east of the tailings dam had a northerly flow direction (GeoTrans, 1995, Figure 2-4). Recently, there are fewer wells for constraining the water-level elevation contour lines, but it does not appear that the presence of two separate flow paths has changed between 1986, 1996, and 2011.

The flow path along Lang Draw measures approximately 2700 feet from the tailings impoundment to the site boundary. The northern flow path measures approximately 3700 feet from the tailings impoundment to the site boundary along the unnamed draw in which MW-111 is installed. The gradients along these paths appear to have changed over time, likely due to the startup, then cessation, of the recovery pumping system.

### **2.2.2 Temporal changes in water levels**

In discussing the temporal changes observed in water levels at the site, two events are important to consider. First, in 1986, a seepage recovery system using pumping wells was initiated downgradient of the tailings impoundment to intercept seepage and reapply it to the tailings impoundment for evaporation. Second, in 1996, the seepage recovery system was terminated (pumping ceased). These two events had an effect on water levels observed in a number of site wells.

Figure 9 shows the changes in water-level elevations through time for selected wells. Some of these wells are part of the current monitoring program (MW-9, -12, -14, -43, and -74). In addition, since some of the current wells were installed after major site changes occurred, some historical wells that have since been abandoned are included on Figure 9 (MW-22, -40, -41, and -42). There are two groups of data that are immediately apparent. The group with the higher elevations was measured in monitoring wells east of Lang Draw, and these wells will be called



the upland group. They are, generally speaking, located between the Lang Draw and the unnamed draw. The group with the lower groundwater elevations includes the wells along Lang Draw. Also noticeable on Figure 9 is the decline in water levels that began in about March of 1989. Recovery pumping had begun in 1986, and there was not a significant increase in pumping rate in the spring of 1989. The noticeable decrease in water levels that occurred in the upland group in 1989 may have been caused by redistribution of pumping. The rate of pumping from the recovery system was reduced in 1994 (and was turned off in 1996), and water levels began to recover.

MW-43 is an upland well that has been monitored during the entire period from the early 1980's to 2011. Water levels in this well were approximately 5098 ft when its record began in the early 1980's. Water levels rose and reached a peak in 1987. From the early 1980's until 1987, MW-43 was probably responding to rising levels in the tailings impoundment. With the beginning of recovery pumping, water levels began to decline, and continued to decline until 1994 when the recovery pumping decreased. Water levels then recovered until about 2000, when a period of declining levels began. The decline in water levels since 2000 is attributed to the reduction in seepage from the tailings as they dewatered in response to construction of a cover, which reduced the recharge rate. This trend of declining water levels will likely continue for several more years.

Another well shown on Figure 9 is MW-14, which is located along Lang Draw. While its behavior is similar to MW-43 with respect to the larger changes, its early behavior is somewhat different. When water levels were rising at the beginning of the record for MW-43, those in MW-14 were declining for a short period before beginning to rise. This different behavior is probably caused by the greater distance between MW-14 and the rising water levels in the tailings, and the greater isolation provided by the cut-off wall and recovery dam. With cessation of the operation of the recovery system, water levels increased in MW-14, but to higher levels than were present before recovery pumping began.

In summary, the cessation of the pumping in the recovery well system caused water levels to increase, and a change in the flow directions as the cones of depressions of the recovery wells dissipated. Water levels are now declining, assumed to be related to continued reduction in the rate of seepage from the tailings impoundment, and hydraulic gradients are decreasing.

### ***2.3 Groundwater Chemistry***

Since 1995, a number of groundwater sampling events have been completed. The most recent groundwater sampling event included wells MW-9, -12, -14, -43R, -74, -108, -109, -110, and -111. The analytes for each location are provided in Table 1. The following sub-sections discuss the February 2011 concentration data and provide a brief analysis of apparent trends, if any, observed in the data over time. The data are plotted on Figures 10 to 15. In each series, the "A" figure is a map illustrating the February 2011 concentrations, the "B" figure shows the historical data for the Lang Draw flow path, and the "C" figure shows the historical data along the Northern flow path.

Temporal plots separated by well and analyte are provided as Attachment I.

Predictions for beryllium, cadmium, chromium, molybdenum, and thorium-230 were not made because the concentrations of these parameters have remained below or very near their detection limits since the recovery system was turned off. GeoTrans (1995) found that concentrations of

Be and Cd have a strong dependence with pH, with very low concentrations at pH greater than 5. Molybdenum showed a similar dependence. The concentrations of beryllium, cadmium, and molybdenum measured since 1994 were reported by DOE to be less than the detection limit, or appeared to be less than the detection limit (based on the reported value and the reporting of identical values for MW-12 and MW-74). Chromium has been detected at concentrations as high as 0.04 mg/L, but concentrations have been typically less than 0.01 mg/L and were less than 0.001 mg/L when sampled in February 2011. Thus, these metals are not believed to be mobile under the current conditions, and the modeling, which will be discussed below, indicates that pH is unlikely to decrease below approximately 6.2, and will increase after the pH front moves through.

Thorium-230 could not be modeled because thermodynamic data were not available in the PHREEQC database. However, thorium should not be mobile under conditions of near-neutral pH. The sampling data demonstrate this. In the current monitoring wells, reported thorium-230 values have been low. The three highest reported values since the recovery system was turned off were 1.4 and 1 pCi/L in MW-43R in 1995 and 1996, and 1.1 pCi/L in MW-9 in 1996. In contrast, samples from TS-5 (pH 3.7) were as high as 14,000 pCi/L and MW-77 (pH 4.2 to 4.6) (downgradient of the tailings dam) had values as high as 31 pCi/L. Both of these sampling locations were characterized with low pH. Increasing the pH to above 6 has reduced the concentration of thorium-230 significantly. As a result, the higher values that were observed in the low pH waters are not expected to occur even in the upgradient monitoring wells, based on currently available measurements and the modeling predictions.

Most of the thorium-230 values that are reported in the DOE database are believed to be at or below the detection limits. Thorium-230 values are determined through counting. Most of the values reported in the DOE database are reported without information on the counting statistics. Where the counting statistics are provided, the detection limit is either at or greater than the reported value, suggesting that the concentration of thorium-230 for the samples without reported counting statistics or detection limits was at or below the detection limit. For samples collected from MW-74, MW-108, and MW-110 in July 2009, the reported values and detection limit were all 0.66 pCi/L. For these samples, the U flag was provided, but for most other sampling dates, the reported values were lower but no U flag was entered. Thus, the plots of thorium concentrations in Attachment I are believed to indicate the detection limits for the period after operation of the recovery system.

### 2.3.1 Uranium

Figure 10A provides a map of the February 2011 uranium concentrations. Uranium ranged from 1.6 pCi/L in MW-110 to 439 pCi/L in MW-14. The wells monitored are located along the Lang Draw and Northern flow paths.

**Lang Draw Path:** As indicated by Figure 10B, both MW-12 and MW-14 were increasing in concentration until late 1986, when the groundwater recovery system was started. Then, both wells experienced decreases in concentration, although there was a lag of a couple years between start of pumping and when concentrations began to decrease. Decreasing concentrations continued until 1994, when the groundwater recovery ceased. After that point, MW-12 and MW-14 both increased significantly in uranium concentration. The concentrations in MW-12

near the south end of the Lang Draw, nearest to the tailings impoundment, peaked after the groundwater recovery system was shut down in 1994, but are now decreasing. Similarly, concentrations at MW-14, located about 500 feet north of MW-12, peaked about two years ago and now appear to be decreasing. Concentrations at MW-108 are fairly stable, but concentrations at MW-109 are slightly increasing. This is because the peak has passed MW-12 and likely MW-14, and is moving northward in the direction of groundwater flow. Concentrations at MW-108 and MW-109 would therefore be expected to increase somewhat over the next few years, then decrease. It is noteworthy that MW-14 seems to have peaked at a concentration about 30% lower than was observed in MW-12. This would indicate that some natural attenuation or dilution is occurring along the Lang Draw flow path. Therefore, peaks observed at MW-108 and MW-109 would be expected to be significantly less than that observed at MW-14.

**Northern Path:** Figure 10C illustrates that peak concentrations have already passed MW-74 and MW-43. Concentrations at MW-110 and MW-111 appear to be fairly stable. As a result, it is not clear whether peak concentrations will actually reach MW-110 and MW-111. The highest concentrations observed along this flow path were prior to the shutdown of the groundwater recovery system in 1994. In addition, due to geologic and spatial heterogeneity, it appears that not all wells on this flow path are located in the plume center.

### 2.3.2 Sulfate

Figure 11A provides a map of the February 2011 sulfate concentrations. Overall, the sulfate concentrations ranged from 1190 mg/L in MW-111 to 2810 mg/L in MW-12 during the sampling event. The sulfate concentrations near the tailings impoundment are, in general, noticeably higher than the sulfate concentrations further downgradient.

**Lang Draw Path:** As indicated by Figure 11B, the sulfate concentrations have generally increased over time in wells MW-12 and MW-14, although they briefly decreased during the operation of the groundwater recovery system. The current sulfate concentrations in wells MW-12 and MW-14 continue to represent an increase over previous sampling events. The concentrations in well MW-9 began to increase after the shutdown of the groundwater recovery system in 1994. Wells MW-108 and MW-109 have had fairly constant sulfate concentrations since they were installed.

**Northern Path:** Figure 11C shows that sulfate concentrations in MW-43 increased steadily until at least the late 1990's, but have recently decreased. In addition, MW-74 has experienced increases in sulfate concentrations since the groundwater recovery system was shut down in 1994. Well MW-74 seems somewhat slower to reach its peak concentration than MW-43; possibly it is not located in the center of the plume due to geologic heterogeneity. Sampling in wells MW-110 and MW-111 since 2002 has indicated that sulfate concentrations are increasing in MW-111 but stable in MW-110.

### 2.3.3 Chloride

Figure 12A provides a map of the February 2011 chloride concentrations. Overall, the chloride concentrations ranged from 89 mg/L in MW-109 to 371 mg/L in MW-12 during the sampling event.

**Lang Draw Path:** Figure 12A shows that chloride concentrations decrease along the Lang Draw flow path from MW-12 (371 mg/L, nearest the tailings impoundment) to MW-14 (358 mg/L), MW-108 (302 mg/L), and MW-109 (89 mg/L). Concentrations in well MW-9 (334 mg/L) are also elevated, indicating that downward migration has occurred into this deeper-screened well. As indicated by Figure 12B, the chloride concentrations in MW-12 were increasing until the groundwater recovery system was implemented in 1986; after that, concentrations decreased until after the pumping ceased in 1994. Recent sampling events indicate that concentrations of chloride in well MW-12 have risen again. Chloride concentrations in well MW-14 seem to follow the same general pattern as in well MW-12, but delayed by about 5 years such that the decreases due to pumping are first seen in after 1991. Recent sampling shows that chloride concentrations in this well have increased since pumping ceased. Wells MW-108 and MW-109 have experienced steady increases since sampling began in 2002. Well MW-9 has experienced chloride concentration increases since about 1995, after the groundwater recovery system was shut down.

**Northern Path:** Figure 12A shows that MW-110 has the highest concentration (290 mg/L) and MW-111 has the lowest concentration (102 mg/L). Therefore, there is not a consistent decrease in chloride concentrations between the tailings impoundment and MW-111; this is likely due to some wells along this flow path not being located along the plume centerline as a result of geologic heterogeneity. As shown by Figure 12C, chloride concentrations in MW-43 increased steadily until reaching a peak in about 1994, and have since decreased. Chloride concentrations in well MW-110 have been on a decreasing trend since sampling began in 2002. Well MW-111 experienced some initial increase in chloride concentrations but has since been fairly stable.

#### 2.3.4 pH

Figure 13A provides a map of the pH measured during the February 2011 sampling event. The measured pH ranged from 6.56 in MW-12 to 7.6 in MW-111 during the sampling event. These are all near neutral pH values and therefore do not indicate a significant low-pH plume emanating from the tailings impoundment.

**Lang Draw Path:** As indicated by Figure 13B, pH values along the Lang Draw flow path decreased slightly after the shutdown of the groundwater recovery system in 1994. The current sampling event seems to indicate a slight increase in most of the pH values; this potential new trend will continue to be monitored during future sampling events.

**Northern Path:** Figure 13C shows the pH values along the Northern flow path. Few monitoring points were available for this flow path prior to 2002. However, available data seem to indicate that a small decrease in pH may have occurred on the Northern flow path after the recovery system shutdown in 1994, though there seems to have been a lag of several years. The current sampling event appears to represent an increase in pH for most wells, but again, this potential trend will continue to be monitored during upcoming sampling events.

#### 2.3.5 Radium

Figure 14A provides a map of the February 2011 combined radium-226 and radium-228 concentrations. The combined radium concentrations range from 0.9 pCi/L in well MW-9 to 10.5 pCi/L in MW-110.

**Lang Draw Path:** As indicated by Figure 14B, wells MW-12, MW-14, and MW-9 were increasing in concentration during the 1980's, and peaked after the start of pumping in 1986. Once the effects of pumping began to decrease concentrations in the late 1980's, concentrations have decreased fairly steadily over time. The highest concentration of radium in the Lang Draw flow path is still located at well MW-12 (3.0 pCi/L), though it has decreased significantly since the 1980's. Concentrations of radium in wells MW-108 and MW-109 have experienced slow increases since the wells were installed. These factors indicate that the peak has passed at MW-12 and MW-14, but has not yet reached MW-108 or MW-109.

**Northern Path:** Figure 14C indicates that concentrations are stable in well MW-74, decreasing in MW-43, possibly increasing in MW-110, and stable in MW-111. This pattern indicates that the plume peak has passed MW-74 and MW-43. The overall increasing trend in MW-110 seems to indicate that the peak has not yet passed this location. The low, stable concentrations at MW-111 indicate that the core of the plume has not reached this well.

### 2.3.6 Nickel

Figure 15A provides a map of the February 2011 nickel concentrations. The nickel concentrations range from 0.004 mg/L in well MW-111 to 0.043 mg/L in MW-108.

**Lang Draw Path:** Figure 15A indicates that the highest nickel concentrations on this flow path are near MW-14 and MW-108. Figure 15B shows that these two wells have experienced some increase in concentration over the last few years. Figure 15B also shows that overall concentrations in MW-12 and MW-14 have significantly decreased since the 1980's and 1990's. Nickel concentrations in MW-109 and MW-9 have remained fairly stable since 2002.

**Northern Path:** Figure 15A indicates that concentrations of nickel along the Northern flow path decrease as distance from the tailings impoundment increases, with the highest concentration being 0.042 mg/L in well MW-74. Figure 15C indicates that nickel concentrations in well MW-43 significantly decreased since the 1980's, but have slightly increased in recent years. Nickel concentrations in well MW-74 have increased since 2002, while concentrations in MW-110 and MW-111 have remained fairly stable since the wells were installed.

## 2.4 Site Geochemistry

### 2.4.1 Geochemical speciation results

Aqueous geochemical speciation models are computational tools for improving the understanding of the chemical reactions that occur in water and between constituents in the water and minerals that the water may contact or that may dissolve or precipitate. The models are based on equations that describe chemical reactions, thermodynamic data that collectively define equilibrium conditions, and the assumption that aqueous reactions are at equilibrium but reactions between the aqueous species and minerals may not be. These models are particularly useful for providing an understanding of the effects of reactions on chemical behavior of the water, and for predicting changes in water chemistry that may occur if conditions change. Changes can occur by many mechanisms, such as mixing of waters of different chemistry, and dissolution or precipitation of minerals.

One of the output parameters from a geochemical speciation model is known as the saturation index, or SI, that provides information on the state of saturation of minerals given the chemistry

of the water. Although complicated to calculate, the SI has a value of 0.0 when the water appears to be in equilibrium with a mineral. When the SI is 0, the mineral will neither precipitate nor dissolve unless conditions change. A value of SI greater than zero indicates that the water is supersaturated with respect to the mineral, and the mineral would have a tendency to precipitate. Conversely, a negative value for SI indicates that the mineral would have a tendency to dissolve, if it is present. Quite commonly, the chemical reactions do not occur rapidly enough for the water to be in equilibrium with the mineral. However, some minerals can dissolve or precipitate quite rapidly and exert controls on the chemistry of the water. Examples include the dissolution and precipitation of calcite, gypsum, and ferrihydrite, three minerals that are important in the chemical characteristics of the water in the groundwater system at Bear Creek.

The 1995 speciation model using MINTEQA2 indicated supersaturation with respect to a number of iron, aluminum, and sulfate minerals, with gibbsite, ferrihydrite, and gypsum identified as the most likely to control aqueous phase concentrations. The waters were found to be in equilibrium with calcite and undersaturated with respect to siderite. Four geochemically distinct pH zones were identified ranging from acidic (<3.5 pH) to neutral.

The 2011 speciation model using PHREEQC indicated many of the same conclusions. Low pH water was not observed, indicating that the pH front had not reached any of the monitoring wells, or that the neutralization capacity of the calcite in the rock is sufficiently high to maintain the pHs above 6. pH conditions beneath the impoundment are unknown, and may be acidic. Prior to dewatering of the tailings, the acid flux was great enough to overwhelm the neutralization capacity of the calcite in the soil and rock (i.e., the calcite that had been present in the soil and rock prior to disposal of the acidic tailings had been consumed). Currently, no data are available to indicate whether the influx of upgradient water is sufficient to neutralize any water which is draining or infiltrating through the tailings. As a result, the modeling (to be discussed later) will assume that low pH conditions continue to exist beneath the tailings to provide conservative results.

The water along the Lang Draw pathway is oversaturated with respect to calcite and the CO<sub>2</sub> pressures are greater than atmospheric CO<sub>2</sub> pressure ( $10^{-3.5}$  atmospheres) (Table 2). This indicates that the water has dissolved calcite, resulting in high CO<sub>2</sub> pressures, and is now trying to degas, which will cause precipitation of calcite. The waters are also supersaturated with ferrihydrite (iron hydroxide), indicating that it will tend to precipitate. Because uranium sorbs to ferrihydrite, the precipitation or dissolution of ferrihydrite affects the mobility of uranium. Waters along the flow path are at equilibrium with gypsum, the result of dissolution of calcite by sulfuric acid in the tailings seepage, with resultant precipitation of gypsum. One important outcome of the speciation modeling is that the waters are undersaturated with respect to all of the uranium minerals, and therefore uranium minerals have not been precipitating out of the groundwater. These results were also obtained when speciation modeling was performed using water-chemistry data from the 1980s and 1990s. Therefore, re-dissolution of uranium minerals is not expected. This result is expected, as the intent of the milling process is to mobilize the uranium from the ore, and remove it. Thus, the chemistry of the tailings solution does not favor precipitation of uranium bearing minerals for later remobilization. However, as will be seen later, the sorption of uranium onto ferrihydrite, followed by subsequent dissolution of the ferrihydrite as the pH front moves, can result in temporary remobilization.

Speciation modeling along the northern pathway produced similar results (Table 3).

In summary, the geochemical speciation modeling based on the recently collected samples produced the same conclusions as the earlier calculations with respect to mineralogic controls on the water chemistry. The low pH water from the tailings reacted with calcite, which raised the pH but caused gypsum to precipitate. The dissolved iron in the water precipitated as ferrihydrite when the pH increased. The waters have remained supersaturated with respect to ferrihydrite. Although not addressed by the speciation modeling, the uranium tends to sorb to ferrihydrite, which provides an attenuation/retardation mechanism for uranium.

### **3.0 Updated predictive transport modeling**

The model that was developed in 1995 to predict transport of constituents in the water was performed using BIO1D, a one-dimensional transport code that uses linear sorption to simulate retardation. Because the pH front was estimated to move more slowly than other constituents in the water, the model was simulating transport downstream of the lower pH area.  $K_d$  values for uranium and other constituents were based on a combination of geochemical modeling and literature values. Initial concentrations were based on water samples collected as part of that study. The model assumed that water would begin moving down the flow paths when the groundwater recovery system was turned off. Capture of the COCs beneath and a short distance downgradient of the tailings impoundment would end, and impacted water would begin moving downgradient again.

As noted by NRC, the 1995 model under-predicted the U concentrations that would reach MW-14. The 1995 model in BIO1D used the observed concentrations as the modeling initial conditions downgradient from the low pH part of the plume. For the upstream boundary condition, it used the observed uranium concentration at the downstream edge of the pH front, 92 pCi/L. The assumption that was made was that this concentration was a good estimate of future uranium concentrations. As observed in Figure 10B, MW-12 had a uranium concentration of approximately 110 pCi/L in 1994, , while MW-9 had a concentration of around 80 pCi/L. Because the modeling was only addressing transport downgradient of the pH front, these values appeared to be reasonable, based on the measurements.

What the modelers did not consider was the effect of dilution during the recovery pumping on the observed concentrations. The recovery pumping was causing steeper gradients west of Lang Draw than present after the pumping was stopped. The steeper gradients produced more water moving into the Lang Draw area than would occur after pumping stopped and water levels recovered. When pumping stopped, the dilution provided by this lateral inflow decreased. This water probably assisted in the neutralization of the acidic plume. The net result was that after water levels recovered, the uranium concentrations increased. Referring again to Figure 10B, the highest uranium concentration in MW-12 was approximately the same as was measured in this well in March 1989, before the full effects of the recovery system were apparent. Because the 1995 model used an upgradient boundary condition that was based on concentrations that were “artificially” low because of the recovery pumping, it underestimated the peak concentrations that were to develop.

The 1995 model estimated the future movement of uranium and other constituents using a  $K_d$  approach, in which the  $K_d$  values were estimated from speciation modeling and literature values for other locations and lithologies, and using estimates of groundwater flow velocities. There were no monitoring data with which to calibrate the models, as is normally done, and the more

recent monitoring data have indicated that the 1995 model overestimated the retardation of uranium, and thus underestimated the rate of its movement.

In response to NRC's request for a revised ACL application based on the additional 13 years of data, a new predictive transport model was developed. The new model has two significant advantages over the 1995 model. First, data are available regarding the transport of uranium and other constituents along Lang Draw and the Northern Pathway for use in calibration of the model. The 1995 model was performed in a purely predictive mode, without information on transport rates at the site. Second, modeling technology has improved allowing direct incorporation of the chemical reactions into the transport model. Separate models were constructed for Lang Draw and for the Northern Pathway.

### ***3.1 Model construction and calibration***

The current model in PHREEQC uses higher, undiluted source area concentrations and incorporates coefficients for U sorption onto ferrihydrite. The current model also assumes equilibrium with gypsum and supersaturation with respect to ferrihydrite. These assumptions are in keeping with the findings of the speciation model discussed above. The initial water concentrations at various points in model are adjusted to match observed concentrations during the earlier part of the simulation period, and concentrations upgradient of the pH front were adjusted to match observed breakthrough concentrations in downgradient monitoring wells. Further, the influx of water from tailings was decreased through time to reflect the decline in the rate of seepage from the tailings following construction of the cover. For example, the chemistry of the water for the upstream boundary of the Lang Draw model was calculated by mixing water from upgradient (represented by samples collected from MW-36) with MW-86, reflecting the tailings fluid. MW-86 had a pH of 4.5, a sulfate concentration of 9,040 mg/L, and iron concentration of 926 mg/L. Chemistries of downgradient water used in the model were based on samples that had been collected from monitoring wells at about the time that the recovery system was turned off.

The models were constructed to begin beneath the tailings impoundment and extend downgradient to the northern property boundary, along each flow path. Model lengths of 968 meters (3,175 ft) and 1,040 meters (3,412 ft) were used for Lang Draw and the Northern Pathway, respectively. The grid spacing was 4 meters, resulting in models with 242 cells and 260 cells, respectively. Time steps of approximately 1 month were used in each model. As would be expected with a reactive transport model with sharp changes in chemical parameters, especially pH, some minor numerical issues occurred early in the simulations. These quickly smoothed out both laterally and temporally as the sharp fronts were smoothed by the dispersive process that the model can simulate.

The model optimization code ucode (Poeter et al, 2005) was used to obtain initial estimates of various parameters (ferrihydrite concentration, water pore velocity, source decay rate, and concentration step factors). Concentration data for U, SO<sub>4</sub>, Cl, Ra, and Ni observed in monitoring wells MW-12, -14, -108, and -109 were used as calibration targets for the Lang Draw flow path, and in wells MW-74, -43, -110, and -111 for the Northern flow path. Once a reasonable match to site data was obtained, hand calibration was used to fine tune parameters, such as the length of the low pH zone, which required adjustments to the model grid. Changes such as this are not easily made by ucode or other parameter-estimation approaches because of



the multiple steps involved in modifying the dataset, and the fact that cell designations can only be changed in integer steps.

During calibration of the models, the primary emphasis was on developing acceptable matches to the timing and magnitude of the breakthrough of uranium at the different monitoring wells, followed by simulating the sulfate and chloride concentrations. Other observations (radium for example) did not show a breakthrough pattern that could be used to assist the calibration of the model. A fact that became apparent early in the calibration process was that there was considerable spatial variability in the breakthrough behavior at different wells. MW-9 is a well that is completed at greater depth than MW-14, and even though MW-9 is closer to the tailings impoundment than MW-14 is, breakthrough occurs more slowly in MW-9. The breakthrough curves for chloride for MW-14 and MW-108 are nearly identical, even though they are nearly 700 feet apart. This complexity cannot be captured in a one-dimensional model. Because the peak uranium concentrations have already been observed in MW-12 and -14 along Lang Draw, the more recent data provide significant information on the rate of movement and the peak concentrations needed for predicting future movement.

For the Northern Pathway, the peak of the uranium breakthrough appears to have passed through MW-74. However, the data are noisier and the concentrations lower than in the wells along Lang Draw. The chloride peak appears to have already passed through MW-74, -4, and -110. As with Lang Draw, geologic variability will affect the actual movement of water and the constituents of interest, and therefore will affect the ability of the model to accurately predict the breakthrough of the constituents.

The input datasets for PHREEQC are provided in Attachments II and III for Lang Draw and the Northern Pathway, along with plots showing the initial concentrations for uranium, chloride, sulfate, pH, radium, and nickel.

For radium, the model considered only Ra-226 transport, because the great majority of the mass of radium is Ra-226, and the model is a chemical model that is based on the mass of the elements present. The activities presented assume that the radium is all Ra-226. Because Ra-226 and Ra-228 should be in secular equilibrium (and the monitoring data support this assumption), the total activity can be estimated by doubling the activities from the monitoring results.

An improved and expanded geochemical database for uranium and radium thermodynamic data was used. This dataset is described in Attachment IV.

### **3.2 Model Results**

Modeling was performed based on two pathways, Lang Draw and the Northern Pathway. For each pathway, the calibration process will be discussed first. Predictions of future transport will then be presented. Data on concentrations of sulfate, chloride, uranium, radium, and nickel; and on pH were used for the calibration. Predictions for concentrations of these same parameters were also made.

#### **3.2.1 Lang Draw**

**Calibration:** The initial concentrations used for the Lang Draw model are shown in Figures 16A through 16F. The upgradient water was a mixture of MW-36 and MW-86 waters. MW-86 is characterized with low pH (4.5), high sulfate (9,040 mg/L), iron (926 mg/L), and high uranium

(2,038 pCi/L). The proportion of MW-86 water was decreased using an exponential function, in steps. Figures 17A through 17F present the simulated breakthrough curves and the measured values for uranium, sulfate, chloride, pH, Ni, and Ra. Uranium is presented first, as it is the constituent of primary interest. The groundwater pore velocity determined through the model calibration was 130 feet per year.

Uranium – Uranium is retarded in its movement by sorption to ferrihydrite, and its transport is therefore affected by the amount of ferrihydrite present in the aquifer solids, as well as by the rate of water movement and by dispersion. The amount of ferrihydrite is primarily determined by the amount of dissolved iron in the low pH water at the upgradient end of the pathway, and by the change in pH downstream of the pH front, which causes the dissolved iron to precipitate as ferrihydrite. At MW-12, the most upgradient monitoring well, uranium concentrations peaked at 731 pCi/L in July 2003. At MW-9, which is the next monitoring well down the flow path, concentrations are lower and it is not clear at this time whether they have peaked. MW-9 is monitoring bedrock beneath the alluvial channel, and thus the uranium breakthrough is different in this well than in the more rapid alluvial channel part of the flow system. Uranium concentrations in MW-14 have also peaked (July 2008) and are declining. This well is completed in the alluvial materials, and the breakthrough is similar to that observed in MW-12, but delayed. At MW-108 and -109, it is not clear whether the peak has arrived yet.

The calibrated model matches the observed uranium concentrations in MW-12 and -14 reasonably well. At MW-12, the simulated breakthrough occurs earlier than observed, and the concentrations drop off more quickly than observed. The tailing (slower decline than rise) in the data is probably caused by the heterogeneity in the sediments. Concentrations in the future will probably decrease more slowly than the model will predict. The model predicts peak concentrations should have already reached MW-9, where the data indicate that transport is occurring much more slowly. Because the model is addressing transport in the more permeable alluvial sediments, it predicts more rapid transport to this location than was observed. Similarly, the model has predicted much more rapid transport to MW-108 and -109, than has been observed. These wells are also completed in the bedrock, and thus would be expected to peak more slowly than predicted.

Sulfate - The movement of sulfate is determined by the water velocity and whether gypsum will dissolve or precipitate. As gypsum is composed of calcium and sulfate, the concentration of sulfate is inversely proportional to the concentration of calcium if gypsum is present. The geochemical speciation modeling discussed above indicated that gypsum is present throughout the area. The model simulates a peak for sulfate at MW-12 approximately 8 years after the pumping stopped. There is a gap in the measurements at about that time, but concentrations measured later are higher than the simulated values, suggesting that either breakthrough occurred more slowly than simulated, or that heterogeneity is causing tailing. The timing of the simulated peaks are coincident with those of uranium. At MW-12, the model matches the sulfate concentrations reasonably well, but over predicts them at other locations. This may indicate that the concentrations of calcium used in the model are too low.

Chloride – Chloride behaves conservatively. In other words, it is not retarded by a chemical mechanism such as sorption or precipitation. The peaks of the simulated breakthrough occur earlier than the peaks for uranium and sulfate. Although the data are quite variable, the model matches the breakthrough of chloride reasonably well except at MW-109. The difference in the measured breakthrough curves for MW-108 and -109 is surprising. Breakthrough of uranium

and sulfate has not occurred at these two wells, so it is surprising that chloride did breakthrough as early as it did. Peak chloride concentrations are matched well.

pH – The pH values varied over the range of approximately 6.1 to 7.5 in the data. The data indicate that pH has decreased in MW-12, -9, -14, -108, and perhaps -109. The lowest measured pH during the post-recovery system period was 6.1. The model simulates the pH over the same approximate range as the measurements with an initial decline followed by rising pH in the three most upgradient wells.

Radium – Concentrations of radium have been variable over this time frame, and may have peaked in approximately 2003. In MW-14, concentrations have generally been declining since the beginning of the period. Concentrations in MW-14 and MW-12 appear to have been higher than in MW-9, -108, and -109. Because radium concentration is determined by counting, and because the concentrations are low, the observed variability is likely due in large part by random counting error. There did not appear to be a reliable signal against which to calibrate the model. As a result, the timing of the peaks is essentially unconstrained, and determined by the groundwater velocity. In the resulting predictions, the range of concentrations is believed to be representative, but the timing of the breakthrough is not.

Nickel – Nickel appears to be increasing in concentration in MW-12 and -14, but concentrations have typically been higher in MW-14, the downgradient well. Some of the results at MW-109 have been nearly as high as those in upgradient wells. Thus, the high variability in the data made it difficult to select calibration targets. Nickel concentrations are lower than prior to the recovery system pumping, but may be trending upward. In the simulation, nickel is retarded by sorption onto ferrihydrite.

**Predictions:** For the predictions, the Lang Draw model was run until concentrations stopped changing. At that time, the water chemistry was primarily determined by the upgradient water chemistry and the simulated precipitation/dissolution reactions (i.e., equilibrium with calcite and gypsum, slight under saturation with aluminum hydroxide and supersaturation with ferrihydrite). The results are shown in Figures 18A through 18F.

Uranium – The uranium results show a double peak. The second peak is approximately one-third to one-half of the height of the first peak. The second peak is caused by the movement of the pH front. Even though the reduction in pH is small, it causes dissolution of ferrihydrite and releases some of the sorbed uranium which migrates downgradient creating the second peak. Because the model assumes homogeneity within different parts of the model, whereas the natural system is heterogeneous, the natural system may not show a clearly discernable second peak. It may create a long tailing effect, similar to what is shown for the most downgradient well, MW-109. The model predicts that uranium concentrations will be approaching background concentrations in approximately 2050; there is uncertainty in this estimate primarily because of heterogeneity, but also because there are many parameters, such as groundwater velocity, dispersion, and thermodynamic data that are uncertain. The availability of the uranium concentration data through and past the time when the first peak occurred provides a constraint on the calibration of the model, especially with respect to the peak concentration. While the timing of the return to background concentrations is not well-defined because the peak has just passed MW-12 and -14, it is unlikely that uranium concentrations will exceed the peak concentrations previously observed.



Sulfate – sulfate concentrations are predicted to have a single peak, as sulfate does not sorb to ferrihydrite. The model simulates that the sulfate peak will pass through the wells, and the concentration in each will then decline to a value of approximately 1,600 mg/L. This concentration is determined by the solubility of the gypsum that was precipitated, and the concentration of the dissolved calcium in the water, which is based on a sample from MW-36. If the simulation had been longer, it should show sulfate concentrations beginning to decrease again as the gypsum is dissolved from the upstream end.

Chloride – The breakthrough of chloride is also single-peaked. Concentrations decrease downgradient because of dispersion processes. The model predicts that concentrations at the monitoring wells will decline to the upstream input concentration within about 25 to 40 years after the pumping stopped, or in about 2025 to 2040. However, heterogeneity causes slower recovery than predicted by homogeneous models, and recovery may take longer than predicted.

pH – The model showed the pH front (from higher to lower pH) during the calibration period, with MW-12 and MW-9 showing increasing pH toward the end of it. In the longer run of the model, the pH increases at all locations to a value of approximately 7. The model predicts that about 4 decades will be required for the pH to become stable, but the range in pH over this period is small.

Radium – As discussed above, radium was assumed not to sorb because of the difficulty in interpreting the measurements. As a result, it is predicted to peak relatively quickly, with maximum concentrations between 2.0 and 2.5 pCi/L. This concentration is based on the observed concentrations over the previous 15 years. Radium concentrations had been as high as 18 pCi/L in the early 1990s, but have not risen much since pumping stopped. The simulations predict that the peak has already passed for many of the monitoring wells, but retardation of radium was not simulated because it does not sorb appreciably to ferrihydrite.

Nickel – Retardation of nickel was simulated using sorption to ferrihydrite. The model predicts that the nickel peak will pass through a little slower than that of chloride, with the concentrations not increasing appreciably above those seen today.

In summary, the modeling predictions for uranium are believed to be representative of the future transport of uranium, because the observed passage of peaks at two of the monitoring wells constrains the transport process. The variability (heterogeneity) of the properties of the soils and rocks further downgradient will cause the observed results to differ from the predicted results. A second peak is predicted for uranium due to pH changes. As ferrihydrite dissolves, sorbed uranium will be released into the groundwater. The second peak will be smaller than the first peak. Longer term sulfate concentrations are predicted to be controlled by the solubility of gypsum and the concentrations of calcium. The pH is expected to decline slightly, then return to present-day or slightly higher values. Predictions of the transport of radium and nickel are less certain, because of the variability in the data and the lack of current-day information on radium and nickel concentrations upgradient of MW-12.

### 3.2.2 Northern Pathway

**Calibration:** Figures 19A through 19E show the initial concentrations used in the model. The upgradient water was as described under the Lang Draw discussion. Results are shown in Figures 20A through 20E.

Uranium – Data variability at MW-74 makes it difficult to determine whether the uranium peak has passed this well. Concentrations at MW-43 were declining through the calibration period. Both MW-110 and -111 have low concentrations. The model simulates a peak for MW-74 that falls within the range of the observed data. The simulated peak for MW-43 occurred later than the data would suggest. Actual concentrations at MW-43 were much higher before the recovery system was installed and during its early operation. At MW-110 and -111, the model indicates slow breakthrough was occurring during the calibration period.

Sulfate – The measurements of sulfate concentrations for MW-74, -43, and -110 do not show appreciable changes during the calibration period, while MW-111 shows a slow increasing trend. The model shows slow upward trends at each location. Thus, the model probably over predicts sulfate concentrations during the coming several years.

Chloride - During the calibration period, chloride has been relatively constant in MW-74, has been declining in MW-43, may have peaked in MW-110, and may be slowly increasing in MW-111. The model simulates each of these trends, but is predicting higher concentrations at MW-111 than have been occurring.

pH – The pH measurements suggest that a weak acid front moved through the locations of MW-74 and -110. The pH in the intervening well, MW-43, has remained reasonably constant. The current measurements in MW-74 and MW-110 are higher than the previous values, and measurements over the next several years should indicate whether these values are likely to be representative. The model simulations indicate that all values are tending toward a pH of 6.5; this value is probably determined in the model by the water chemistry and the specification that the water is to be in equilibrium with calcite and gypsum.

Radium – The data for the wells indicate stable or slowly declining values. The model, on the other hand, predicts increasing concentrations in MW-74 and MW-43. A value of 6.8 pCi/L was assumed for the area upgradient of MW-74 and MW-43. No data are available on concentrations of Ra today beneath the tailings impoundment near these wells. If a lower value had been used for this segment of the model, the fit may have improved.

Nickel – It is difficult to discern whether there are trends in the nickel concentration data. Concentrations in MW-74 may have been increasing since 2005, and perhaps in MW-43. The concentrations are low and there appear to be some elevated detection limits. In the late 1980s, concentrations were as high as 0.33 in MW-43, but have been low since the recovery system was terminated. The model showed slow rises during the calibration period.

**Predictions:** The predictions were made by extending the time of the simulation until concentrations stabilized. One thing to note is the much longer time frame for the Northern Pathway for concentrations to become stable. This is a consequence of the slower velocity (65 ft/year) and longer flow path than for Lang Draw.

Uranium – The transport of uranium along the Northern Flowpath is similar to that along Lang Draw, except that the concentrations are lower and the rate of movement is slower. The second peak is predicted to occur along both flow paths, as described previously.

Sulfate – The breakthrough curves for sulfate are remarkably similar to those for Lang Draw, reaching the same long-term equilibrium concentration of approximately 1,600 mg/L. The peak concentrations for the Northern Pathway are slightly lower than those for Lang Draw.

Chloride – Peak concentrations for chloride are higher than those for Lang Draw because of the higher initial condition used.

pH – Both the Northern Pathway and Lang Draw models predict that pH will decrease, and then rise to a constant value. For the Northern Pathway, the lowest pH is predicted to be about 6.5, and the final pH will be about 6.9. These values are slightly different from those along Lang Draw (low of 6.4, long-term value of approximately 7.0).

Radium – Radium concentrations are predicted to peak above 6 pCi/L. This value is the result of the assumed concentration (6.8 pCi/L) in the water beneath the tailings impoundment. The double-peak feature of some of the breakthrough curves (MW-111 is the best example) was caused by having two areas of higher concentration in the initial concentrations dataset, and is not associated with dissolution of ferrihydrite. The lower concentration area was further downgradient, causing the first peak to be smaller than the second peak.

Nickel – The peak nickel concentration is predicted to be about 0.04 mg/L. It is sorbed slightly by ferrihydrite, causing the slight decrease in concentration below 0.01 mg/L before rising to 0.01 mg/L, the upgradient concentration used in the model.

#### **4.0 Conclusions**

The re-evaluation of the geochemistry of the groundwater at the Bear Creek Disposal Facility was based on monitoring data collected from the period of operation of the facility to the present. The geochemistry had previously been evaluated in 1987 and 1995. The chemical mechanisms controlling the groundwater chemistry identified in those previous investigations (namely, attenuation of the acid front by dissolution of calcite, and subsequent precipitation of gypsum and ferrihydrite) were found to remain true, based on new samples and geochemical modeling.

Monitoring data collected after cessation of the groundwater recovery system provided information with which to calibrate reactive transport models for predicting future movement of uranium, radium, and nickel along the Lang Draw and Northern pathways. When modeling was done in 1995, data to constrain the calibration did not exist. Estimates of the retardation factors were based on geochemical speciation modeling and on Kds (distribution coefficients) developed for other locations. The monitoring data that have been collected since 1995 have provided site-specific information with which to determine the retardation. For Lang Draw, which is the more significant of the two pathways, uranium concentrations have now peaked in two wells, providing information on the highest concentrations that might be expected in the future. The peaks observed in the data set also provided information on the rate of movement of uranium. For the Northern Pathway, uranium appears to have peaked in one, and perhaps two, of the monitoring wells, providing the same types of information.

The models predict that there will be a second peak of uranium that occurs in the monitoring wells, caused by movement of lower pH water that can dissolve the ferrihydrite that has sorbed uranium. The second peak would be caused by the release of the uranium through this process. The magnitude of the second peak is predicted to be less than that of the first peak. However, geologic heterogeneity and resulting dispersion may make the peaks difficult to distinguish in actual sample data.

The radium data that have been collected since cessation of the recovery pumping did not provide a clear indication of radium transport behavior. Therefore, radium was modeled as

essentially being conservative. Its sorption to ferrihydrite was considered in the model, but the mass sorbed was inconsequential. Radium is likely to be attenuated by ion exchange.

Information on the transport of nickel was also hard to discern in the data because of the low concentrations and the variability. Nickel attenuation was simulated through sorption on ferrihydrite. Thus, the movement of the pH front affects nickel transport behavior.

## 5.0 References

- Allison, J.D., D.S. Brown, and K.J. Novo-Gradac, 1991. MINTEQA2/PRODEFA2: A geochemical assessment model for environmental systems, version 3.0 user's manual: EPA/600/3-91/021, USEPA, Athens, Georgia.
- GeoTrans, Inc. (1995). *Hydrogeologic and Geochemical Transport Analyses Converse County, Wyoming*.
- Parkhurst, D.L. and C.A.J. Appelo, 1999. *User's guide to PHREEQC (version 2) – a computer program for speciation, batch-reaction, one-dimensional transport, and inverse geochemical calculations*. USGS, Denver, Colorado, Water-Resources Investigations Report 99-4259, 312 pages.
- Poeter, E.P; M.C. Hill, E.R. Banta, S. Mehl, and S. Christensen, 2008 revision. *UCODE\_2005 and six other codes for universal sensitivity analysis, calibration, and uncertainty evaluation*. USGS, Reston, Virginia, Techniques and Methods 6-A11, 283 pages.



## FIGURES

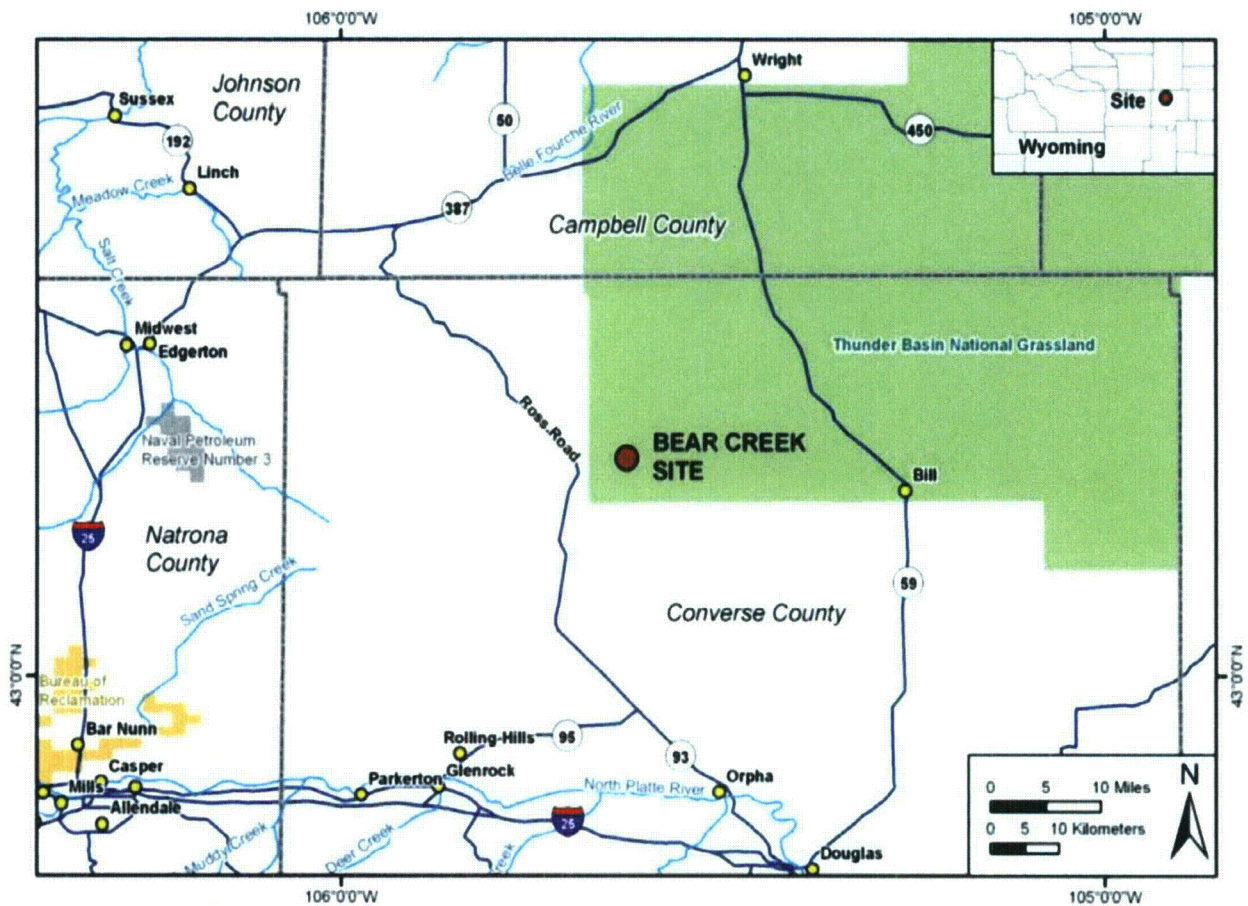


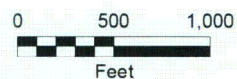
**Figure 1. Bear Creek Uranium Mill Site Location**

Source: 2009 NRC Information Sheet for Bear Creek Uranium Mill Site





Monitoring Wells, February 2011



ISSUED BY:



336 Centennial pkwy, Suite 210  
Louisville, Colorado 80027

ISSUED FOR:

**Bear Creek Disposal Site**  
Bear Creek, Wyoming

PROJECT NAME:

Bear Creek Uranium

DATE:

August 5, 2011

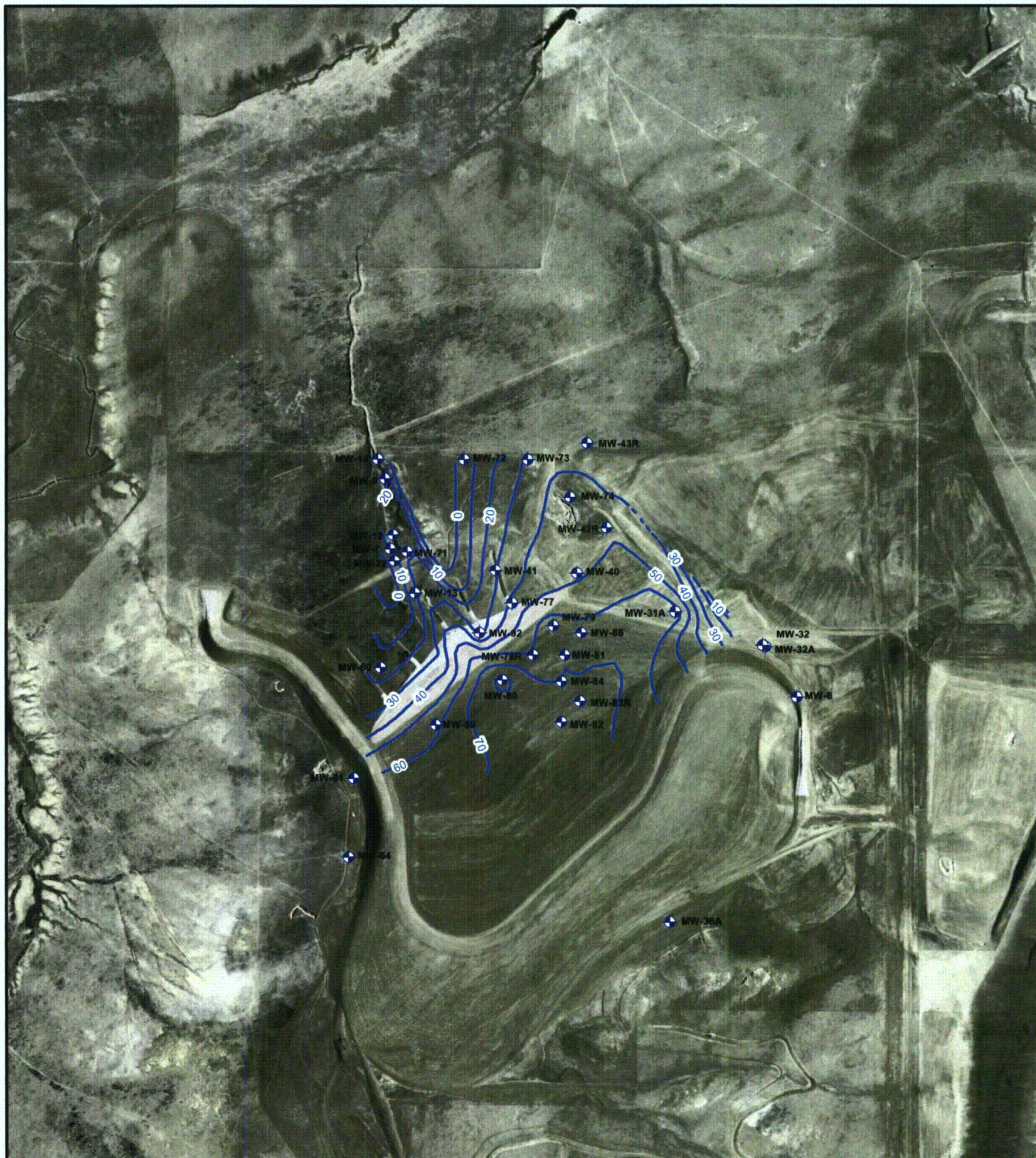
PROJECT NO.:

117-7252001

TITLE:

**Figure 2. Existing Site  
Features**

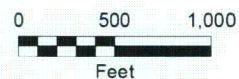




Monitoring Wells, June 1986



Saturated Thickness, June 1986



ISSUED BY:



336 Centennial pkwy, Suite 210  
Louisville, Colorado 80027

ISSUED FOR:

**Bear Creek Disposal Site**  
Bear Creek, Wyoming

PROJECT NAME:

Bear Creek Uranium

DATE:

August 5, 2011

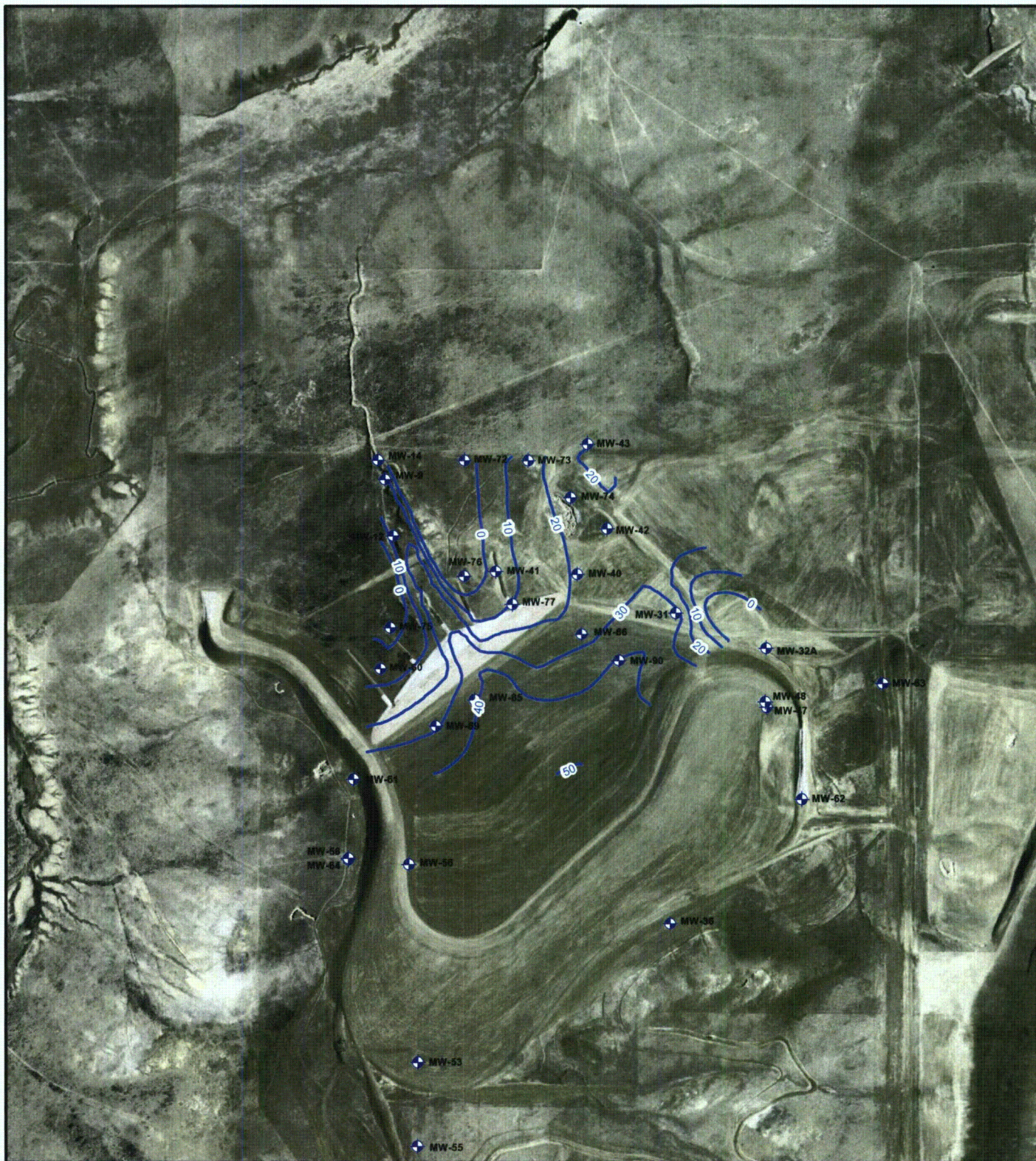
PROJECT NO:

117-7252001

TITLE:

**Figure 3. Saturated  
Thickness of N Sand,  
June 1986**





Monitoring Wells, March 1996



Saturated Thickness, March 1996



0 500 1,000  
Feet

ISSUED BY:



336 Centennial pkwy, Suite 210  
Louisville, Colorado 80027

ISSUED FOR:

**Bear Creek Disposal Site**  
Bear Creek, Wyoming

PROJECT NAME:

Bear Creek Uranium

DATE:

August 5, 2011

PROJECT NO.:

117-7252001

TITLE:

**Figure 4. Saturated  
Thickness of N Sand,  
March 1996**





Monitoring Wells, February 2011



Saturated Thickness, February 2011



0 500 1,000  
Feet

ISSUED BY:



TETRA TECH GEO

336 Centennial pkwy, Suite 210  
Louisville, Colorado 80027

ISSUED FOR:

**Bear Creek Disposal Site**  
Bear Creek, Wyoming

PROJECT NAME:

Bear Creek Uranium

DATE:

August 5, 2011

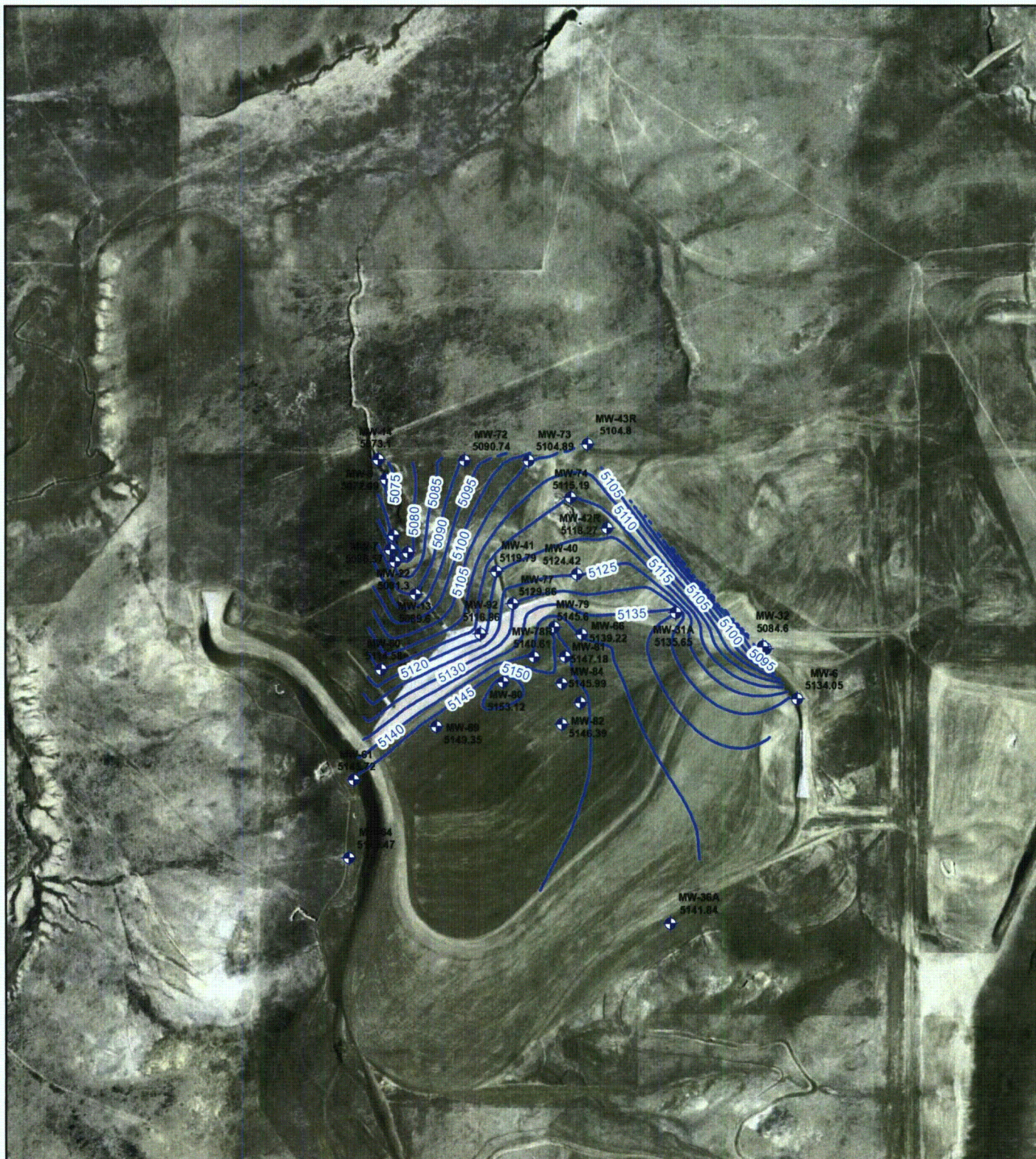
PROJECT NO.:

117-7252001

TITLE:

**Figure 5. Saturated  
Thickness of N Sand,  
February 2011**









Monitoring Wells, March 1996  
Groundwater Elevation, March 1996

0 500 1,000  
Feet



ISSUED BY:



336 Centennial pkwy, Suite 210  
Louisville, Colorado 80027

ISSUED FOR:

**Bear Creek Disposal Site**  
Bear Creek, Wyoming

PROJECT NAME:

Bear Creek Uranium

DATE:

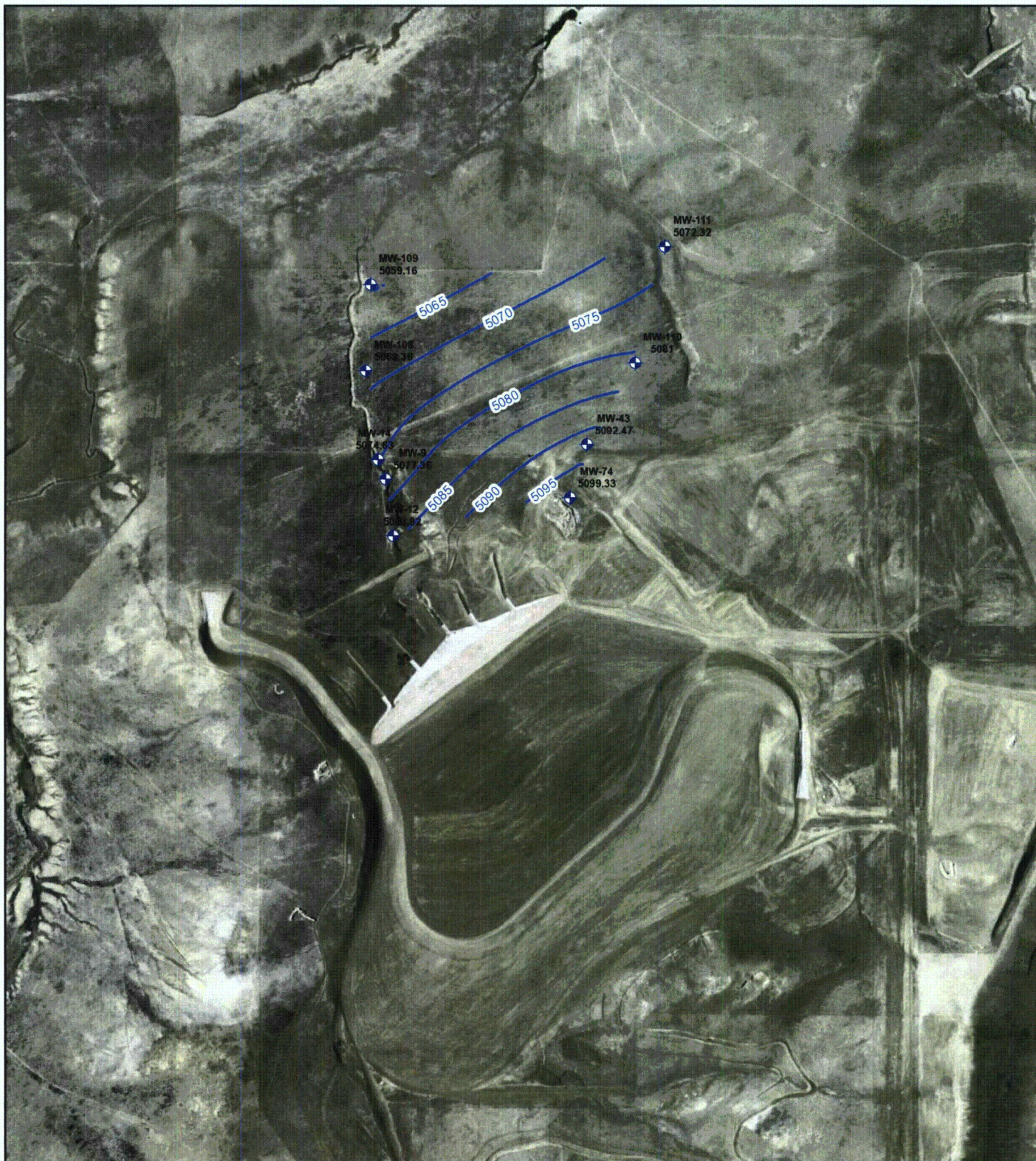
August 5, 2011

PROJECT NO.: 117-7252001

TITLE:

**Figure 7. Water-Level  
Elevations,  
March 1996**





Monitoring Wells, February 2011  
Groundwater Elevation, February 2011

0 500 1,000  
Feet



ISSUED BY:



336 Centennial pkwy, Suite 210  
Louisville, Colorado 80027

ISSUED FOR:

**Bear Creek Disposal Site**  
Bear Creek, Wyoming

PROJECT NAME:

Bear Creek Uranium

DATE:

August 5, 2011

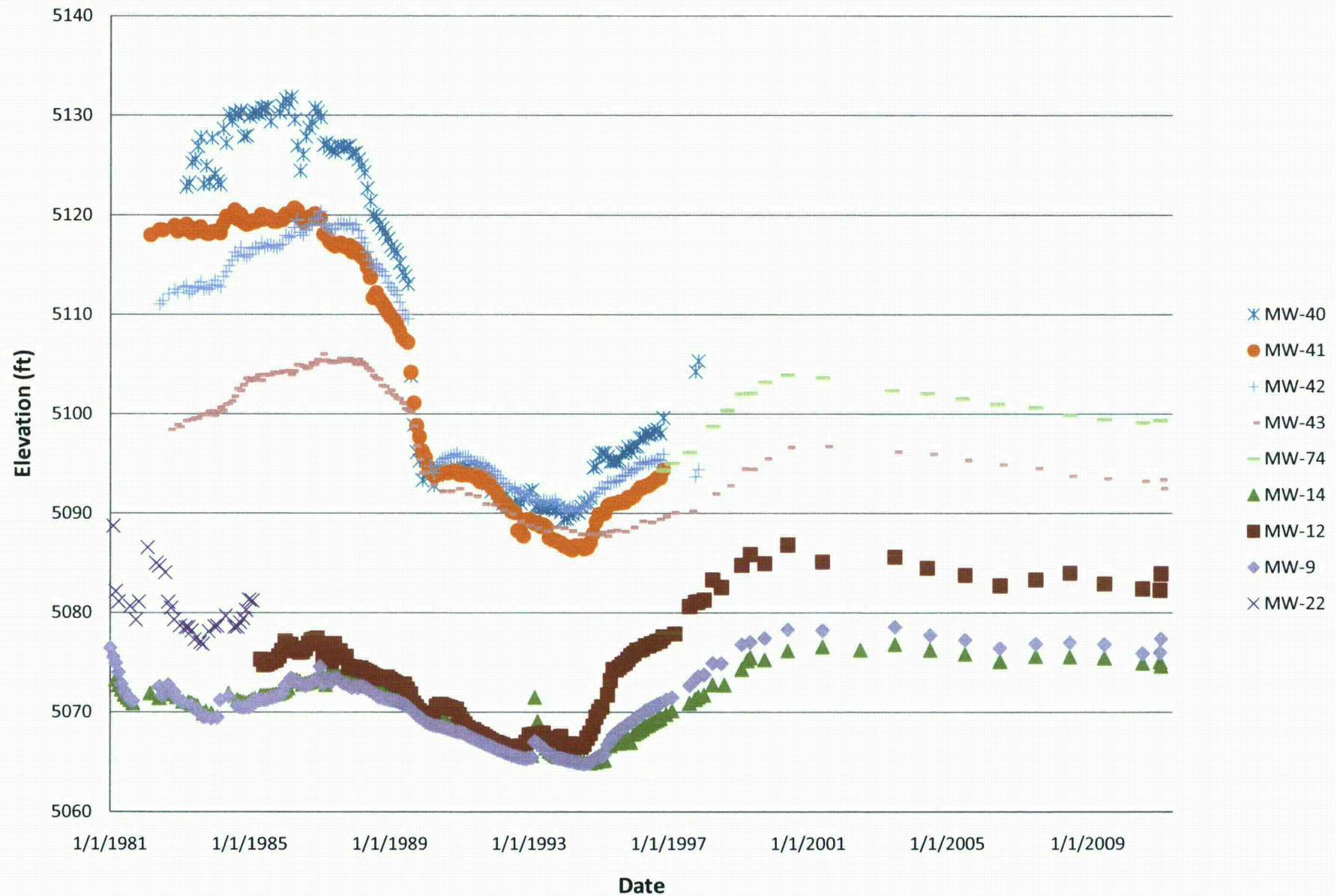
PROJECT NO.: 117-7252001

TITLE:

**Figure 8. Water-Level  
Elevations,  
February 2011**



**Figure 9. Measured Water-Level Elevations, 1981-2011**

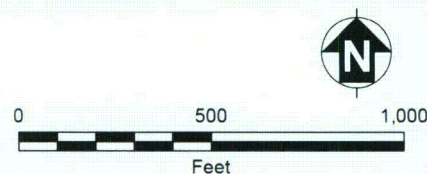






Monitoring Well  
(17.6)

Concentrations are in pCi/L (picocuries per liter)  
ACL (alternate concentration limit) = 2,038 pCi/L



ISSUED BY:



336 Centennial pkwy, Suite 210  
Louisville, Colorado 80027

ISSUED FOR:

**Bear Creek Disposal Site**  
Bear Creek, Wyoming

PROJECT NAME:

Bear Creek Uranium

DATE:

August 5, 2011

PROJECT NO.: 117-7252001

TITLE:

**Figure 10A. Distribution  
of Uranium  
Concentrations,  
February 2011**



**Figure 10B. Temporal Changes in Uranium Concentrations,  
Lang Draw**

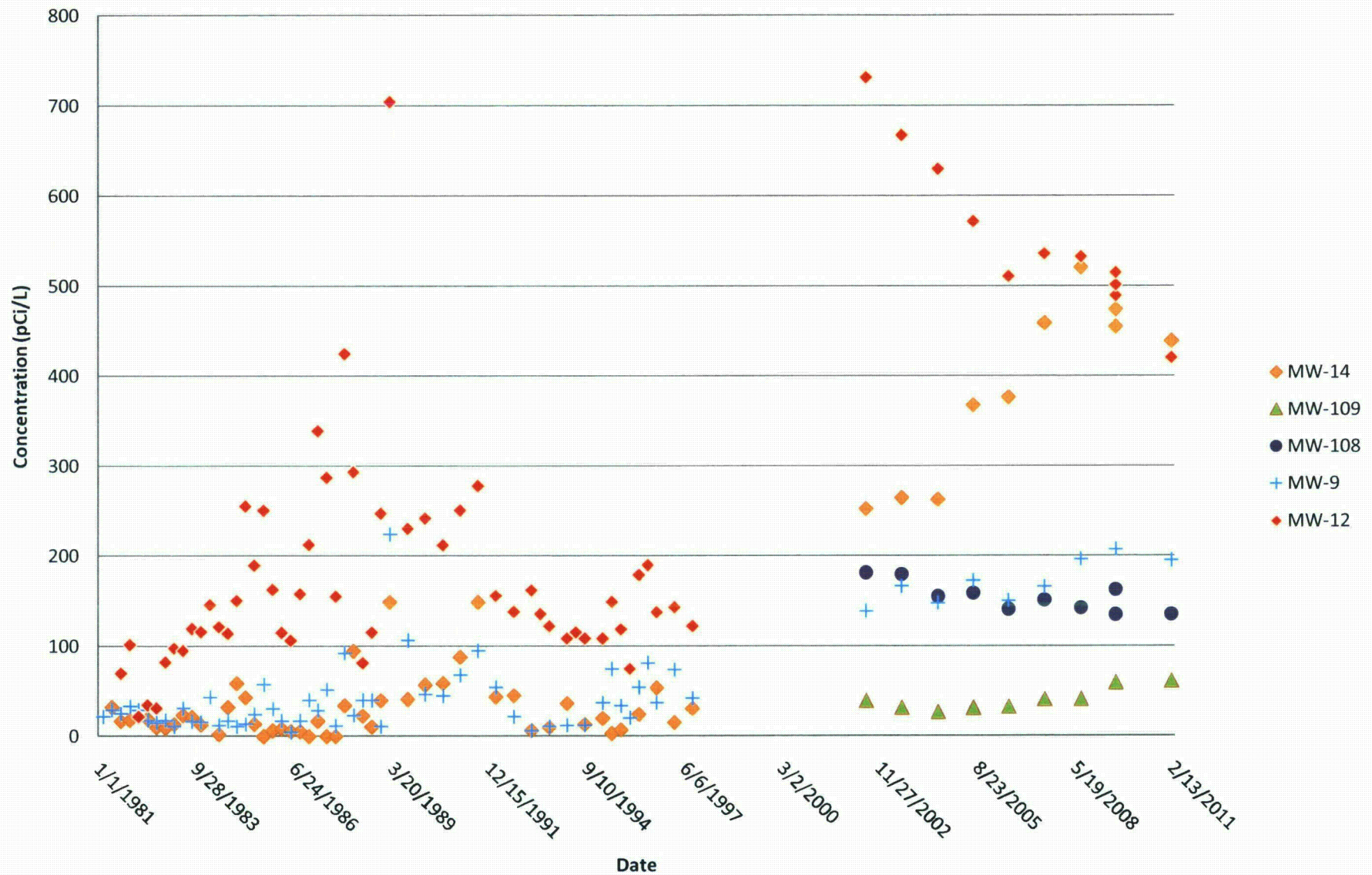
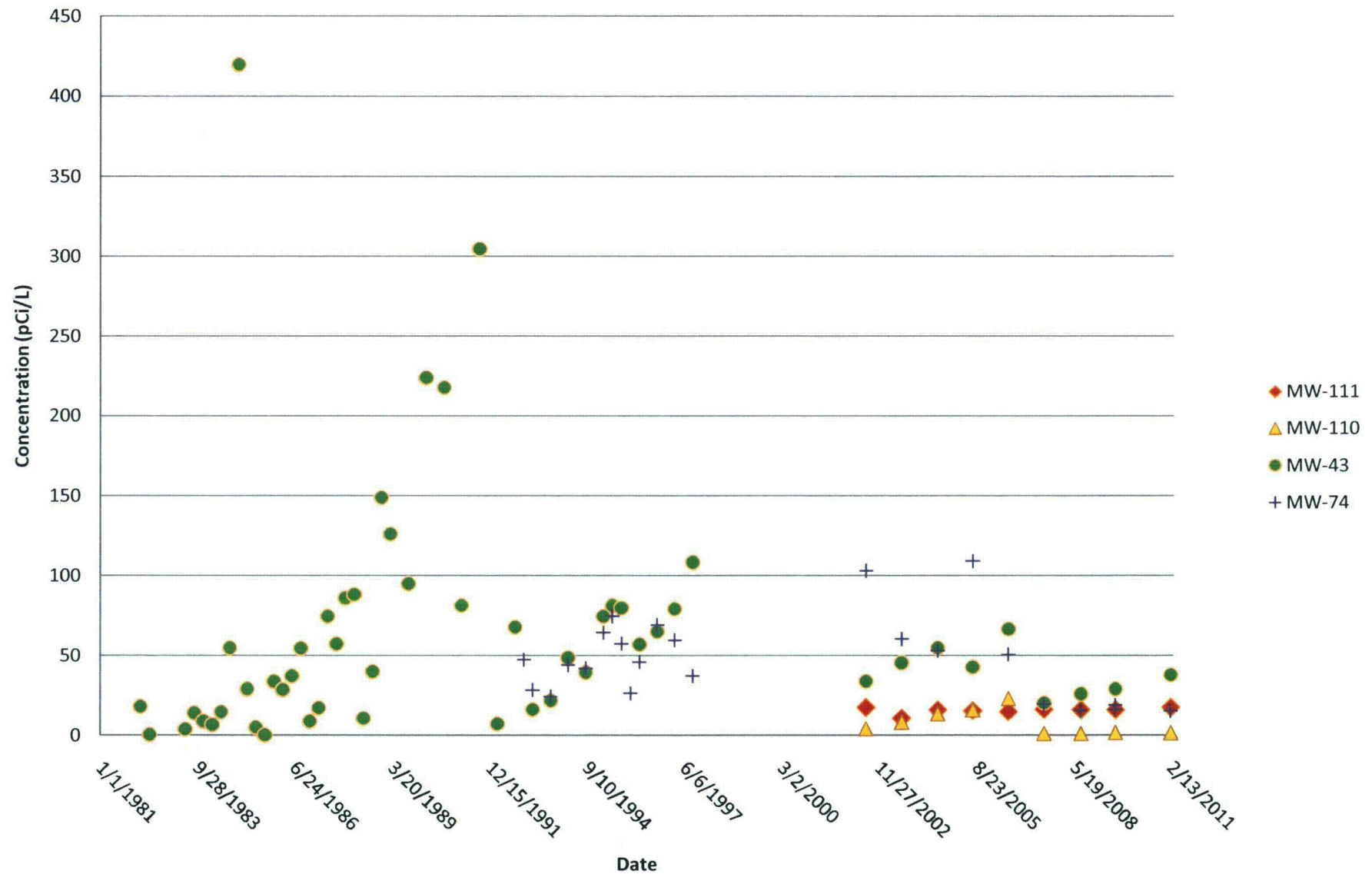



**Figure 10C. Temporal Changes in Uranium Concentrations,  
Northern Pathway**

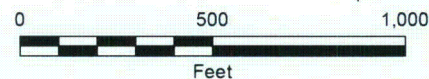






 Monitoring Well  
 (1190)

Concentrations are in mg/L (milligrams per liter)  
 Groundwater Protection Standard = 3,000 mg/L



ISSUED BY:



336 Centennial pkwy, Suite 210  
 Louisville, Colorado 80027

ISSUED FOR:

**Bear Creek Disposal Site**  
 Bear Creek, Wyoming

PROJECT NAME:

Bear Creek Uranium

DATE:

August 5, 2011

PROJECT NO.: 117-7252001

TITLE:

**Figure 11A. Distribution  
 of Sulfate  
 Concentrations,  
 February 2011**



**Figure 11B. Temporal Changes in Sulfate Concentrations,  
Lang Draw**

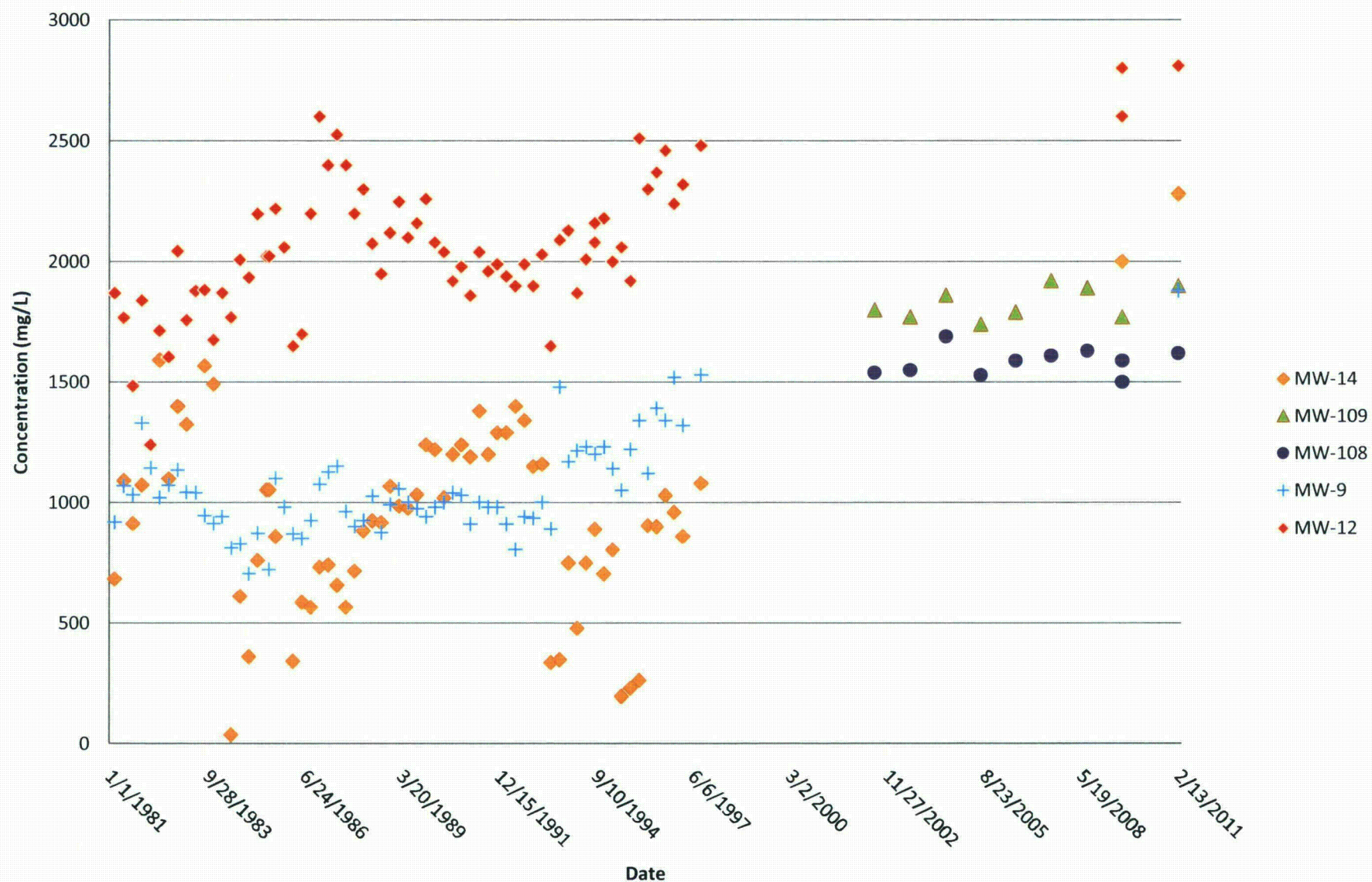
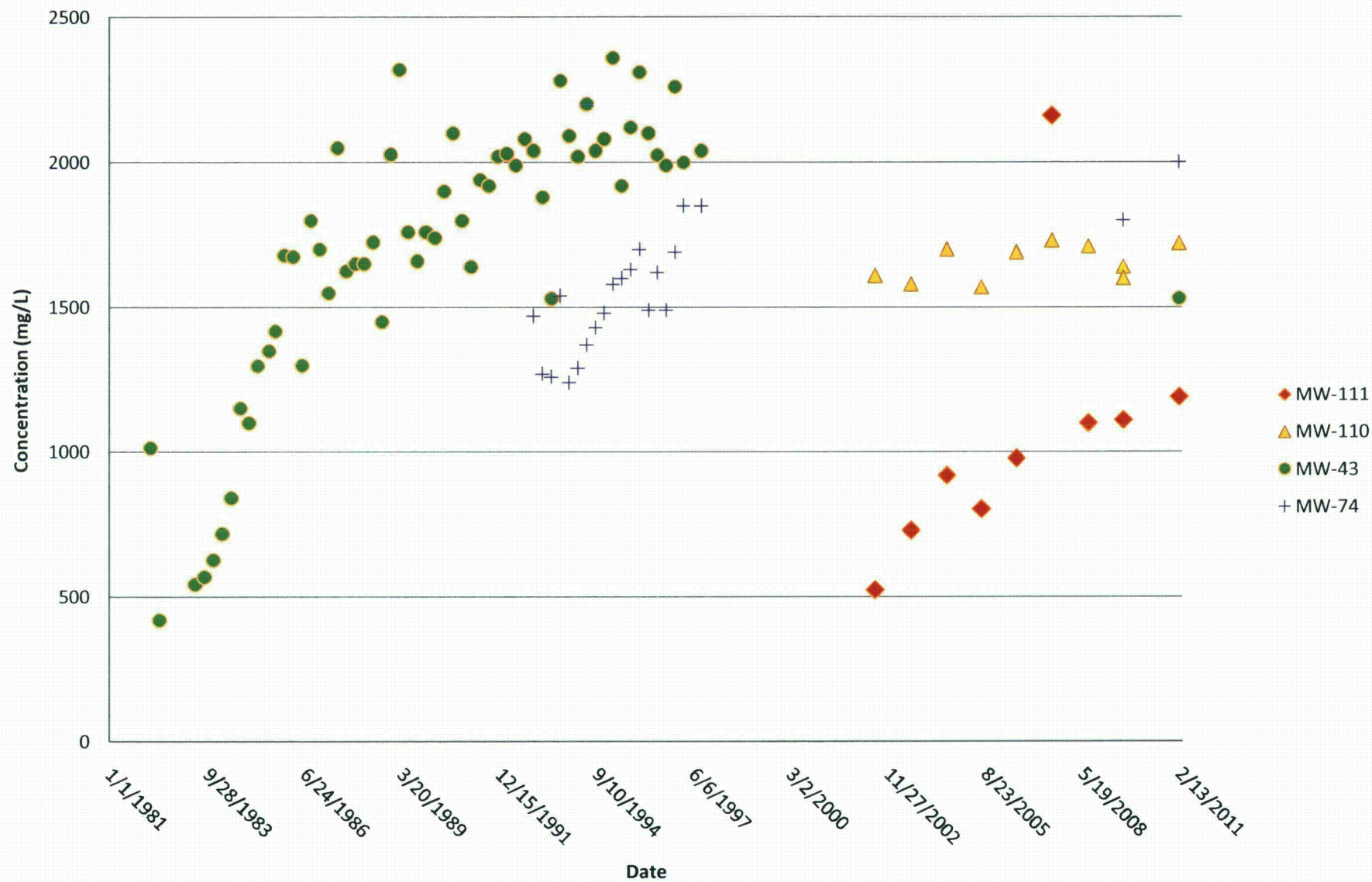



**Figure 11C. Temporal Changes in Sulfate Concentrations,  
Northern Pathway**

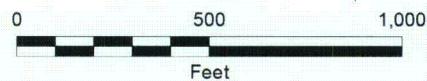






 Monitoring Well  
(102)

Concentrations are in mg/L (milligrams per liter)  
 Groundwater Protection Standard = 2,000 mg/L



ISSUED BY:



336 Centennial pkwy, Suite 210  
 Louisville, Colorado 80027

ISSUED FOR:

**Bear Creek Disposal Site**  
 Bear Creek, Wyoming

PROJECT NAME:

Bear Creek Uranium

DATE:

August 5, 2011

PROJECT NO.: 117-7252001

TITLE:

**Figure 12A. Distribution  
 of Chloride  
 Concentrations,  
 February 2011**



**Figure 12B. Temporal Changes in Chloride Concentrations,  
Lang Draw**

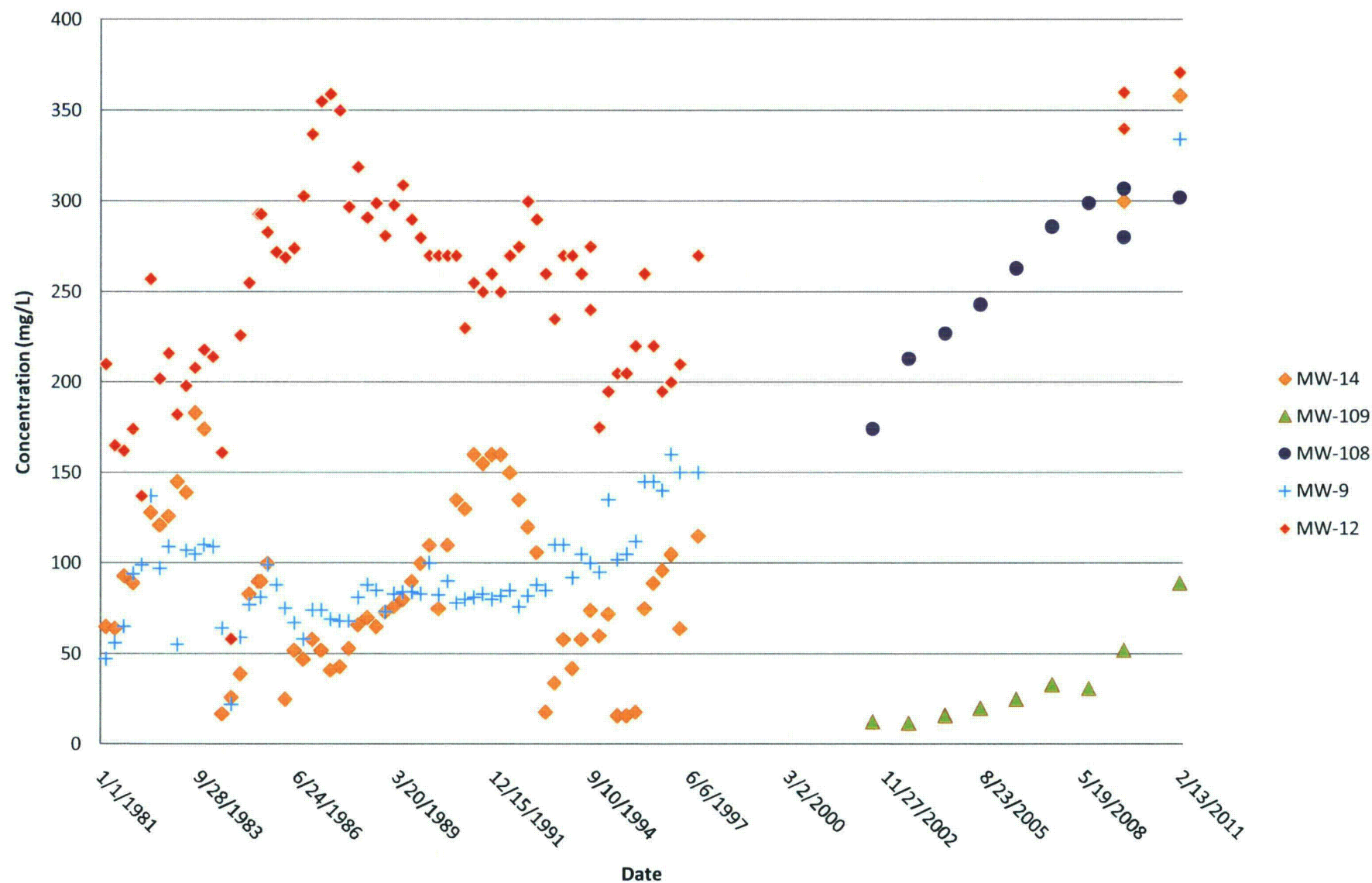
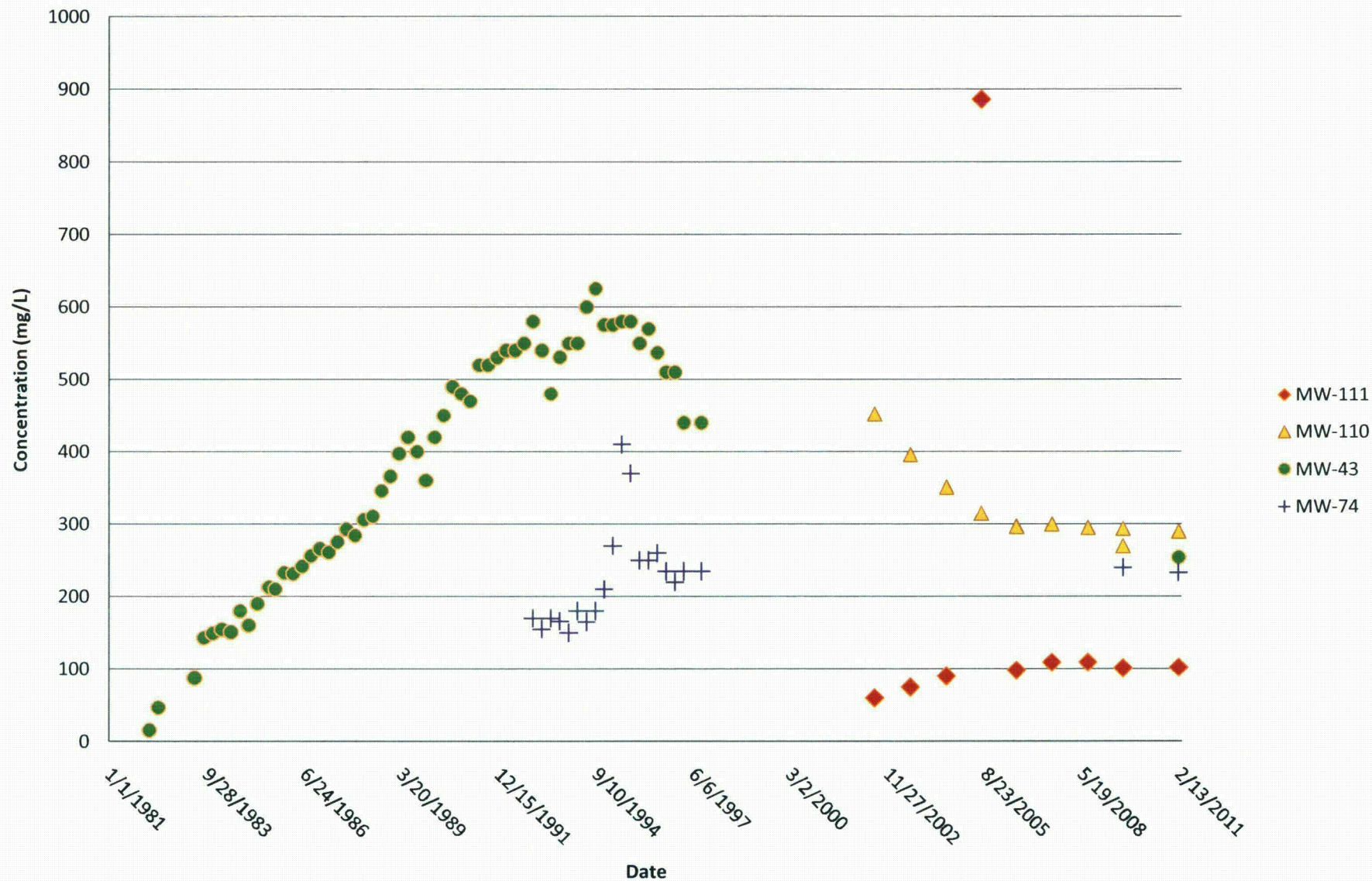



**Figure 12C. Temporal Changes in Chloride Concentration,  
Northern Pathway**

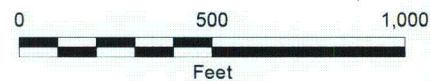






 Monitoring Well  
 (7.6)

Values are in pH units (s.u.)



ISSUED BY:



336 Centennial pkwy, Suite 210  
Louisville, Colorado 80027

ISSUED FOR:

**Bear Creek Disposal Site**  
Bear Creek, Wyoming

PROJECT NAME:

Bear Creek Uranium

DATE:

August 5, 2011

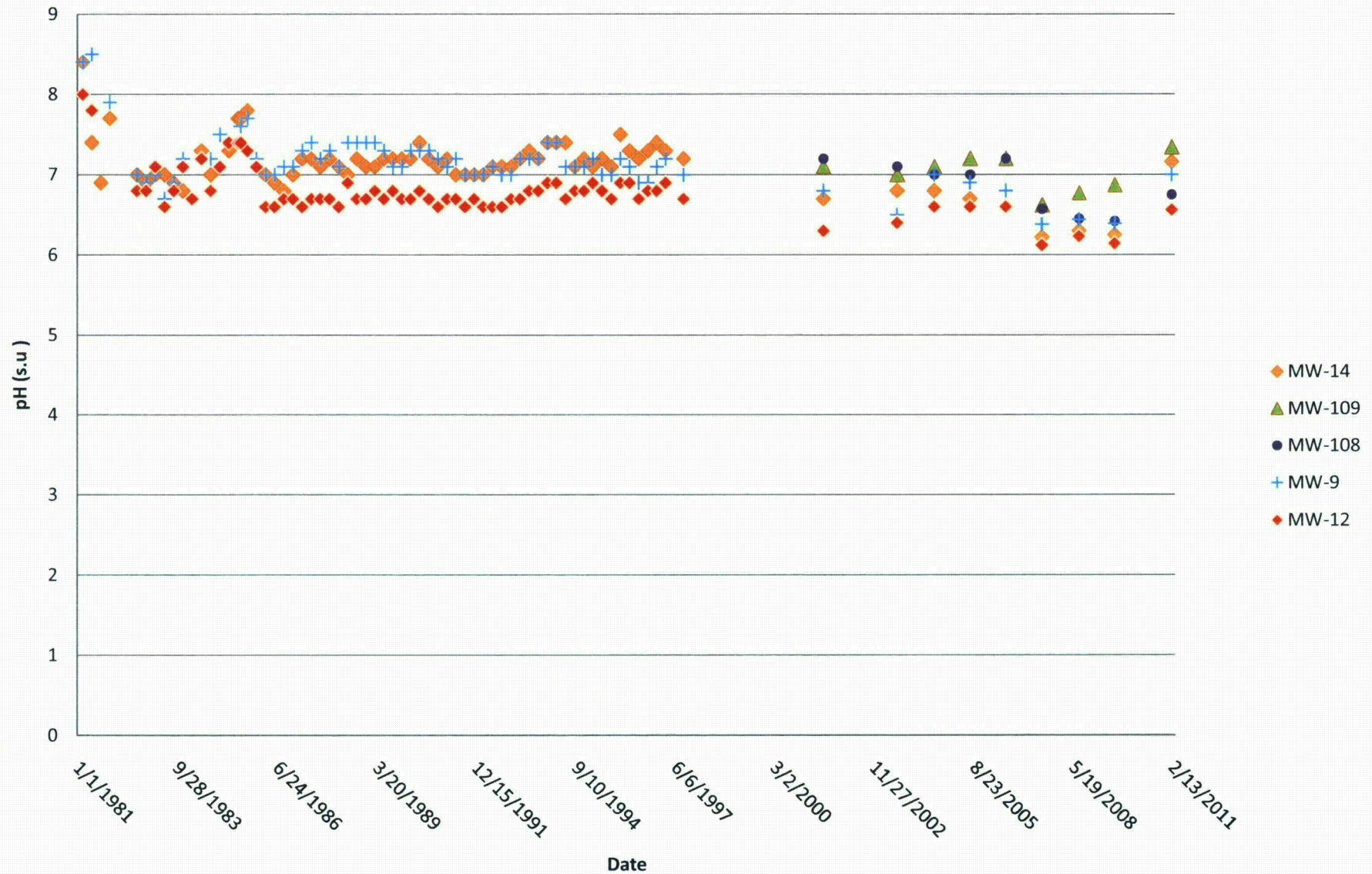
PROJECT NO.: 117-7252001

TITLE:

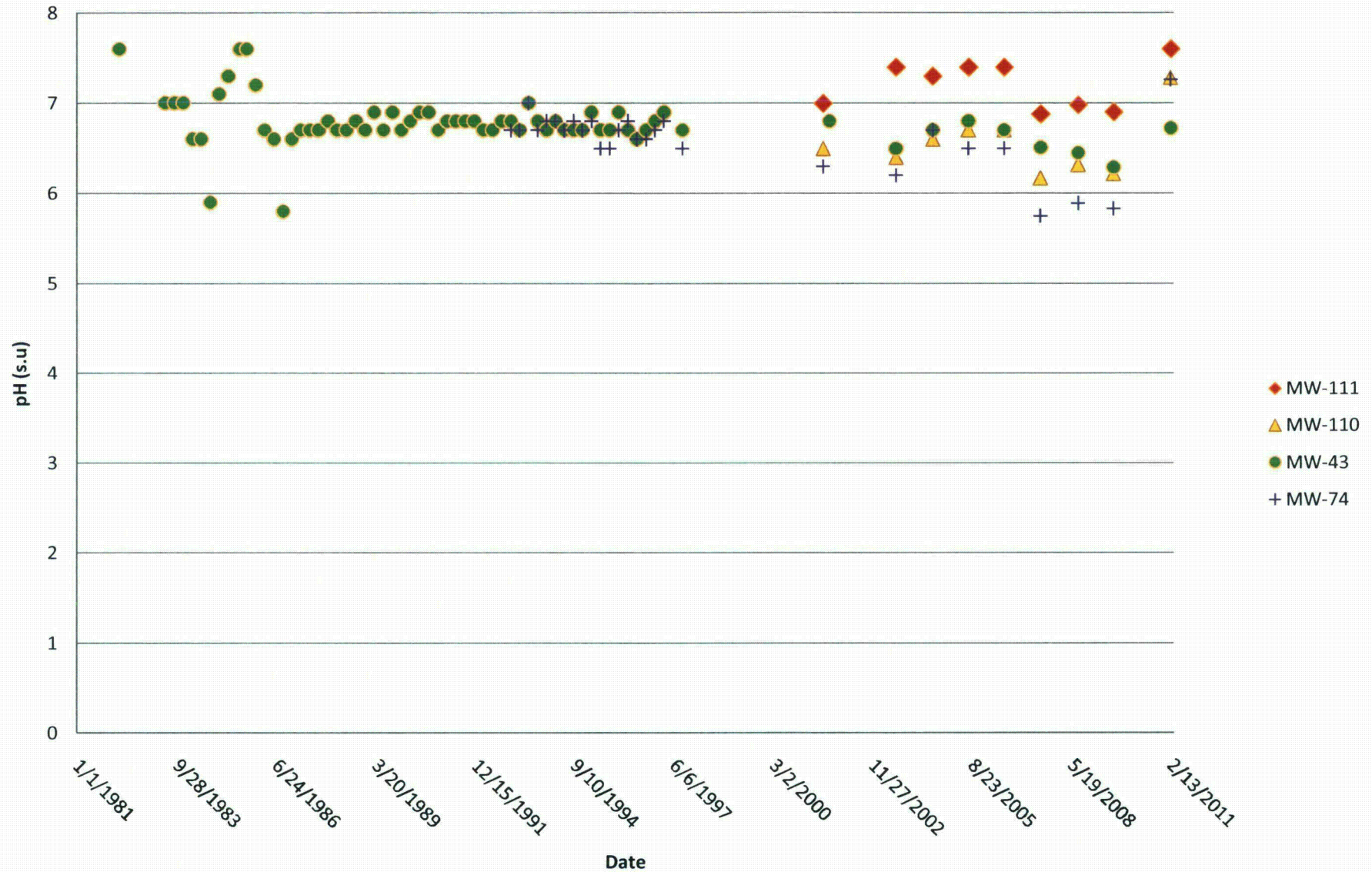
**Figure 13A. Distribution  
of pH, February 2011**



Figure 13B. Temporal Changes in pH,  
Lang Draw





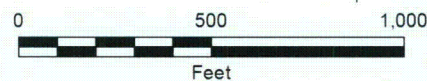
[illegible]





Monitoring Well  
(1.8)

Concentrations are in pCi/L (picocuries per liter)  
ACL (alternate concentration limit) = 46 pCi/L



ISSUED BY:



336 Centennial pkwy, Suite 210  
Louisville, Colorado 80027

ISSUED FOR:

**Bear Creek Disposal Site**  
Bear Creek, Wyoming

PROJECT NAME:

Bear Creek Uranium

DATE:

August 5, 2011

PROJECT NO.: 117-7252001

TITLE:

**Figure 14A. Distribution  
of Radium  
Concentrations,  
February 2011**



**Figure 14B. Temporal Changes in Radium Concentrations,  
Lang Draw**

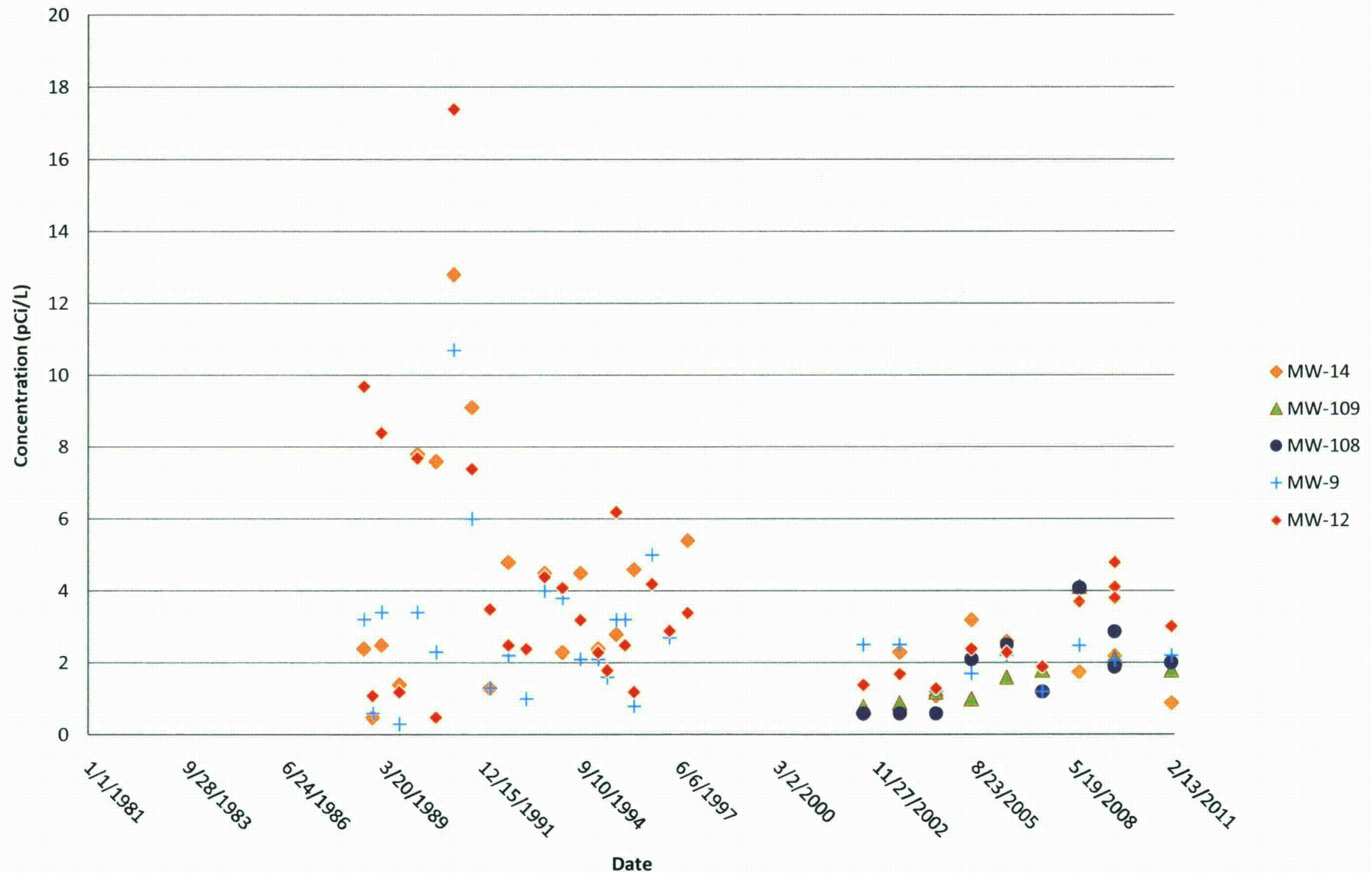
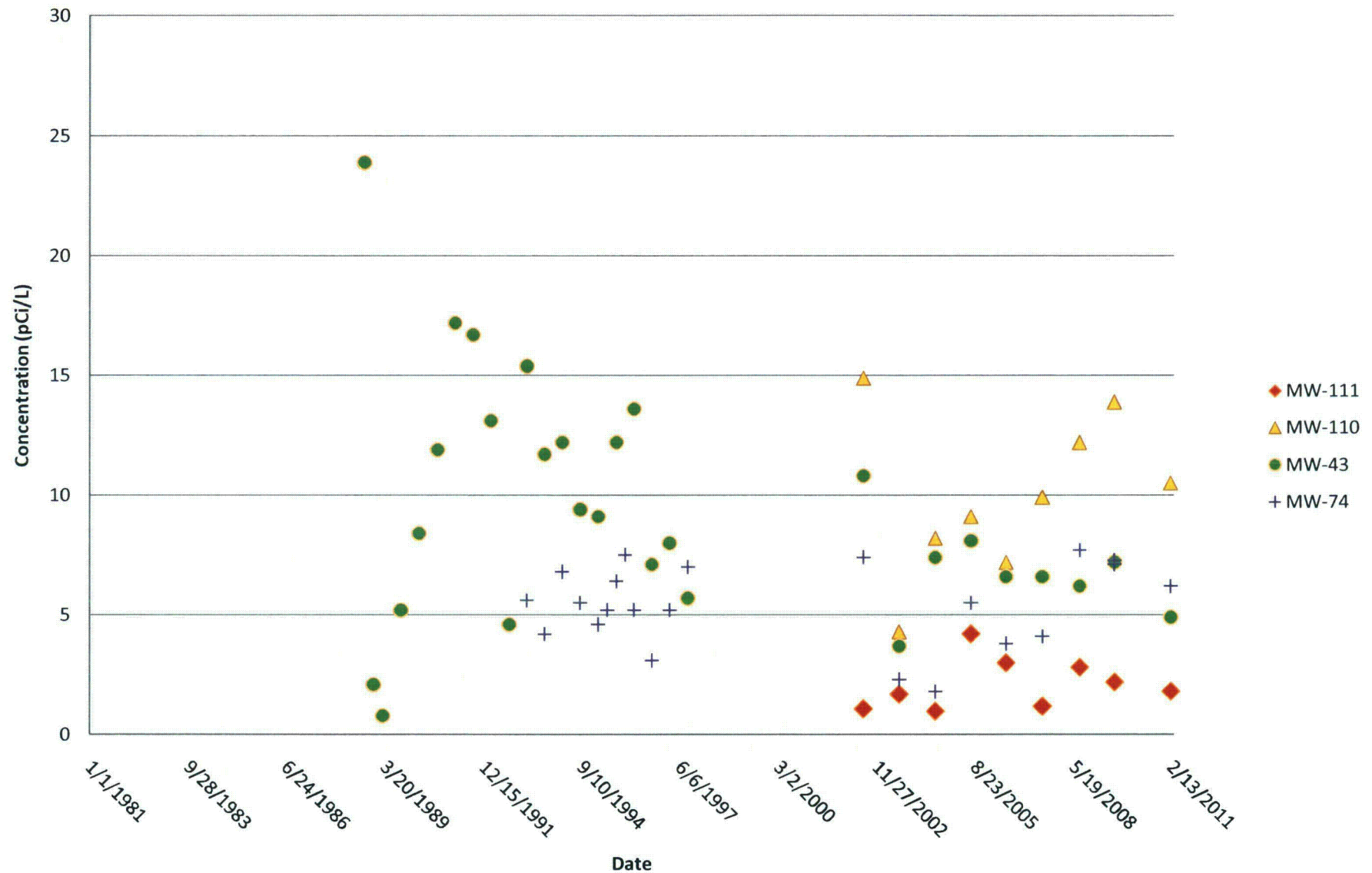


**Figure 14C. Temporal Changes in Radium Concentrations, Northern Pathway**

The figure is a scatter plot titled "Figure 14C. Temporal Changes in Radium Concentrations, Northern Pathway". The y-axis is labeled "Concentration (pCi/L)" and ranges from 0 to 30 in increments of 5. The x-axis is labeled "Date" and shows dates from 1/1/1981 to 2/13/2011. The legend indicates four data series: MW-111 (red diamonds), MW-110 (yellow triangles), MW-43 (green circles), and MW-74 (blue plus signs). MW-43 has the highest concentrations, starting around 24 pCi/L in 1988 and generally decreasing to around 5 pCi/L by 2011. MW-110 shows concentrations between 4 and 15 pCi/L. MW-111 and MW-74 show the lowest concentrations, generally below 10 pCi/L.

Date	MW-111 (pCi/L)	MW-110 (pCi/L)	MW-43 (pCi/L)	MW-74 (pCi/L)
3/20/1989			24	
3/20/1989			2	
3/20/1989			1	
3/20/1989			5	
3/20/1989			8	
12/15/1991			4.5	
12/15/1991			12	
12/15/1991			15	
12/15/1991			17	
12/15/1991			17	
9/10/1994			9	5
9/10/1994			9	5
9/10/1994			12	5
9/10/1994			12	5
9/10/1994			13	5
6/6/1997			5.5	5
6/6/1997			8	5
3/2/2000				
11/27/2002	1	15	11	7
11/27/2002	2	4	4	2
11/27/2002	2	8	7	2
8/23/2005	4	9	8	5
8/23/2005	3	7	6.5	4
8/23/2005	1	10	6.5	4
5/19/2008	3	12	6	7
5/19/2008	2	14	7	7
2/13/2011	2	10.5	5	6

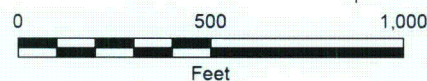






 Monitoring Well  
 (0.017)

Concentrations are in mg/L (milligrams per liter)  
 ACL (alternate concentration limit) = 3.8 mg/L



ISSUED BY:



336 Centennial pkwy, Suite 210  
 Louisville, Colorado 80027

ISSUED FOR:

**Bear Creek Disposal Site**  
 Bear Creek, Wyoming

PROJECT NAME:

Bear Creek Uranium

DATE:

August 5, 2011

PROJECT NO.: 117-7252001

TITLE:

**Figure 15A. Distribution  
 of Nickel  
 Concentrations,  
 February 2011**



**Figure 15B. Temporal Changes in Nickel Concentrations,  
Lang Draw**

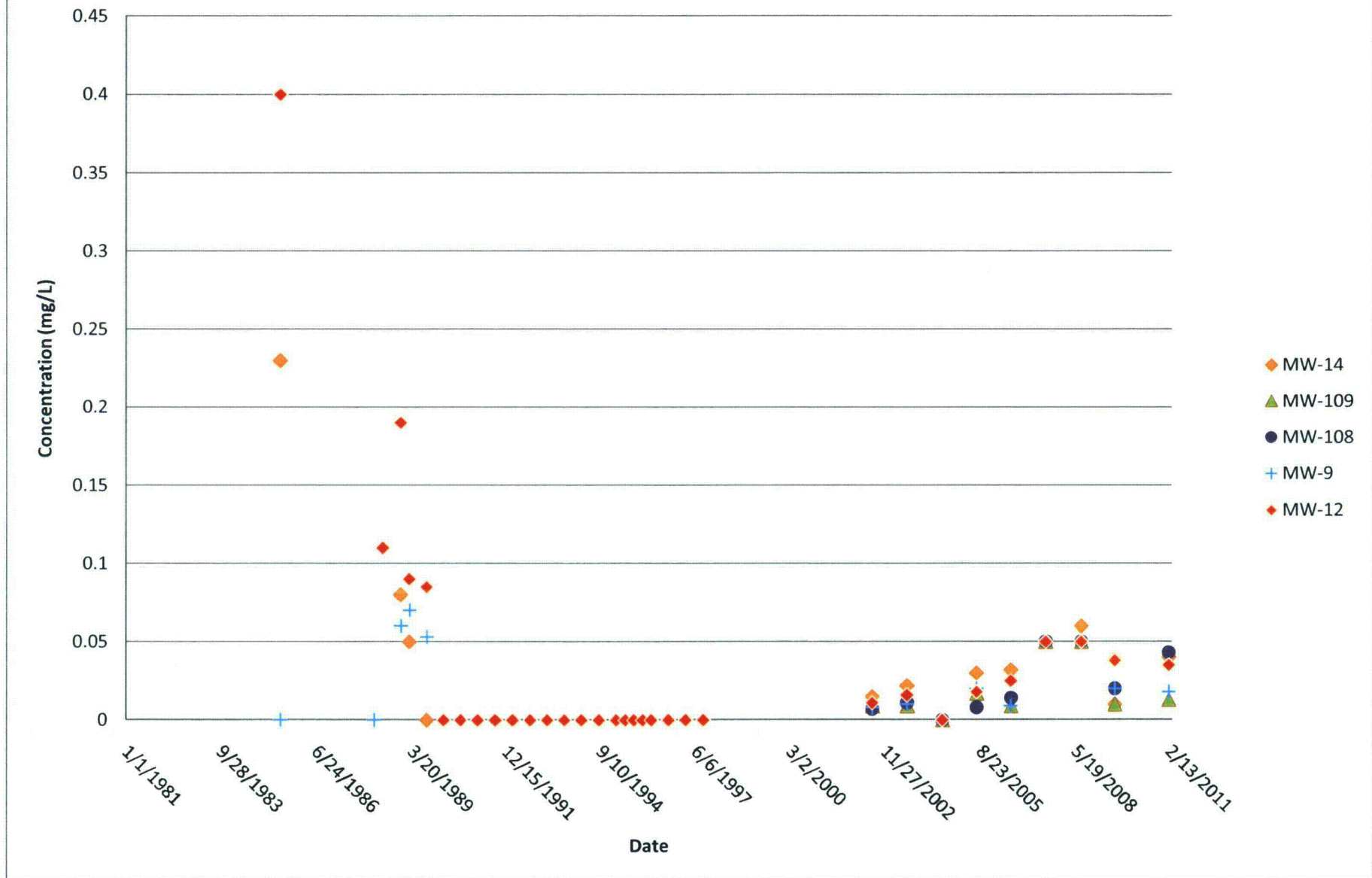




**Figure 15C. Temporal Changes in Nickel Concentration,  
Northern Pathway**

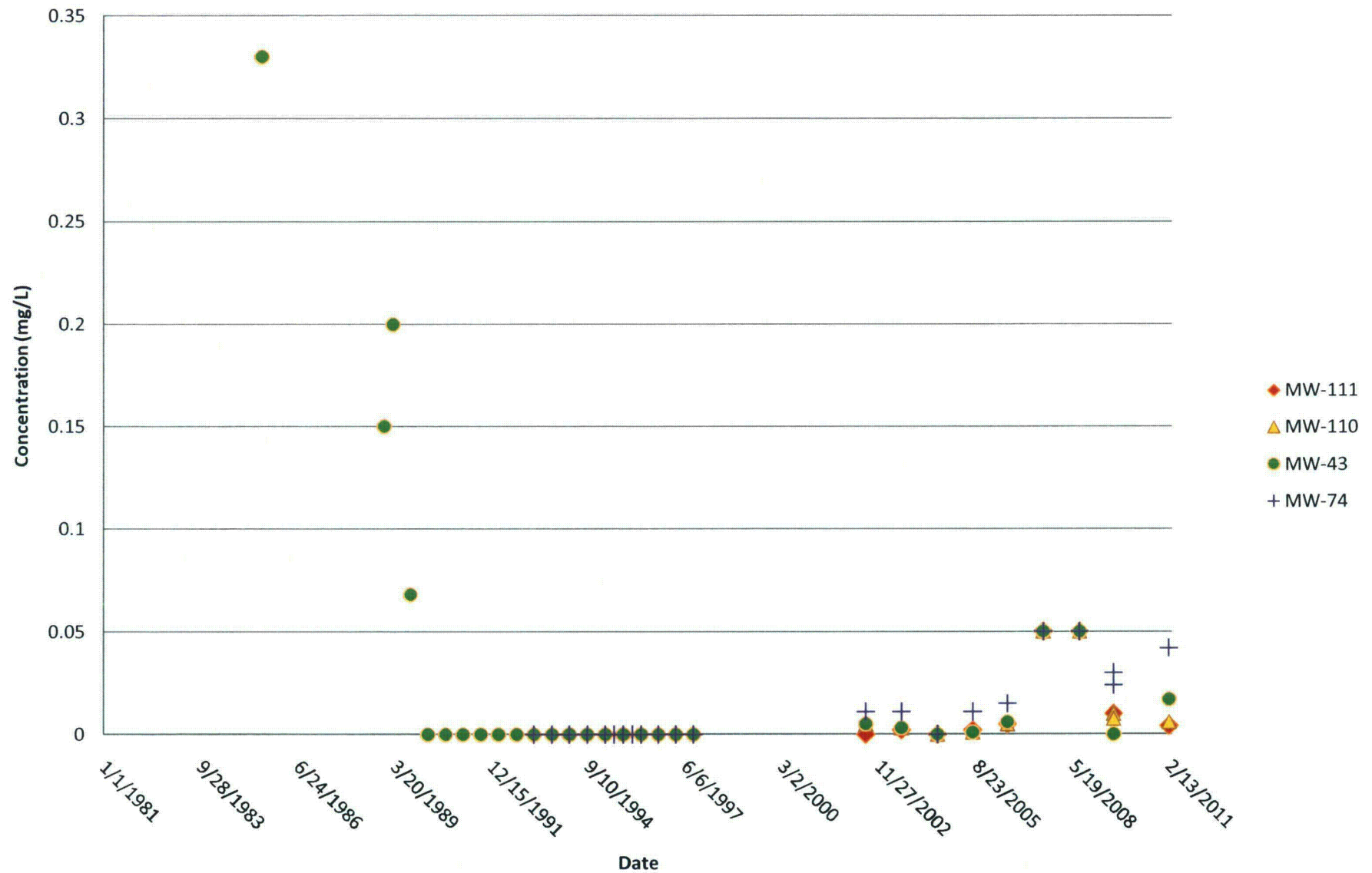


**Figure 16A. Simulated Initial Values of Uranium  
Lang Draw**

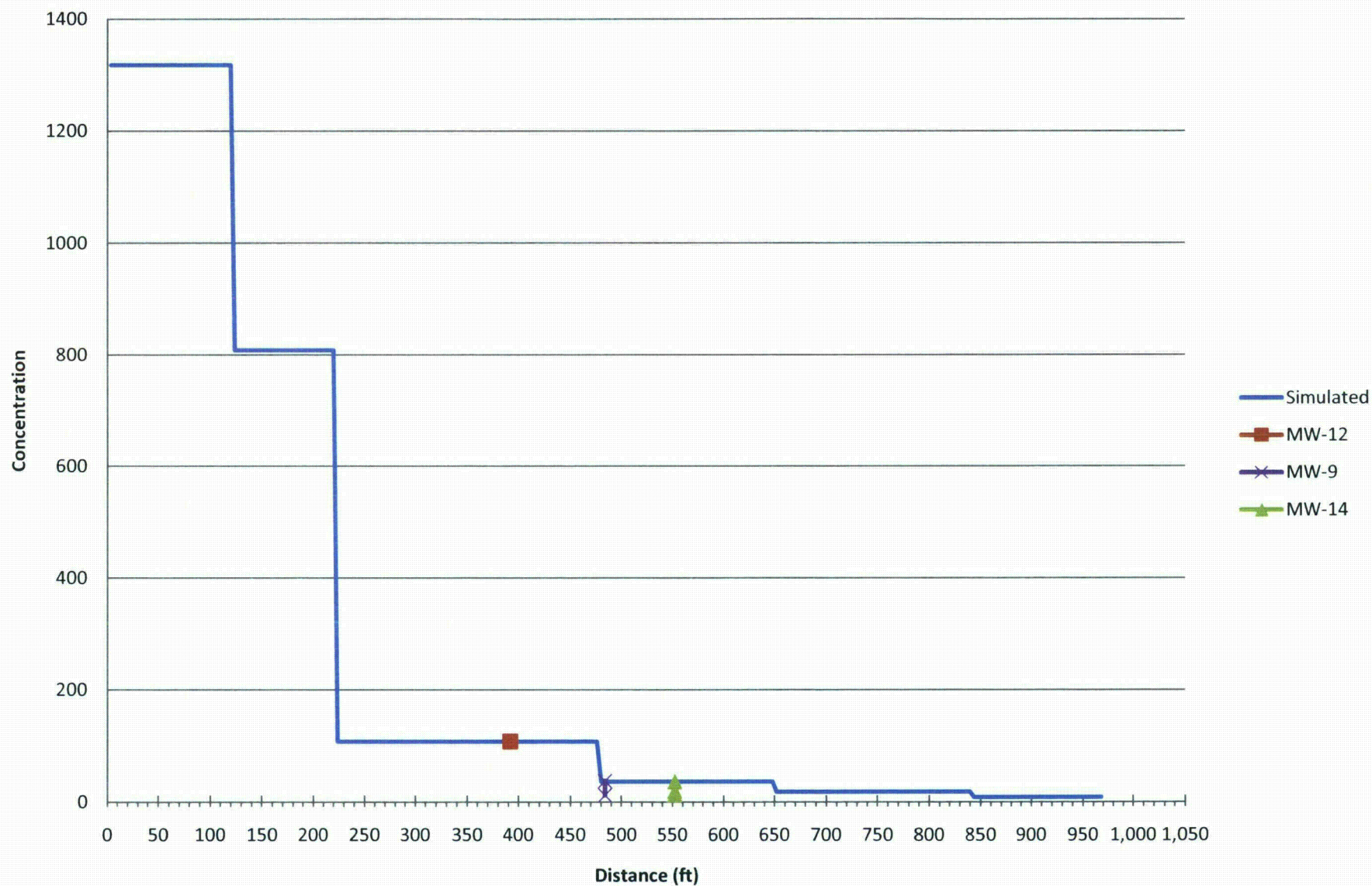


**Figure 16B. Simulated Initial Values of Sulfate  
Lang Draw**

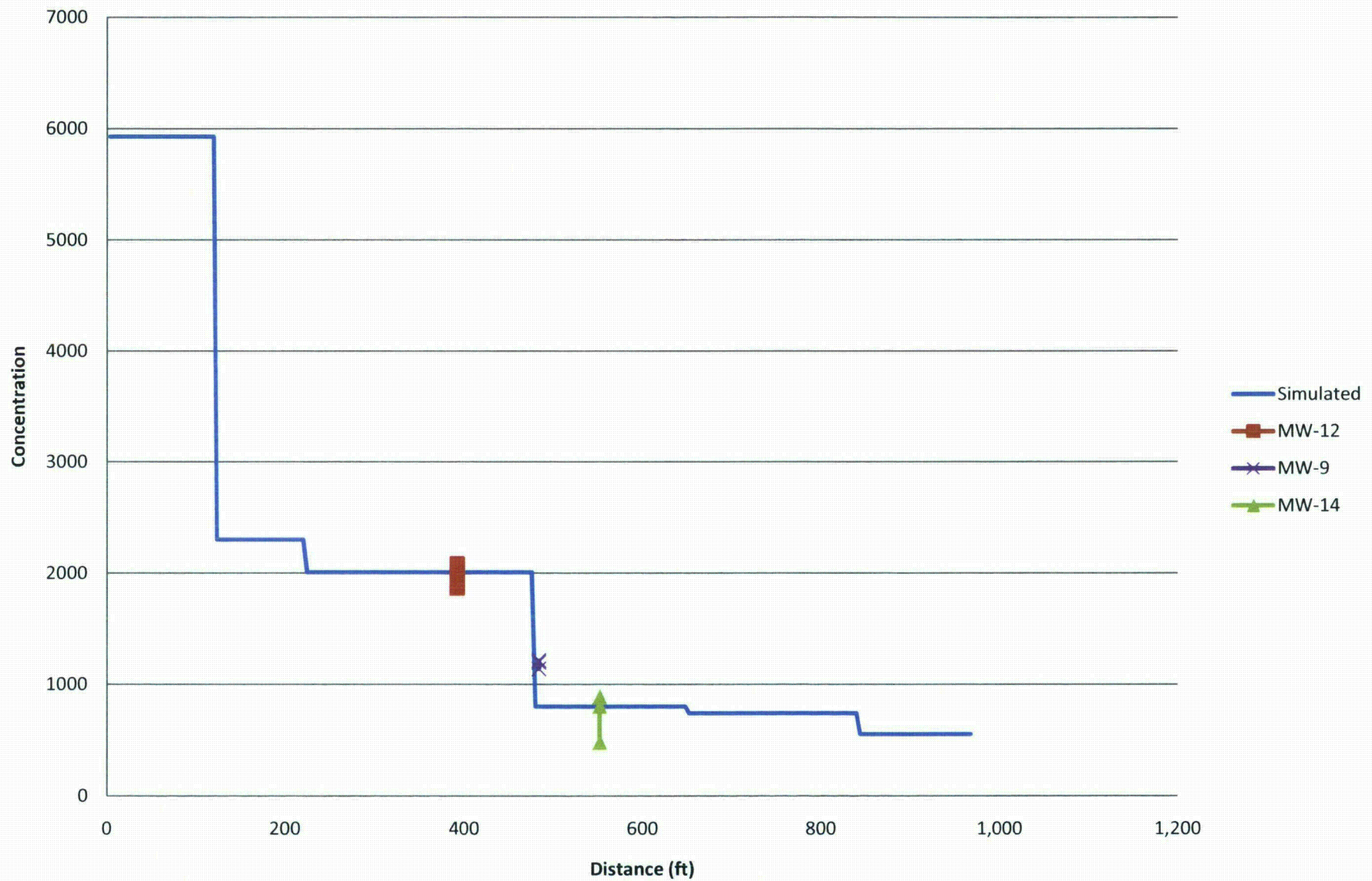




**Figure 16C. Simulated Initial Values of Chloride  
Lang Draw**

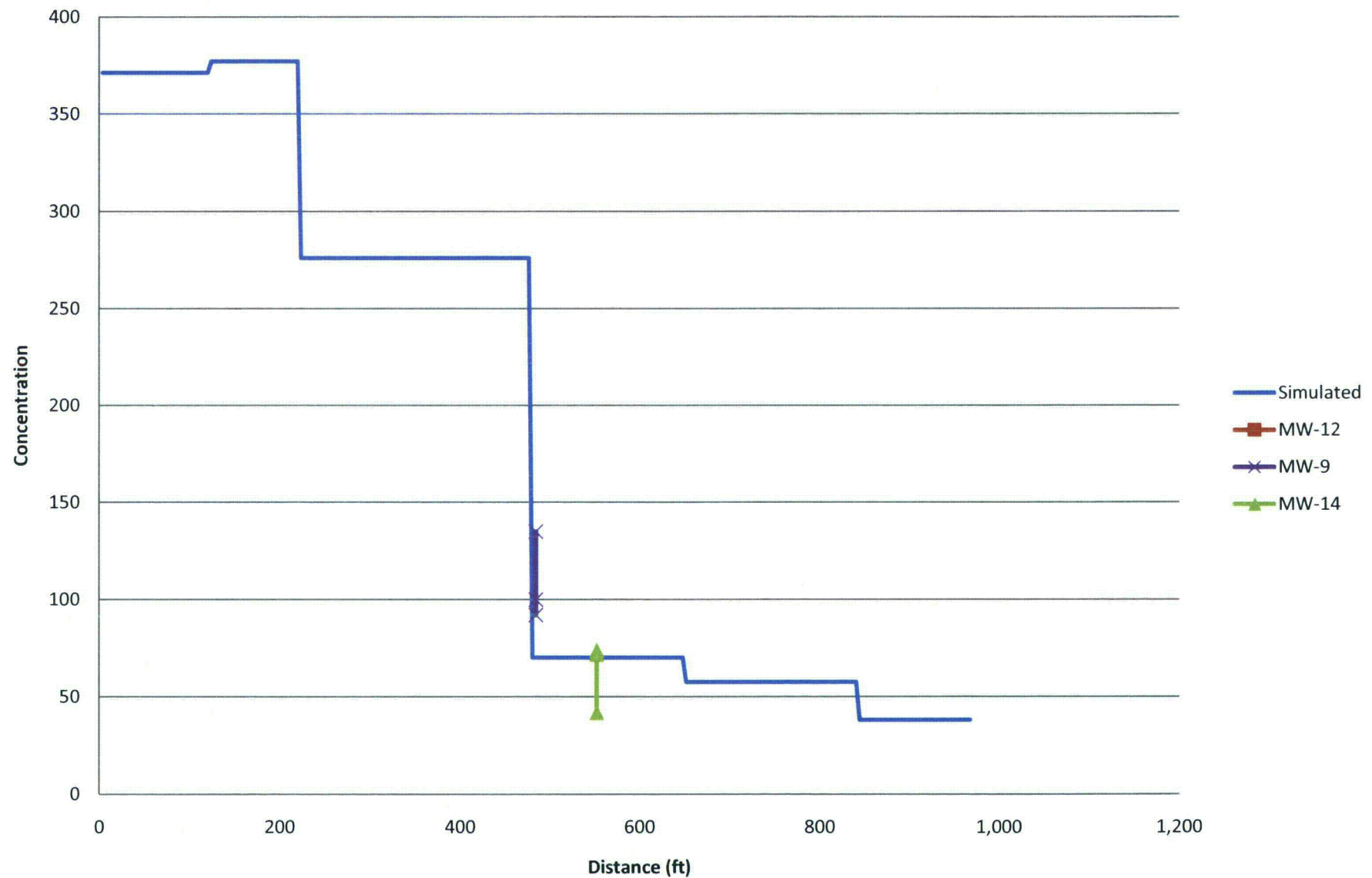


**Figure 16D. Simulated Initial Values of pH  
Lang Draw**

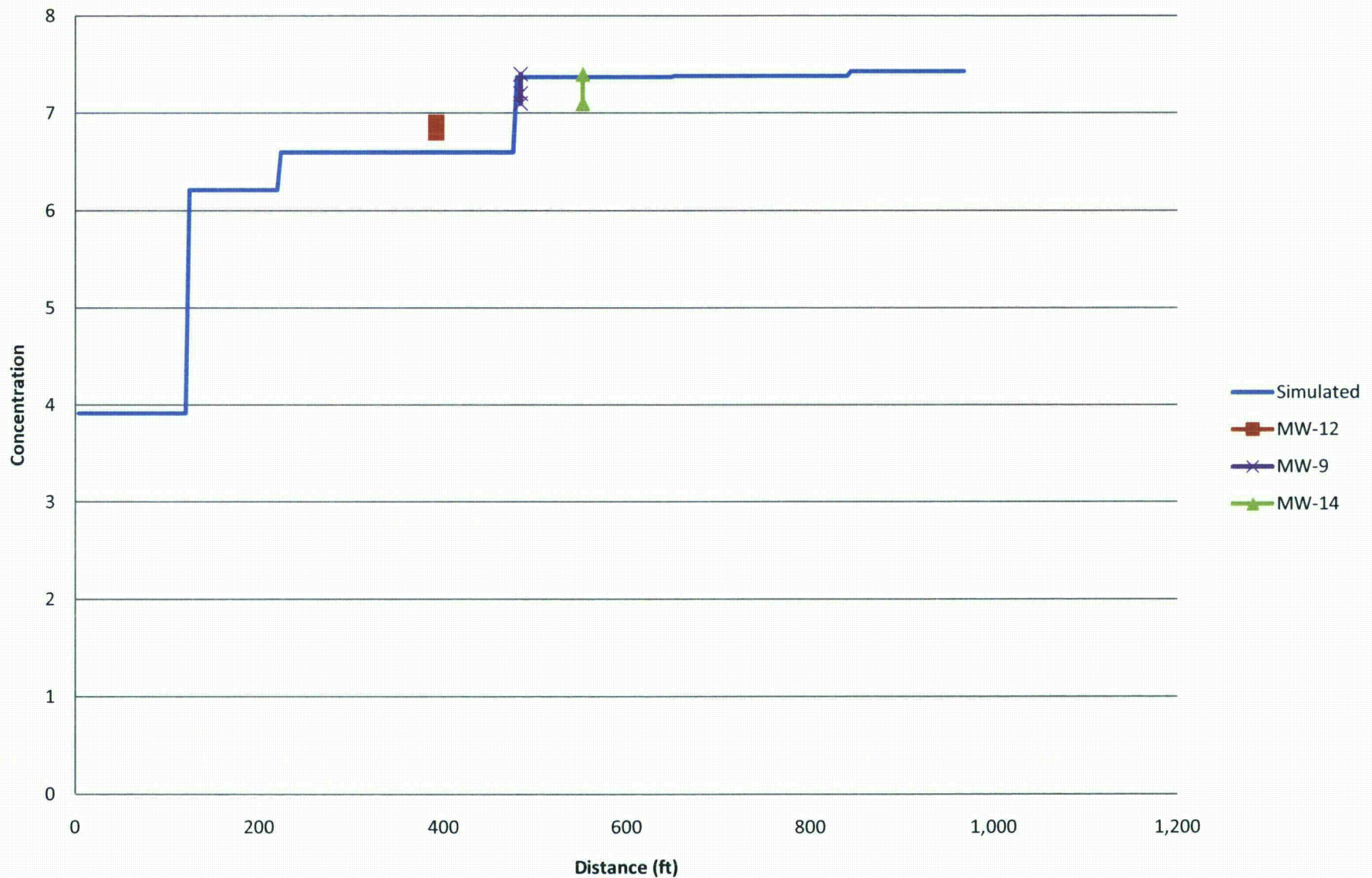


**Figure 16E. Simulated Initial Values of Radium  
Lang Draw**

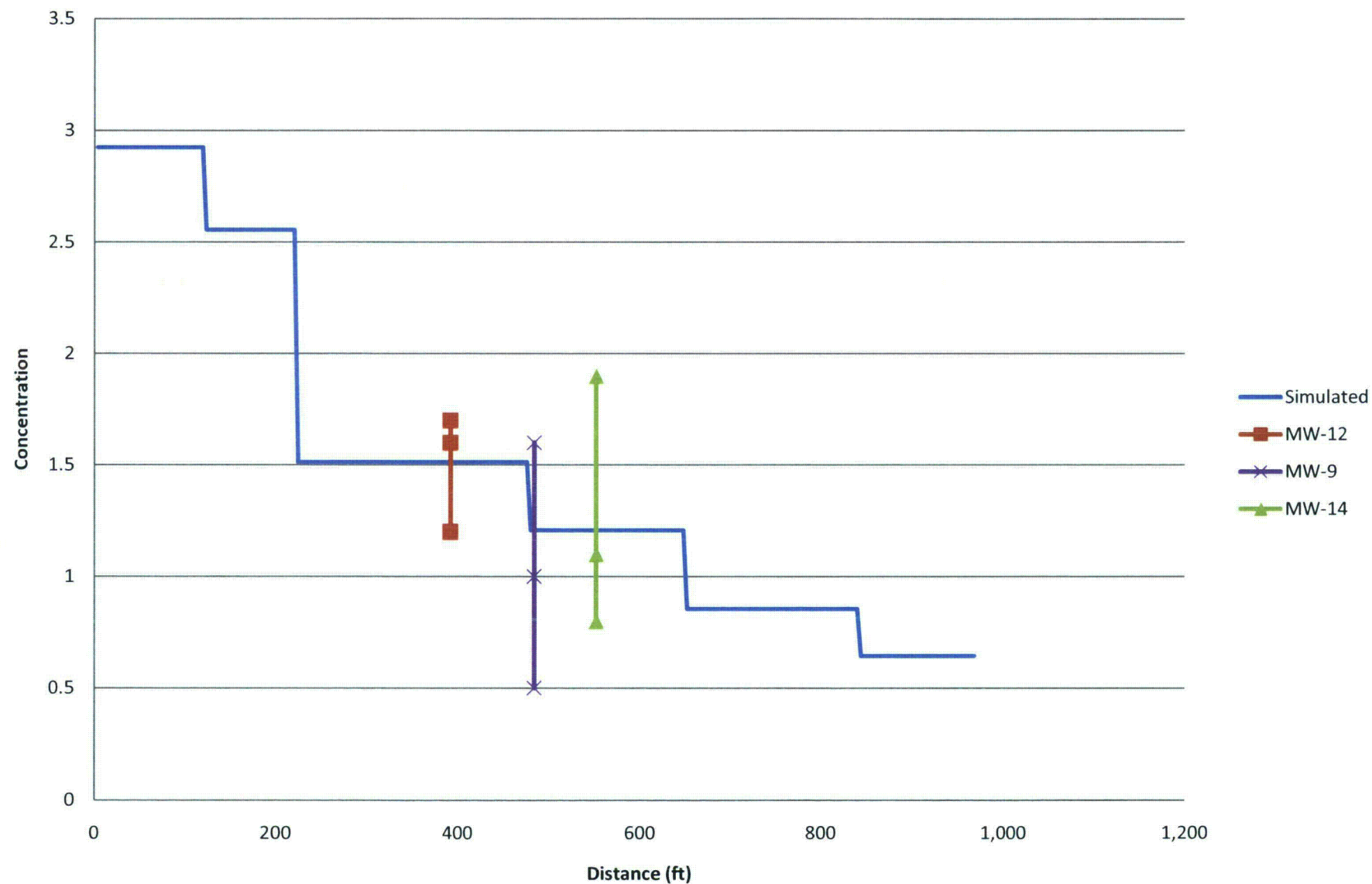




**Figure 16F. Simulated Initial Values of Nickel  
Lang Draw**

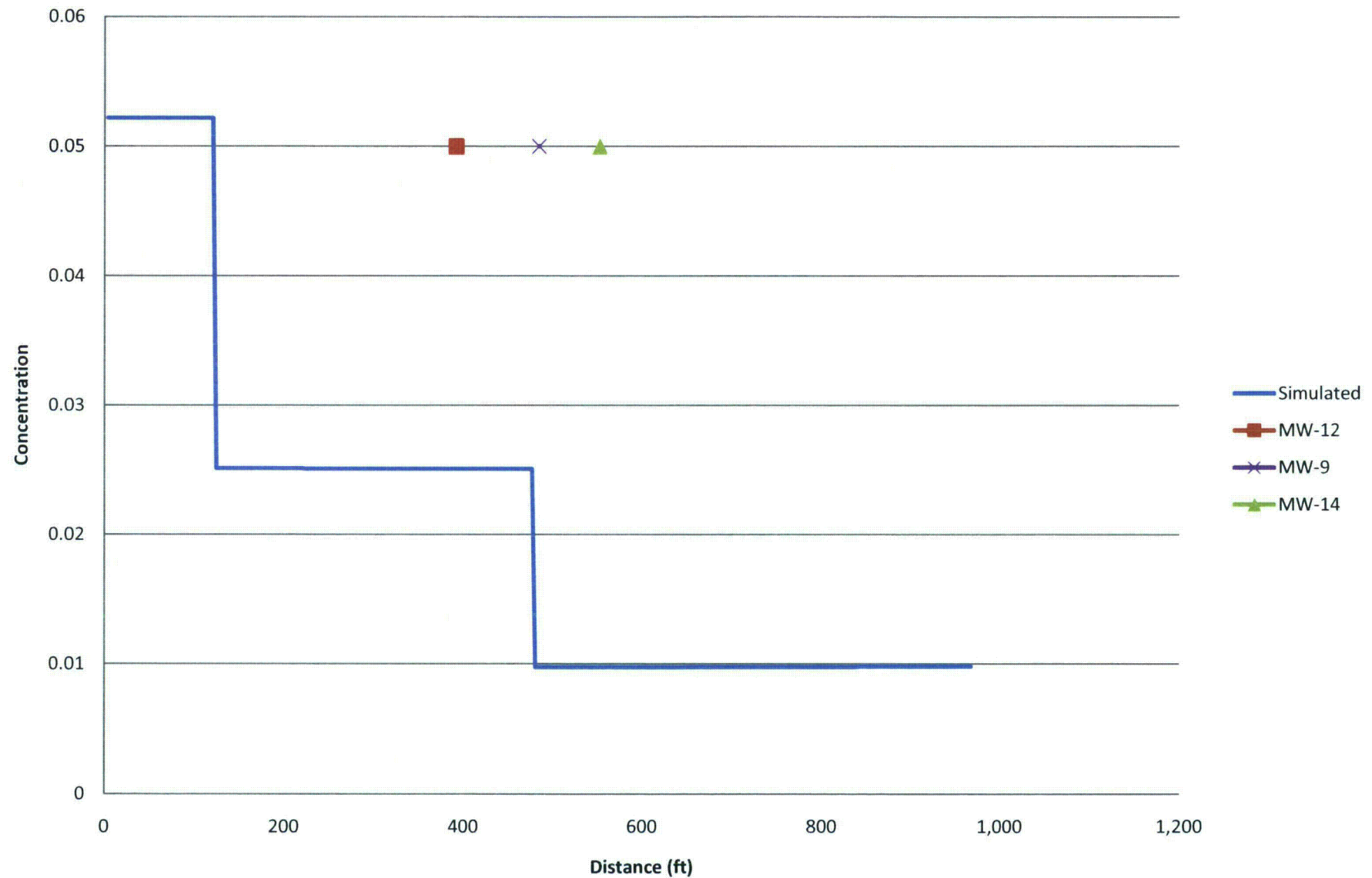


**Figure 17 A. Simulated Breakthrough of Uranium  
Lang Draw**

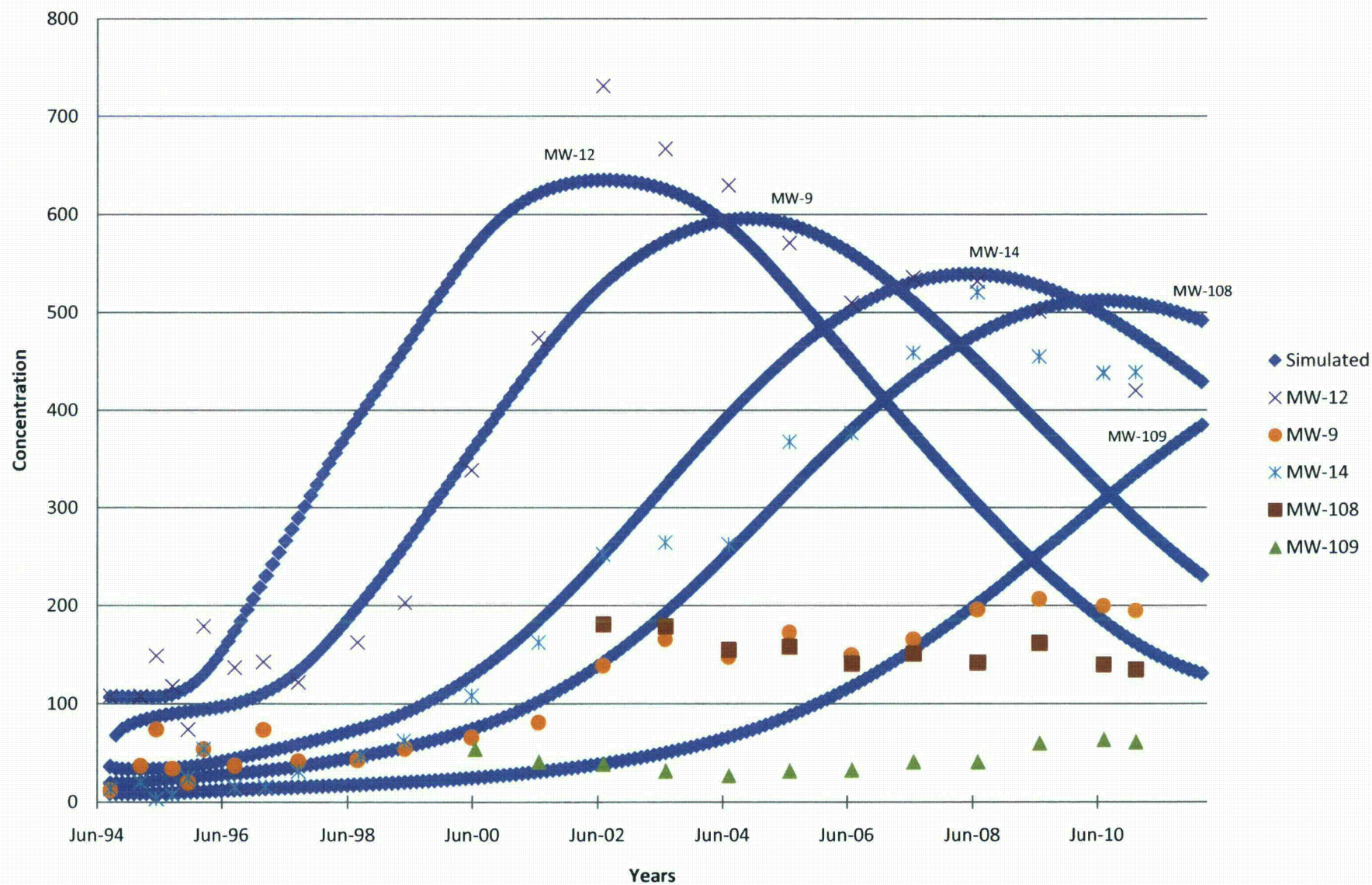


**Figure 17B. Simulated Breakthrough of Sulfate  
Lang Draw**

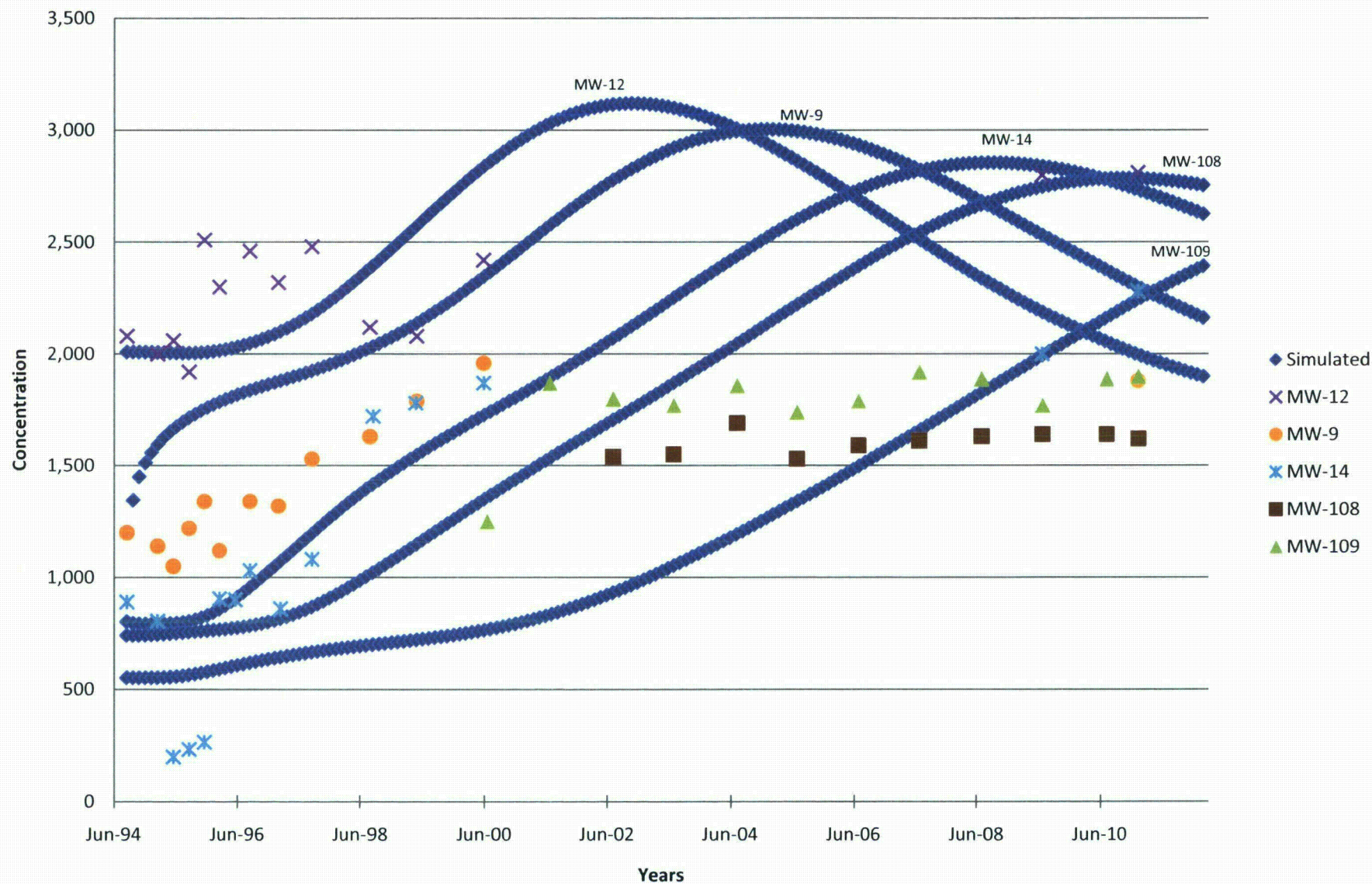




**Figure 17C. Simulated Breakthrough of Chloride  
Lang Draw**

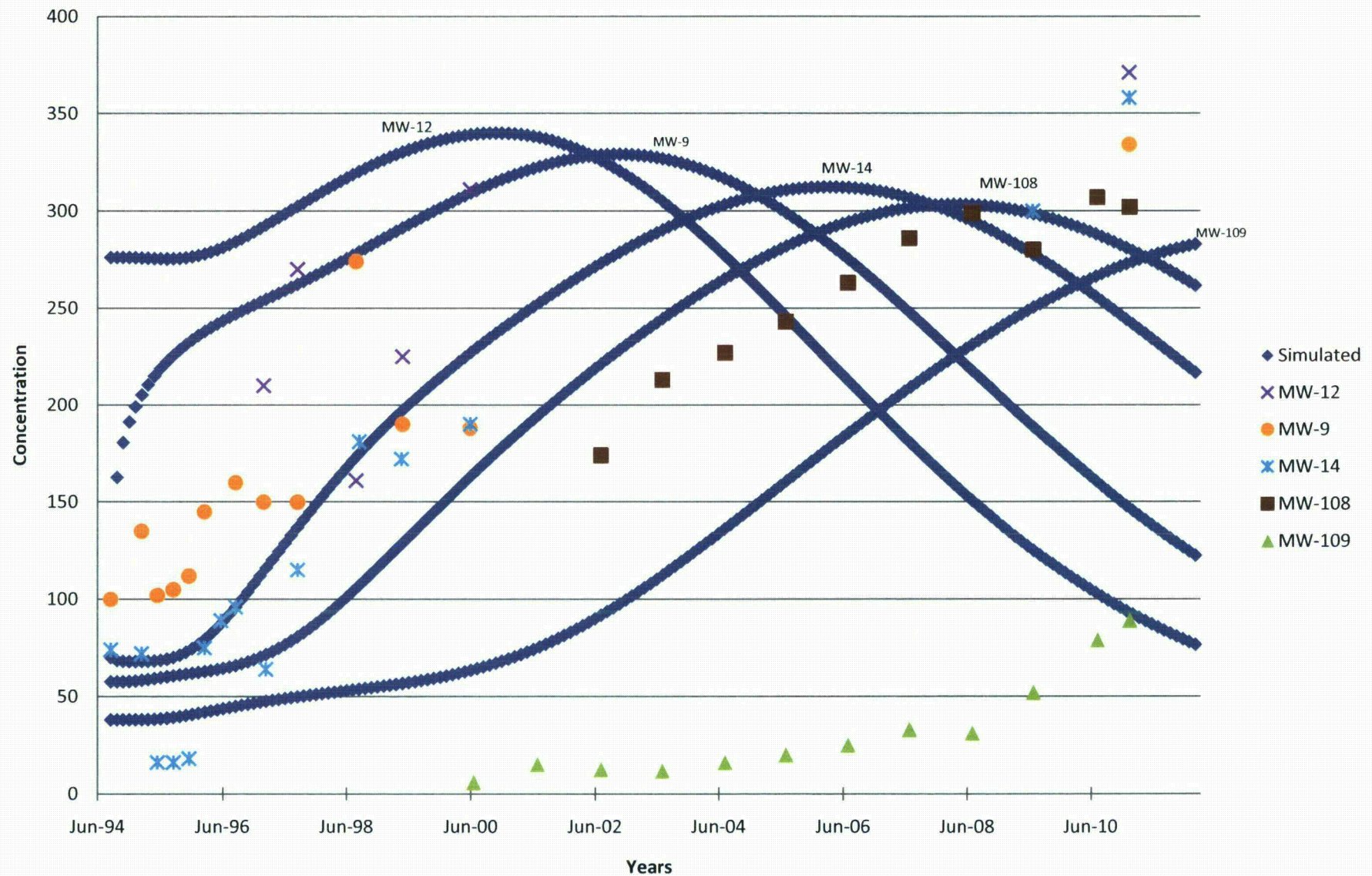


**Figure 17D. Simulated Breakthrough of pH  
Lang Draw**

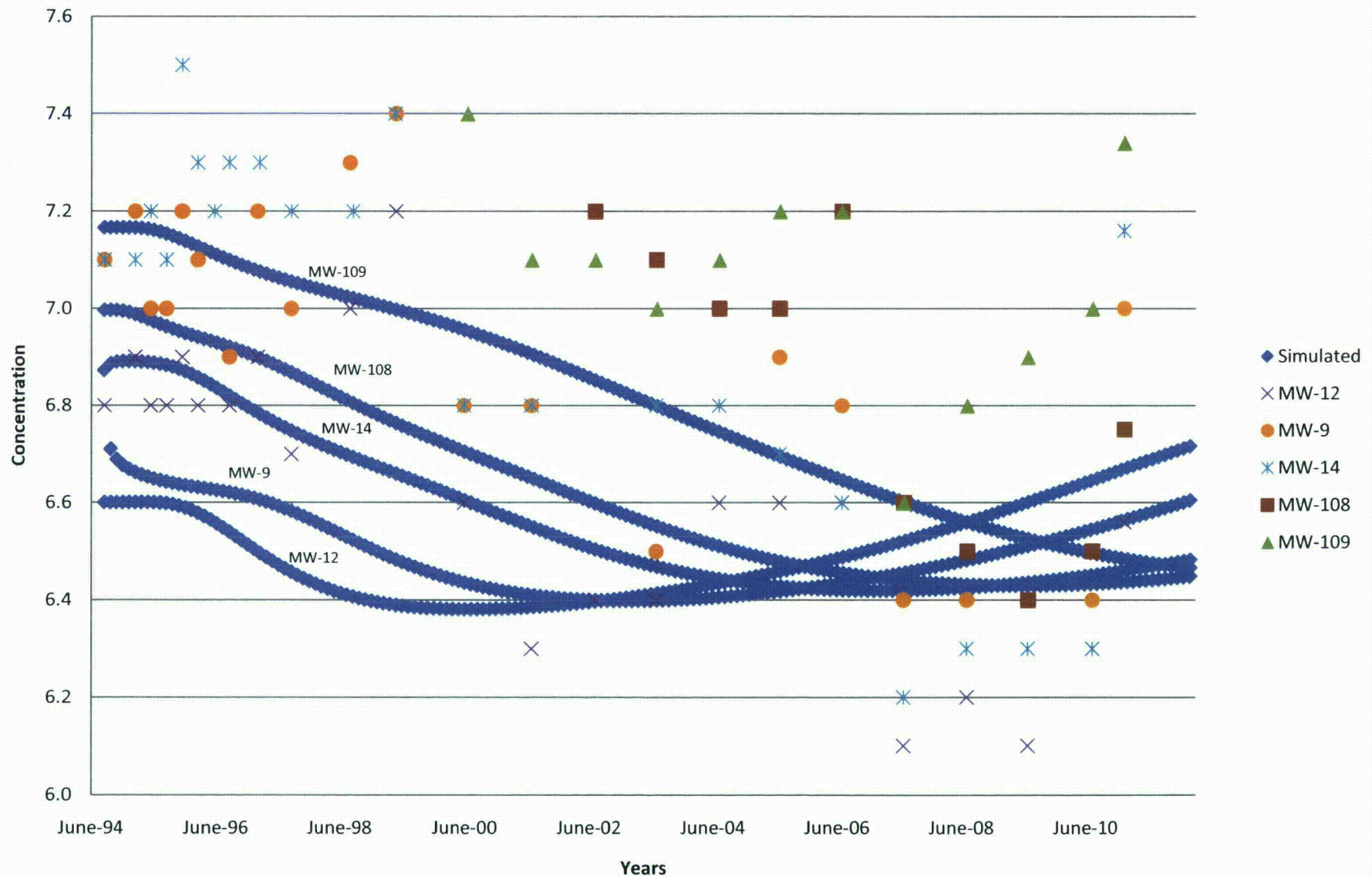


**Figure 17E. Simulated Breakthrough of Radium  
Lang Draw**

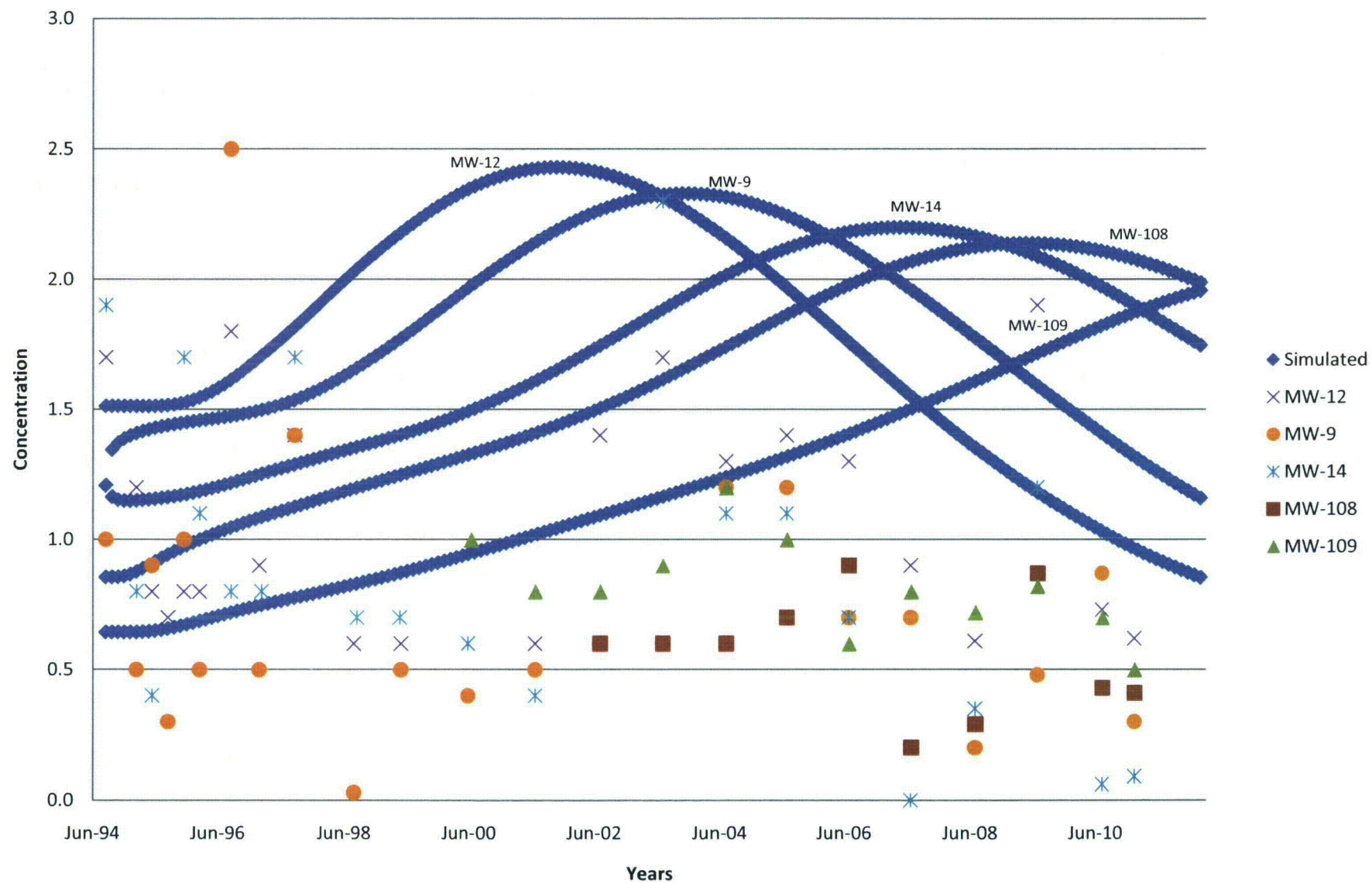




**Figure 17F. Simulated Breakthrough of Nickel  
Lang Draw**

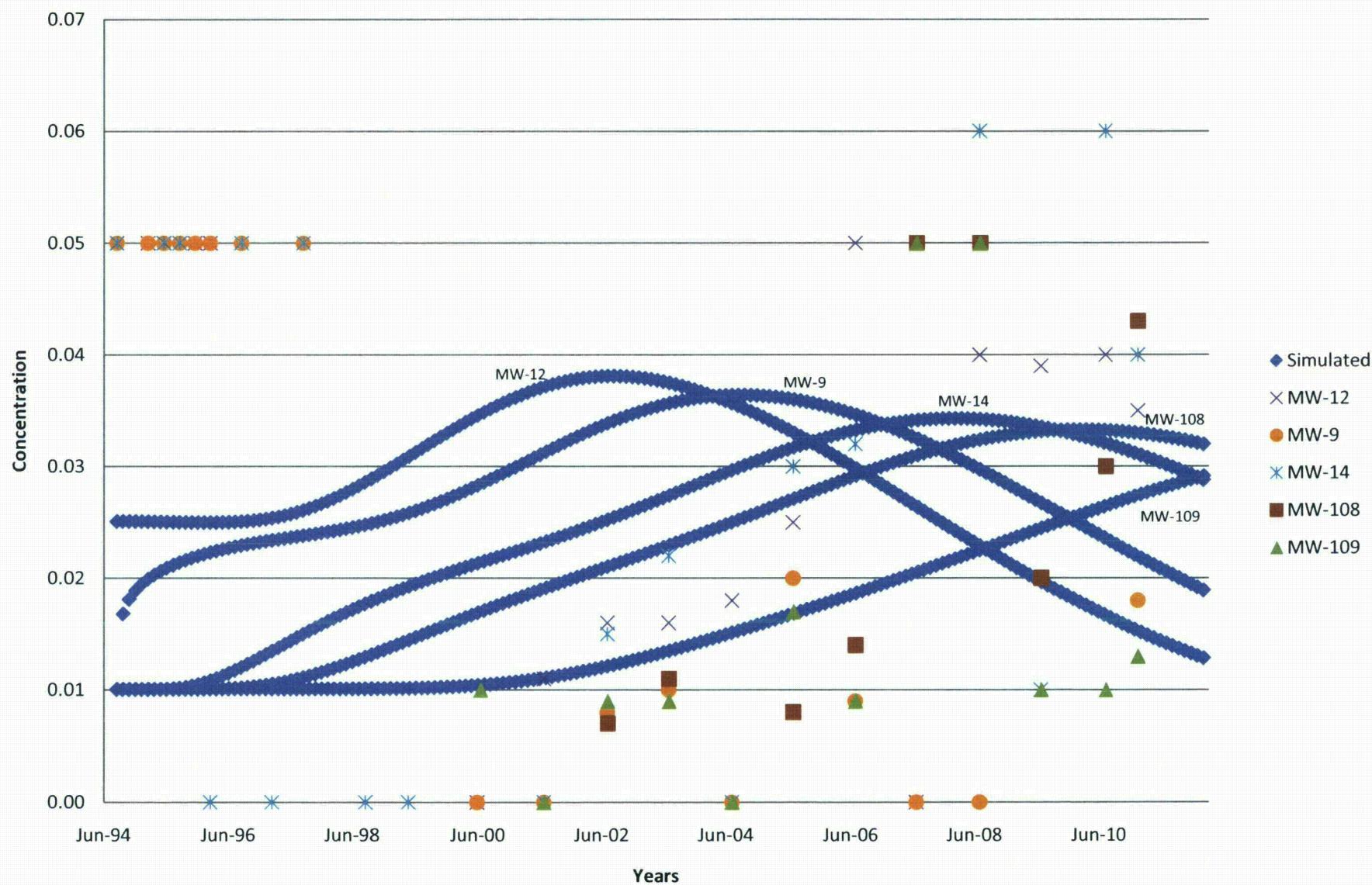


Figure 18A. Predicted Breakthrough of Uranium Lang Draw

The graph displays the predicted breakthrough of uranium concentration over time for various monitoring wells (MW-12, MW-9, MW-14, MW-108, MW-109) and simulated data. The Y-axis represents Concentration (0 to 800), and the X-axis represents Years (Aug-94 to May-49).

Legend:

- Simulated (Blue line with diamond markers)
- MW-12 (Purple 'x' markers)
- MW-9 (Orange circle markers)
- MW-14 (Light blue 'x' markers)
- MW-108 (Brown square markers)
- MW-109 (Green triangle markers)

Key observations from the graph:

- The simulated breakthrough curves show a peak concentration around 600-700 units, occurring between 1994 and 2008.
- Monitoring well data points generally follow the simulated curves, with MW-12 showing the highest peak concentration (around 730 units) and MW-109 showing the lowest (around 60 units).
- The breakthrough curves for MW-12, MW-9, MW-14, MW-108, and MW-109 are shifted to the right, indicating a delayed breakthrough compared to the simulated data.

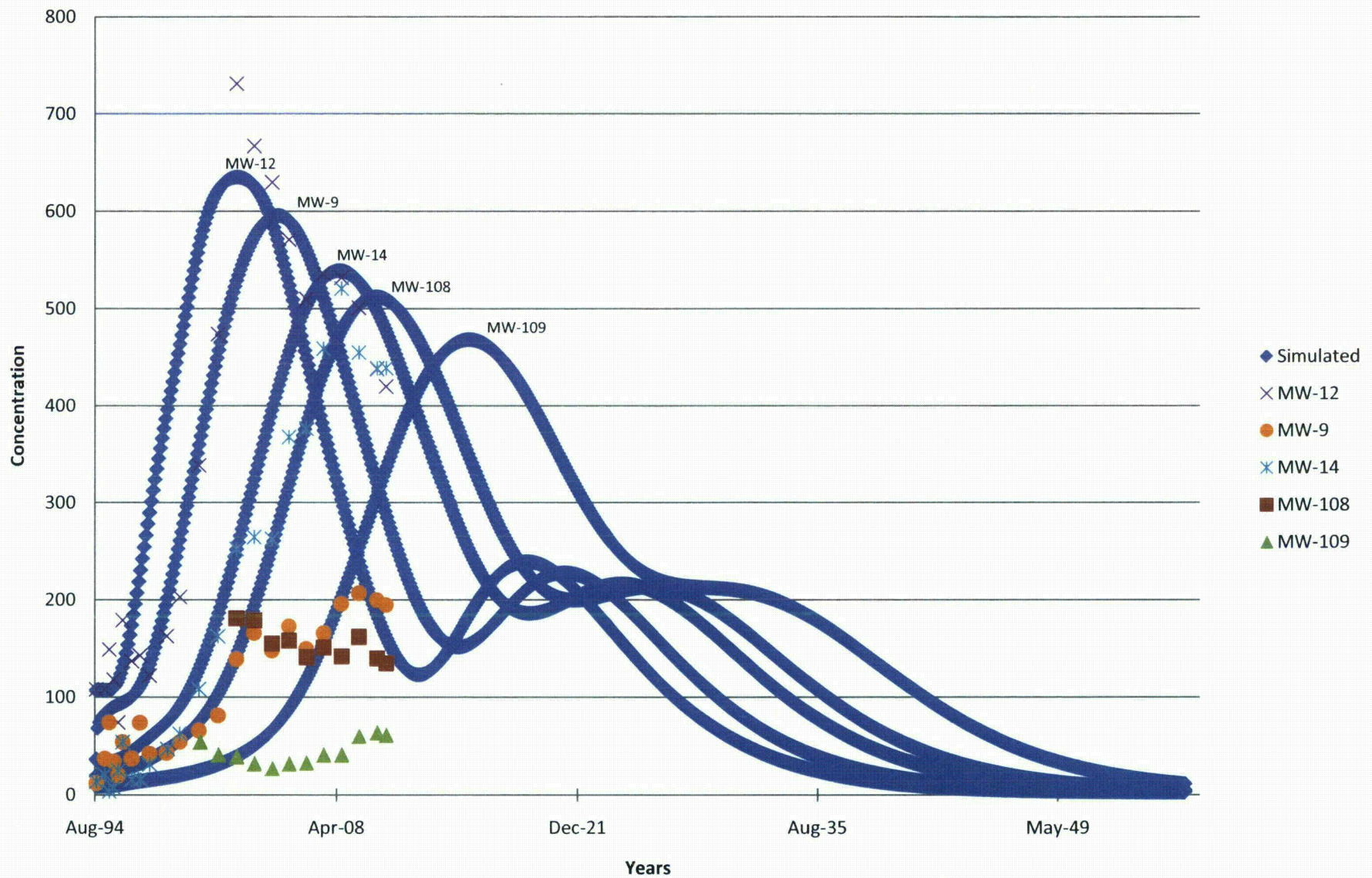


**Figure 18B. Predicted Breakthrough of Sulfate  
Lang Draw**

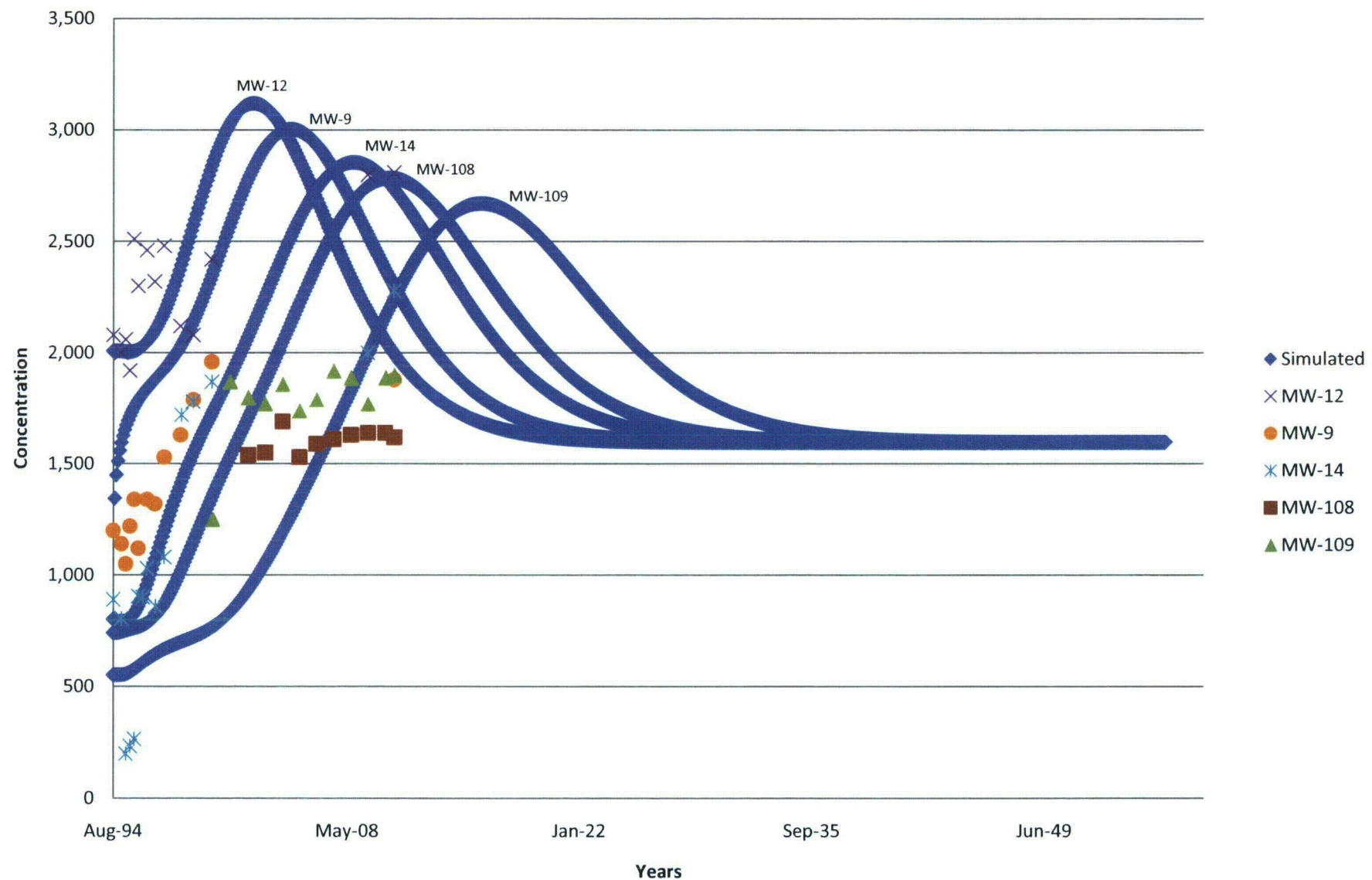




**Figure 18C. Predicted Breakthrough of Chloride  
Lang Draw**

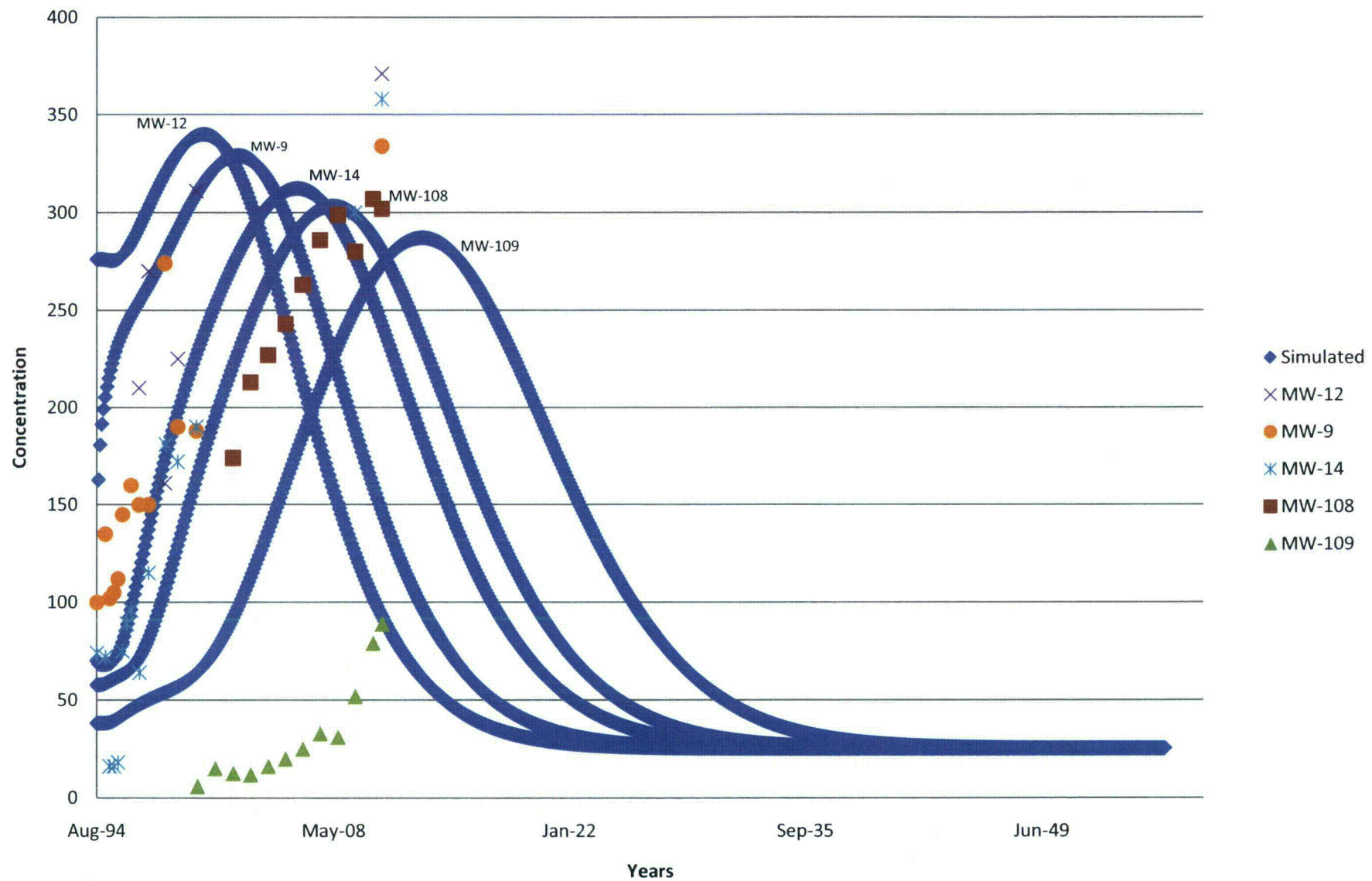


**Figure 18D. Predicted Breakthrough of pH  
Lang Draw**

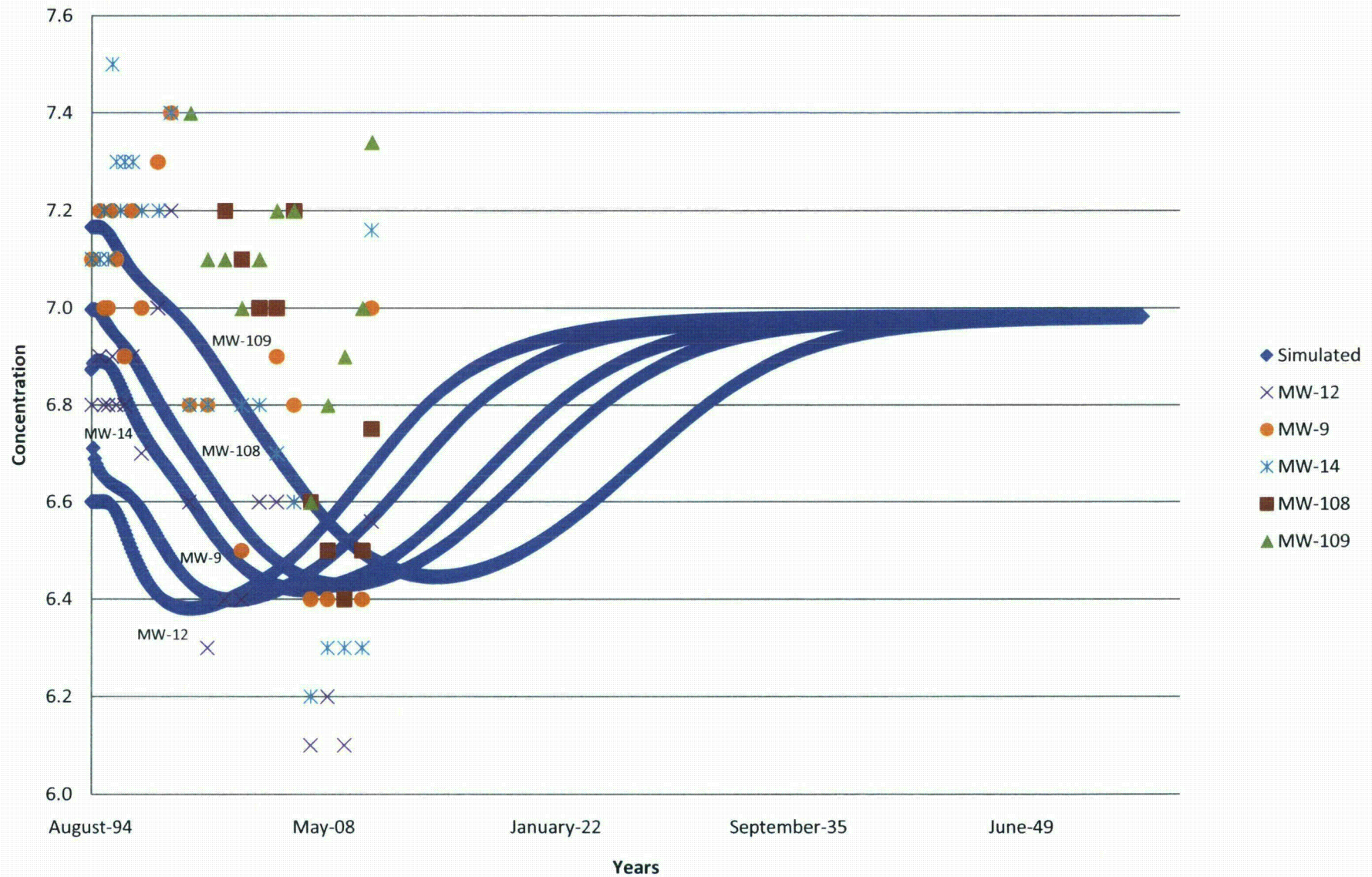


**Figure 18E. Predicted Breakthrough of Radium  
Lang Draw**

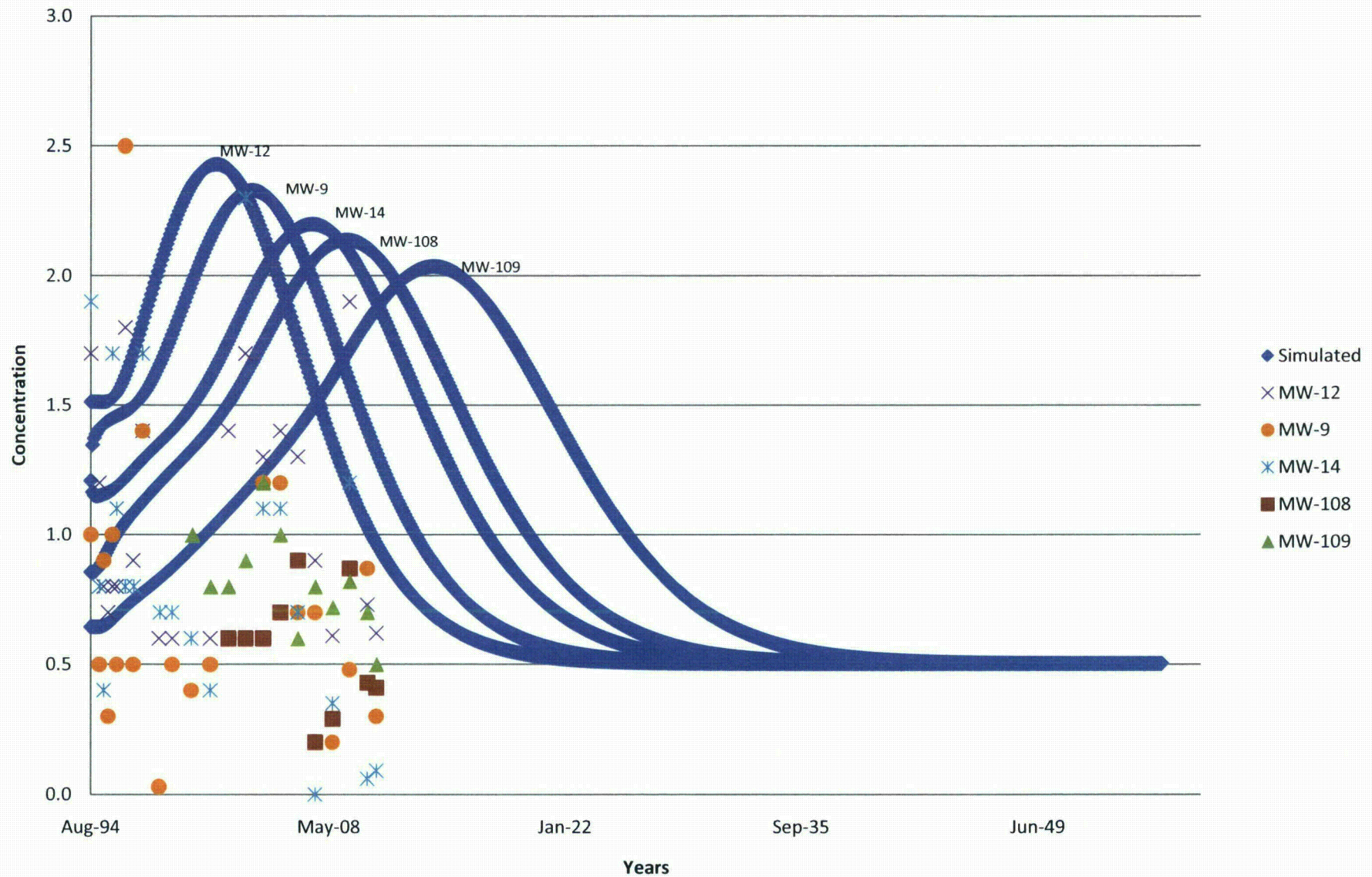




**Figure 18F. Predicted Breakthrough of Nickel  
Lang Draw**

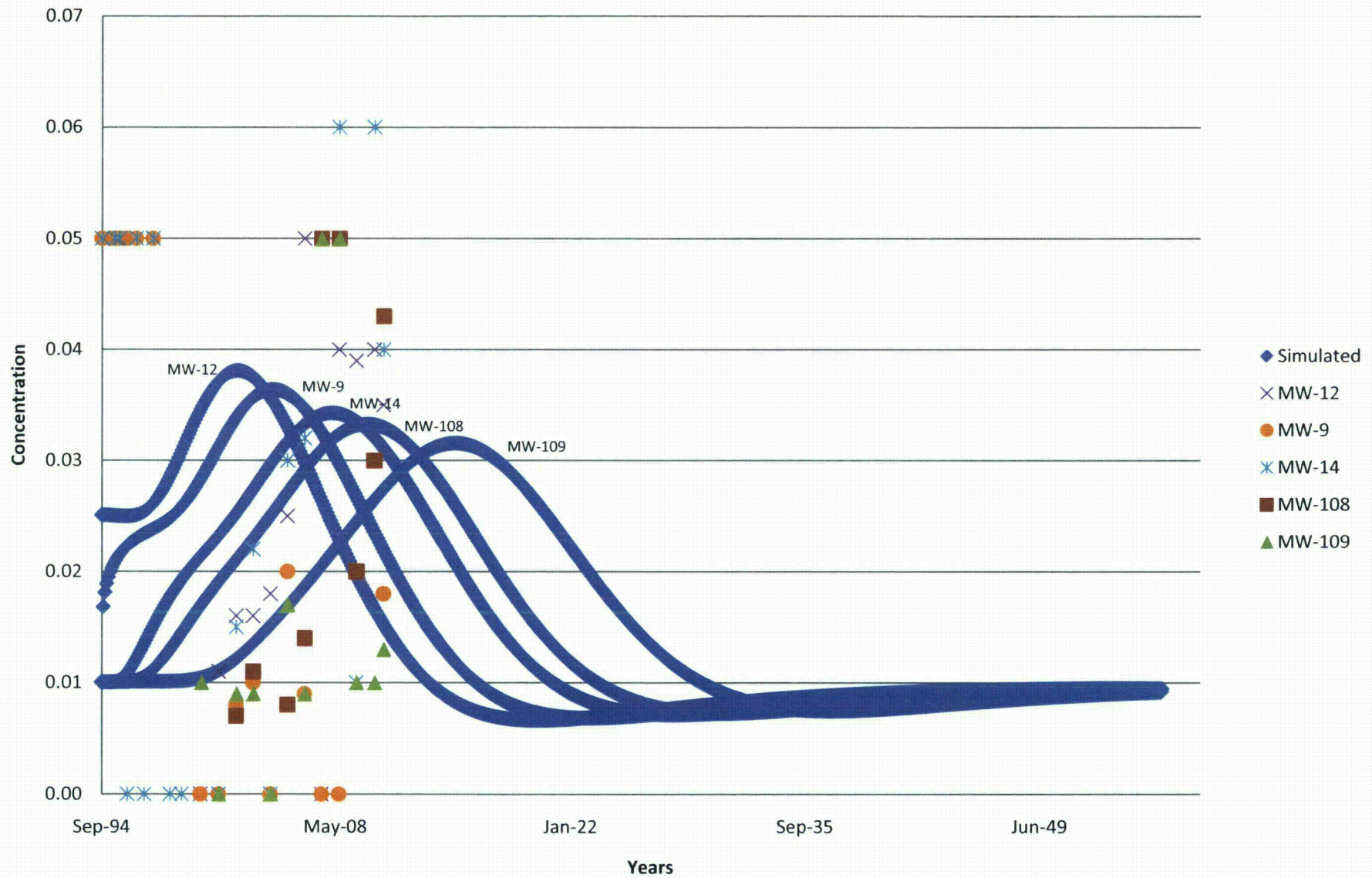


**Figure 19A. Simulated Initial Values of Uranium  
Northern Pathway**

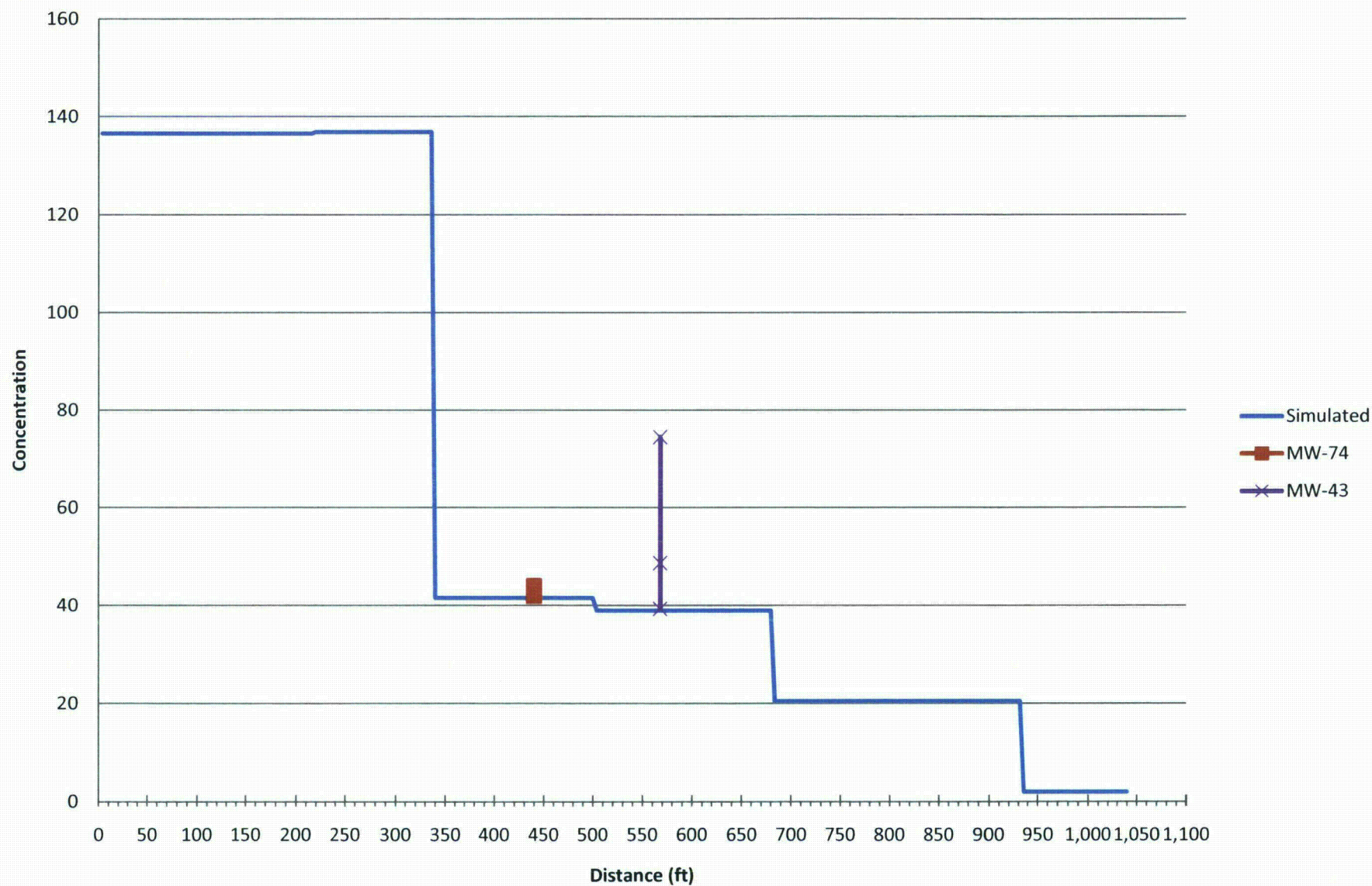


**Figure 19B. Simulated Initial Values of Sulfate  
Northern Pathway**

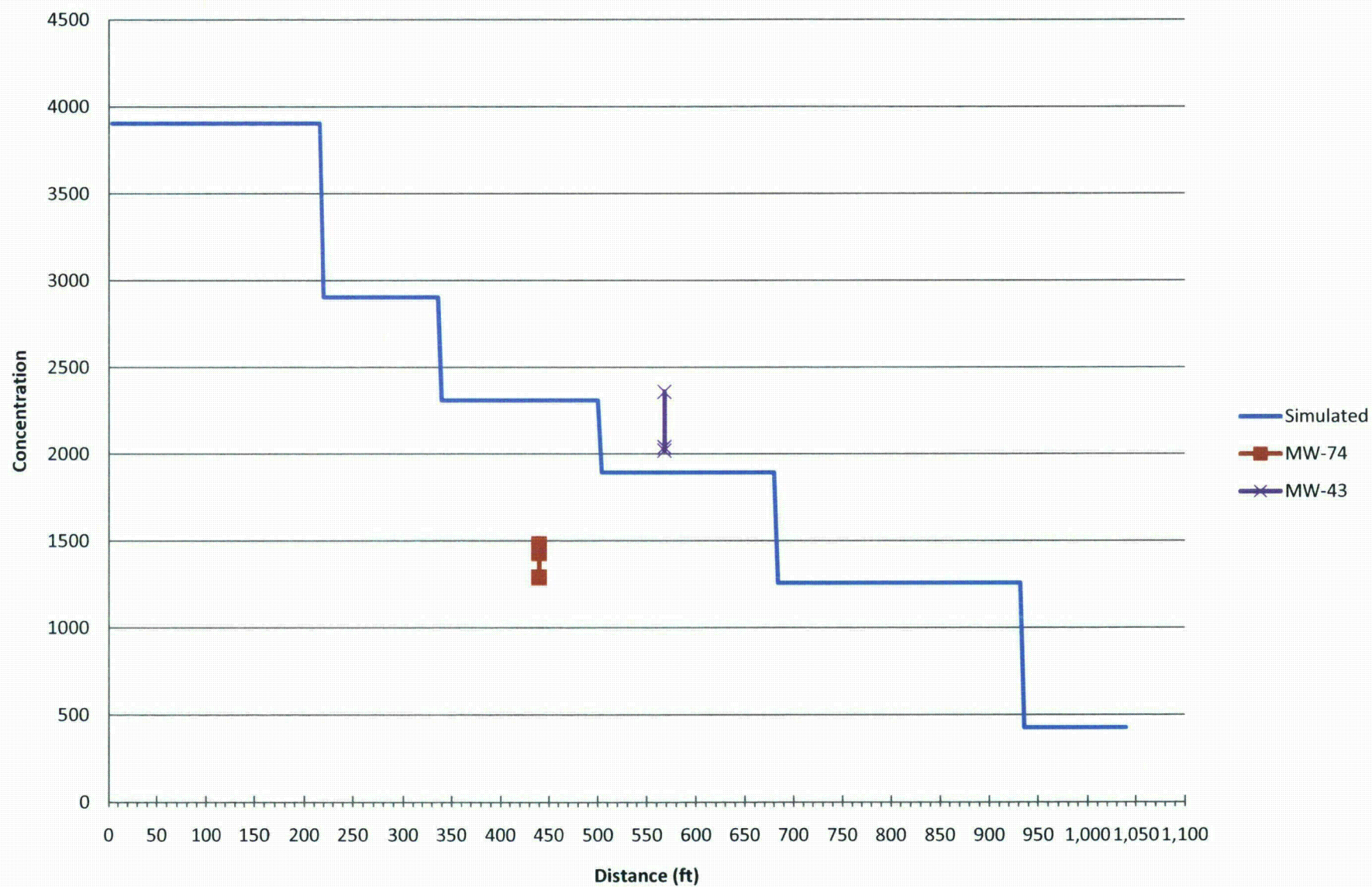




**Figure 19C. Simulated Initial Values of Chloride  
Northern Pathway**

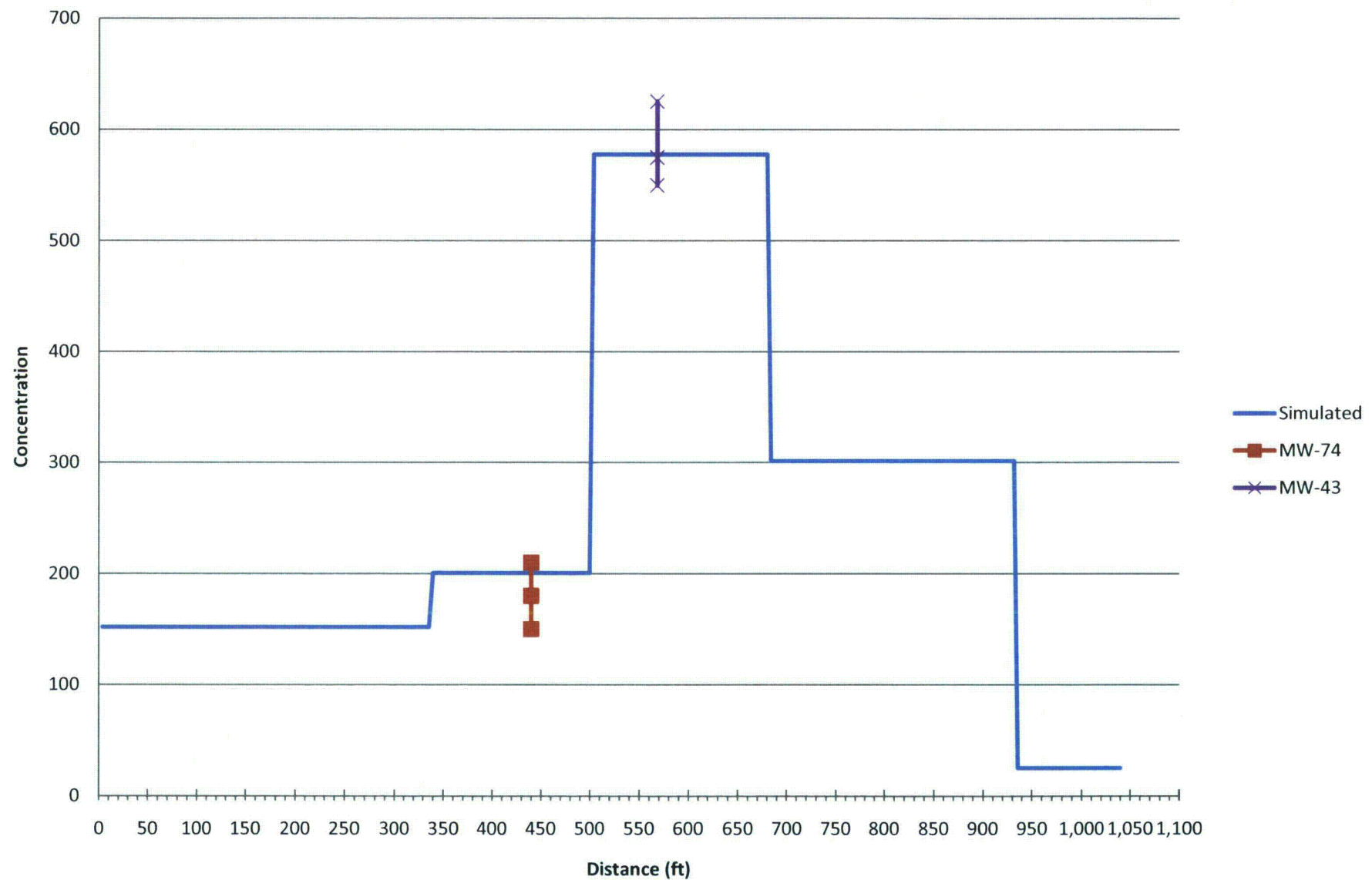


**Figure 19D. Simulated Initial Values of pH  
Northern Pathway**

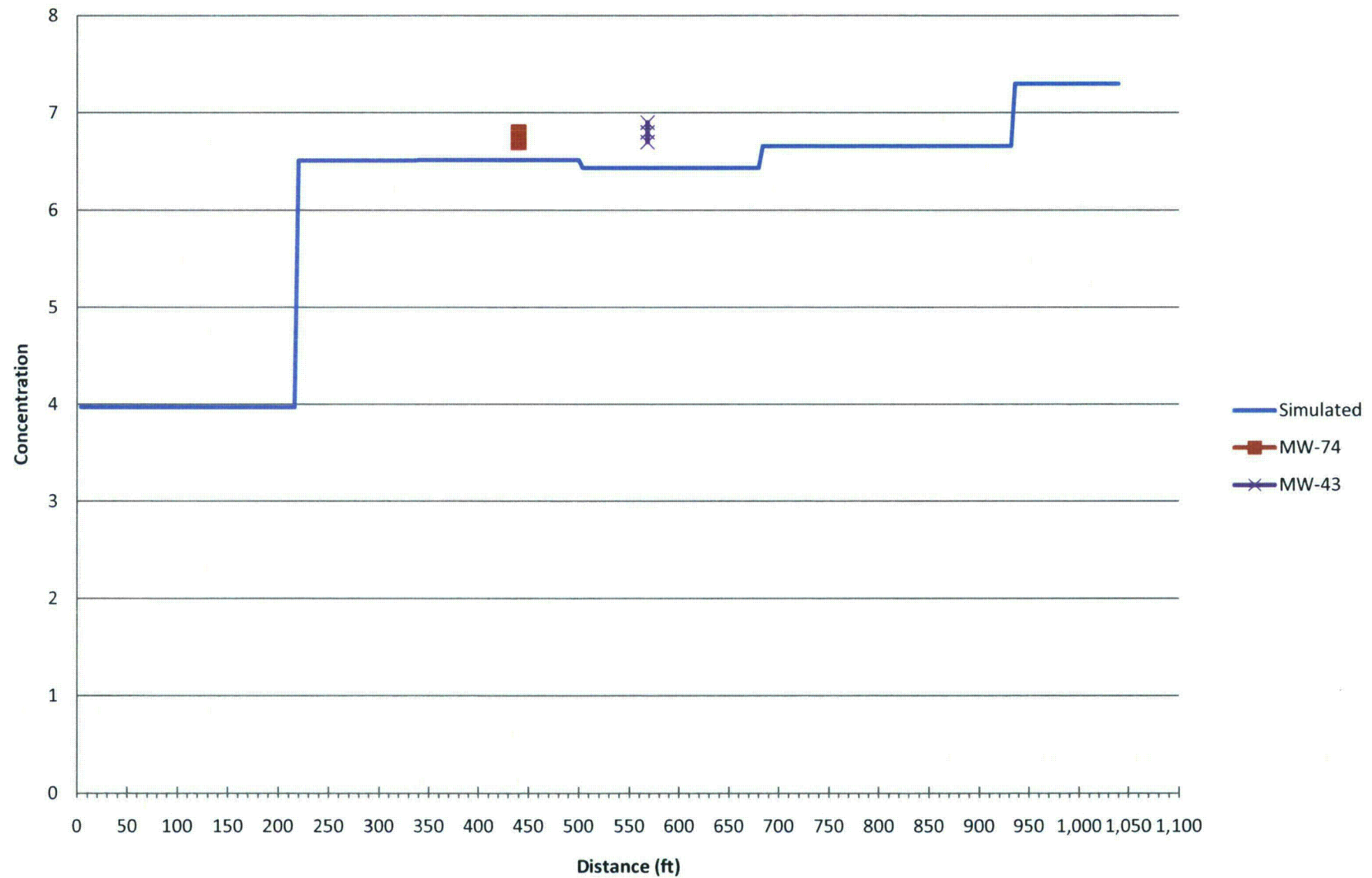


**Figure 19E. Simulated Initial Values of Radium  
Northern Pathway**

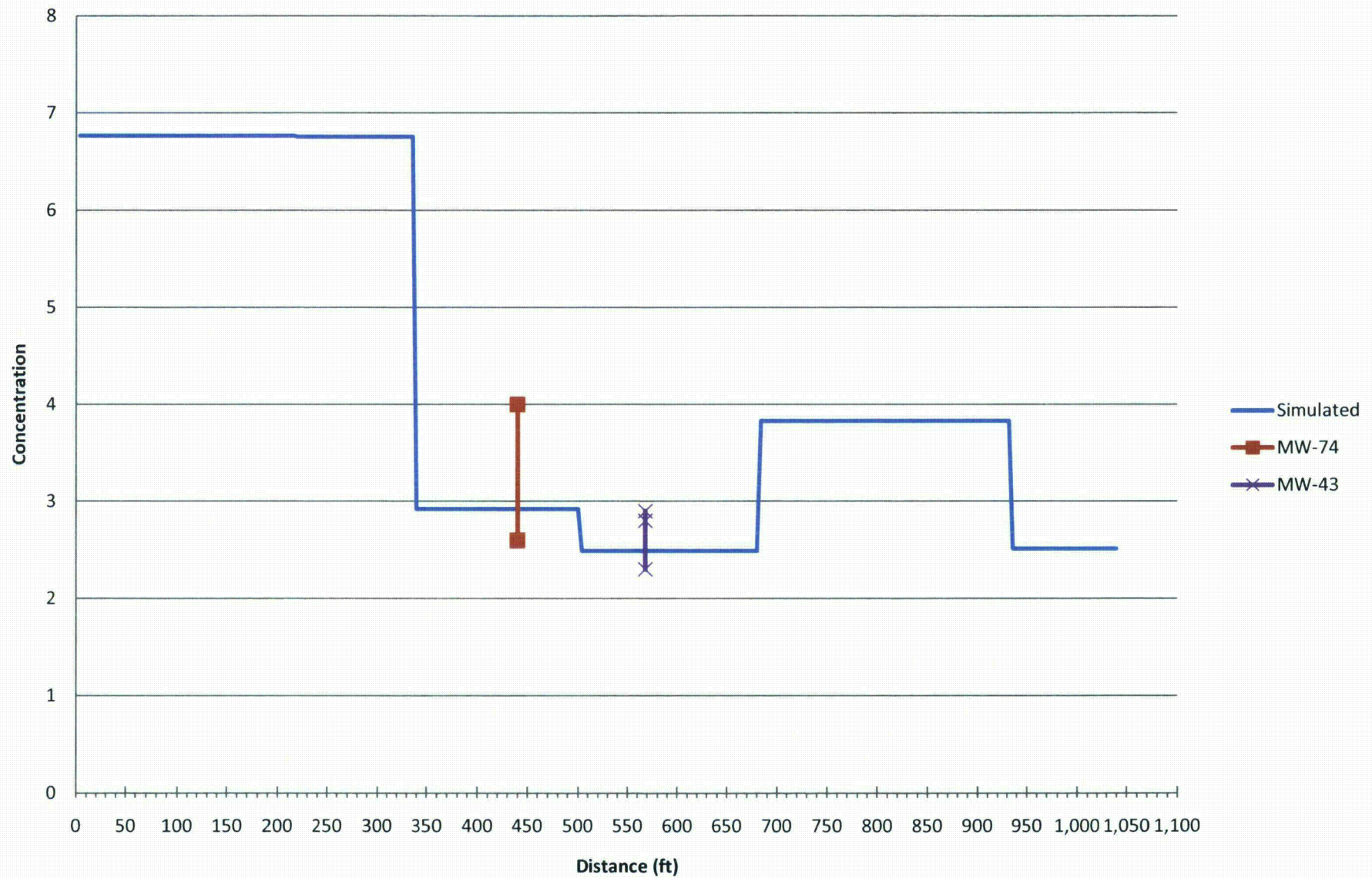




**Figure 19F. Simulated Initial Values of Nickel  
Northern Pathway**

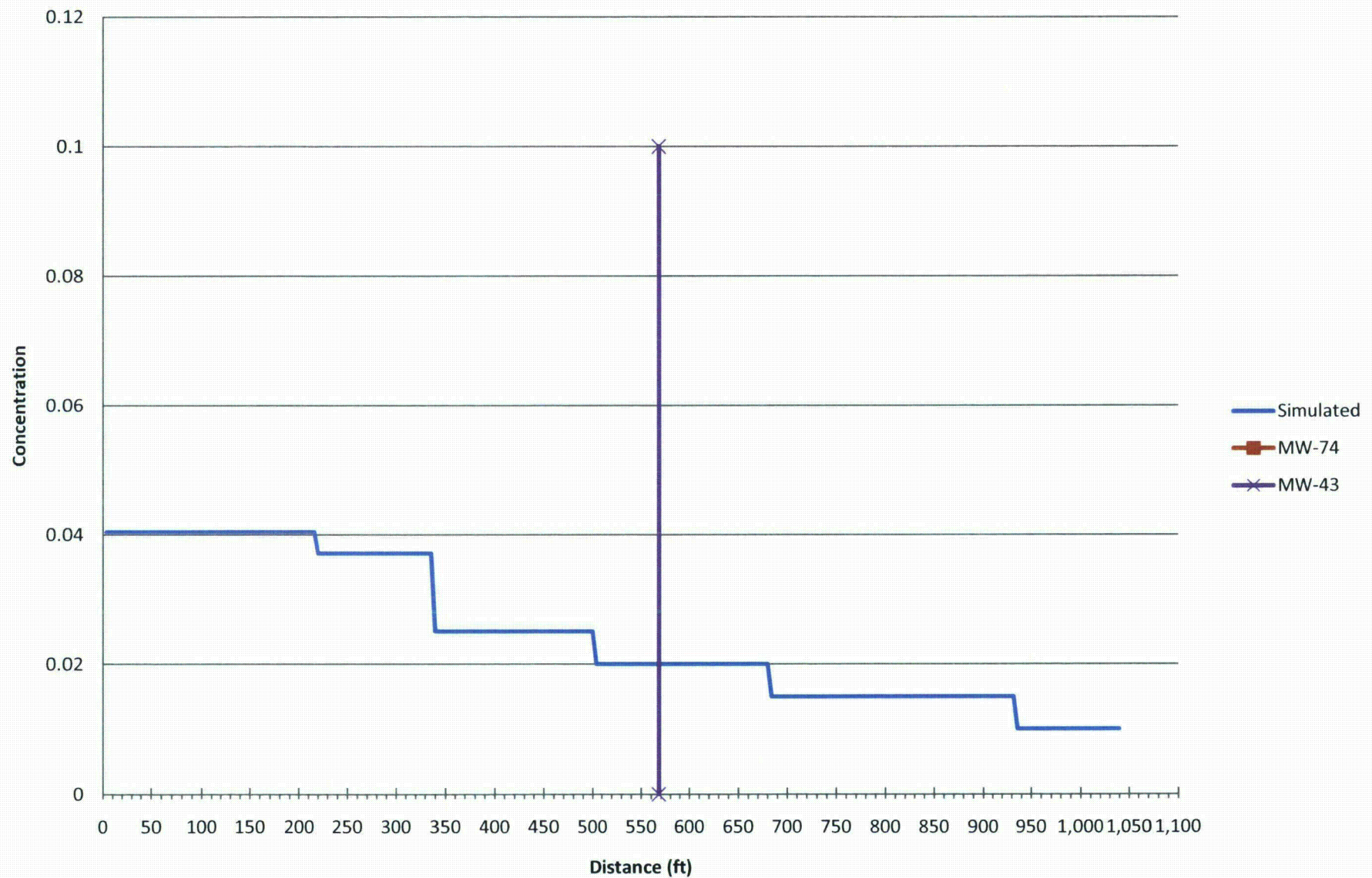


**Figure 20A. Simulated Breakthrough of Uranium  
Northern Pathway**

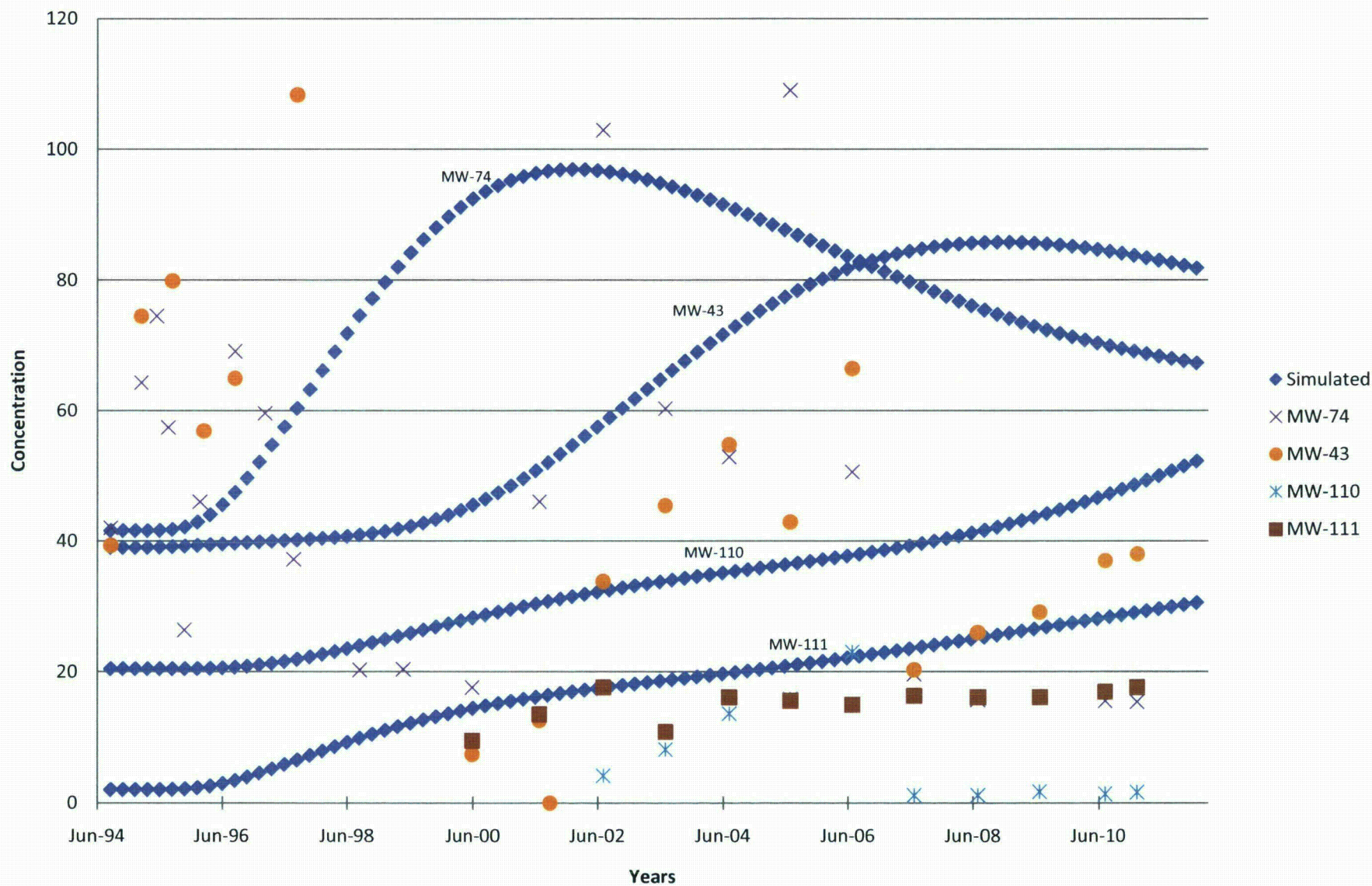


**Figure 20B. Simulated Breakthrough of Sulfate  
Northern Pathway**

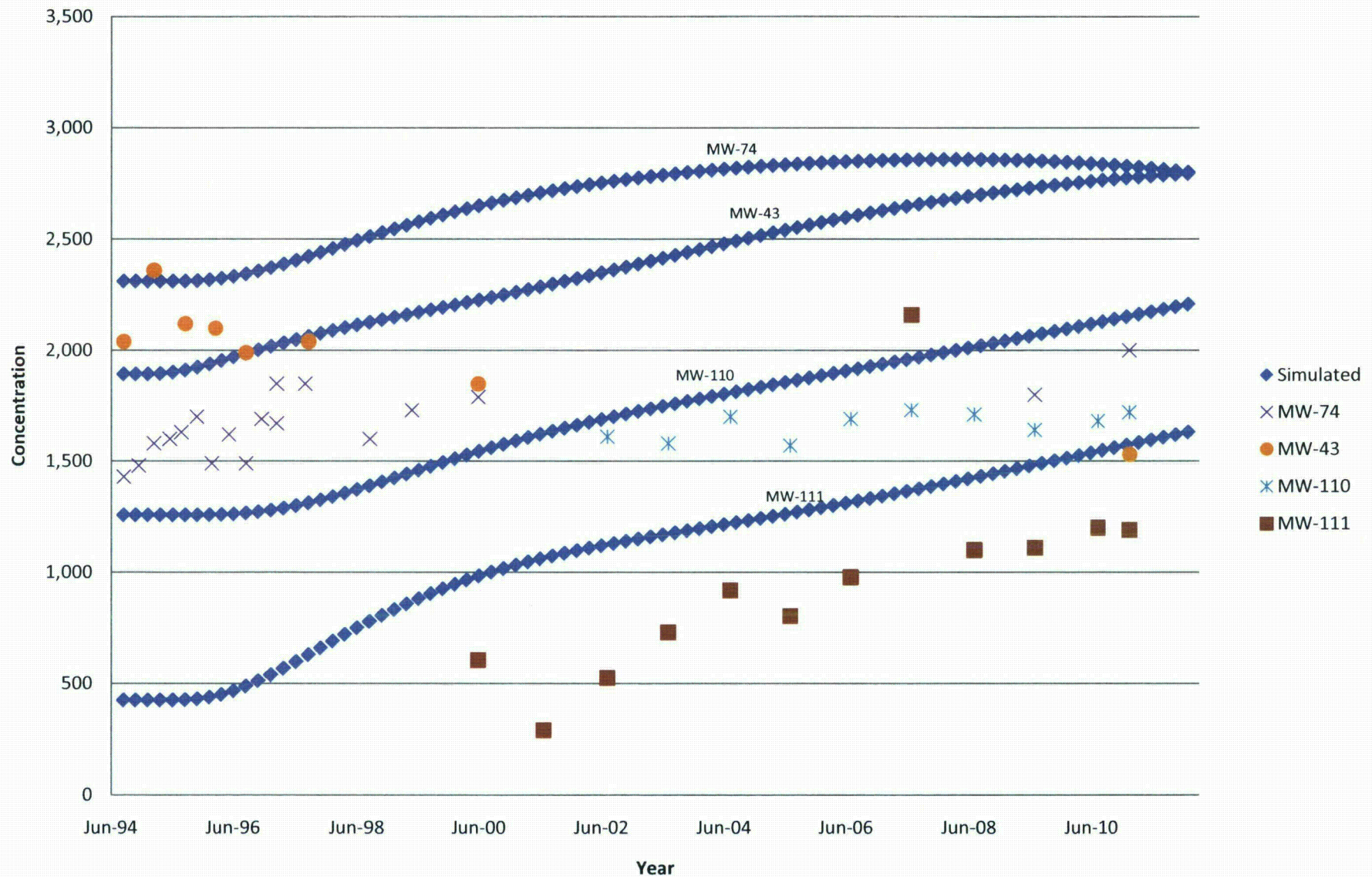




**Figure 20C. Simulated Breakthrough of Chloride  
Northern Pathway**

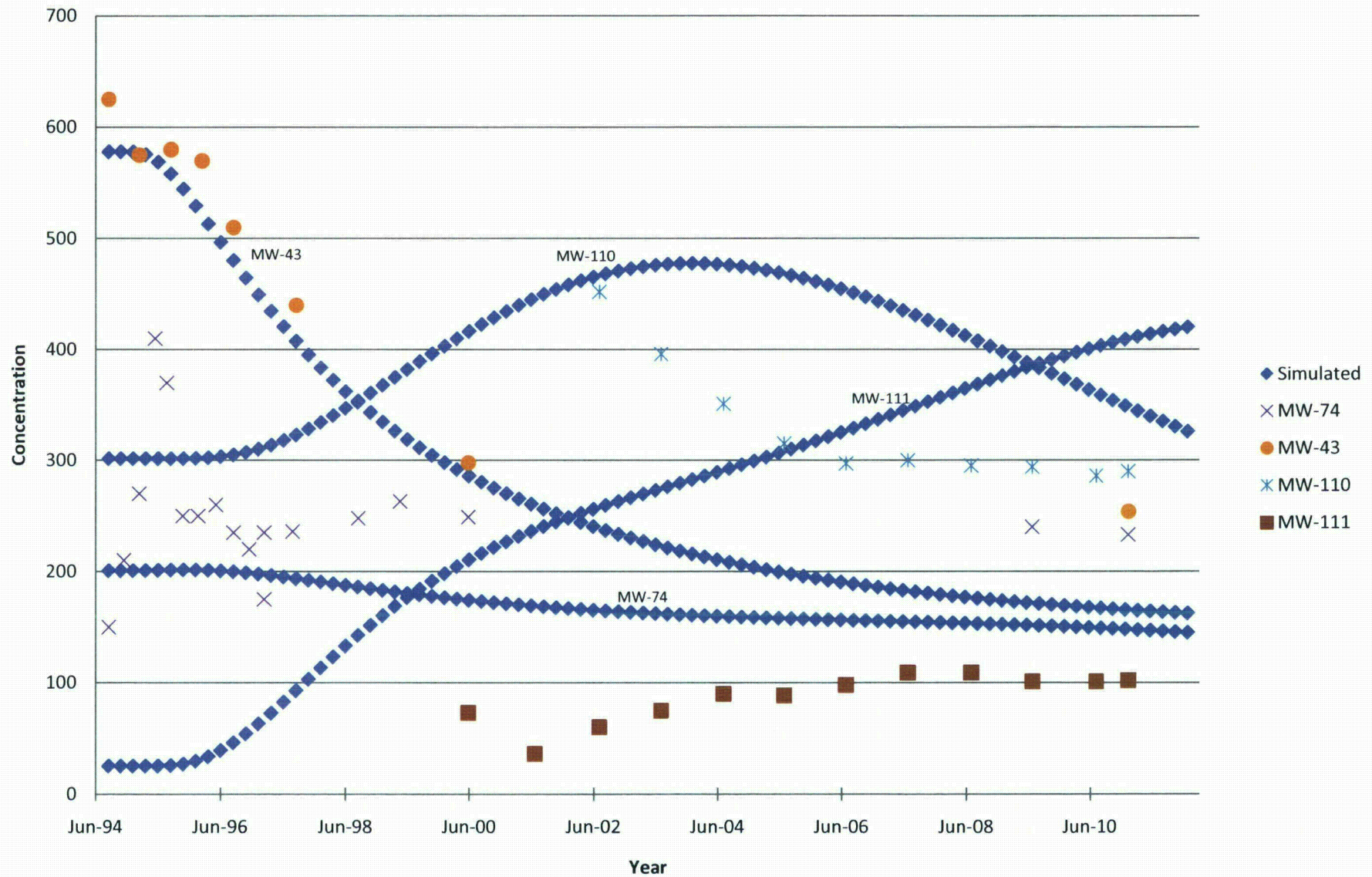


**Figure 20D. Simulated Breakthrough of pH  
Northern Pathway**

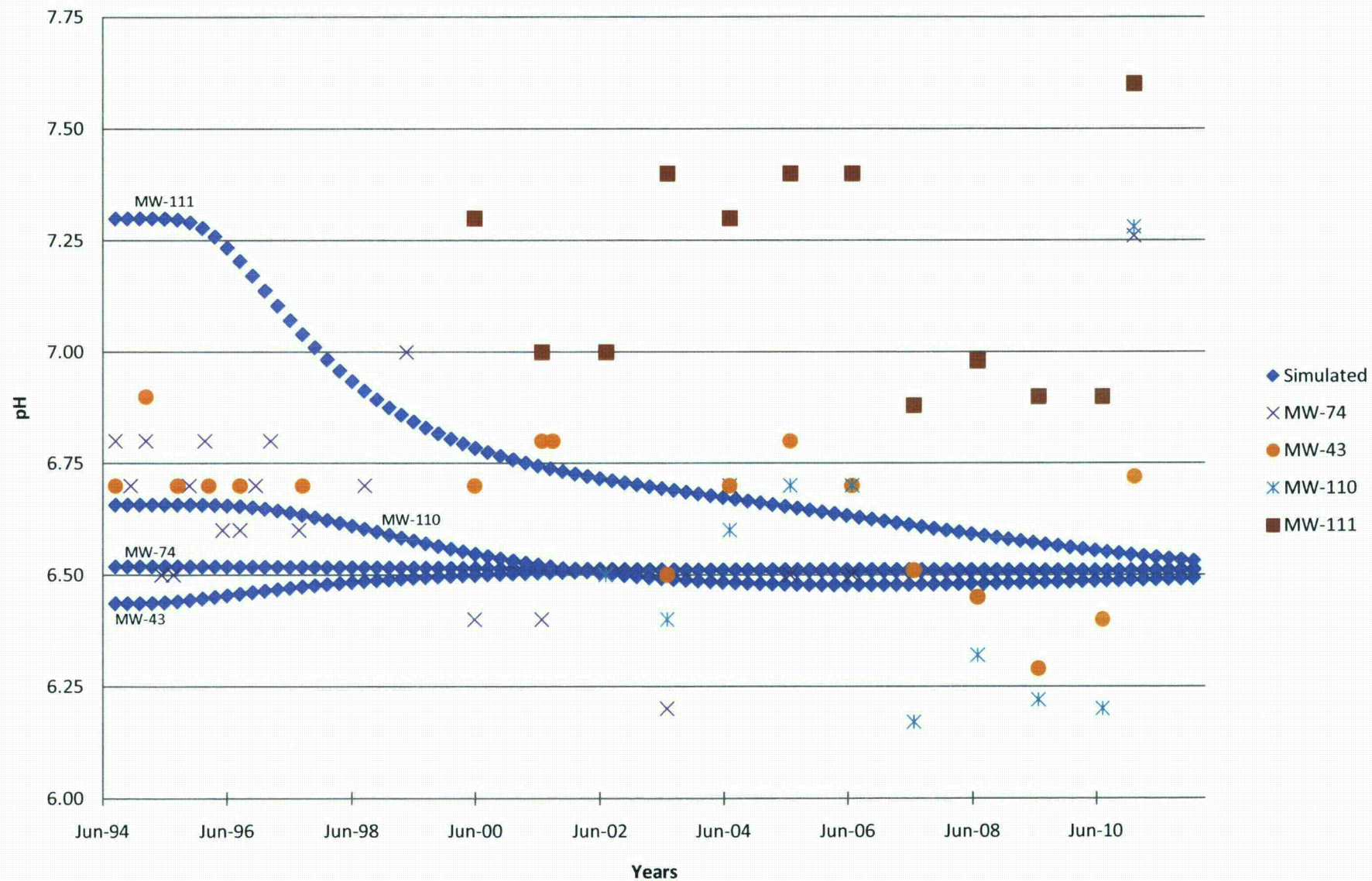


**Figure 20E. Simulated Breakthrough of Radium  
Northern Pathway**

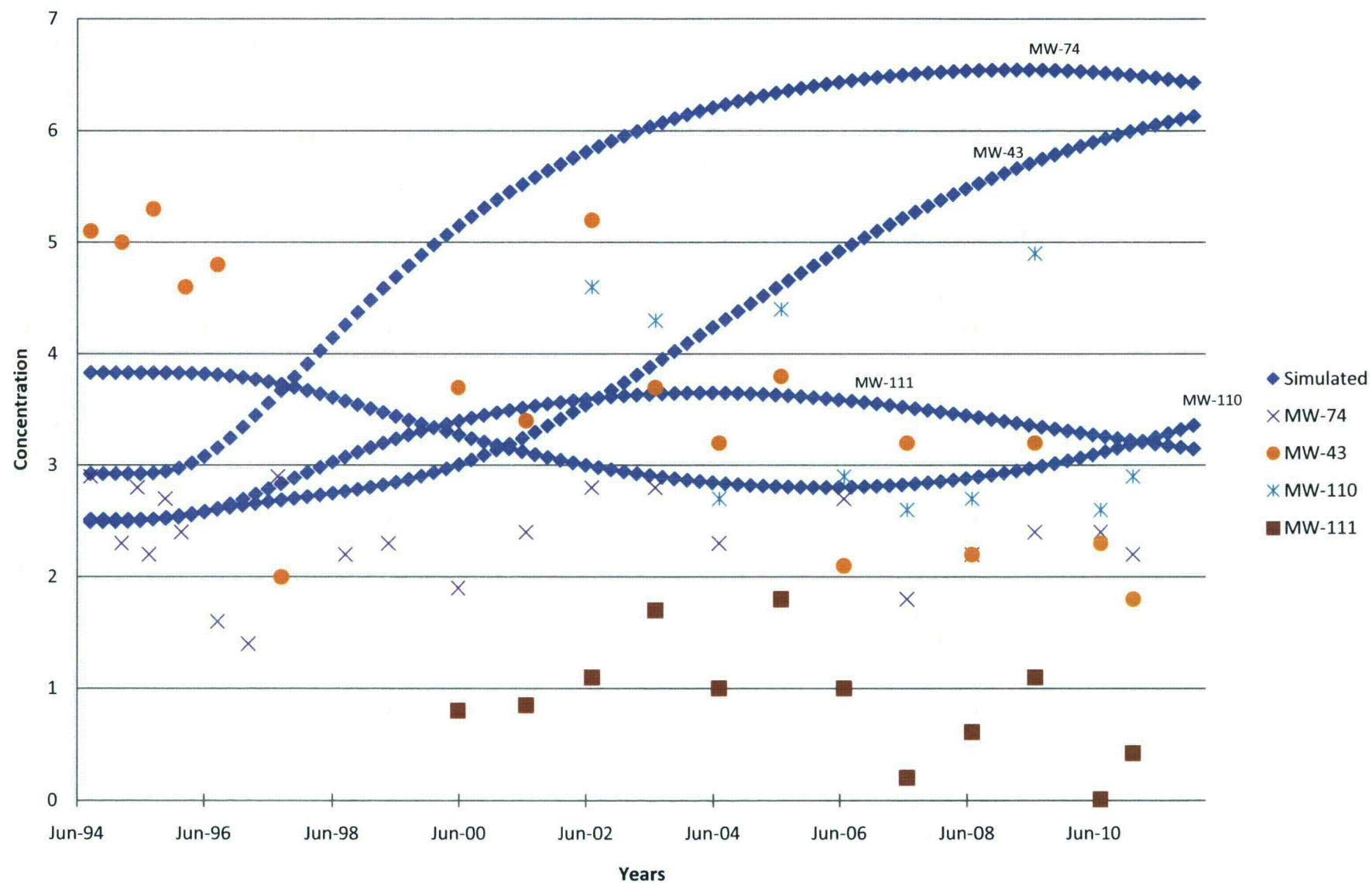




**Figure 20F. Simulated Breakthrough of Nickel  
Northern Pathway**

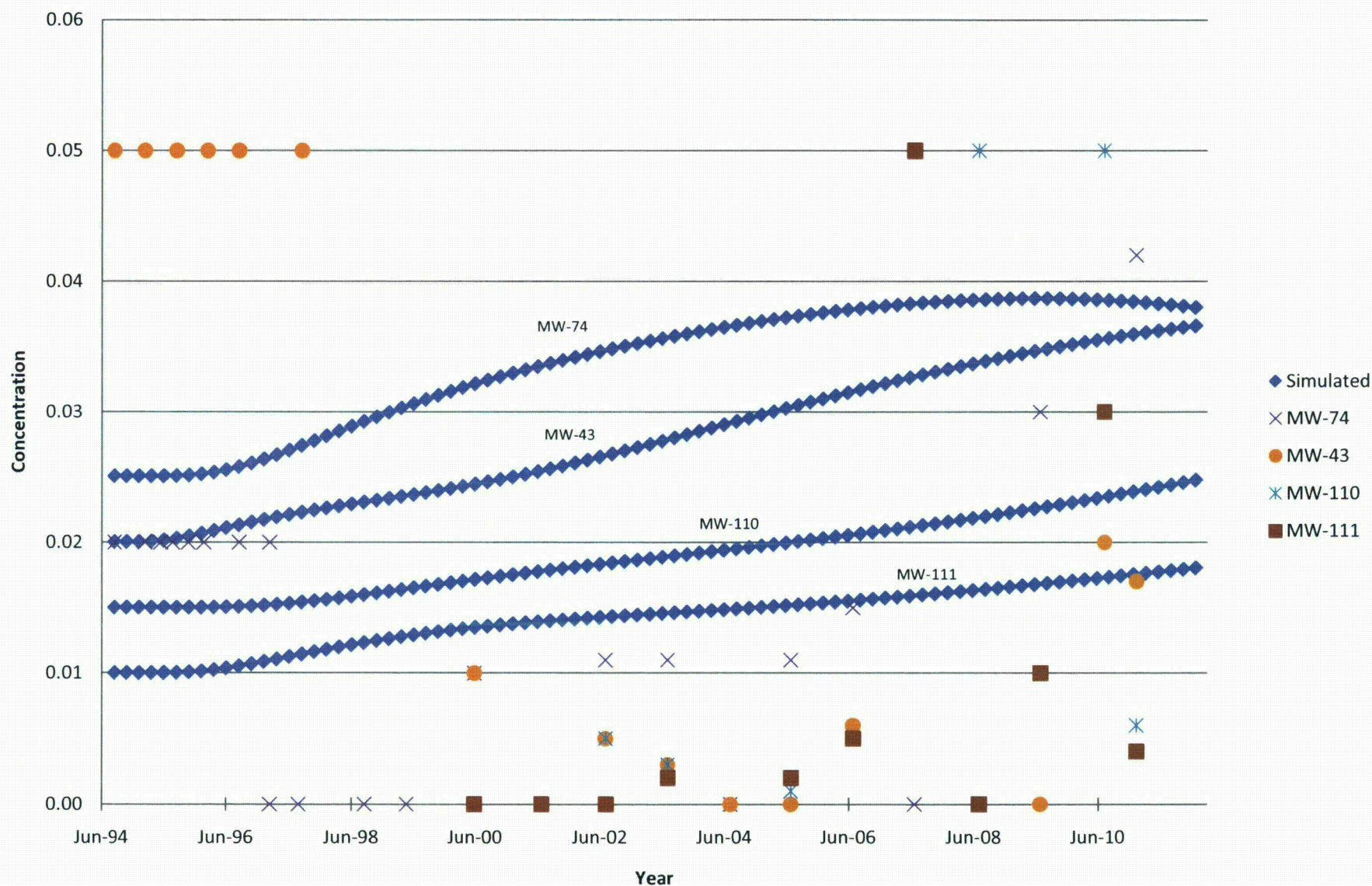


**Figure 21A. Predicted Breakthrough of Uranium Northern Pathway**

The graph displays the predicted breakthrough of uranium concentration over time for the Northern Pathway. The Y-axis represents Concentration (0 to 120), and the X-axis represents Years (1/1/1990 to 1/2/2110).

The legend identifies the data series:

- Simulated (Blue line with diamond markers)
- MW-74 (Blue 'x' markers)
- MW-43 (Orange circle markers)
- MW-110 (Light blue 'x' markers)
- MW-111 (Brown square markers)

The simulated breakthrough curve shows a peak concentration of approximately 95 around 1995. The monitoring well data points (MW-74, MW-43, MW-110, MW-111) show actual measurements that generally follow the simulated trend, with MW-74 having the highest peak concentration and MW-111 the lowest.

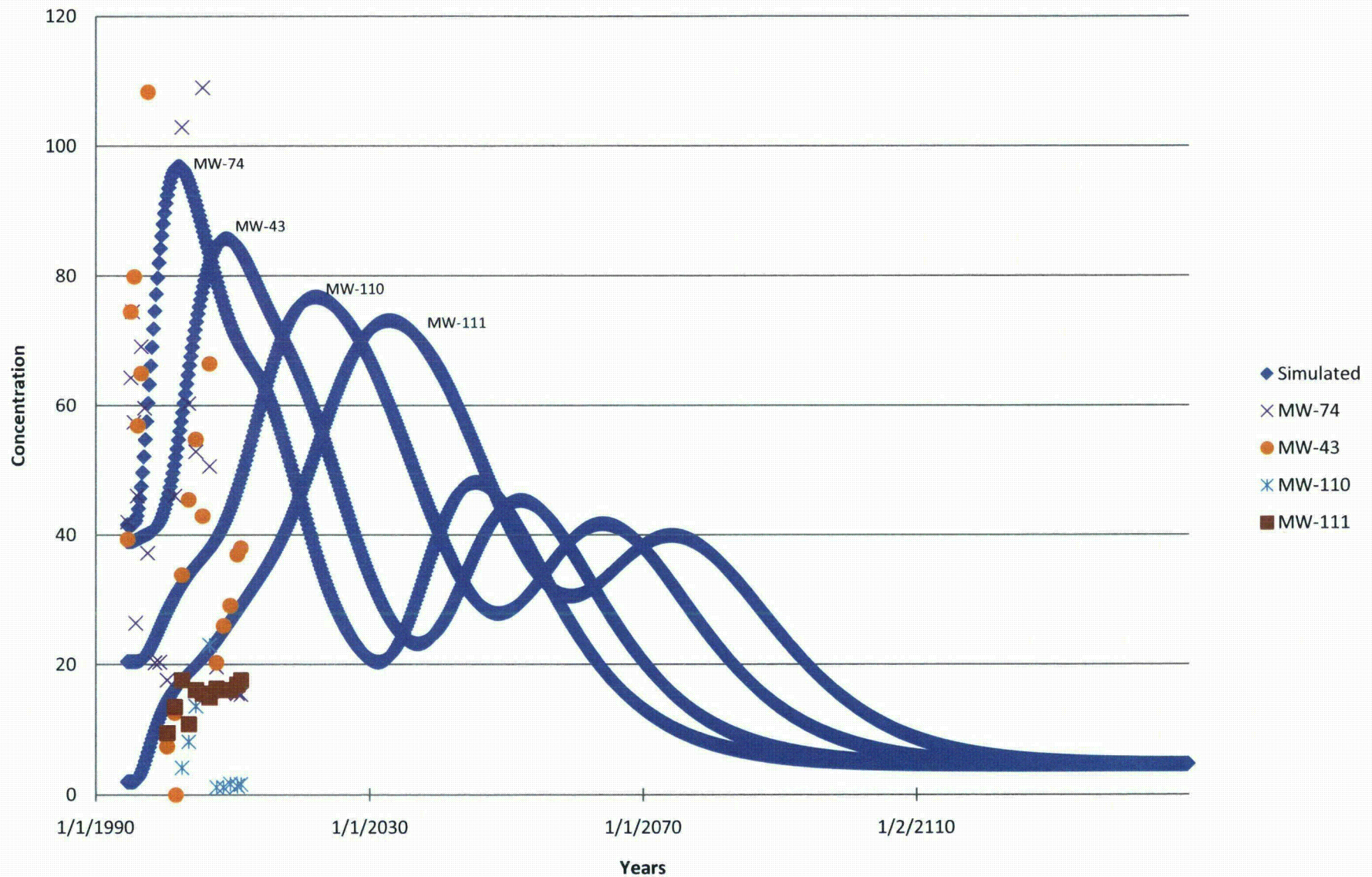


**Figure 21B. Predicted Breakthrough of Sulfate  
Northern Pathway**

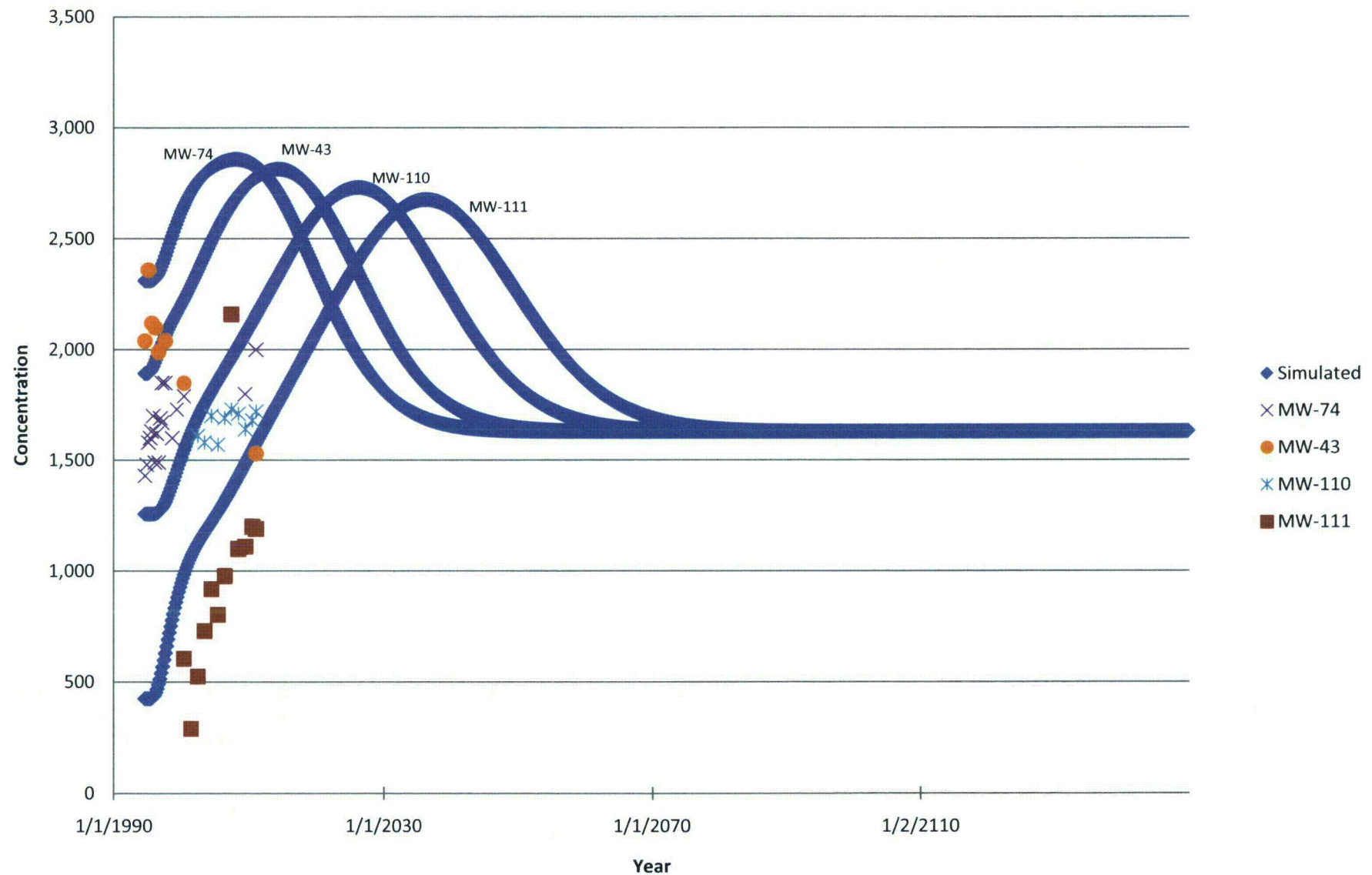




**Figure 21C. Predicted Breakthrough of Chloride  
Northern Pathway**

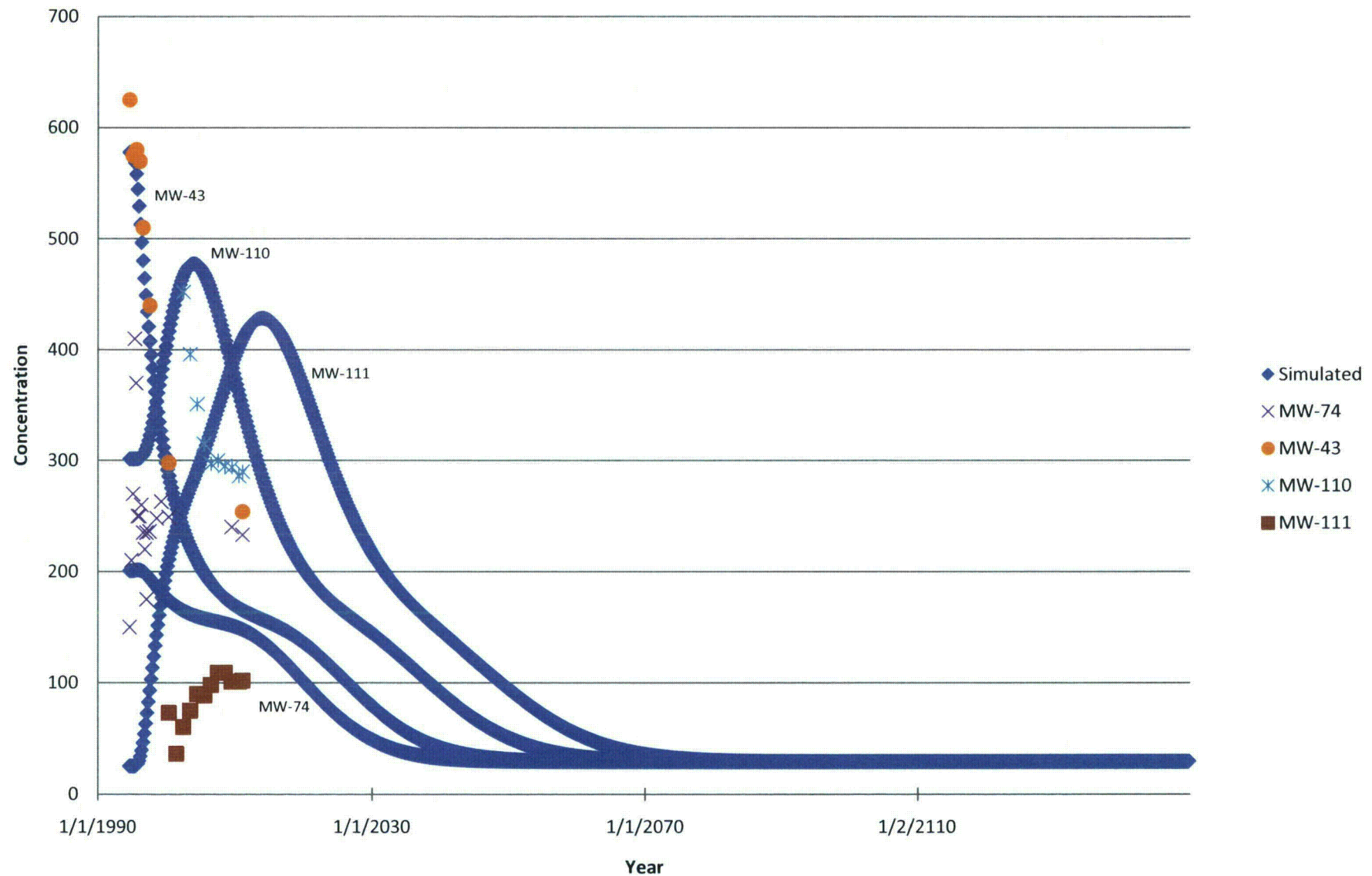


**Figure 21D. Predicted Breakthrough of pH  
Northern Pathway**

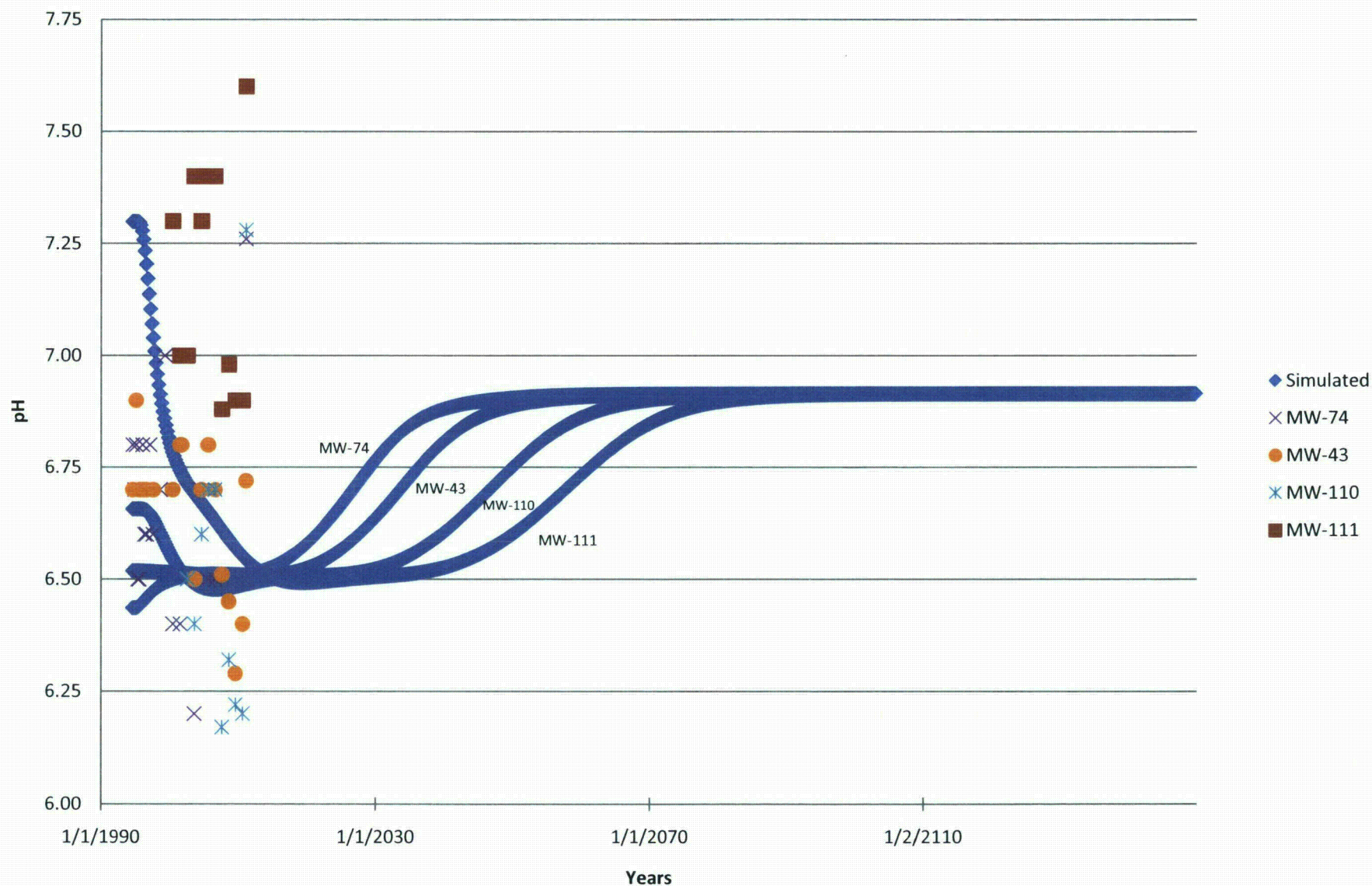


**Figure 21E. Predicted Breakthrough of Radium  
Northern Pathway**

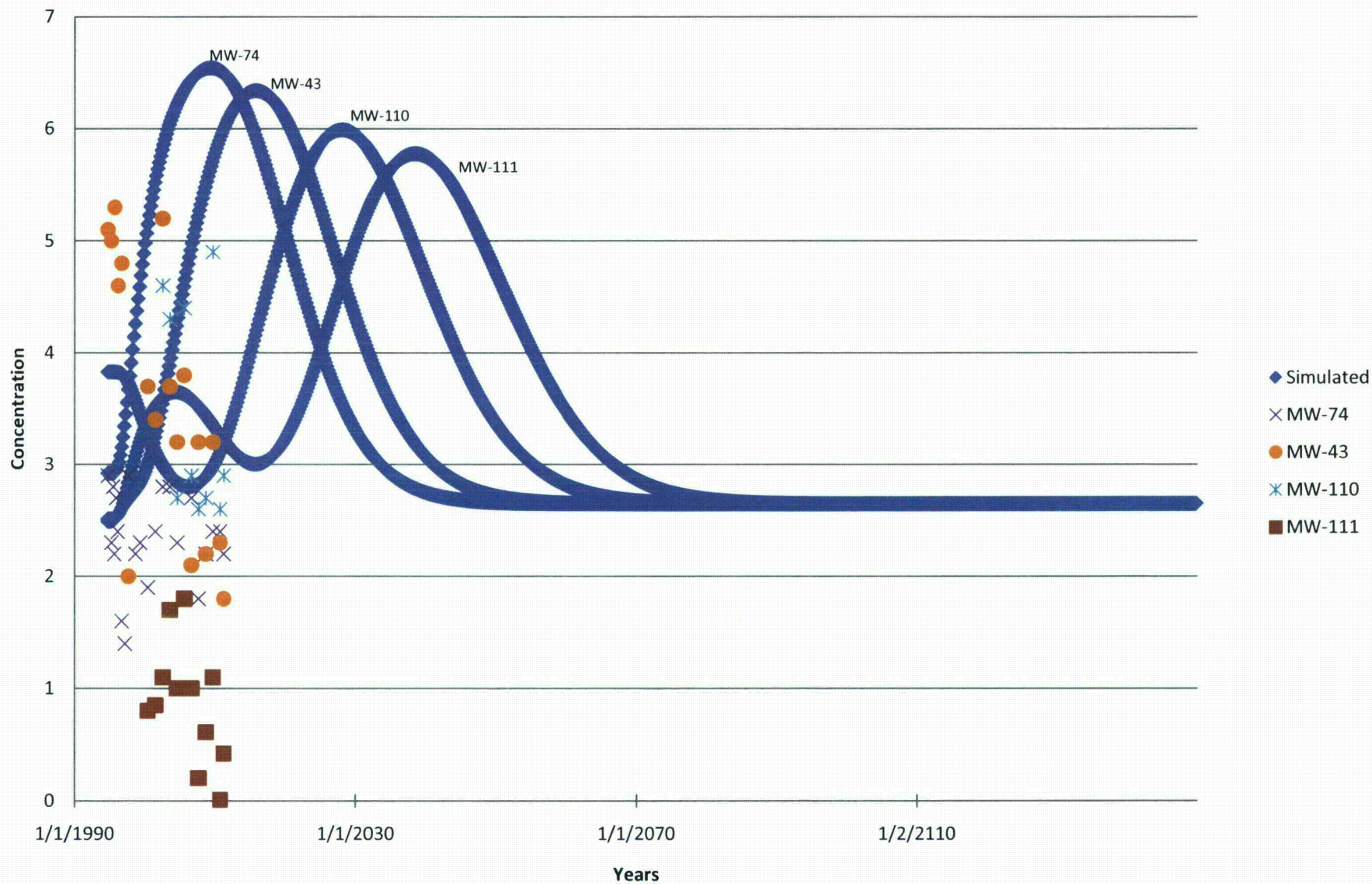




**Figure 21F. Predicted Breakthrough of Nickel Northern Pathway**

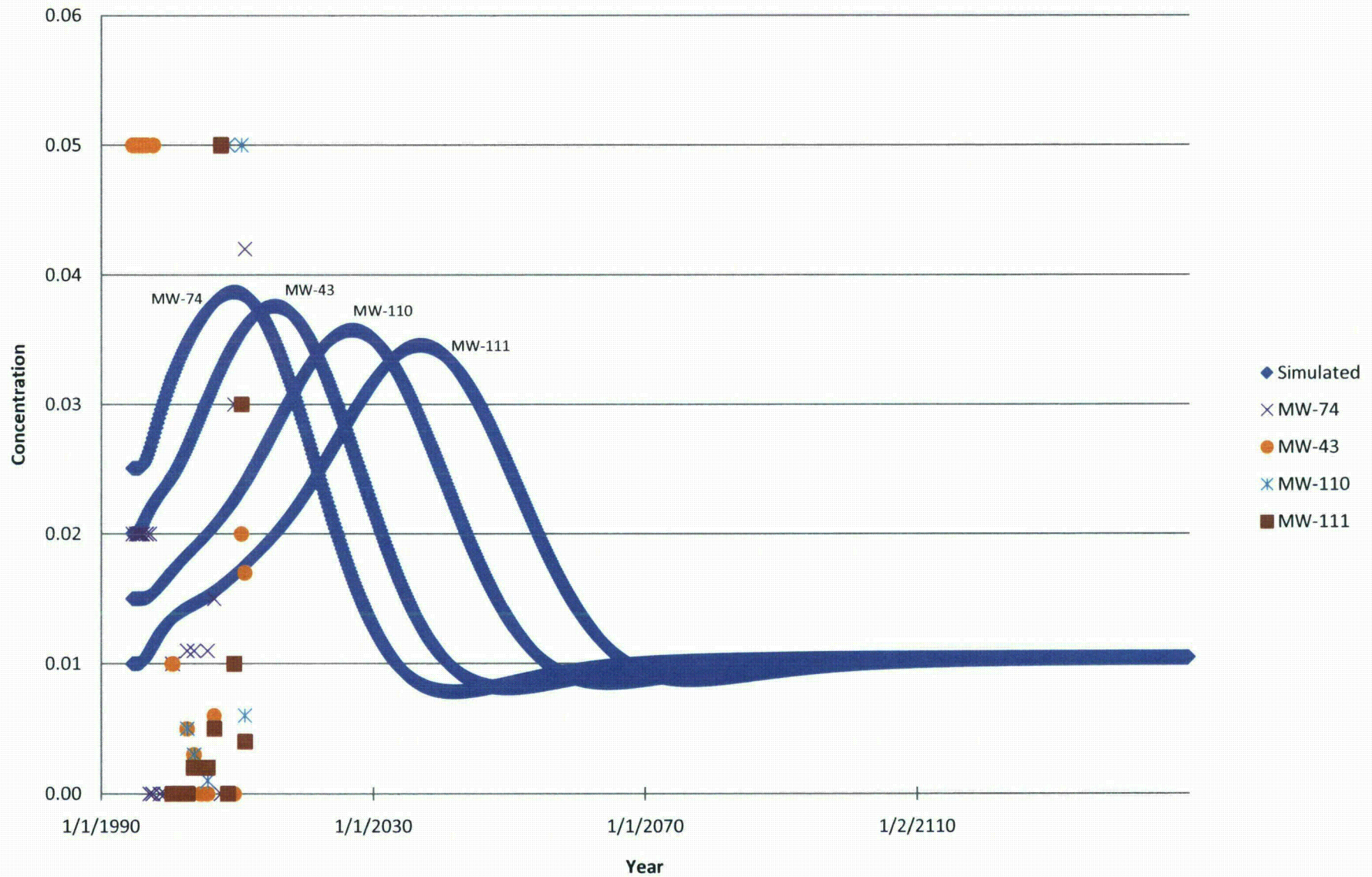
The graph illustrates the predicted breakthrough of nickel concentration over time for four monitoring wells (MW-74, MW-43, MW-110, and MW-111) along the Northern Pathway. The Y-axis represents Concentration (ranging from 0.00 to 0.06), and the X-axis represents Year (ranging from 1/1/1990 to 1/2/2110).

The legend identifies the data series:

- Simulated (Blue diamonds)
- MW-74 (Blue crosses)
- MW-43 (Orange circles)
- MW-110 (Blue asterisks)
- MW-111 (Brown squares)

The simulated curves show the predicted breakthrough of nickel concentration for each well. MW-74 shows the earliest breakthrough, peaking around 1995. MW-43 peaks around 2005, MW-110 around 2025, and MW-111 around 2045. All curves eventually decline to a baseline concentration of approximately 0.01.

Observed data points (symbols) are plotted for each well, showing the actual breakthrough of nickel concentration. The data points generally follow the trend of the simulated curves, with MW-74 showing the highest concentration (around 0.04) and MW-111 showing the lowest concentration (around 0.01).



## TABLES



Table 1. Results of Monitor Well Samples, February 2011

Well ID	MW-12	MW-9	MW-14	MW-108	MW-109	MW-74	MW-43R	MW-110	MW-111
Sample Date	2/11/2011	2/11/2011	2/11/2011	2/12/2011	2/12/2011	2/10/2011	2/12/2011	2/10/2011	2/10/2011
	Lang Draw					Northern Pathway			
Analyte									
Major Ions (mg/L)									
Calcium	883	883	824	868	552	686	739	769	520
Chloride	371	334	358	302	89	233	254	290	102
Magnesium	544	200	343	179	137	175	154	156	90
Nitrogen Nitrate + Nitrite as N	0.01	0.81	<0.01	0.06	0.13	4.4	0.05	0.01	0.04
Phosphorus Total as P	<0.005	0.006	0.058	0.013	0.029	0.008	0.009	0.064	0.01
Potassium	18	6	11	9	10	14	16	17	7
Sodium	297	257	268	180	127	122	66	43	24
Sulfate	2810	1880	2280	1620	1900	2000	1530	1720	1190
Metals Dissolved (mg/L)									
Aluminum	<0.1	<0.1	<0.1	<0.1	0.2	<0.1	<0.1	<0.1	<0.1
Arsenic	<0.001	<0.001	<0.001	<0.001	<0.001	<0.001	<0.001	<0.001	<0.001
Barium	<0.1	<0.1	<0.1	<0.1	<0.1	<0.1	<0.1	<0.1	<0.1
Beryllium	<0.001	N/A	N/A	N/A	N/A	<0.001	N/A	N/A	N/A
Cadmium	<0.001	N/A	N/A	N/A	N/A	<0.001	N/A	N/A	N/A
Chromium	<0.001	N/A	N/A	N/A	N/A	<0.001	N/A	N/A	N/A
Iron	0.41	1.14	1.46	0.55	0.53	4.62	0.59	9.92	0.19
Manganese	6.62	0.18	1.19	0.43	0.04	2.11	1.04	0.53	<0.01
Molybdenum	<0.001	N/A	N/A	N/A	N/A	<0.001	N/A	N/A	N/A
Nickel	0.035	0.018	0.04	0.043	0.013	0.042	0.017	0.006	0.004
Selenium	0.002	<0.001	0.004	N/A	N/A	0.021	0.003	N/A	N/A
Silica	28	23.7	25.9	26.2	14.1	29	19.6	23.6	18.1
Uranium (pCi/L)	420	195	439	135	61.3	15.4	38	1.6	17.6
Metals Total (mg/L)									
Aluminum	<0.1	<0.1	<0.1	1.2	3.1	<0.1	0.3	3	2.1
Iron	0.57	1.25	1.55	1.53	2	4.96	1.55	12.9	1.23
Manganese	6.72	0.19	1.21	0.49	0.03	2.14	1.16	0.54	0.02
Silica	31.6	25.9	27.3	18.5	29	30.9	20.8	38.7	28.2
Radionuclides Dissolved (pCi/L)									
Radium-226	0.62	0.3	0.09	0.41	0.5	2.2	1.8	2.9	0.42
Radium-228	2.4	1.9	0.8	1.6	1.3	4	3.1	7.6	1.4
Thorium-230	-0.3	-0.06	<0.1	-0.1	-0.05	-0.09	-0.07	<0.02	-0.06
Total Dissolved Solids (mg/L)	5770	4390	5050	3980	3050	3700	3410	3340	2260
pH (s.u.)	6.56	7.00	7.16	6.75	7.34	7.26	6.72	7.28	7.60



Table 2. Saturation Indices for Water Samples on Lang Draw Flow Path, 2011

Phase	Formula	MW-108	MW-109	MW-12	MW-14	MW-9
(UO <sub>2</sub> ) <sub>3</sub> (PO <sub>4</sub> ) <sub>2</sub> ·4w	(UO <sub>2</sub> ) <sub>3</sub> (PO <sub>4</sub> ) <sub>2</sub> ·4H <sub>2</sub> O	-36.01	-33.17		-36.37	-38.16
Al(OH) <sub>3</sub> (a)	Al(OH) <sub>3</sub>		-0.7			
Calcite	CaCO <sub>3</sub>	0.74	0.49	0.37	1.17	1.02
Chalcedony	SiO <sub>2</sub>	0.2	-0.07	0.23	0.2	0.16
CO <sub>2</sub> (g)	CO <sub>2</sub> pressure (atmos.)	-0.91	-2.13	-0.74	-1.22	-1.11
Ferrihydrite	Fe(OH) <sub>3</sub>	2.23	2.49	1.97	2.86	2.69
Gypsum	CaSO <sub>4</sub> ·2H <sub>2</sub> O	-0.01	-0.05	0.02	0.04	0.04
Magnesite	MgCO <sub>3</sub>	-0.19	-0.36	0.01	0.55	0.13
MnHPO <sub>4</sub>	MnHPO <sub>4</sub>	-0.28	-0.63		0.79	-0.97
Schoepite	UO <sub>2</sub> (OH) <sub>2</sub> ·H <sub>2</sub> O	-7.67	-6.33	-6.64	-7.72	-7.88
Siderite	FeCO <sub>3</sub>	-7.03	-7.99	-7.12	-6.71	-6.77
U <sub>3</sub> O <sub>8</sub> (c)	U <sub>3</sub> O <sub>8</sub>	-38.21	-34.19	-35.12	-38.37	-38.83
UO <sub>2</sub> (OH) <sub>2</sub> (beta)	UO <sub>2</sub> (OH) <sub>2</sub>	-7.21	-5.87	-6.18	-7.27	-7.42
Uraninite(c)	UO <sub>2</sub>	-26.43	-25.09	-25.4	-26.48	-26.63

Note: SI less than 0 indicates undersaturation and SI greater than 0 indicates supersaturation.

Table 3. Saturation Indices for Water Samples on Northern Pathway

Phase	Formula	MW-110	MW-111	MW-43	MW-74
(UO <sub>2</sub> ) <sub>3</sub> (PO <sub>4</sub> ) <sub>2</sub> ·4w	(UO <sub>2</sub> ) <sub>3</sub> (PO <sub>4</sub> ) <sub>2</sub> ·4H <sub>2</sub> O	-40.91	-39.97	-35.5	-36.95
Calcite	CaCO <sub>3</sub>	0.93	1.05	0.44	0.59
Chalcedony	SiO <sub>2</sub>	0.15	0.03	0.07	0.24
CO <sub>2</sub> (g)	CO <sub>2</sub> pressure (atmos)	-1.73	-2.14	-1.1	-1.96
Ferrihydrite	Fe(OH) <sub>3</sub>	3.74	2.1	2.24	3.4
Gypsum	CaSO <sub>4</sub> ·2H <sub>2</sub> O	0.01	-0.19	-0.04	0.02
Magnesite	MgCO <sub>3</sub>	-0.01	0.04	-0.48	-0.25
MnHPO <sub>4</sub>	MnHPO <sub>4</sub>	0.7		0.03	0.45
Schoepite	UO <sub>2</sub> (OH) <sub>2</sub> ·H <sub>2</sub> O	-9.16	-7.96	-7.45	-7.28
Siderite	FeCO <sub>3</sub>	-6.34	-8.39	-7.2	-6.91
U <sub>3</sub> O <sub>8</sub> (c)	U <sub>3</sub> O <sub>8</sub>	-42.69	-39.1	-37.54	-37.04
UO <sub>2</sub> (OH) <sub>2</sub> (beta)	UO <sub>2</sub> (OH) <sub>2</sub>	-8.71	-7.51	-6.99	-6.82
Uraninite(c)	UO <sub>2</sub>	-27.92	-26.72	-26.2	-26.04

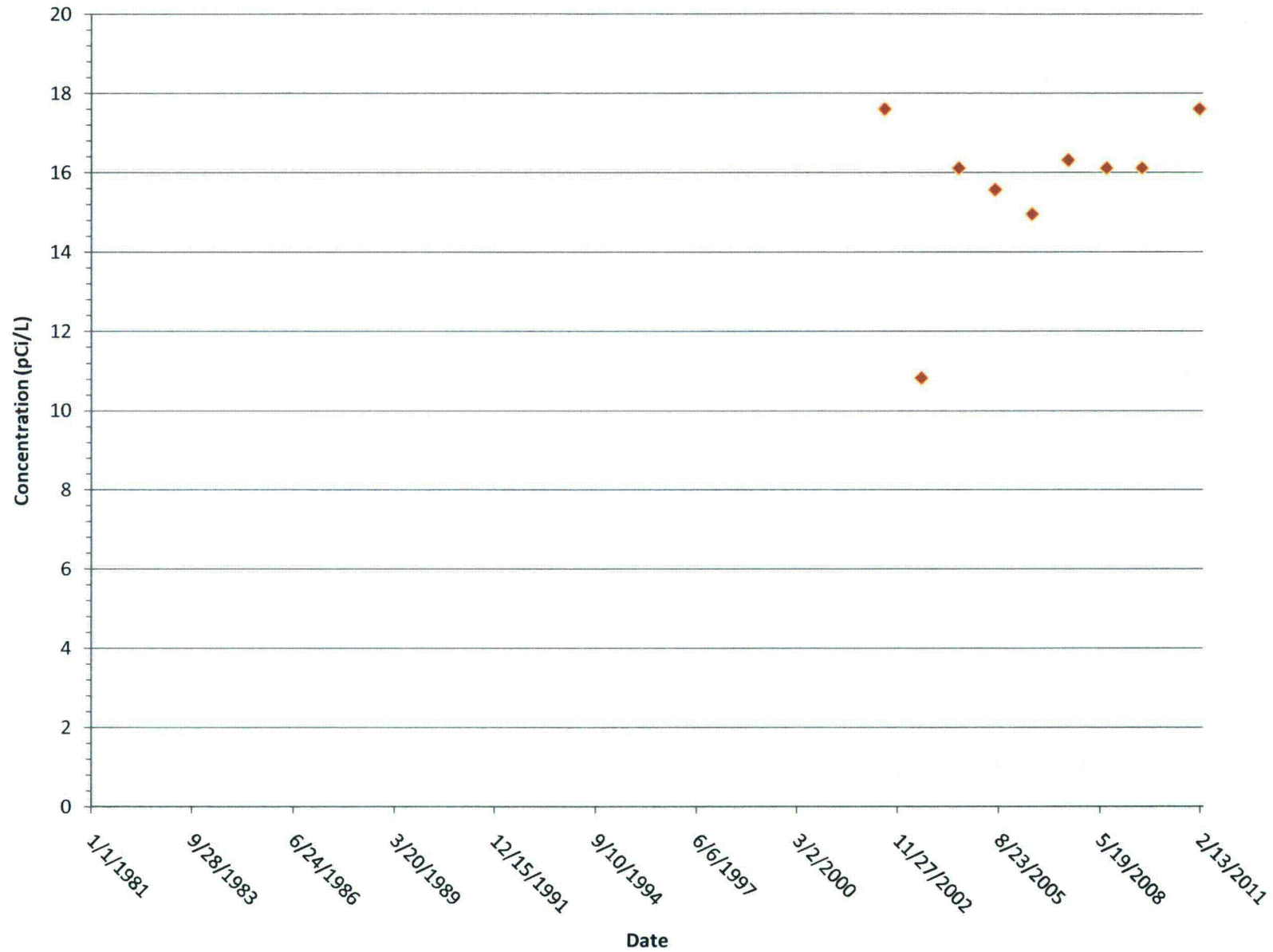
Note: SI less than 0 indicates undersaturation and SI greater than 0 indicates supersaturation.

## **ATTACHMENT I**

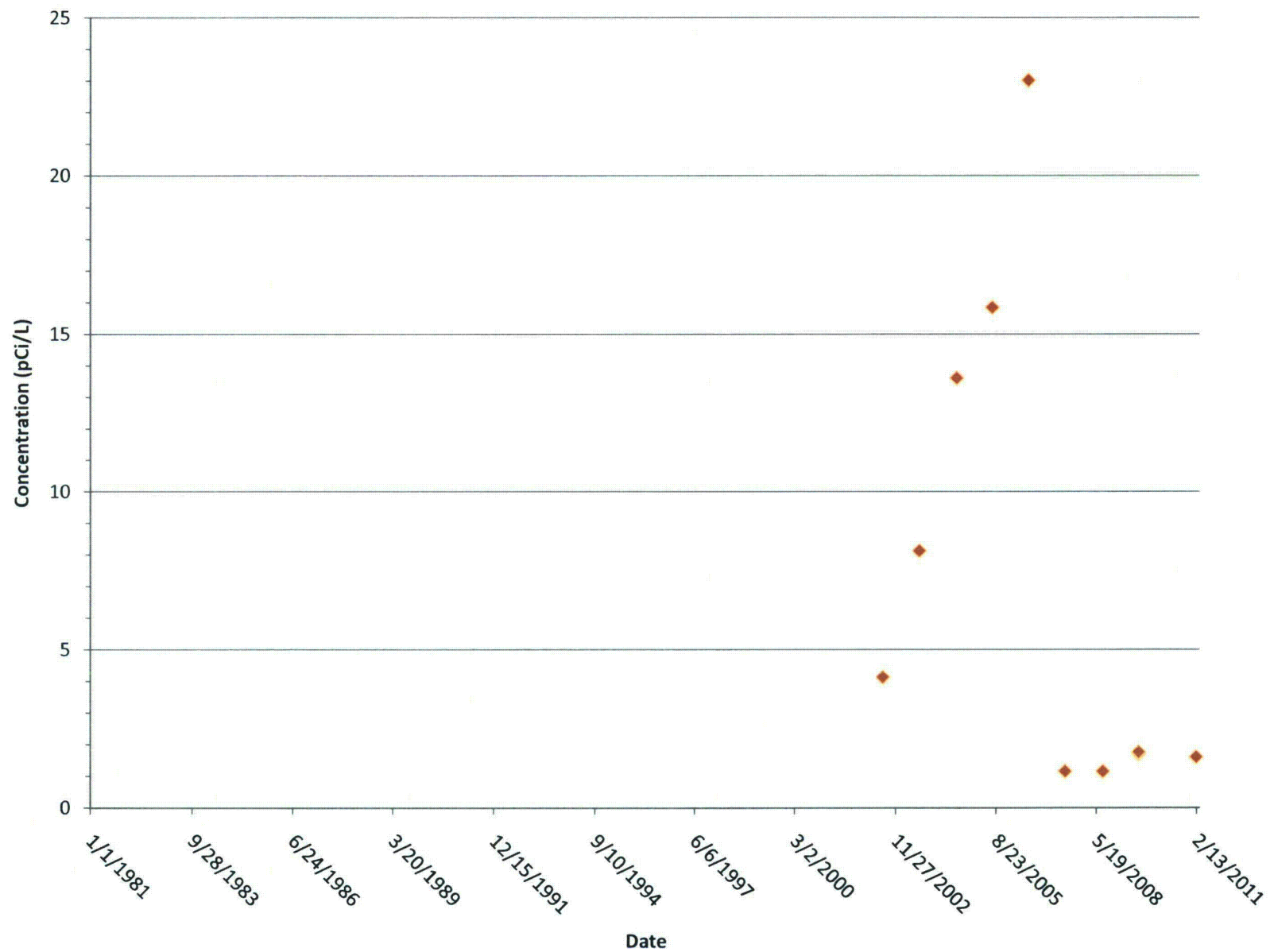
Temporal plots of  
chemical parameters measured  
in monitoring wells



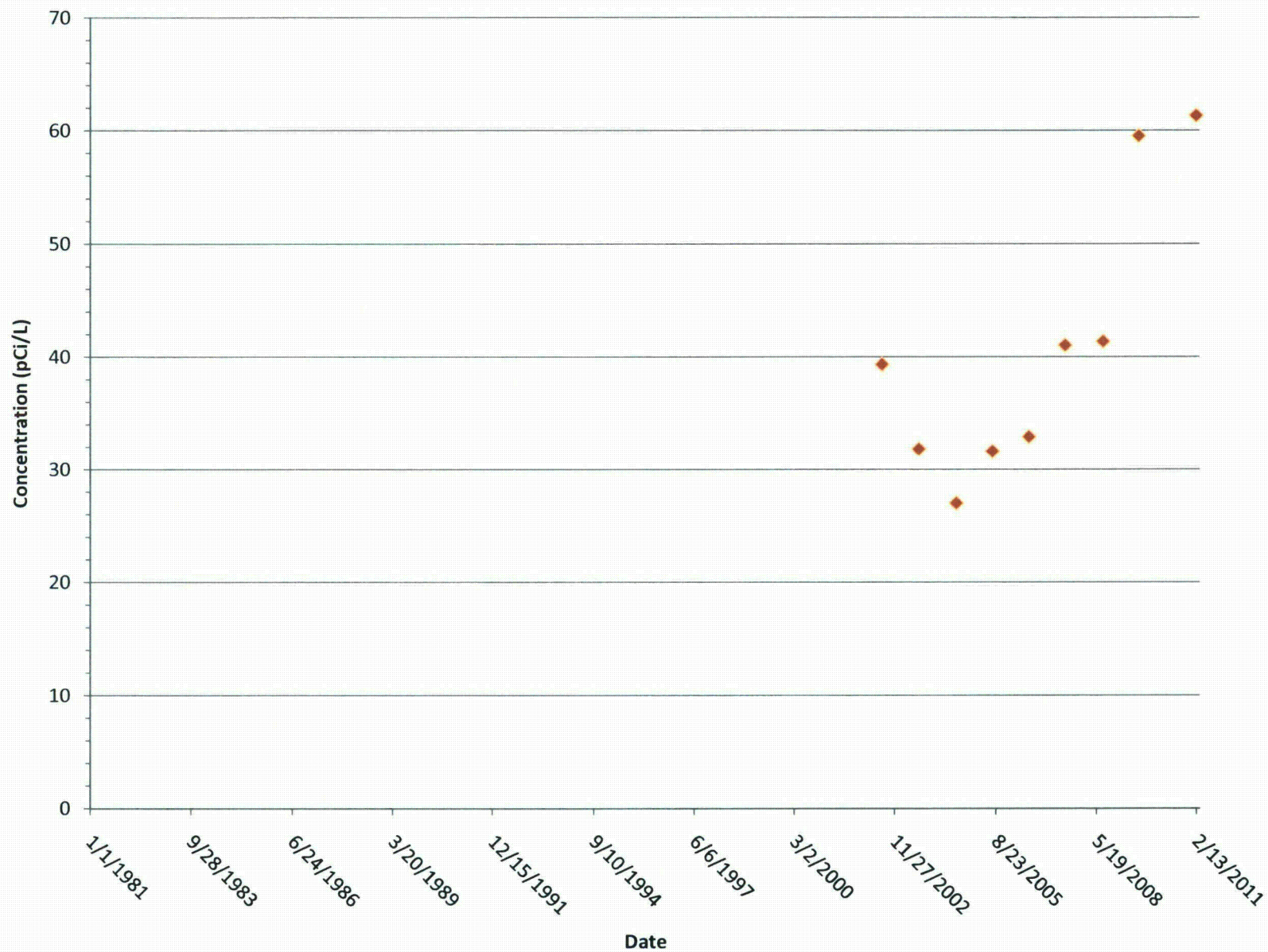
## MW-111 Uranium



## MW-110 Uranium

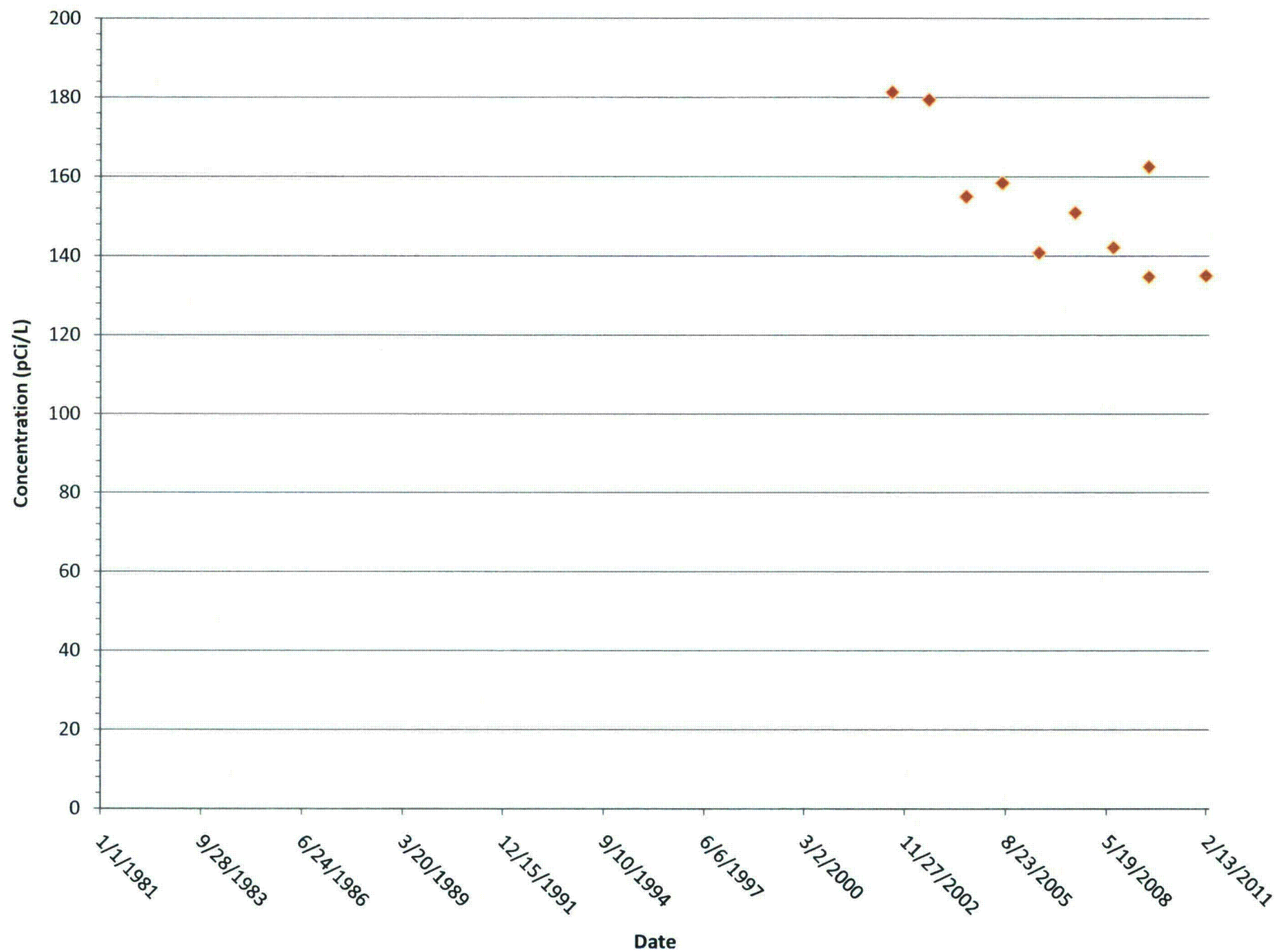


# MW-109 Uranium

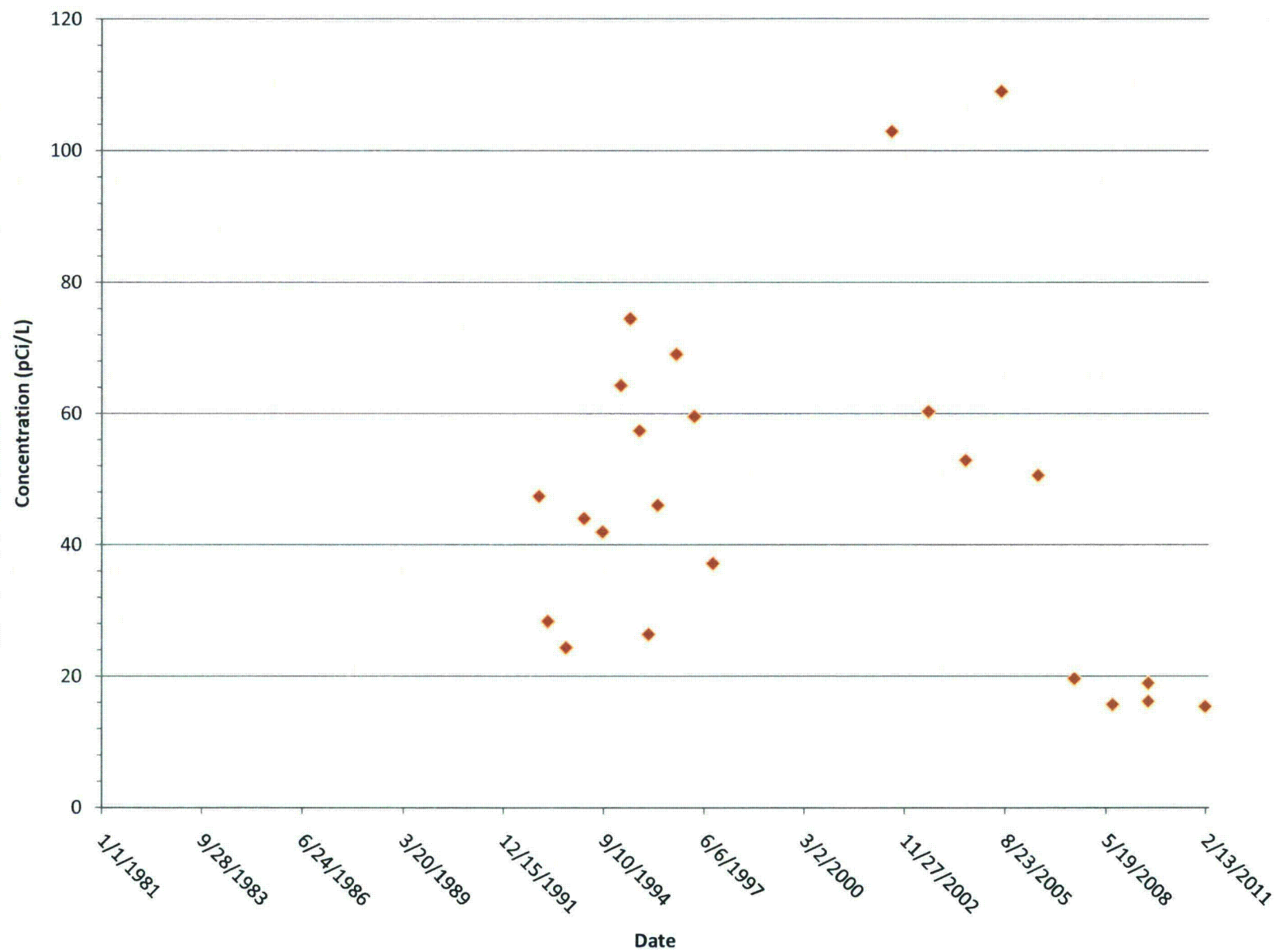




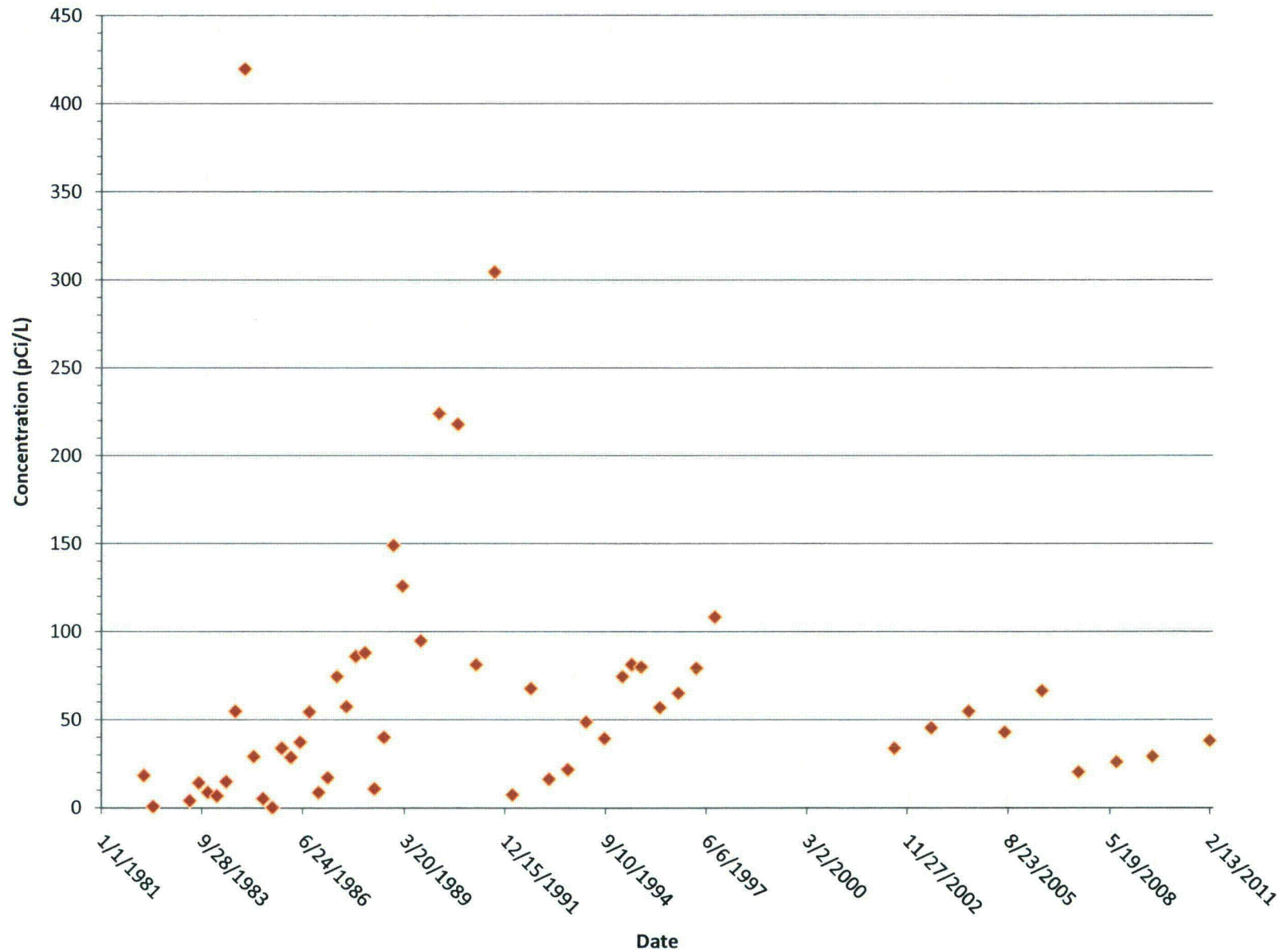
# MW-108 Uranium



## MW-74 Uranium

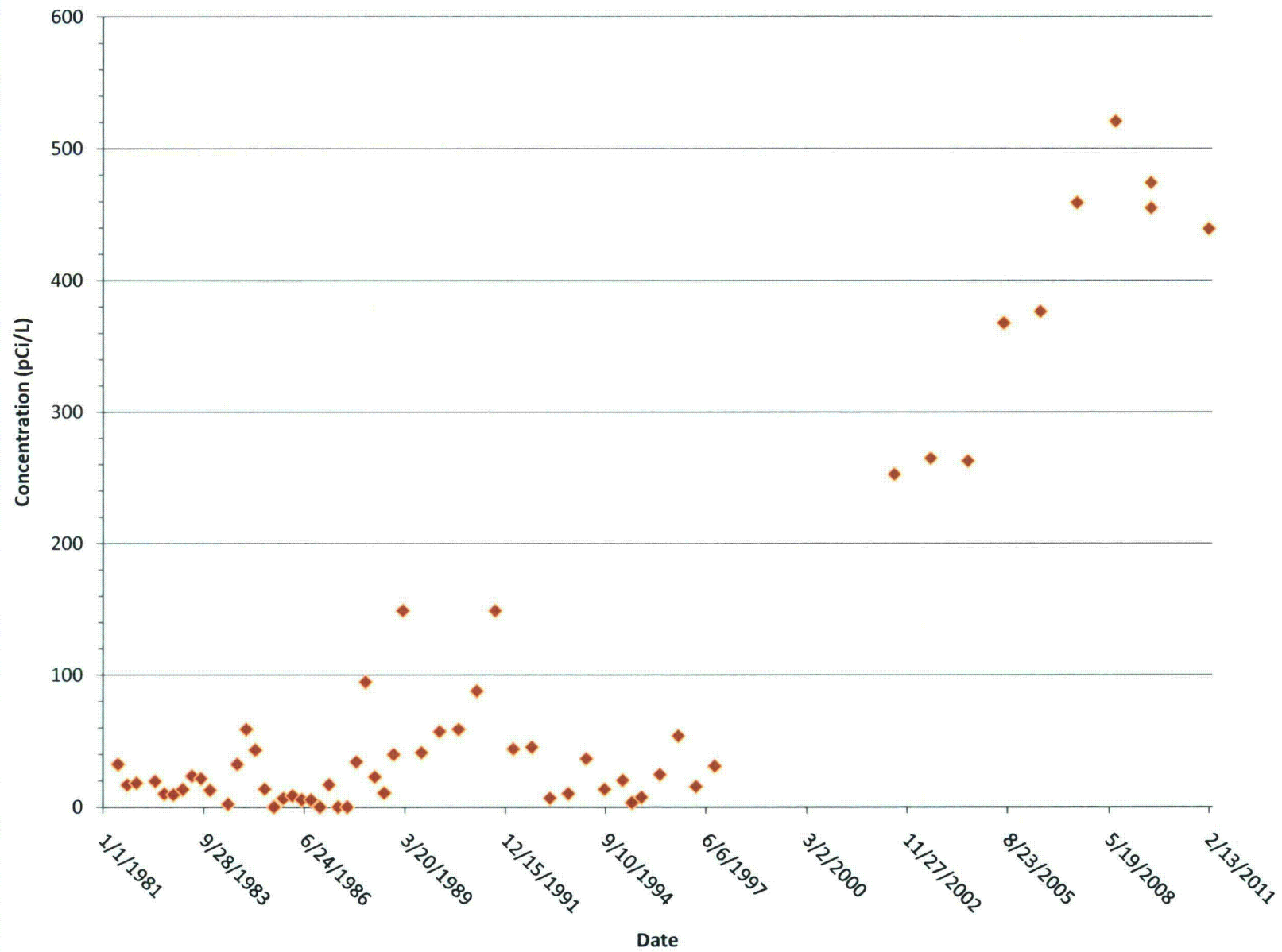


## MW-43 Uranium

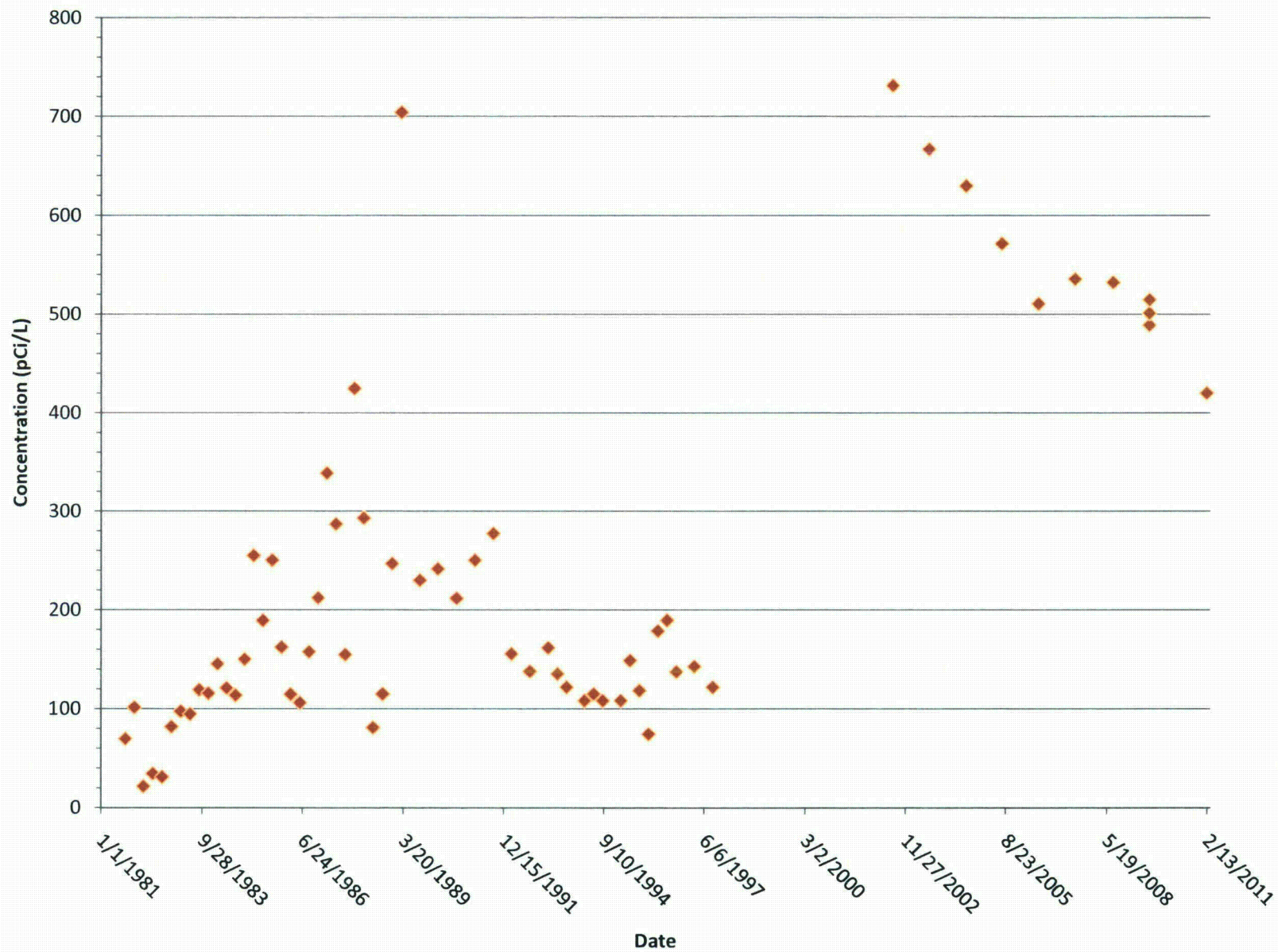




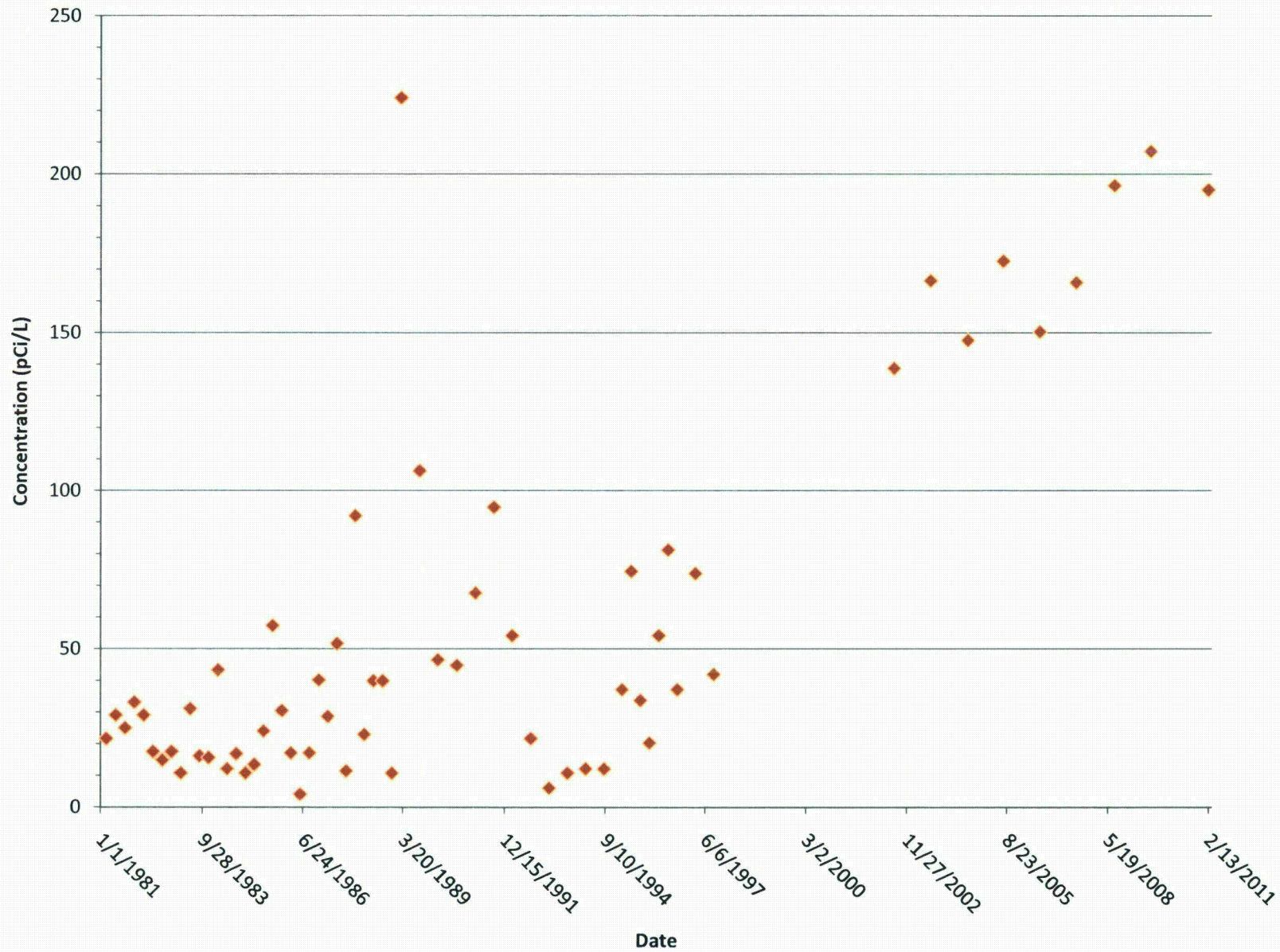
## MW-14 Uranium



## MW-12 Uranium

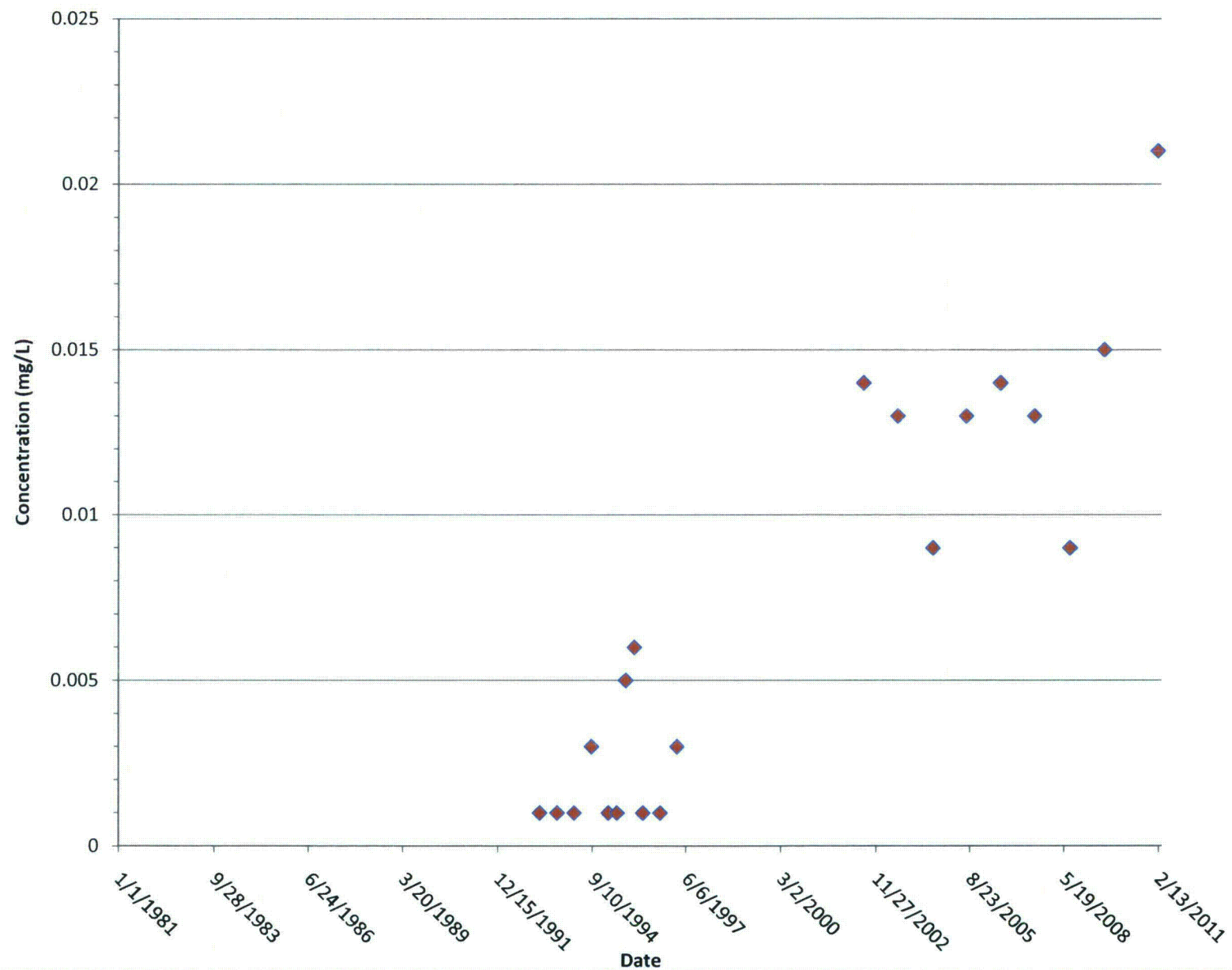


## MW-9 Uranium





# MW-74 Selenium



**MW-43 Selenium**

Date	Concentration (mg/L)
9/28/1982	0.015
1/1/1981	0.010
9/28/1983	0.005
1/1/1984	0.004
6/24/1986	0.006
1/1/1987	0.005
6/24/1986	0.005
1/1/1987	0.005
6/24/1986	0.002
1/1/1987	0.002
3/20/1989	0.001
12/15/1991	0.001
9/10/1994	0.003
6/6/1997	0.001
3/2/2000	0.004
11/27/2002	0.004
8/23/2005	0.006
5/19/2008	0.004
2/13/2011	0.003

Concentration (mg/L)

**MW-14 Selenium**

Date	Concentration (mg/L)
1/1/1981	0.010
9/28/1983	0.016
6/24/1986	0.005
12/15/1991	0.080
9/10/1994	0.005
11/27/2002	0.005
8/23/2005	0.007
5/19/2008	0.003
2/13/2011	0.004

Concentration (mg/L)



**MW-12 Selenium**

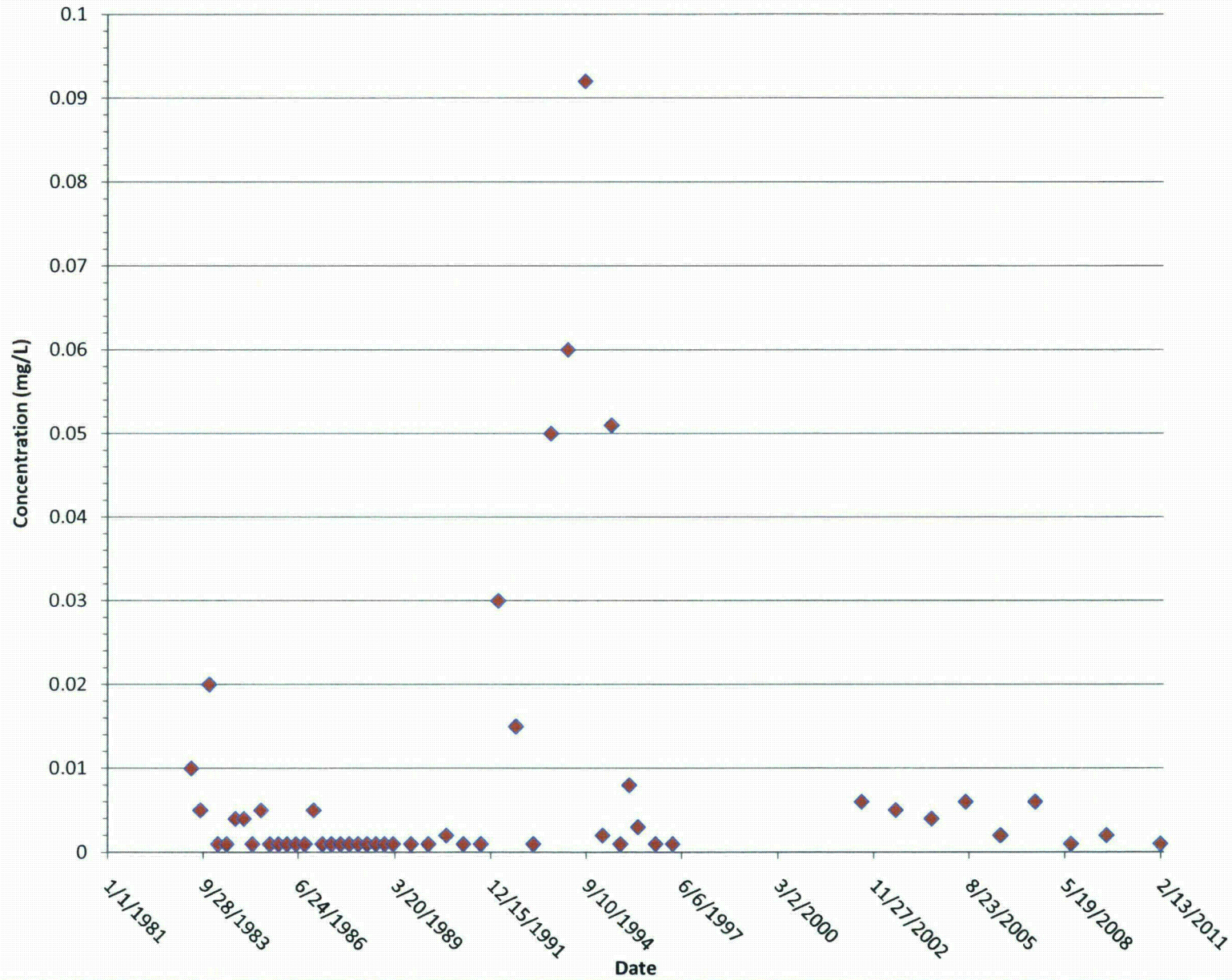
Concentration (mg/L)

Date

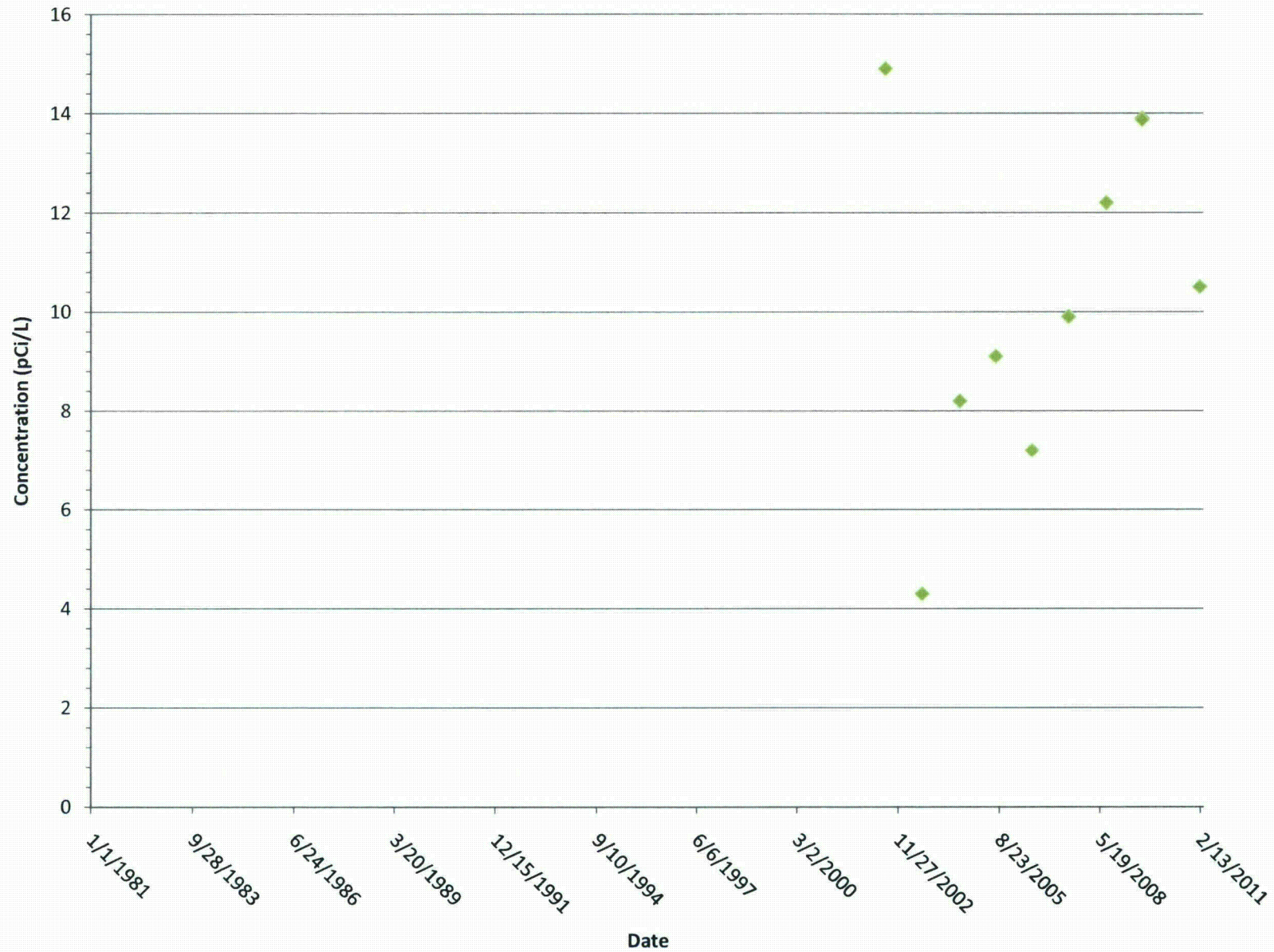
Date	Concentration (mg/L)
9/28/1983	0.024
1/1/1981	0.010
9/28/1983	0.005
1/1/1981	0.005
9/28/1983	0.004
1/1/1981	0.004
6/24/1986	0.005
1/1/1981	0.002
6/24/1986	0.002
1/1/1981	0.001
3/20/1989	0.001
12/15/1991	0.001
9/10/1994	0.004
9/10/1994	0.003
6/6/1997	0.004
6/6/1997	0.002
6/6/1997	0.001
11/27/2002	0.005
11/27/2002	0.007
8/23/2005	0.007
8/23/2005	0.003
5/19/2008	0.003
5/19/2008	0.001
2/13/2011	0.002

Concentration (mg/L)

# MW-9 Selenium

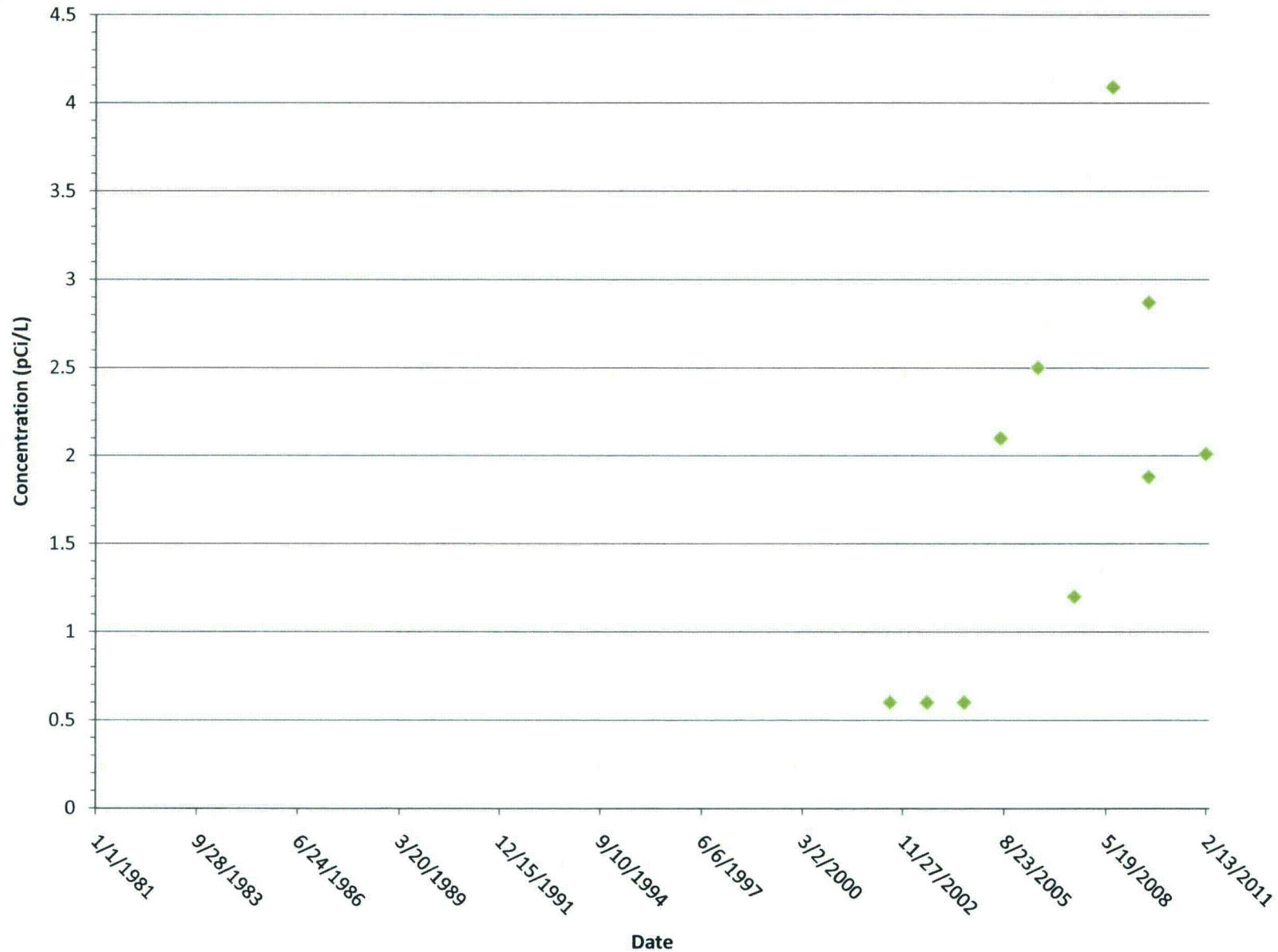


## MW-110 Combined Radium 226 and 228

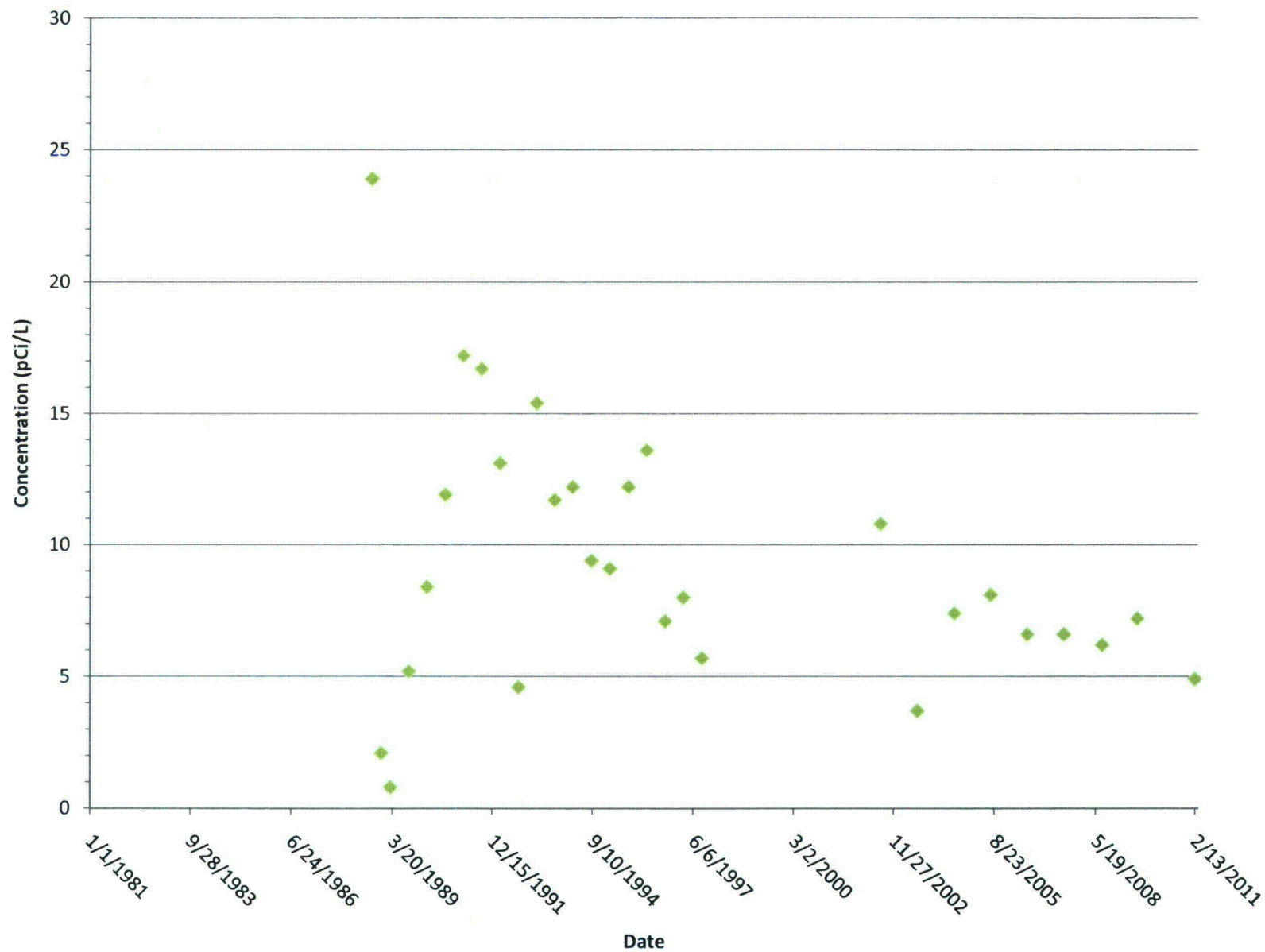




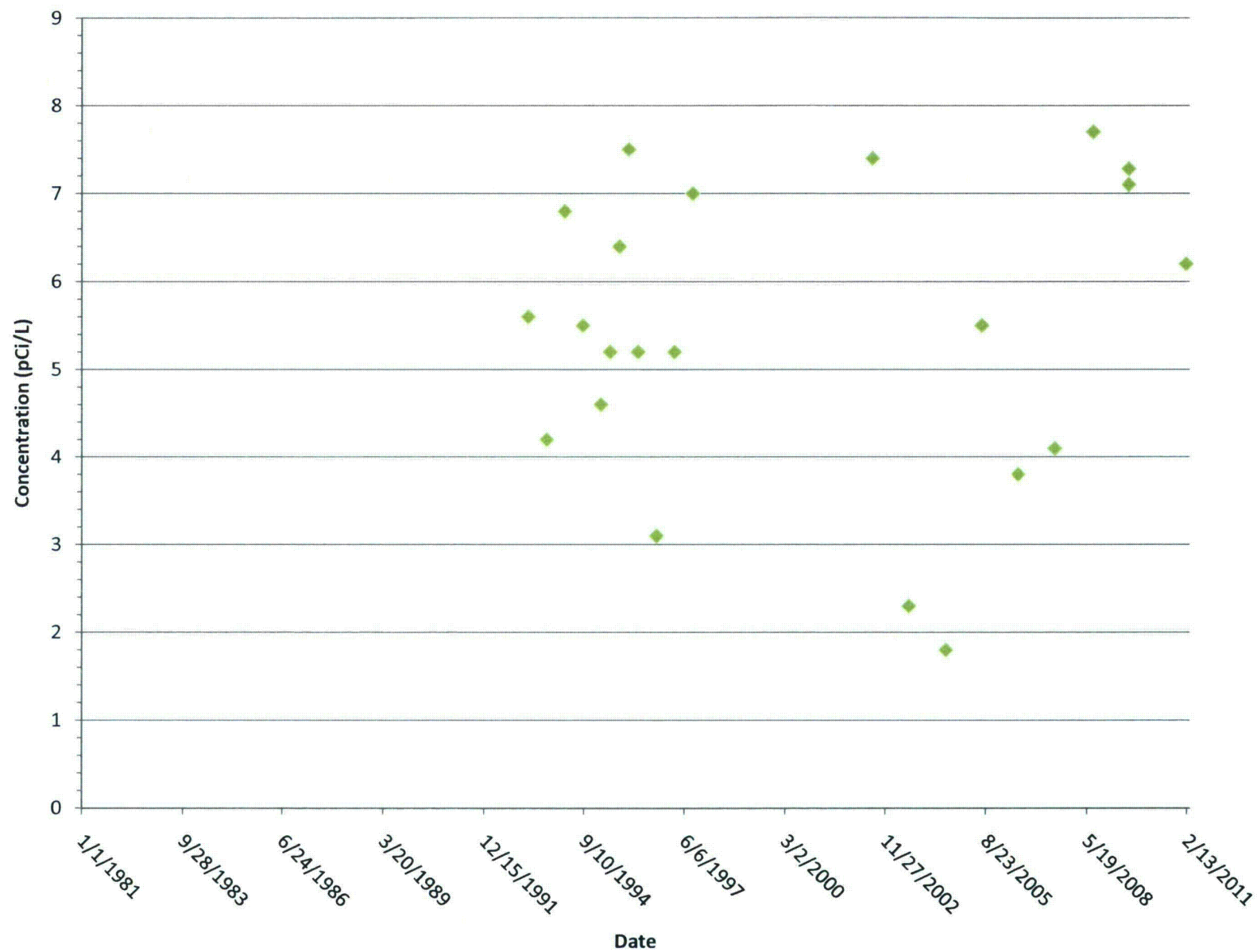
# MW-108 Combined Radium 226 and 228



# MW-43 Combined Radium 226 and 228

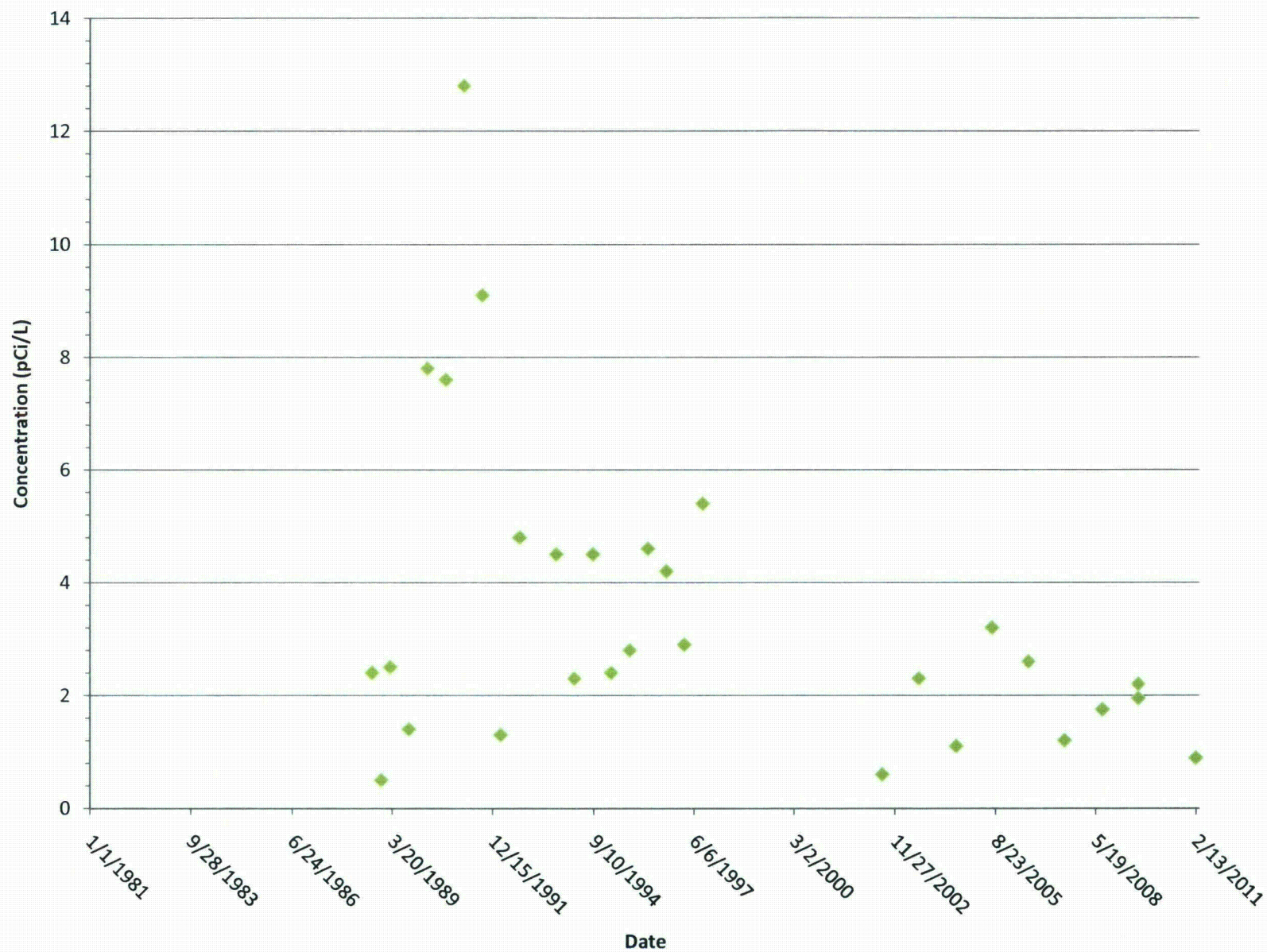


# MW-74 Combined Radium 226 and 228

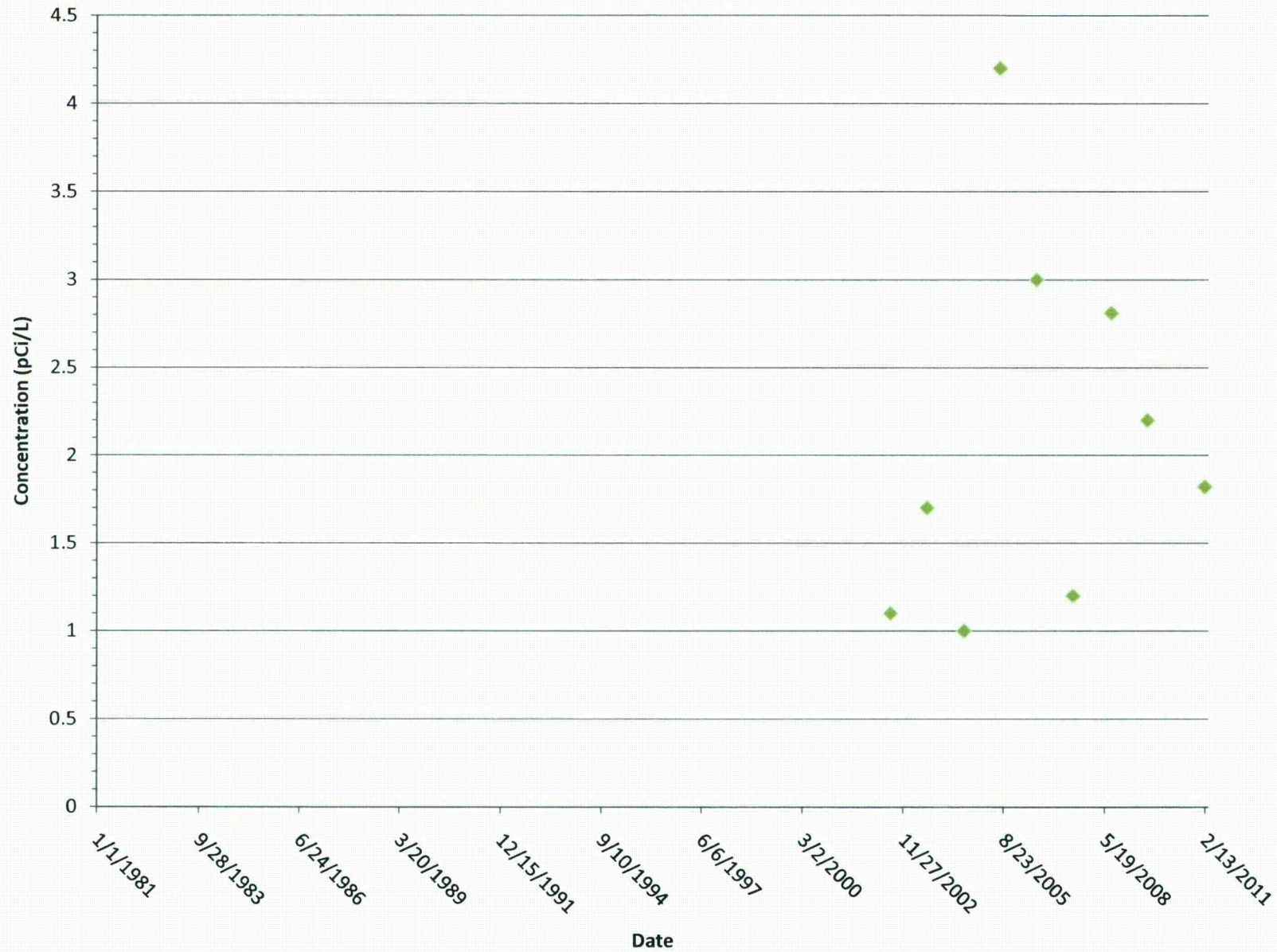




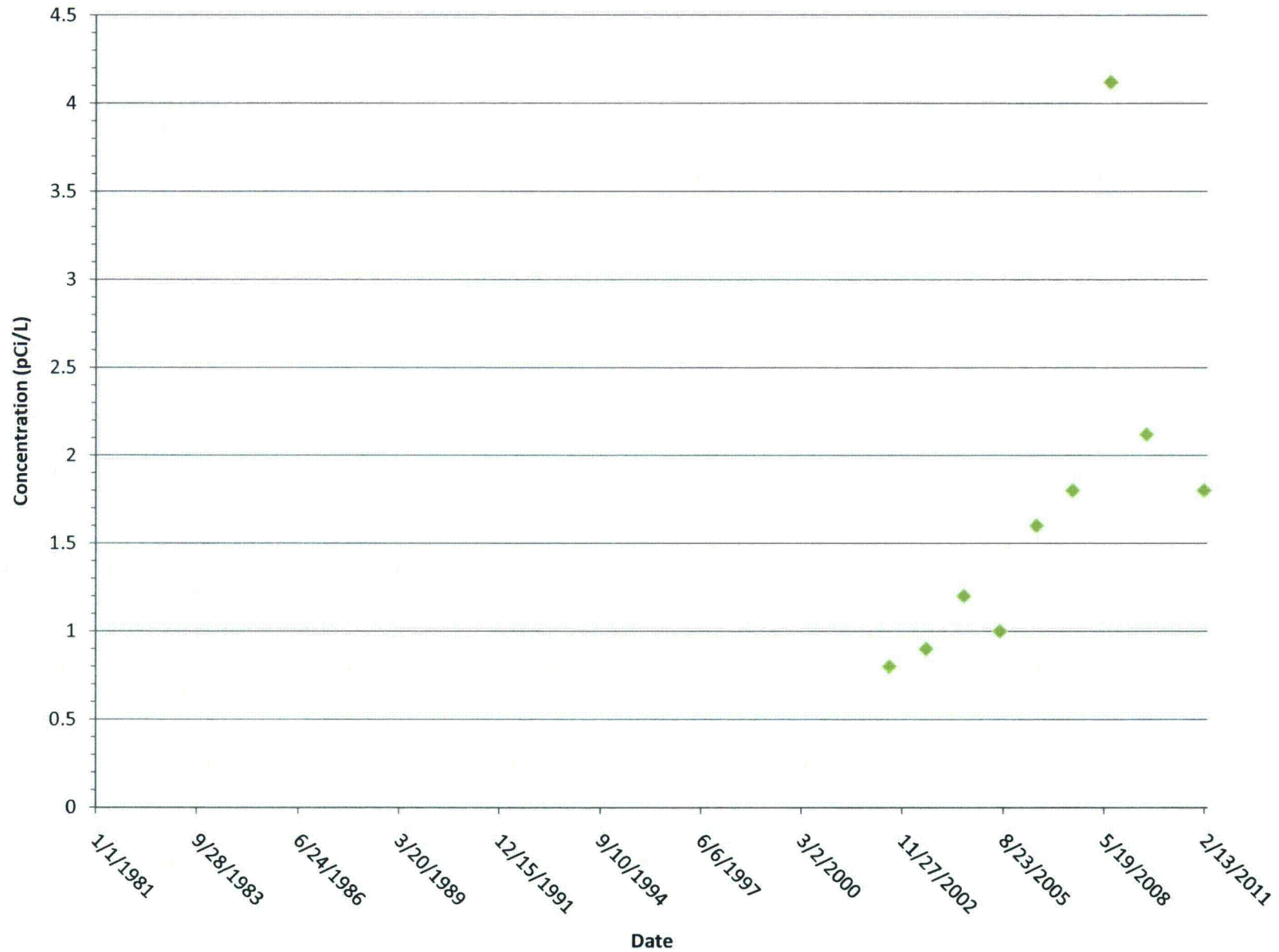
# MW-14 Combined Radium 226 and 228



## MW-111 Combined Radium 226 and 228

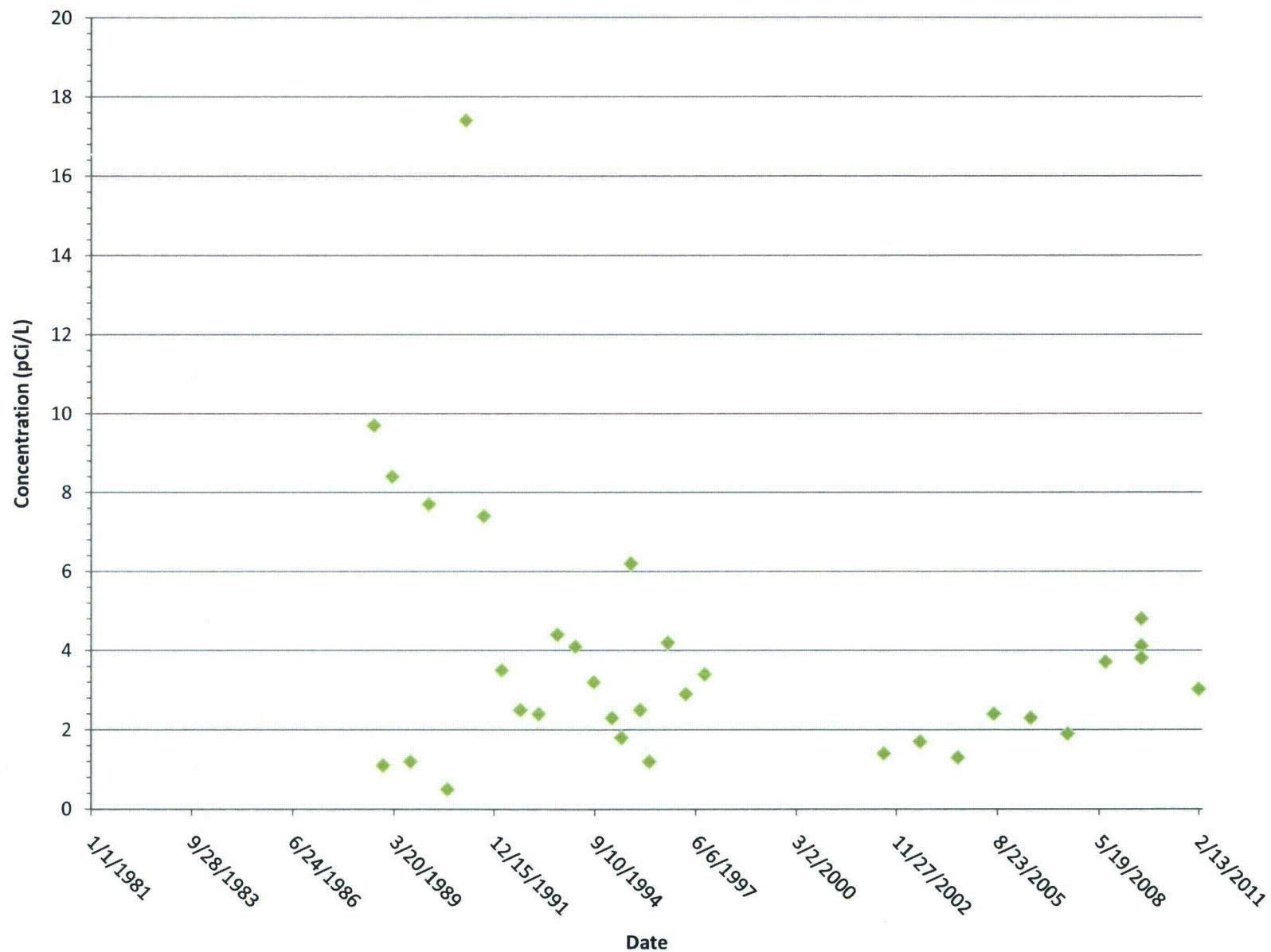


## MW-109 Combined Radium 226 and 228

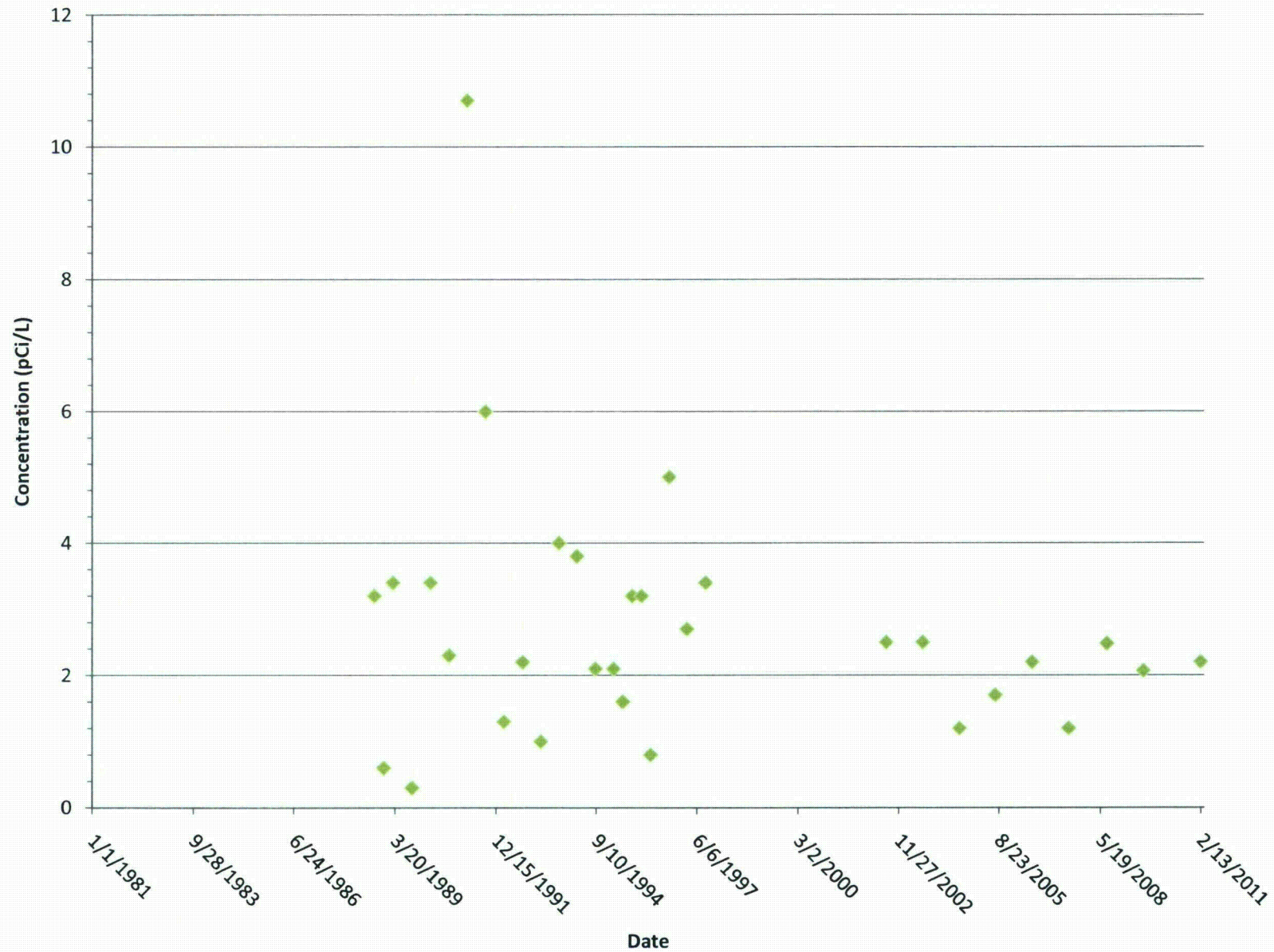




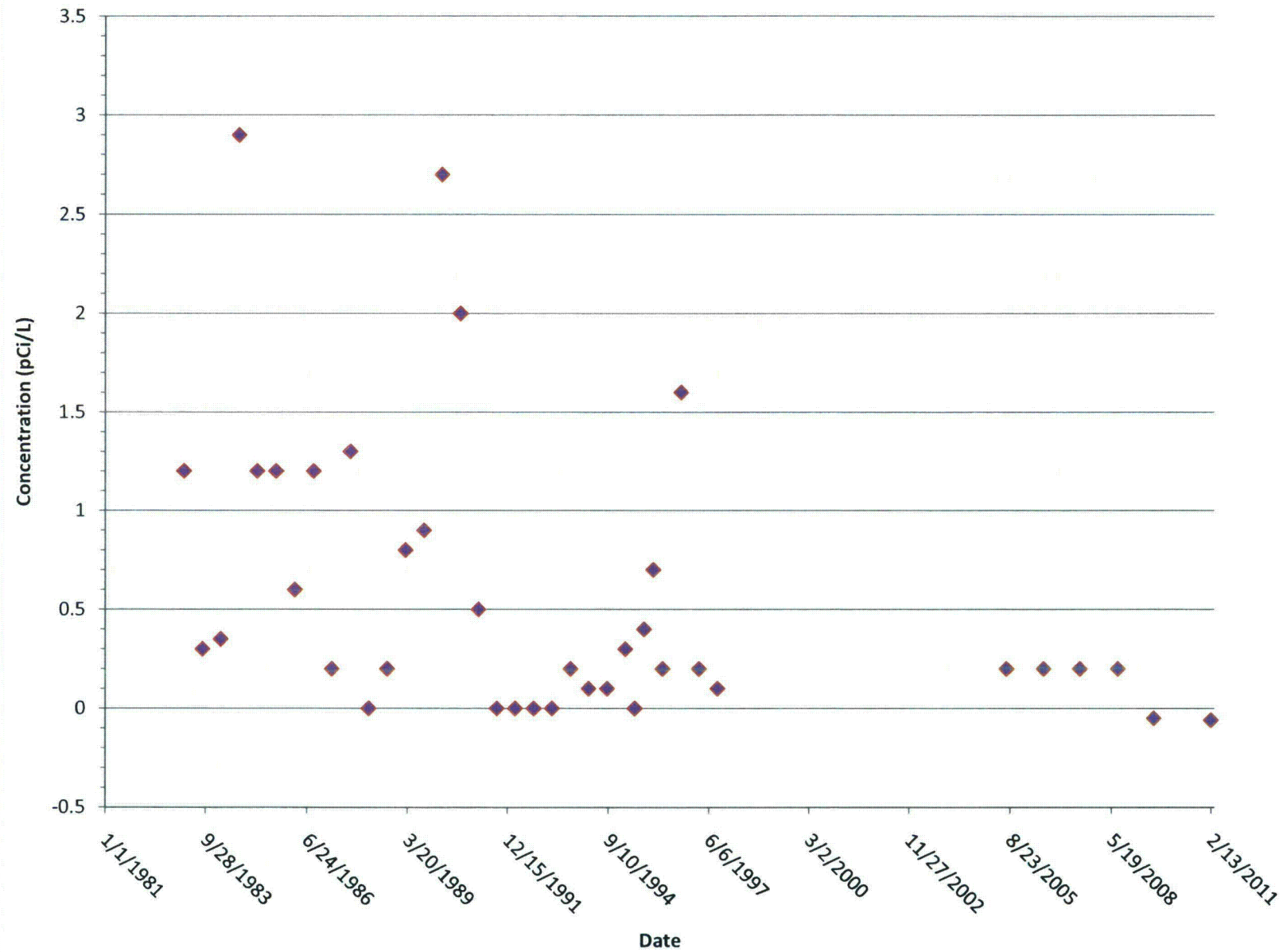
## MW-12 Combined Radium 226 and 228



# MW-9 Combined Radium 226 and 228

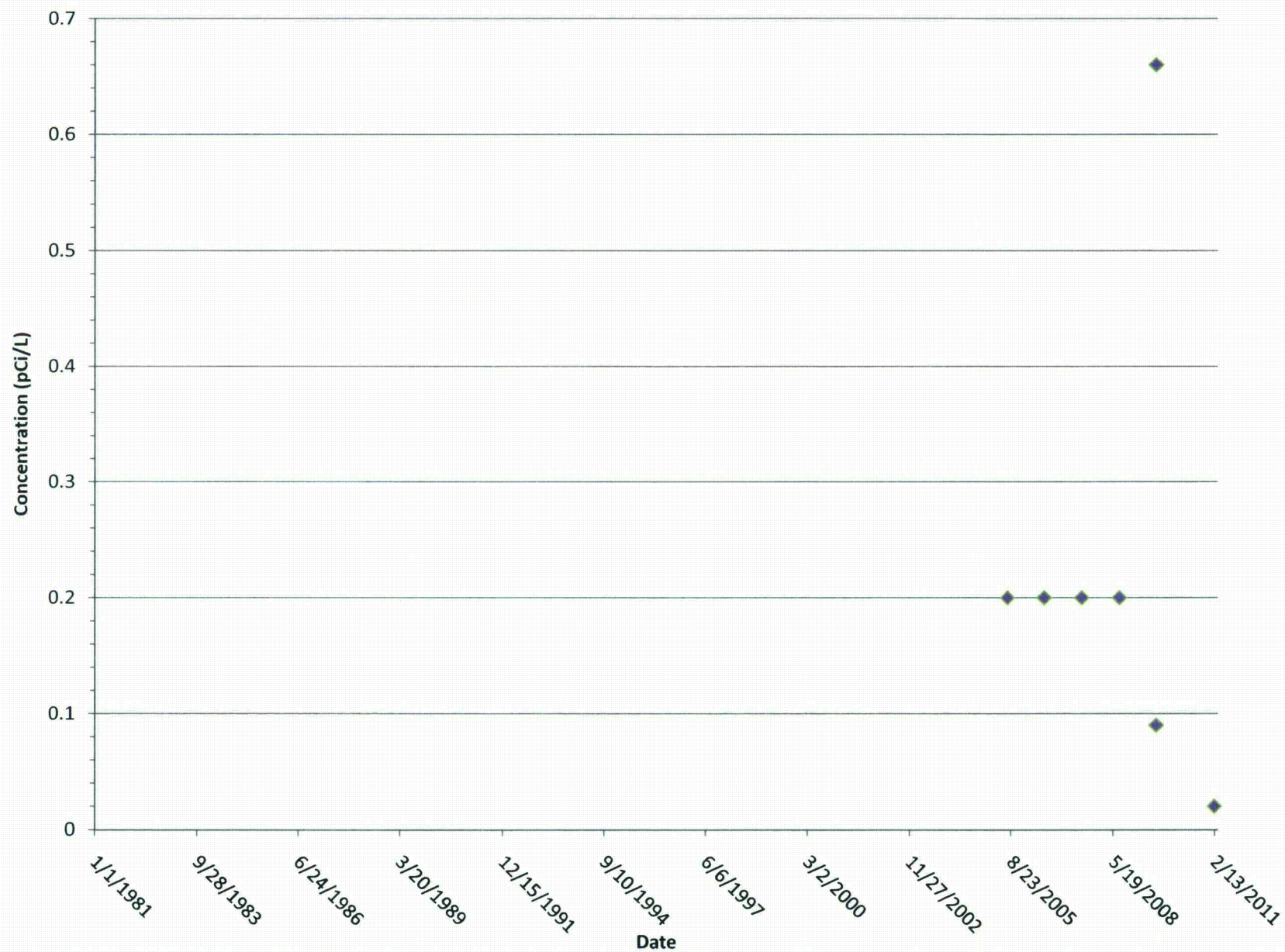


# MW-9 Thorium 230

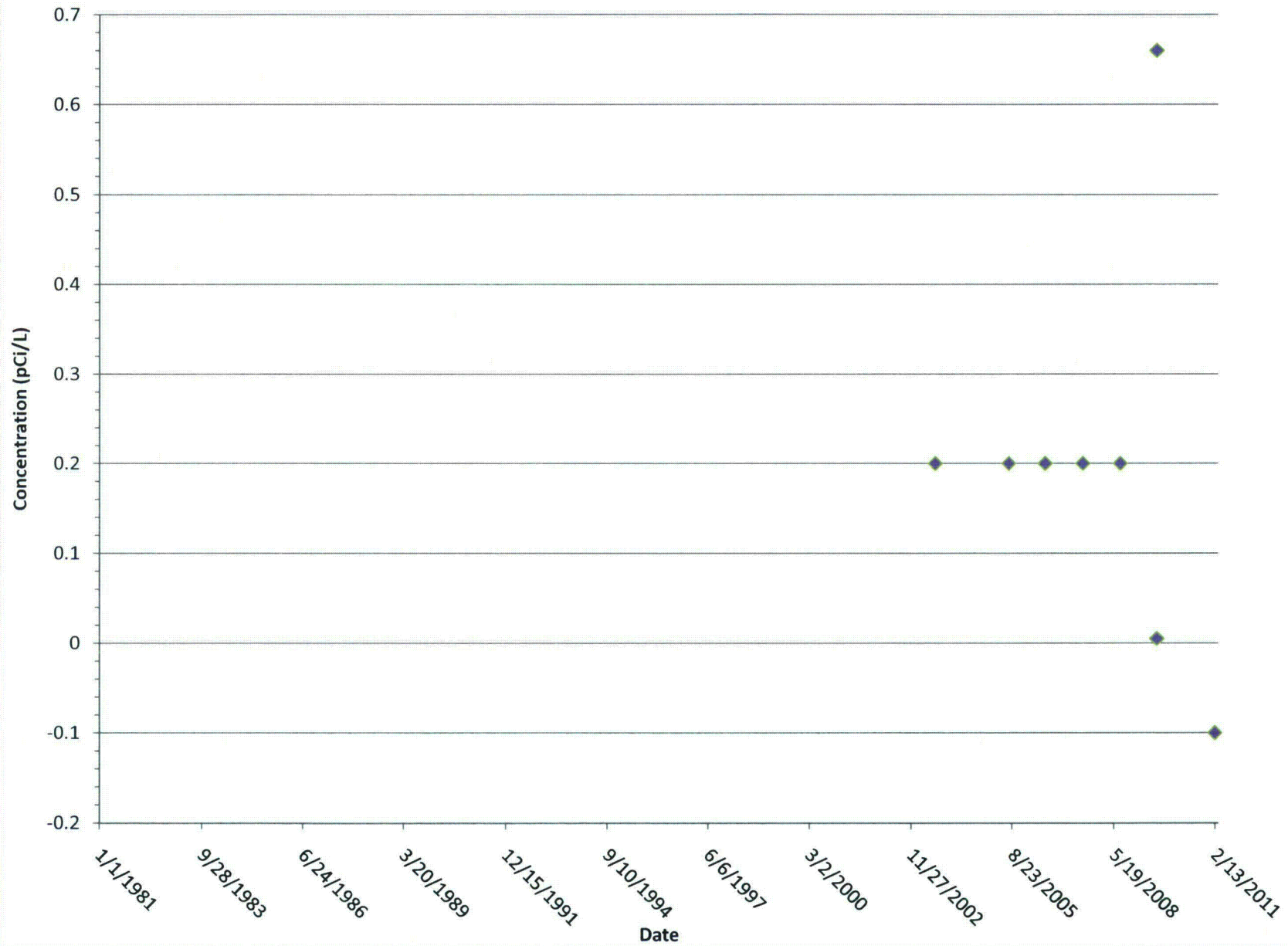




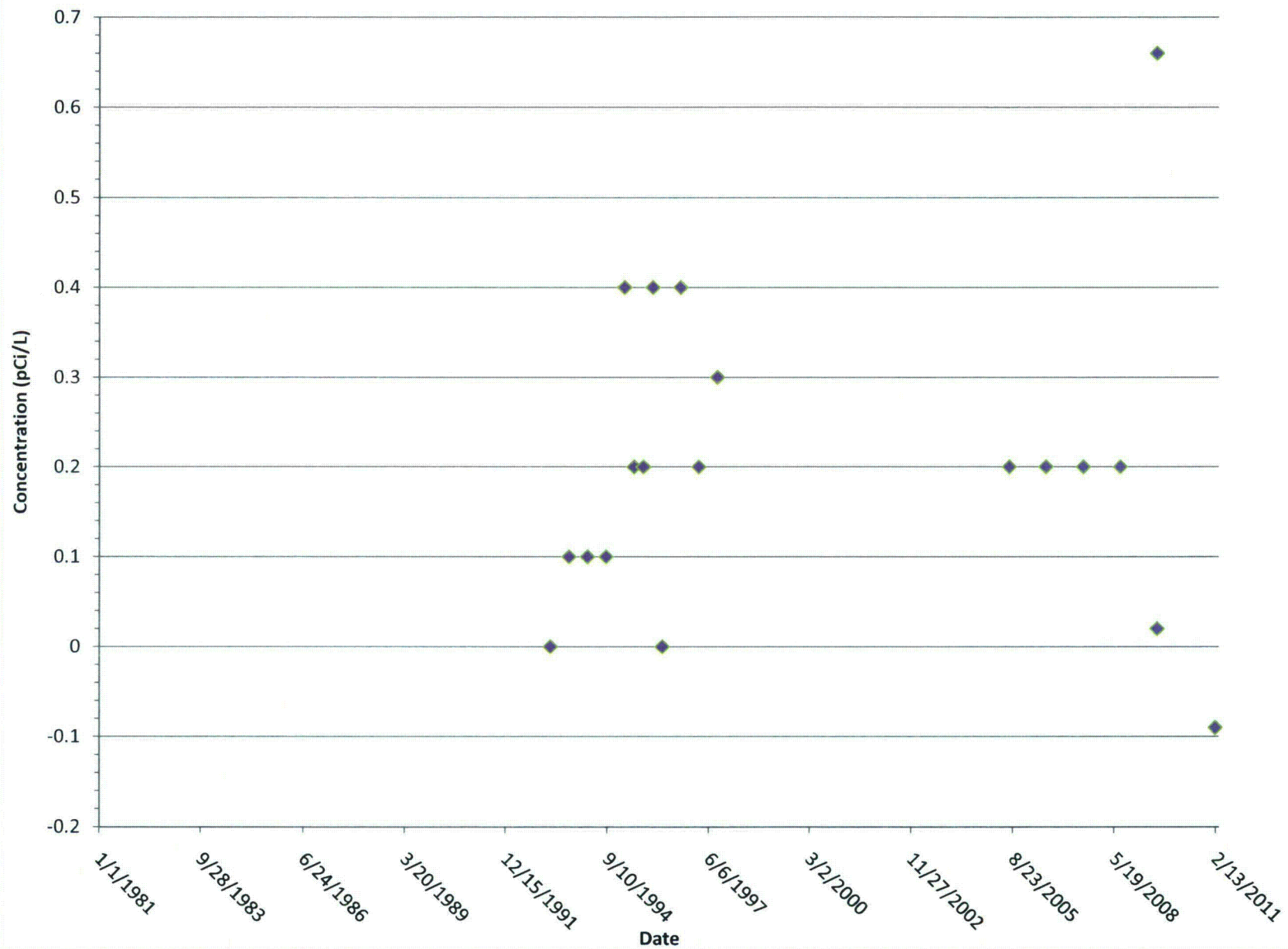
# MW-110 Thorium 230



# MW-108 Thorium 230

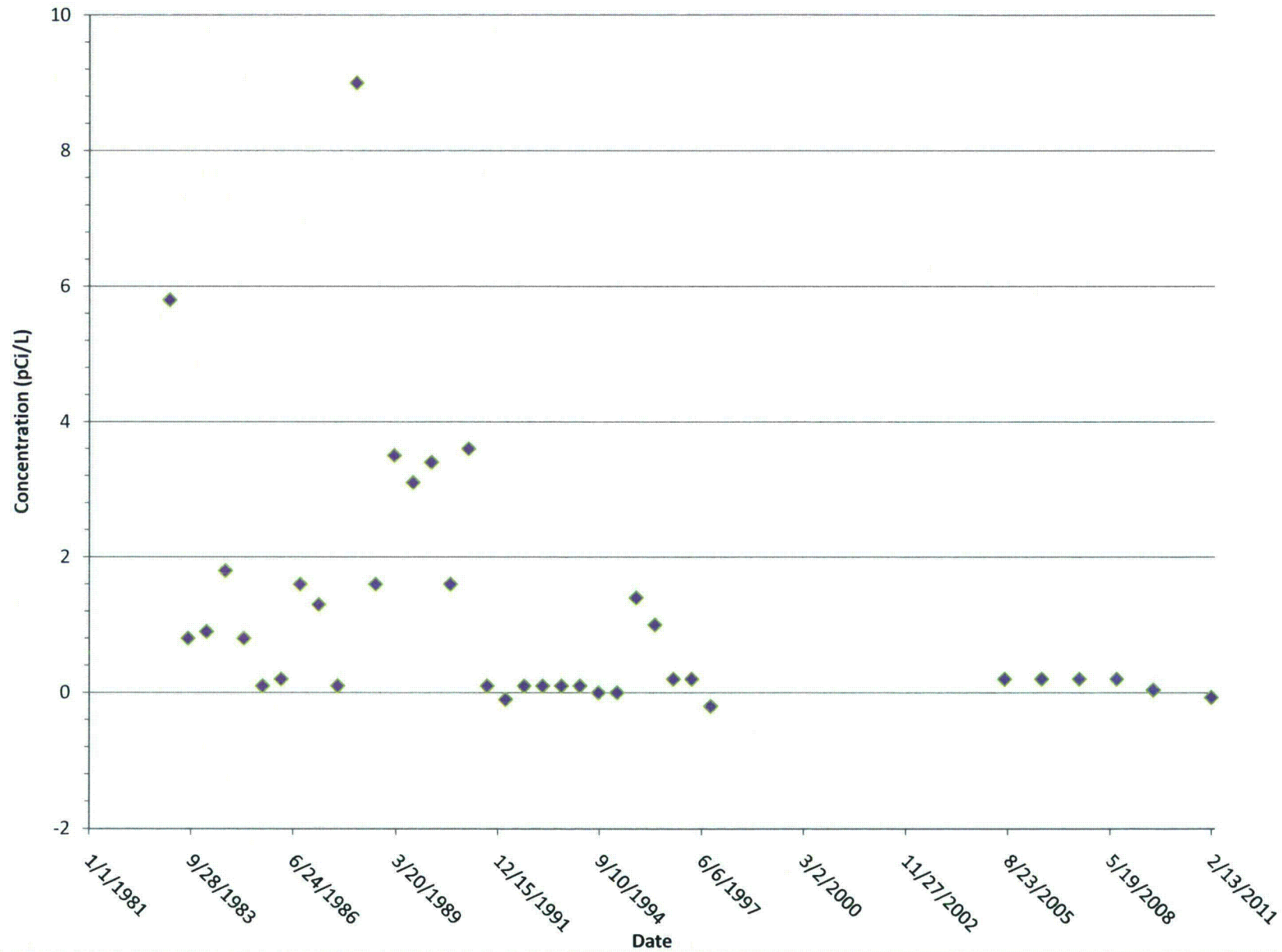


# MW-74 Thorium 230

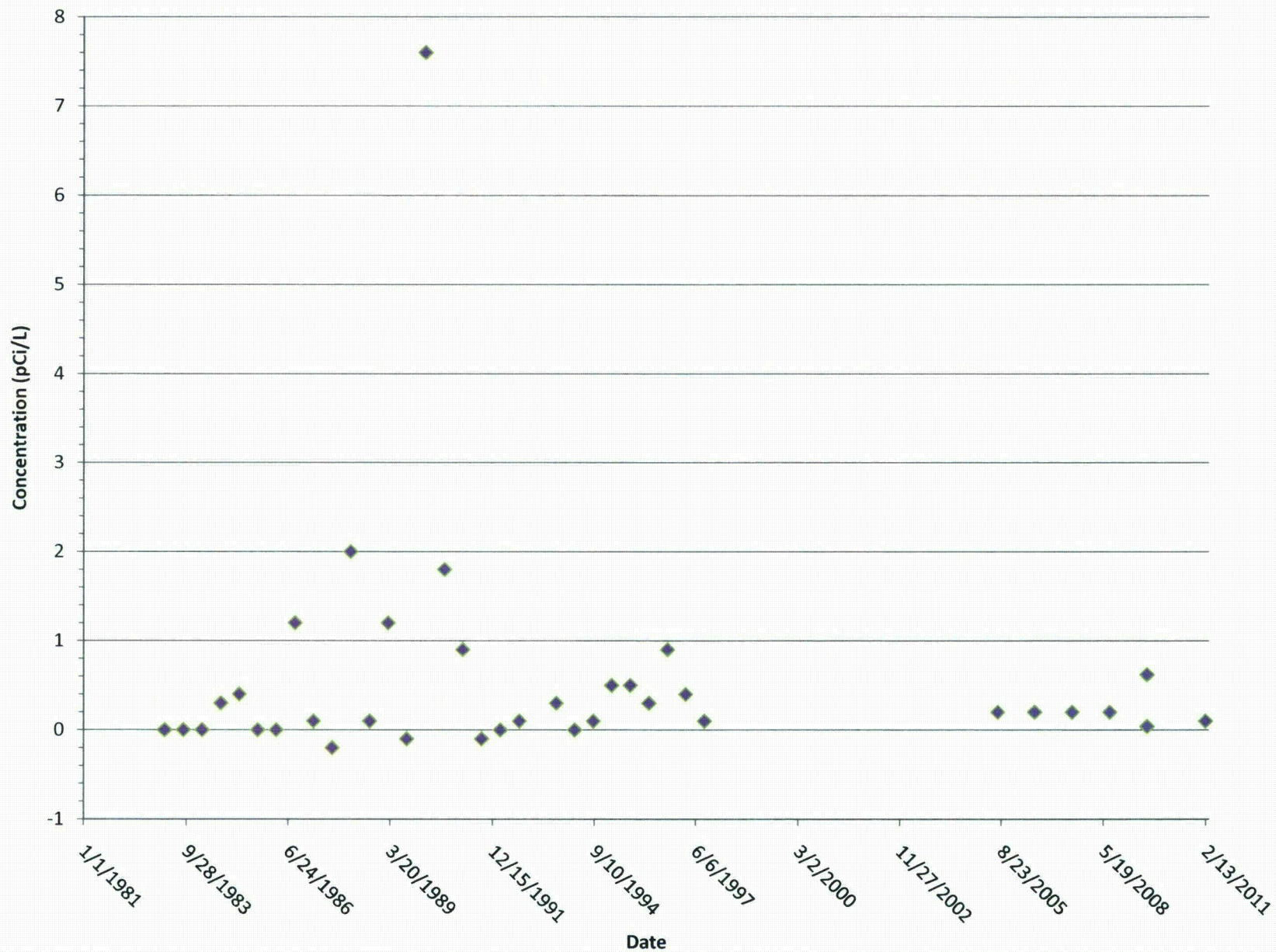




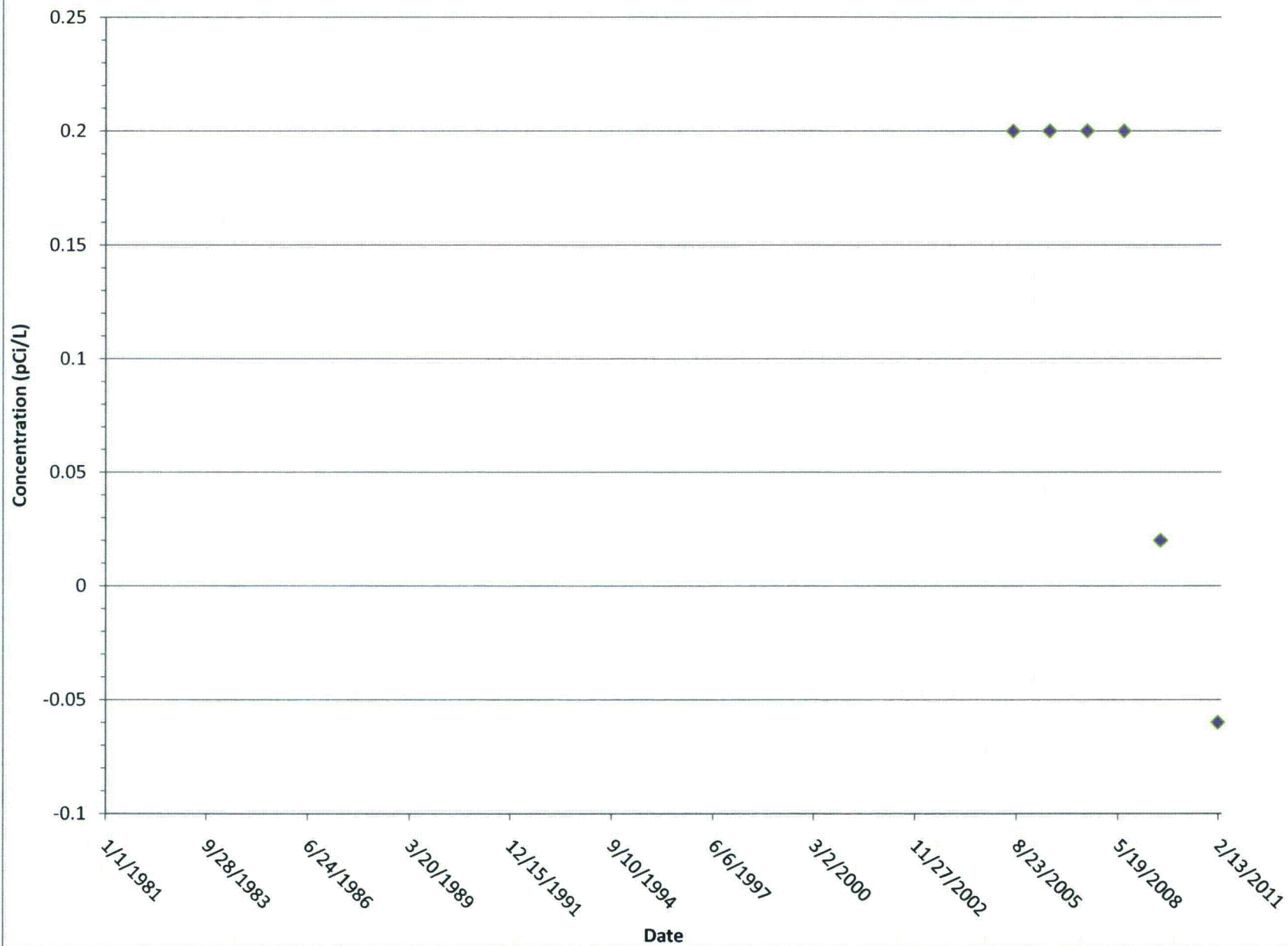
# MW-43 Thorium 230



# MW-14 Thorium 230

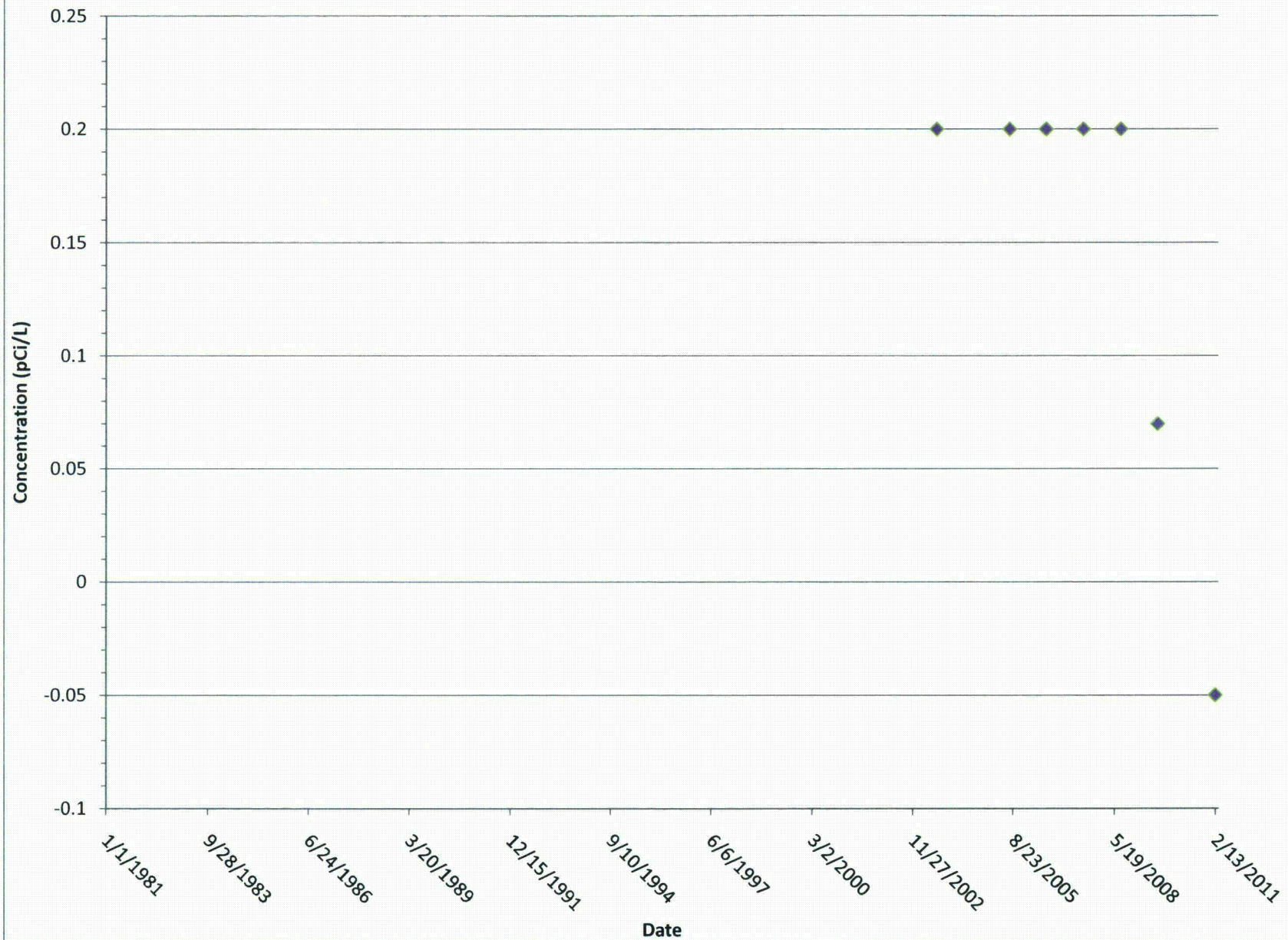


# MW-111 Thorium 230

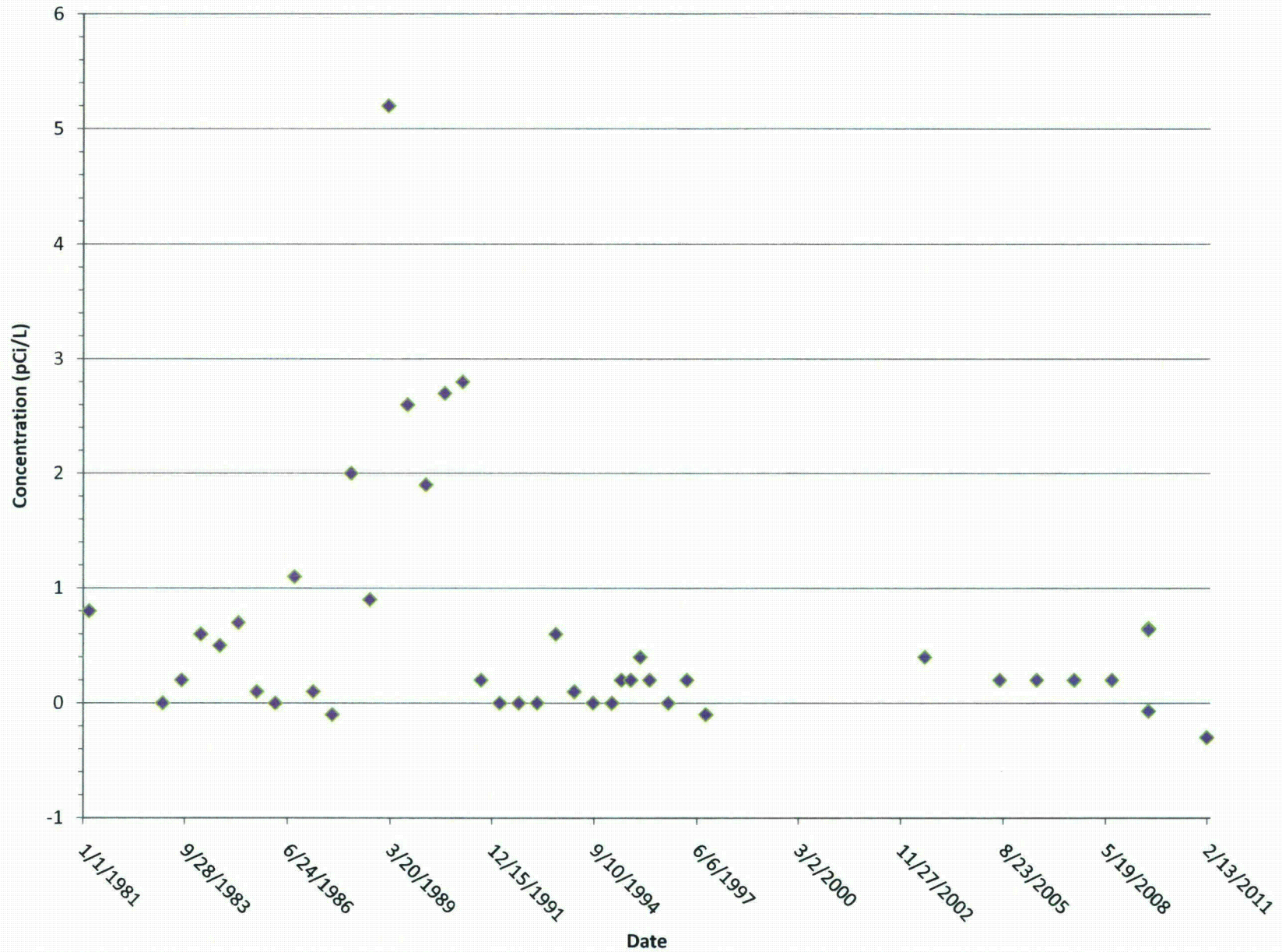




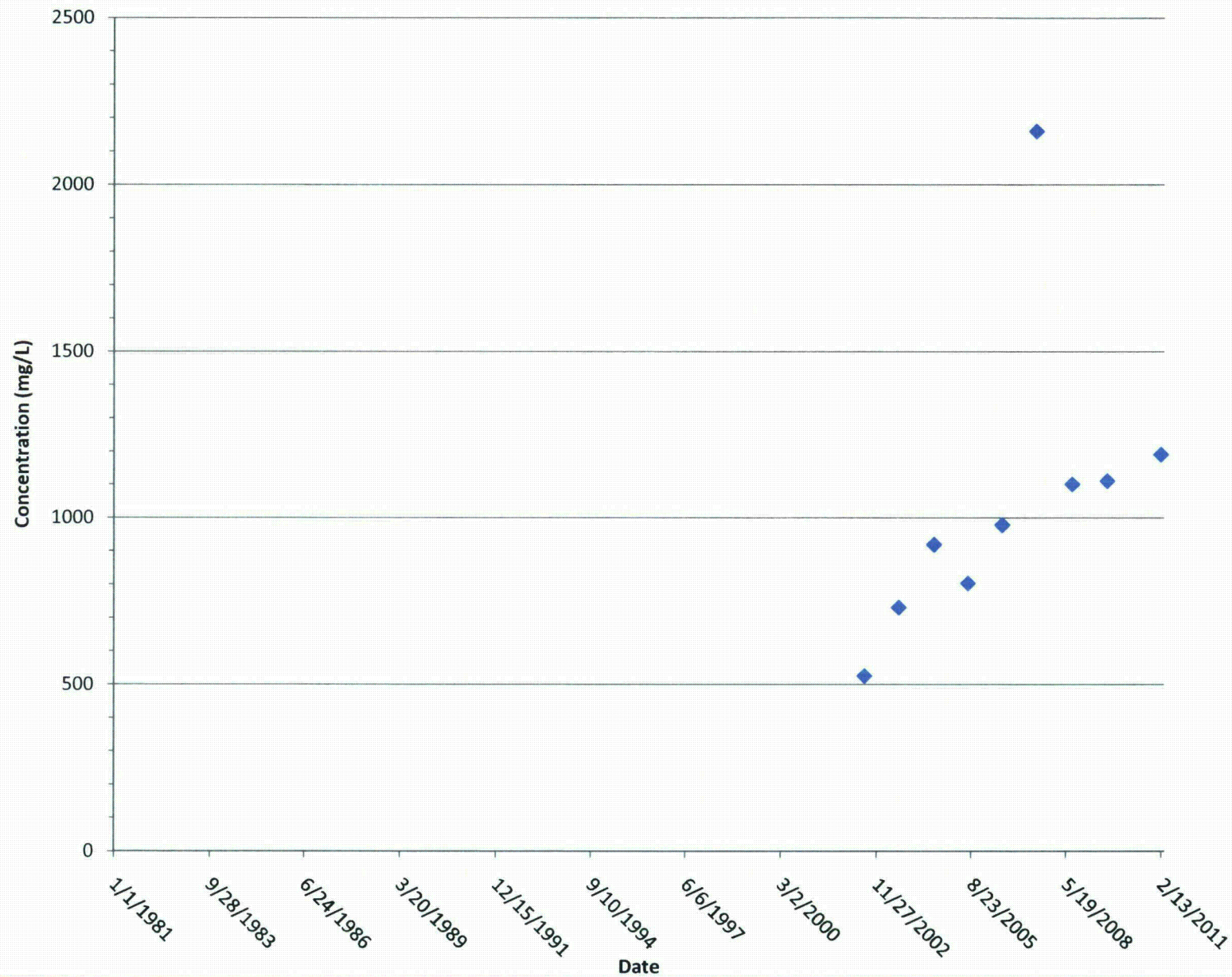
# MW-109 Thorium 230



# MW-12 Thorium 230

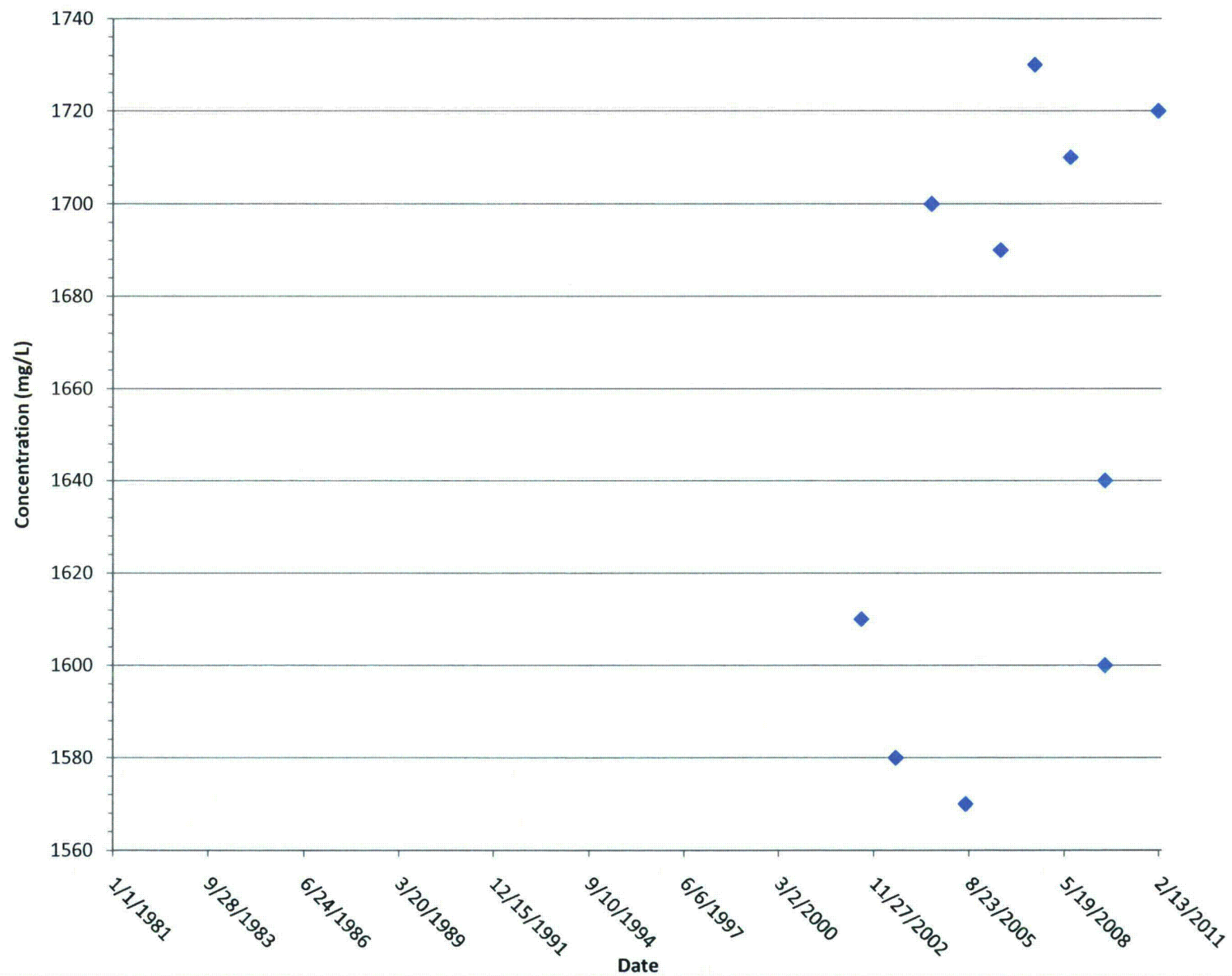


## MW-111 Sulfate

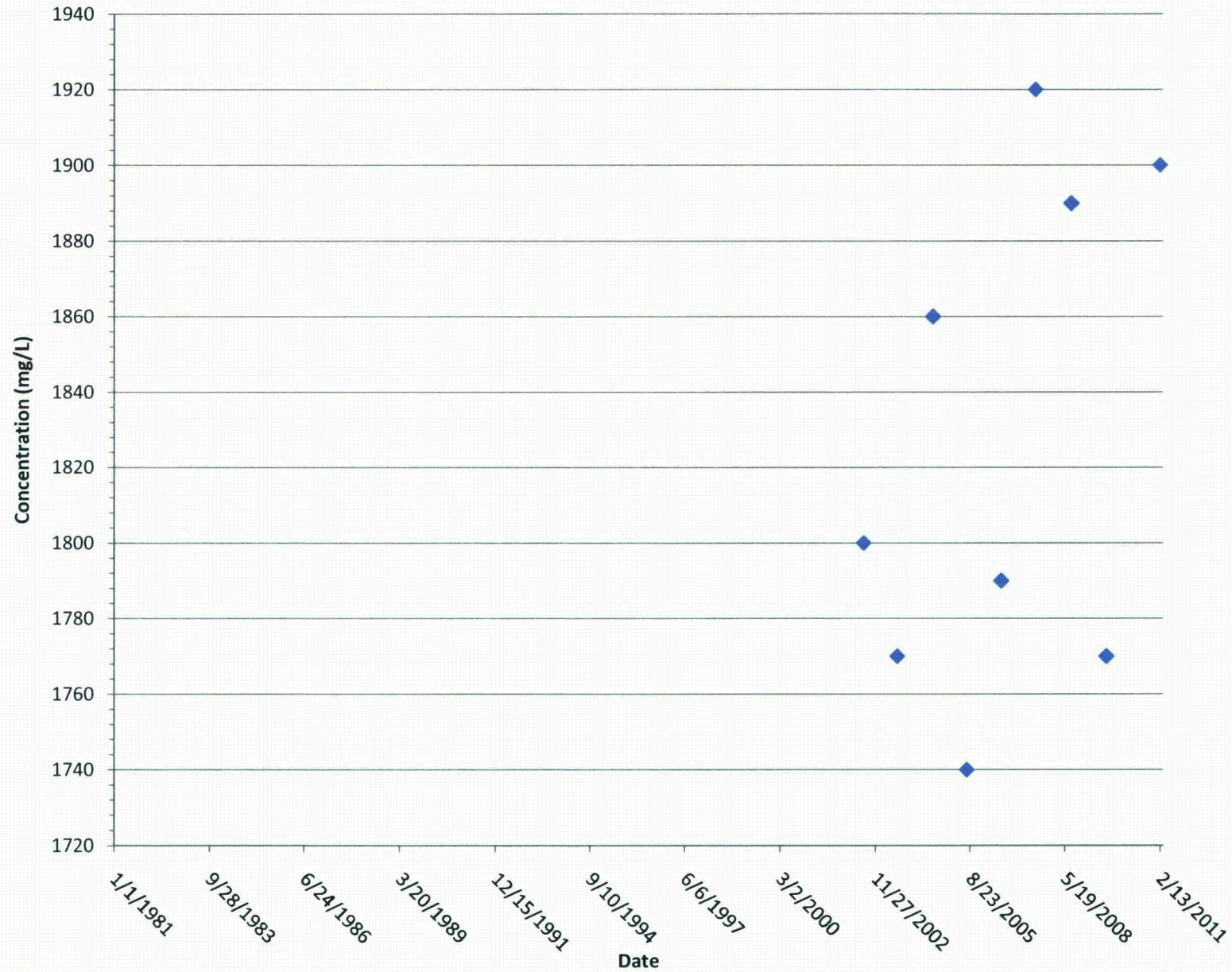




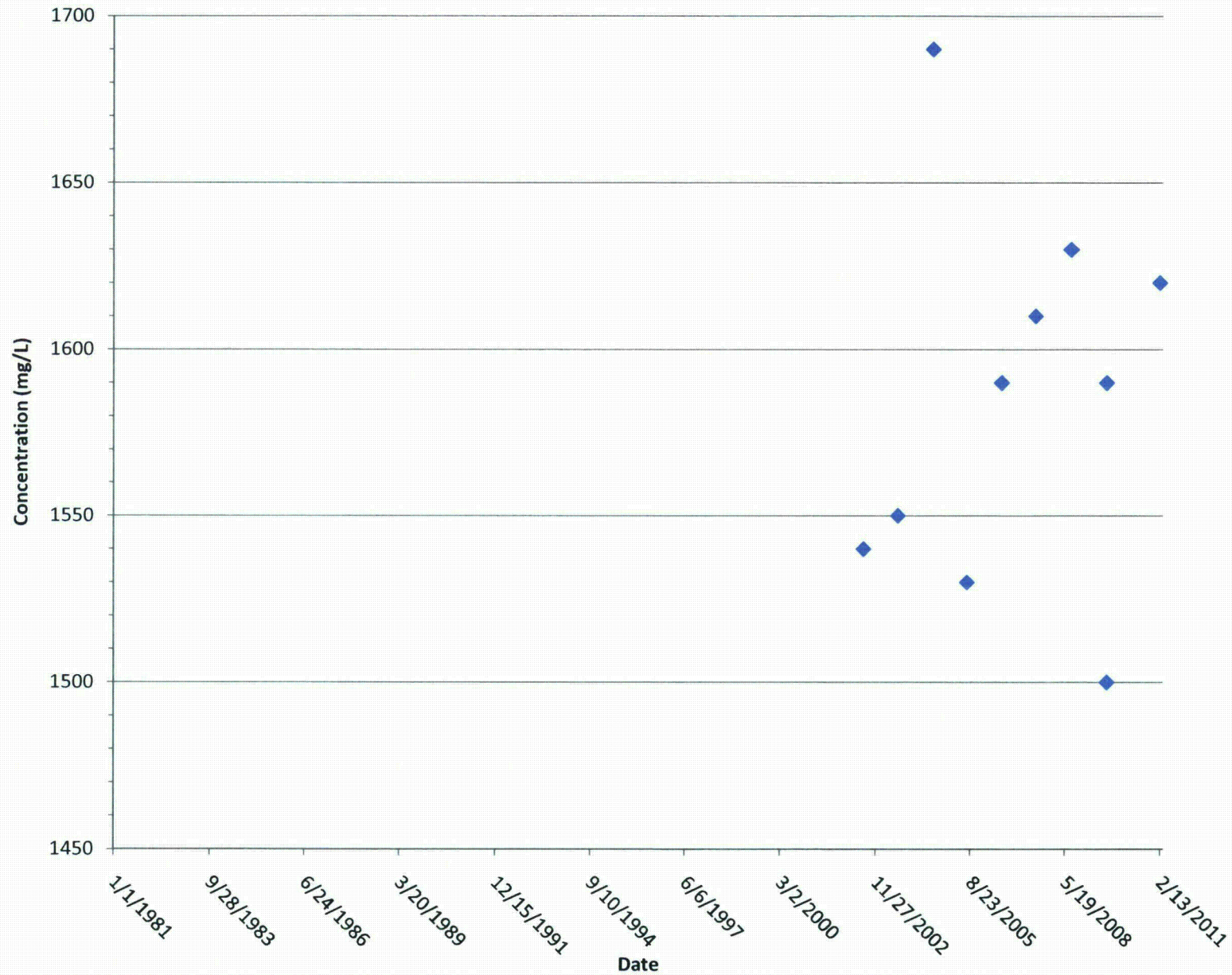
# MW-110 Sulfate



# MW-109 Sulfate

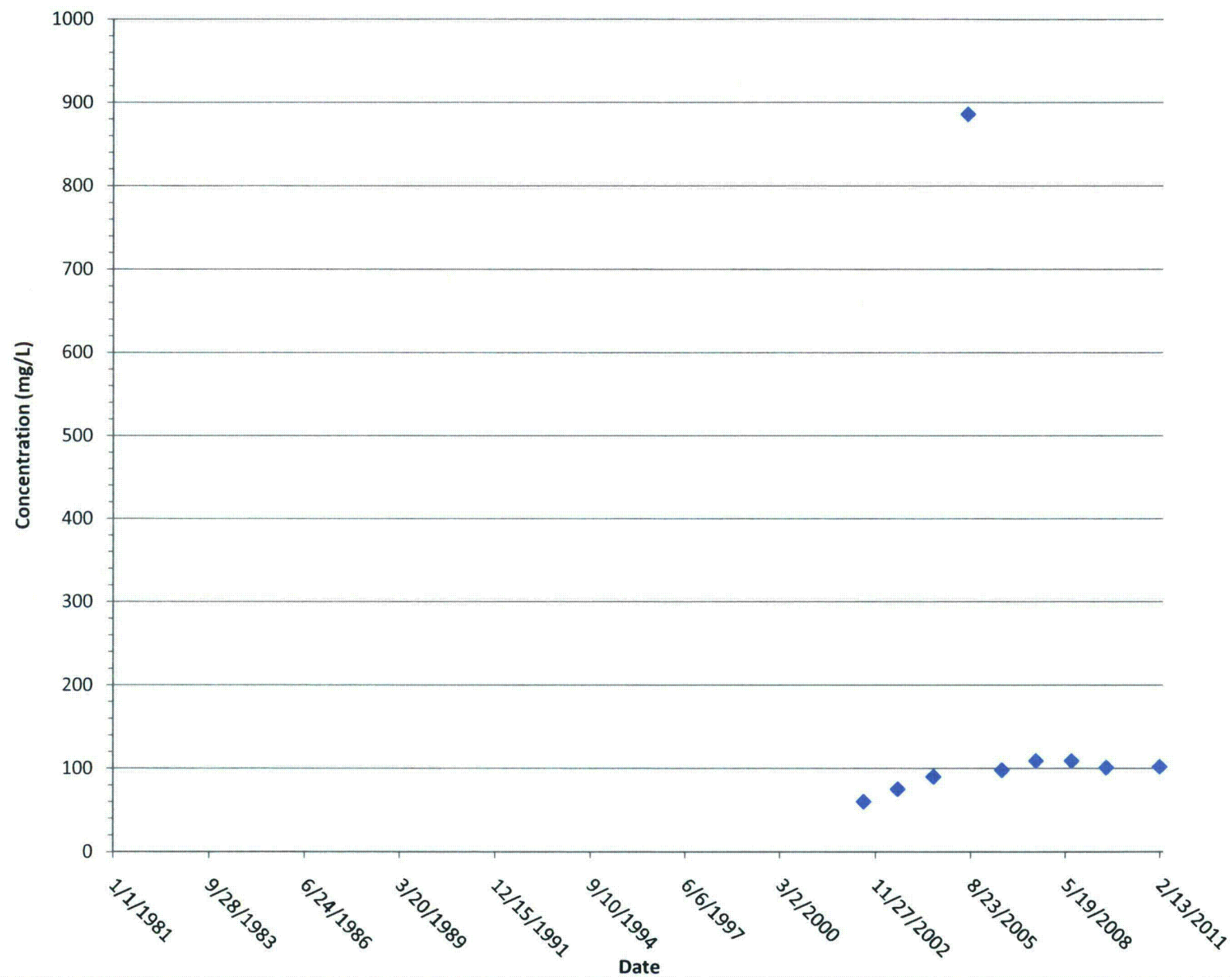


## MW-108 Sulfate

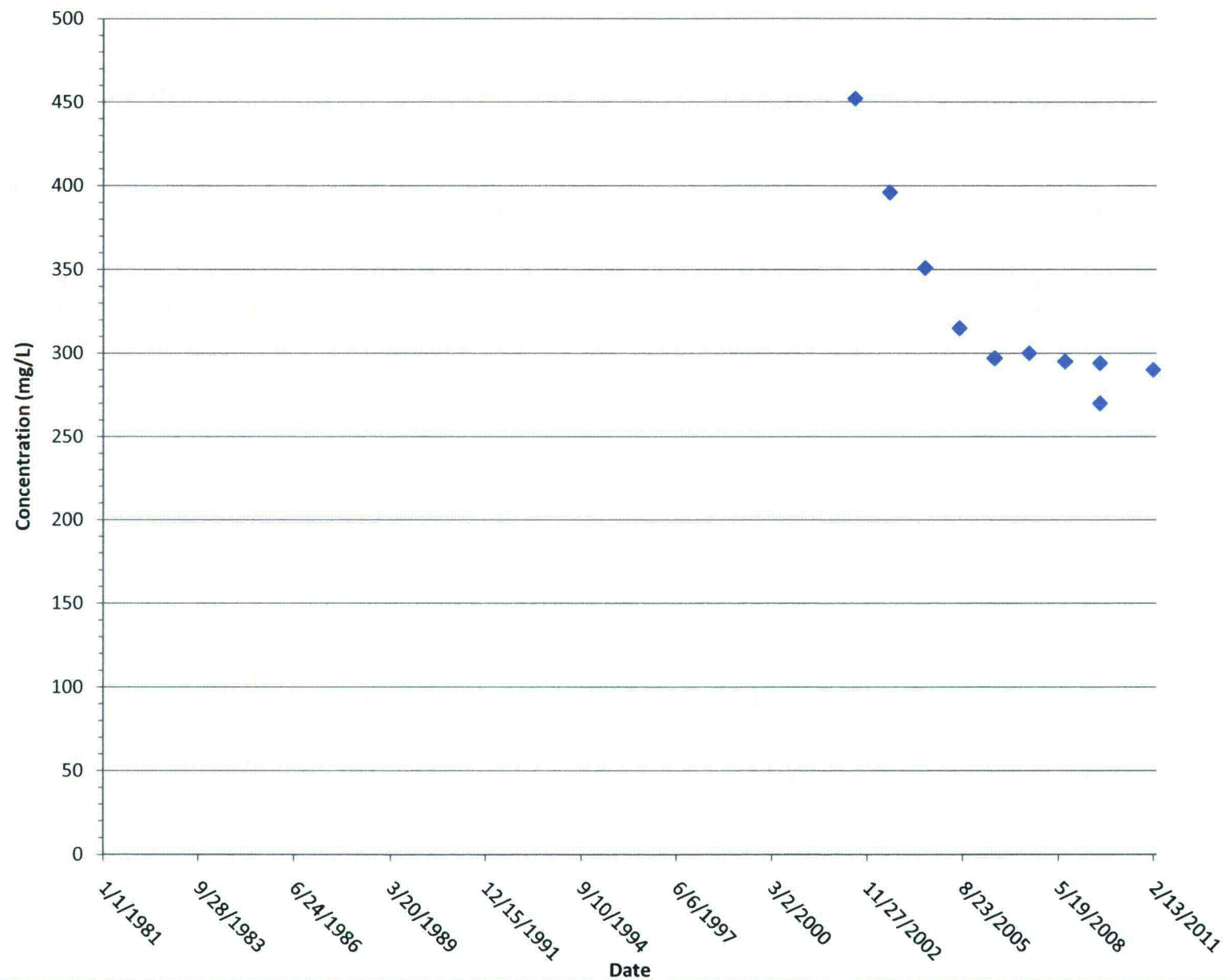




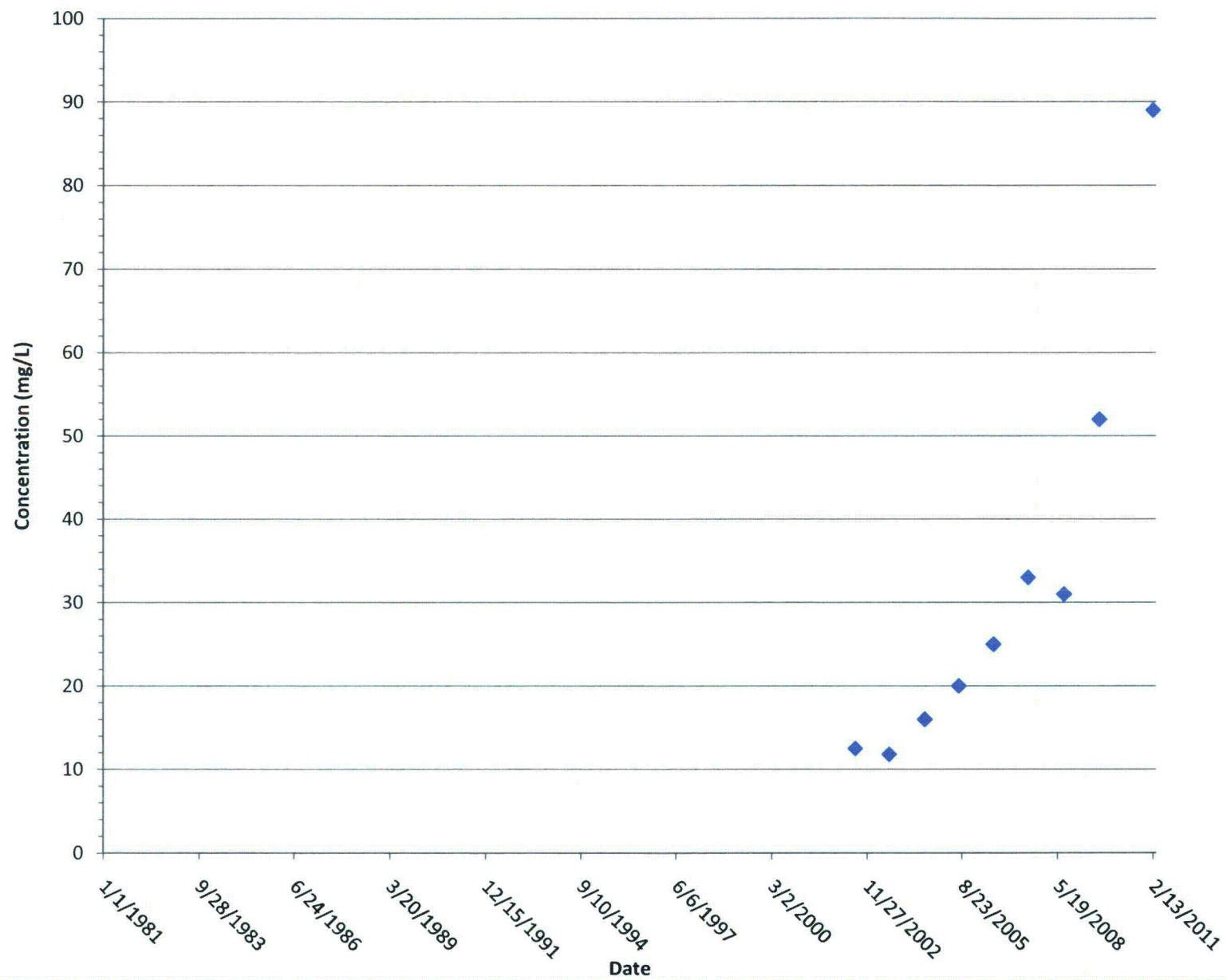
## MW-111 Chloride



## MW-110 Chloride

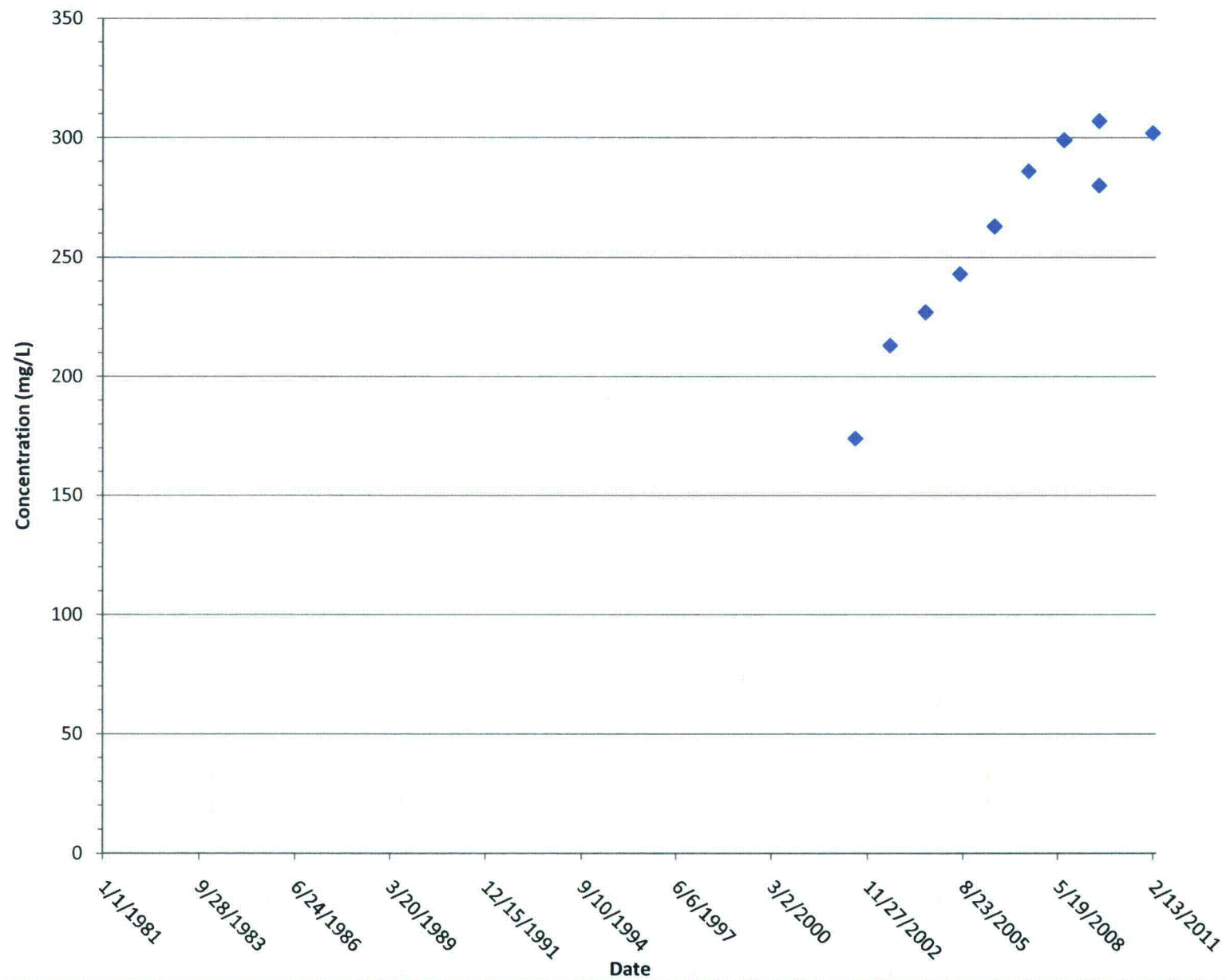


## MW-109 Chloride

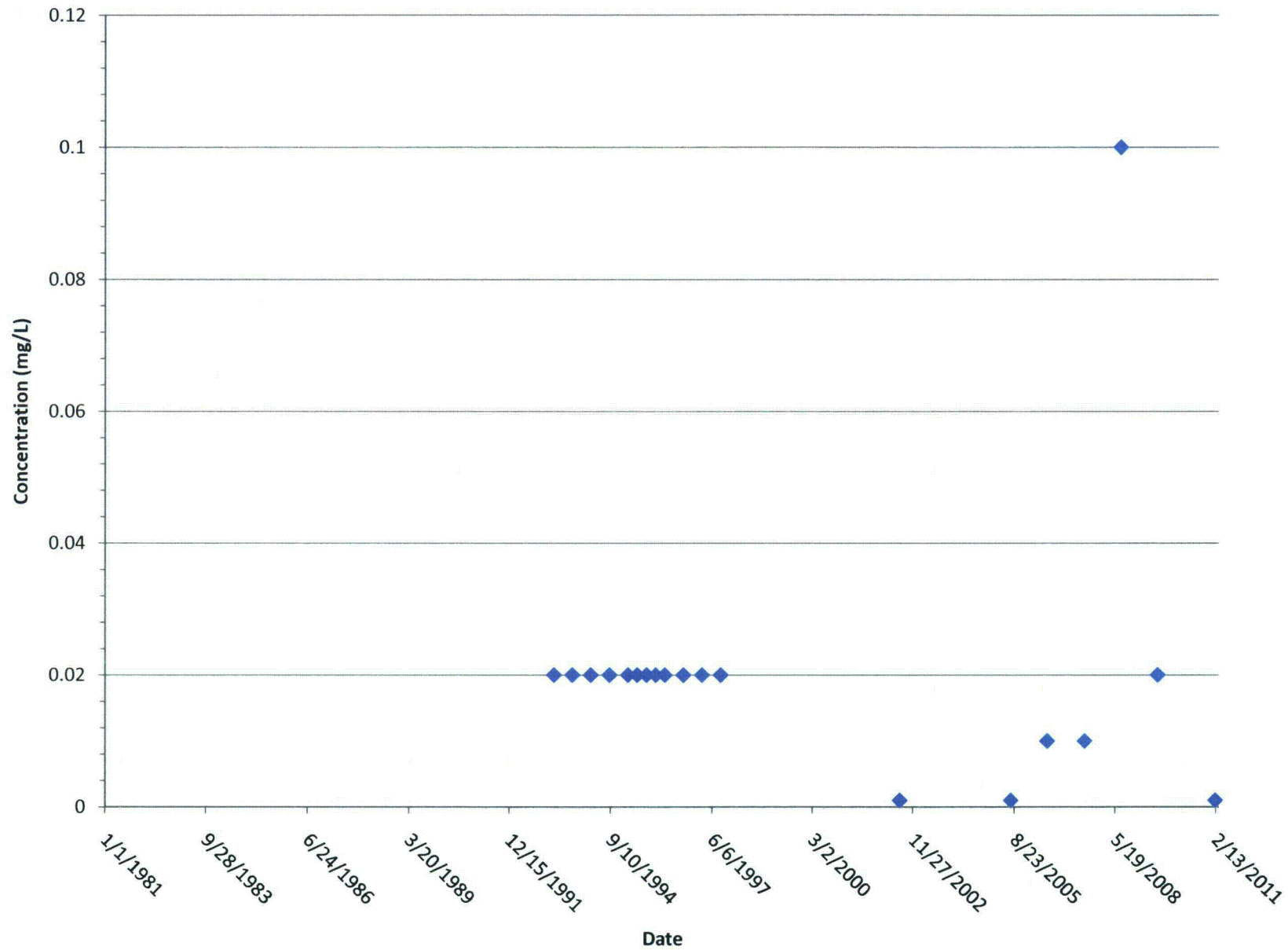




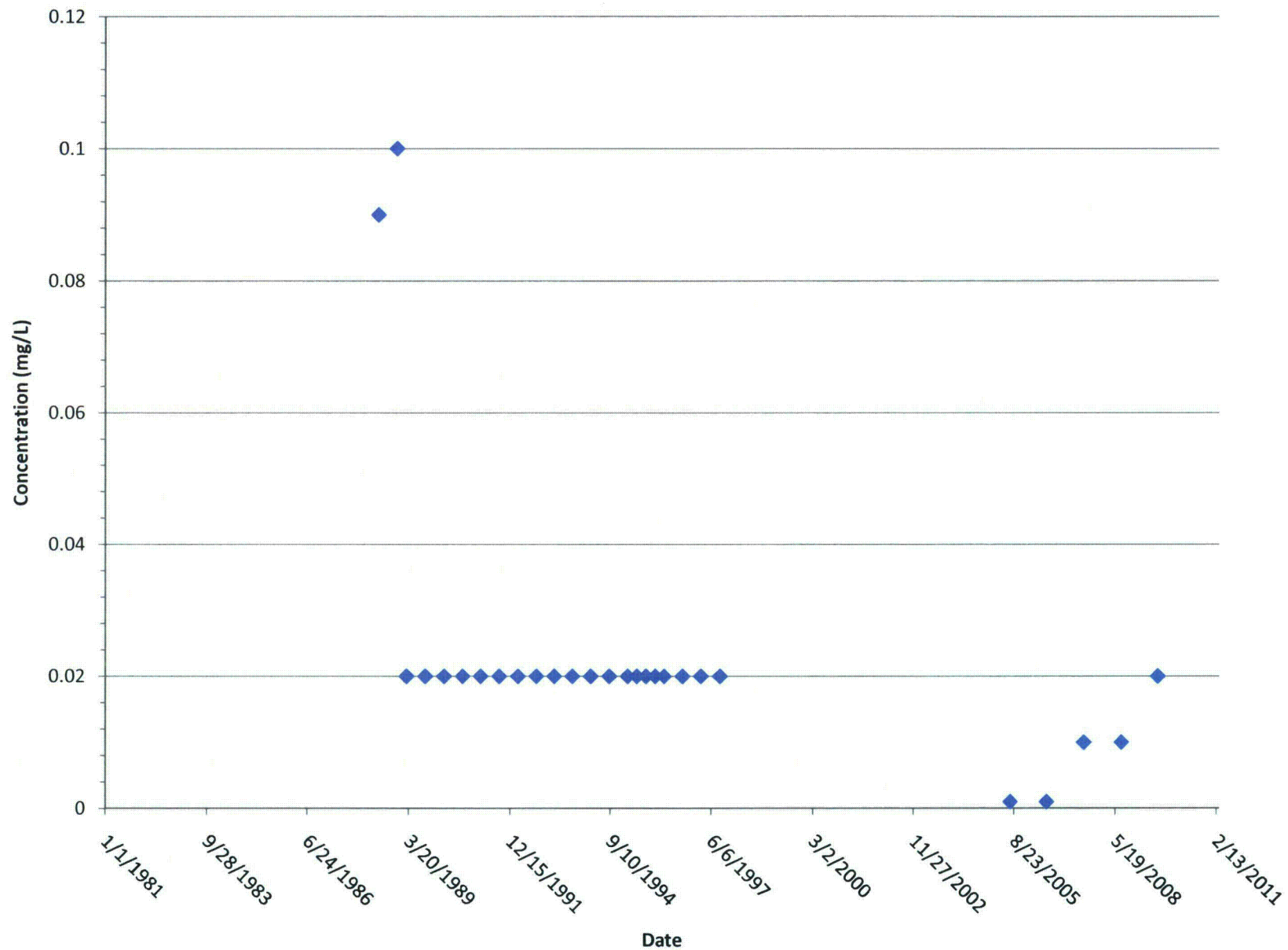
## MW-108 Chloride



## MW-74 Molybdenum



## MW-12 Molybdenum





**MW-74 Chromium**

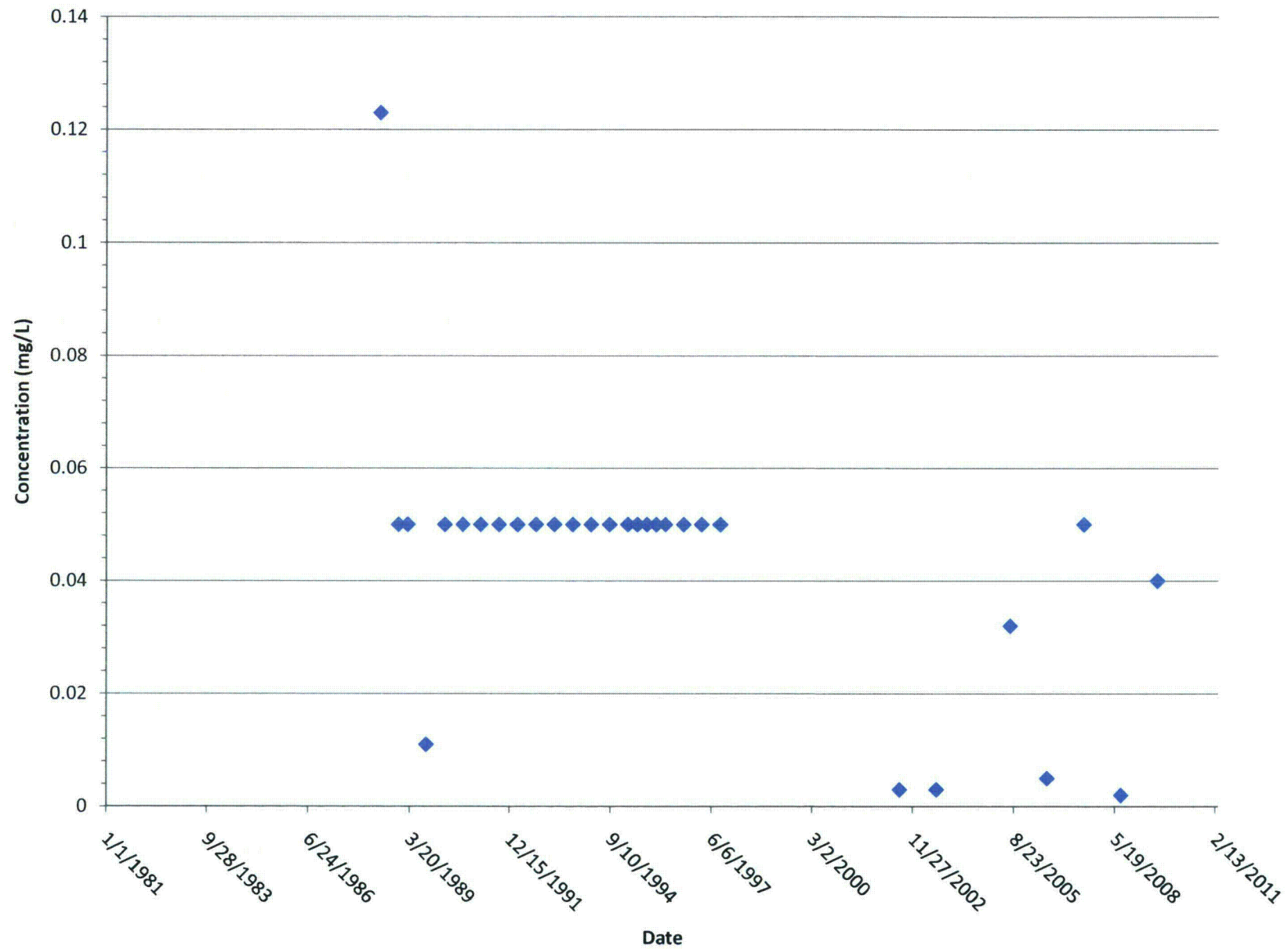
Concentration (mg/L)

Date

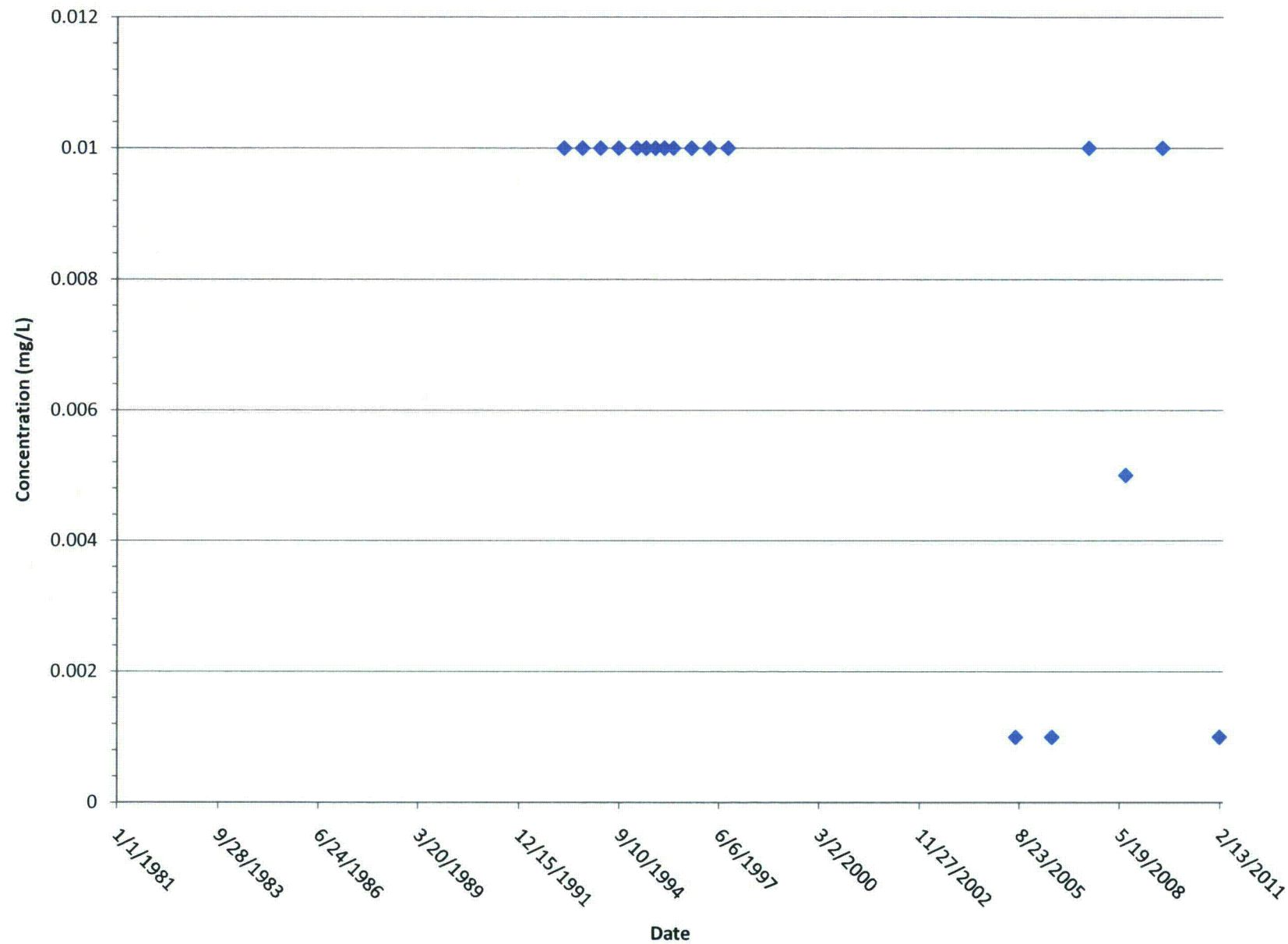
Date	Concentration (mg/L)
12/15/1991	0.05
1992-01-01	0.05
1992-02-01	0.05
1992-03-01	0.05
1992-04-01	0.05
1992-05-01	0.05
1992-06-01	0.05
1992-07-01	0.05
1992-08-01	0.05
1992-09-01	0.05
1992-10-01	0.05
1992-11-01	0.05
1992-12-01	0.05
1993-01-01	0.05
1993-02-01	0.05
1993-03-01	0.05
1993-04-01	0.05
1993-05-01	0.05
1993-06-01	0.05
1993-07-01	0.05
1993-08-01	0.05
1993-09-01	0.05
1993-10-01	0.05
1993-11-01	0.05
1993-12-01	0.05
1994-01-01	0.05
1994-02-01	0.05
1994-03-01	0.05
1994-04-01	0.05
1994-05-01	0.05
1994-06-01	0.05
1994-07-01	0.05
1994-08-01	0.05
1994-09-01	0.05
1994-10-01	0.05
1994-11-01	0.05
1994-12-01	0.05
1995-01-01	0.05
1995-02-01	0.05
1995-03-01	0.05
1995-04-01	0.05
1995-05-01	0.05
1995-06-01	0.05
1995-07-01	0.05
1995-08-01	0.05
1995-09-01	0.05
1995-10-01	0.05
1995-11-01	0.05
1995-12-01	0.05
1996-01-01	0.05
1996-02-01	0.05
1996-03-01	0.05
1996-04-01	0.05
1996-05-01	0.05
1996-06-01	0.05
1996-07-01	0.05
1996-08-01	0.05
1996-09-01	0.05
1996-10-01	0.05
1996-11-01	0.05
1996-12-01	0.05
1997-01-01	0.05
1997-02-01	0.05
1997-03-01	0.05
1997-04-01	0.05
1997-05-01	0.05
1997-06-01	0.05
1997-07-01	0.05
1997-08-01	0.05
1997-09-01	0.05
1997-10-01	0.05
1997-11-01	0.05
1997-12-01	0.05
1998-01-01	0.05
1998-02-01	0.05
1998-03-01	0.05
1998-04-01	0.05
1998-05-01	0.05
1998-06-01	0.05
1998-07-01	0.05
1998-08-01	0.05
1998-09-01	0.05
1998-10-01	0.05
1998-11-01	0.05
1998-12-01	0.05
1999-01-01	0.05
1999-02-01	0.05
1999-03-01	0.05
1999-04-01	0.05
1999-05-01	0.05
1999-06-01	0.05
1999-07-01	0.05
1999-08-01	0.05
1999-09-01	0.05
1999-10-01	0.05
1999-11-01	0.05
1999-12-01	0.05
2000-01-01	0.05
2000-02-01	0.05
2000-03-01	0.05
2000-04-01	0.05
2000-05-01	0.05
2000-06-01	0.05
2000-07-01	0.05
2000-08-01	0.05
2000-09-01	0.05
2000-10-01	0.05
2000-11-01	0.05
2000-12-01	0.05
2001-01-01	0.05
2001-02-01	0.05
2001-03-01	0.05
2001-04-01	0.05
2001-05-01	0.05
2001-06-01	0.05
2001-07-01	0.05
2001-08-01	0.05
2001-09-01	0.05
2001-10-01	0.05
2001-11-01	0.05
2001-12-01	0.05
2002-01-01	0.05
2002-02-01	0.05
2002-03-01	0.05
2002-04-01	0.05
2002-05-01	0.05
2002-06-01	0.05
2002-07-01	0.05
2002-08-01	0.05
2002-09-01	0.05
2002-10-01	0.05
2002-11-01	0.05
2002-12-01	0.05
2003-01-01	0.05
2003-02-01	0.05
2003-03-01	0.05
2003-04-01	0.05
2003-05-01	0.05
2003-06-01	0.05
200	

Concentration (mg/L)

## MW-12 Chromium

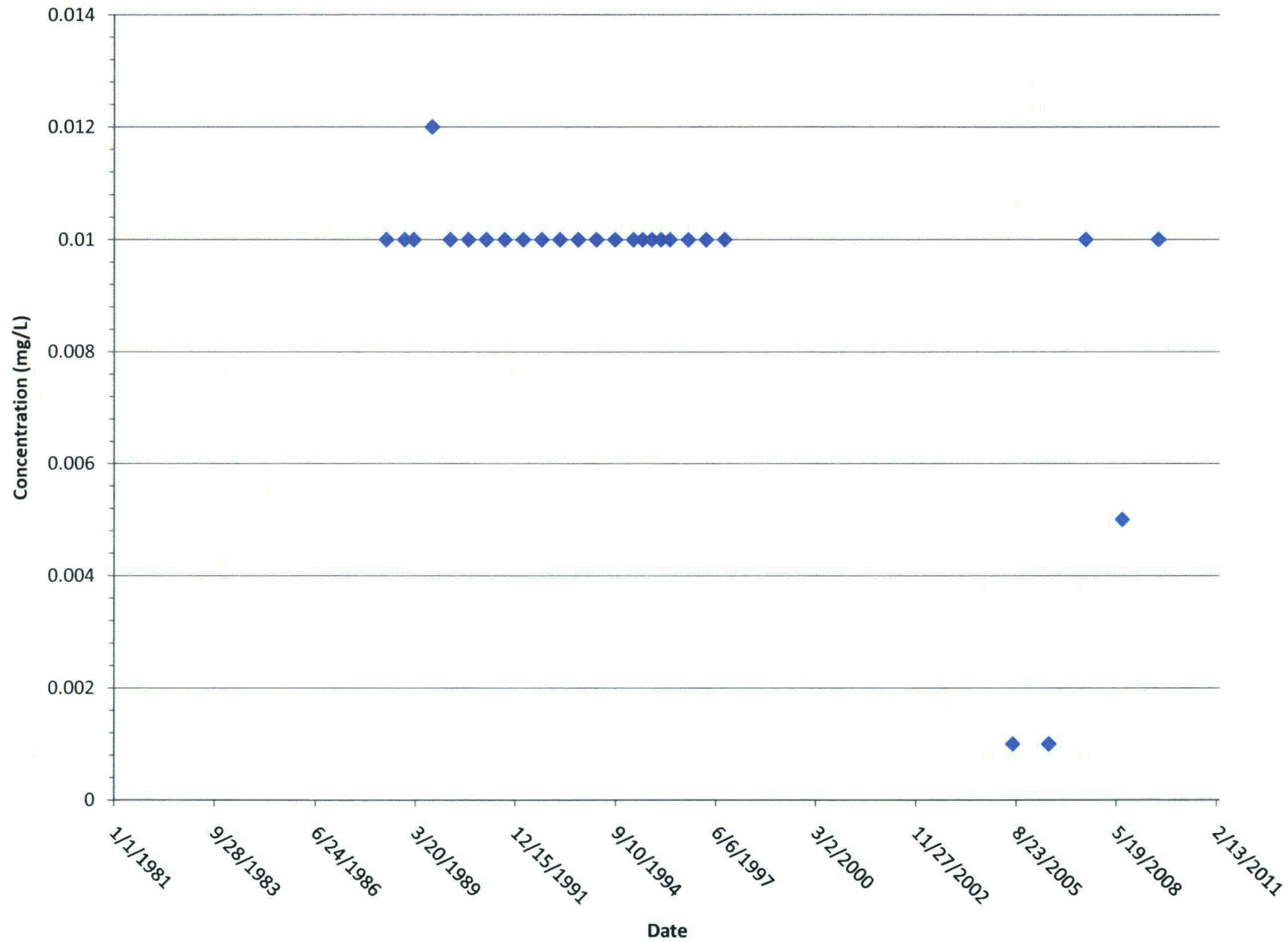


# MW-74 Cadmium





# MW-12 Cadmium



**MW-74 Beryllium**

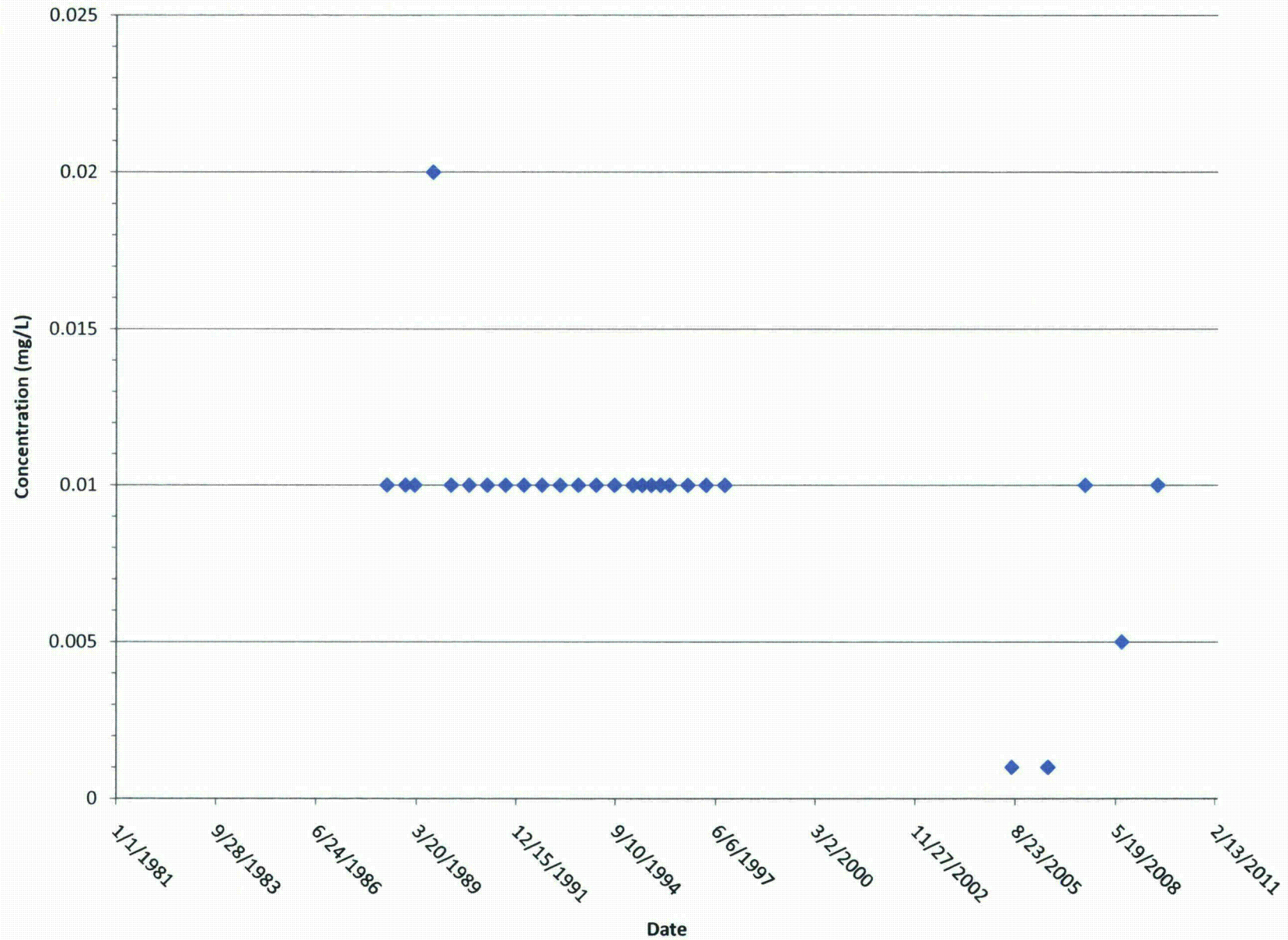
Concentration (mg/L)

Date

Date	Concentration (mg/L)
12/15/1991	0.010
1/10/1992	0.010
2/10/1992	0.010
3/10/1992	0.010
4/10/1992	0.010
5/10/1992	0.010
6/10/1992	0.010
7/10/1992	0.010
8/10/1992	0.010
9/10/1992	0.010
10/10/1992	0.010
11/10/1992	0.010
12/10/1992	0.010
1/10/1993	0.010
2/10/1993	0.010
3/10/1993	0.010
4/10/1993	0.010
5/10/1993	0.010
6/10/1993	0.010
7/10/1993	0.010
8/10/1993	0.010
9/10/1993	0.010
10/10/1993	0.010
11/10/1993	0.010
12/10/1993	0.010
1/10/1994	0.010
2/10/1994	0.010
3/10/1994	0.010
4/10/1994	0.010
5/10/1994	0.010
6/10/1994	0.010
7/10/1994	0.010
8/10/1994	0.010
9/10/1994	0.010
10/10/1994	0.010
11/10/1994	0.010
12/10/1994	0.010
1/10/1995	0.010
2/10/1995	0.010
3/10/1995	0.010
4/10/1995	0.010
5/10/1995	0.010
6/10/1995	0.010
7/10/1995	0.010
8/10/1995	0.010
9/10/1995	0.010
10/10/1995	0.010
11/10/1995	0.010
12/10/1995	0.010
1/10/1996	0.010
2/10/1996	0.010
3/10/1996	0.010
4/10/1996	0.010
5/10/1996	0.010
6/10/1996	0.010
7/10/1996	0.010
8/10/1996	0.010
9/10/1996	0.010
10/10/1996	0.010
11/10/1996	0.010
12/10/1996	0.010
1/10/1997	0.010
2/10/1997	0.010
3/10/1997	0.010
4/10/1997	0.010
5/10/1997	0.010
6/10/1997	0.010
7/10/1997	0.010
8/10/1997	0.010
9/10/1997	0.010
10/10/1997	0.010
11/10/1997	0.010
12/10/1997	0.010
1/10/1998	0.010
2/10/1998	0.010
3/10/1998	0.010
4/10/1998	0.010
5/10/1998	0.010
6/10/1998	0.010
7/10/1998	0.010
8/10/1998	0.010
9/10/1998	0.010
10/10/1998	0.010
11/10/1998	0.010
12/10/1998	0.010
1/10/1999	0.010
2/10/1999	0.010
3/10/1999	0.010
4/10/1999	0.010
5/10/1999	0.010
6/10/1999	0.010
7/10/1999	0.010
8/10/1999	0.010
9/10/1999	0.010
10/10/1999	0.010
11/10/1999	0.010
12/10/1999	0.010
1/10/2000	0.010
2/10/2000	0.010
3/10/2000	0.010
4/10/2000	0.010
5/10/2000	0.010
6/10/2000	0.010
7/10/2000	0.010
8/10/2000	0.010
9/10/2000	0.010
10/10/2000	0.010
11/10/2000	0.010
12/10/2000	0.010
1/10/2001	0.010
2/10/2001	0.010
3/10/2001	0.010
4/10/2001	0.010
5/10/2001	0.010
6/10/2001	0.010
7/10/2001	0.010
8/10/2001	0.010
9/10/2001	0.010
10/10/2001	0.010
11/10/2001	0.010
12/10/2001	0.010
1/10/2002	0.010
2/10/2002	0.010
3/10/2002	0.010
4/10/2002	0.010
5/10/2002	0.010
6/10/2002	0.010
7/10/2002	0.010
8/10/2002	0.010
9/10/2002	0.010
10/10/2002	0.010
11/10/2002	0.010
12/10/2002	0.010
1/10/2003	0.010
2/10/2003	0.010
3/10/2003	0.010
4/10/2003	0.010
5/10/2003	0.0

Concentration (mg/L)

## MW-12 Beryllium



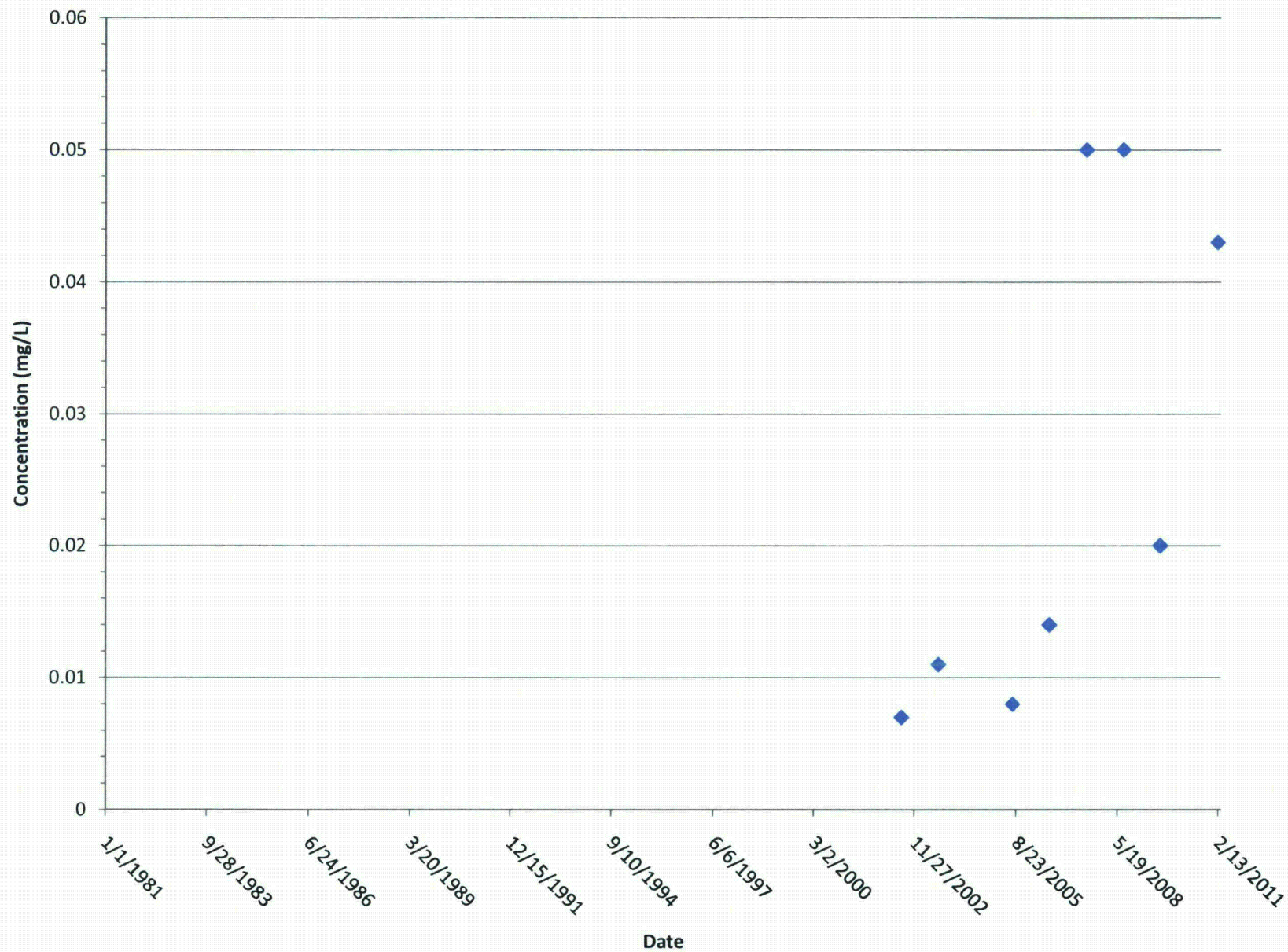


**MW-74 Nickel**

Date	Concentration (mg/L)
12/15/1991	0.050
1992	0.050
1993	0.050
1994	0.050
1994	0.050
1994	0.050
1994	0.050
1994	0.050
1994	0.050
1995	0.050
1996	0.050
1997	0.050
11/27/2002	0.011
1999	0.011
8/23/2005	0.011
2005	0.015
5/19/2008	0.050
2008	0.024
2008	0.030
2/13/2011	0.042

Concentration (mg/L)

# MW-108 Nickel



The scatter plot displays nickel concentration data over time. The y-axis ranges from 0 to 0.25 mg/L with major gridlines every 0.05 units. The x-axis shows dates from 1/1/1981 to 2/13/2011. Data points are blue diamonds. Notable values include two points at approximately 0.20 mg/L in early 1989, followed by a sharp drop to around 0.07 mg/L, and then a long period of stability at 0.05 mg/L until mid-1997. After 1997, concentrations remain very low, mostly below 0.01 mg/L, with a slight increase to about 0.02 mg/L by early 2011.

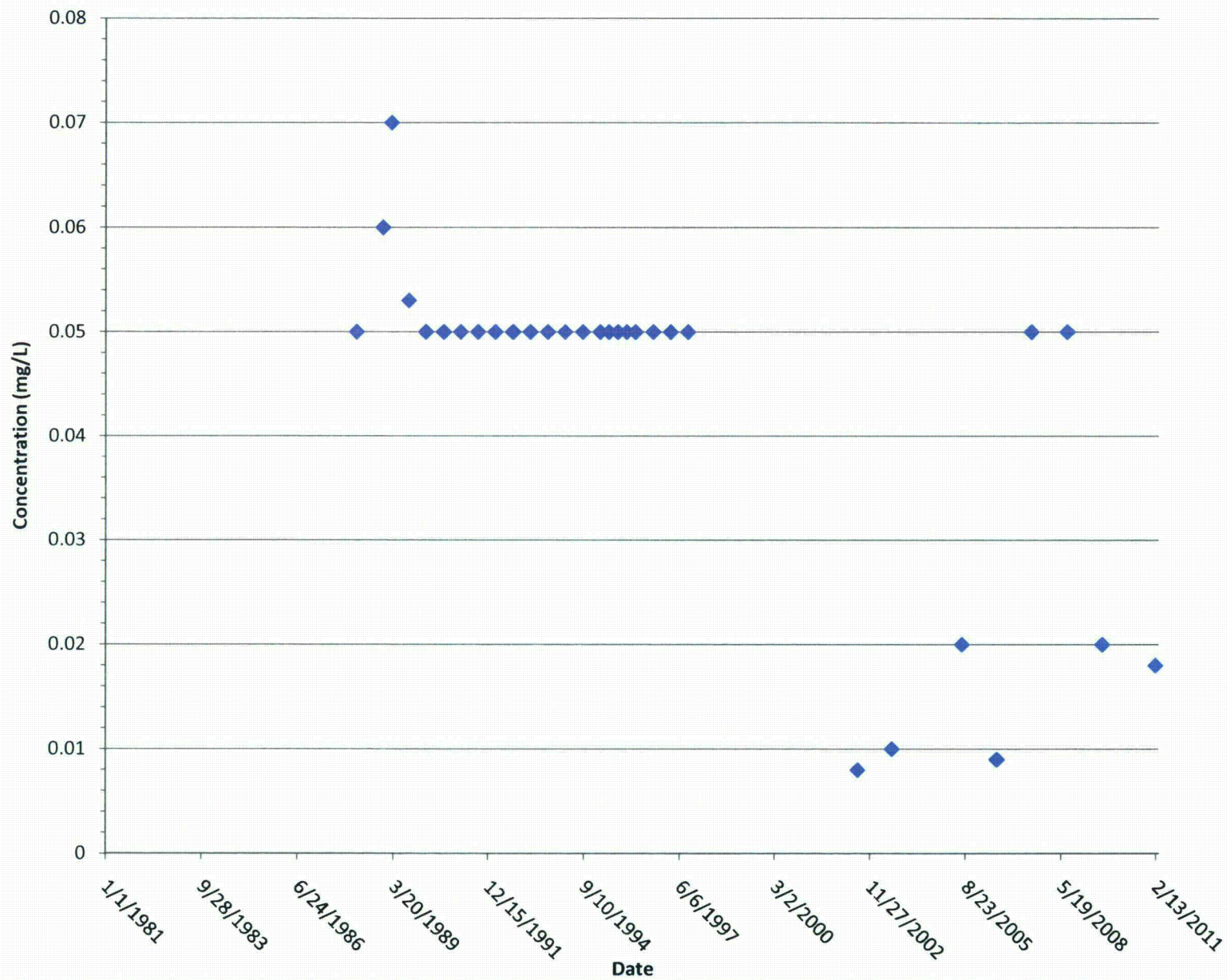
Date	Concentration (mg/L)
~1989-01-15	0.20
~1989-02-15	0.15
~1989-03-20	0.07
~1989-04-20	0.05
~1989-06-20	0.05
~1989-08-20	0.05
~1989-10-20	0.05
~1989-12-15	0.05
~1990-02-15	0.05
~1990-04-15	0.05
~1990-06-15	0.05
~1990-08-15	0.05
~1990-10-15	0.05
~1990-12-15	0.05
~1991-02-15	0.05
~1991-04-15	0.05
~1991-06-15	0.05
~1991-08-15	0.05
~1991-10-15	0.05
~1991-12-15	0.05
~1992-02-15	0.05
~1992-04-15	0.05
~1992-06-15	0.05
~1992-08-15	0.05
~1992-10-15	0.05
~1992-12-15	0.05
~1993-02-15	0.05
~1993-04-15	0.05
~1993-06-15	0.05
~1993-08-15	0.05
~1993-10-15	0.05
~1993-12-15	0.05
~1994-02-15	0.05
~1994-04-15	0.05
~1994-06-15	0.05
~1994-08-15	0.05
~1994-10-15	0.05
~1994-12-15	0.05
~1995-02-15	0.05
~1995-04-15	0.05
~1995-06-15	0.05
~1995-08-15	0.05
~1995-10-15	0.05
~1995-12-15	0.05
~1996-02-15	0.05
~1996-04-15	0.05
~1996-06-15	0.05
~1996-08-15	0.05
~1996-10-15	0.05
~1996-12-15	0.05
~1997-02-15	0.05
~1997-04-15	0.05
~1997-06-15	0.05
~1997-08-15	0.05
~1997-10-15	0.05
~1997-12-15	0.05
~1998-02-15	0.05
~1998-04-15	0.05
~1998-06-15	0.05
~1998-08-15	0.05
~1998-10-15	0.05
~1998-12-15	0.05
~1999-02-15	0.05
~1999-04-15	0.05
~1999-06-15	0.05
~1999-08-15	0.05
~1999-10-15	0.05
~1999-12-15	0.05
~2000-02-15	0.05
~2000-04-15	0.05
~2000-06-15	0.05
~2000-08-15	0.05
~2000-10-15	0.05
~2000-12-15	0.05
~2001-02-15	0.05
~2001-04-15	0.05
~2001-06-15	0.05
~2001-08-15	0.05
~2001-10-15	0.05
~2001-12-15	0.05
~2002-02-15	0.05
~2002-04-15	0.05
~2002-06-15	0.05
~2002-08-15	0.05
~2002-10-15	0.05
~2002-12-15	0.05
~2003-02-15	0.05
~2003-04-15	0.05
~2003-06-15	0.05
~2003-08-15	0.05
~2003-10-15	0.05
~2003-12-15	0.05
~2004-02-15	0.05
~2004-04-15	0.05
~2004-06-15	0.05
~2004-08-15	0.05
~2004-10-15	0.05
~2004-12-15	0.05
~2005-02-15	0.05
~2005-04-15	0.05
~2005-06-15	0.05
~2005-08-15	0.05
~2005-10-15	0.05
~2005-12-15	0.05
~2006-02-15	0.05
~2006-04-15	0.05
~2006-06-15	0.05
~2006-08-15	0.05
~2006-10-15	0.05
~2006-12-15	0.05
~2007-02-15	0.05
~2007-04-15	0.05
~2007-06-15	0.05
~2007-08-15	0.05
~2007-10-15	0.05
~2007-12-15	0.05
~2008-02-15	0.05
~2008-04-15	0.05
~2008-06-15	0.05
~2008-08-15	0.05
~2008-10-15	0.05
~2008-12-15	0.05
~2009-02-15	0.05
~2009-04-15	0.05
~2009-06-15	0.05
~2009-08-15	0.05
~2009-10-15	0.05
~2009-12-15	0.05

Concentration (mg/L)

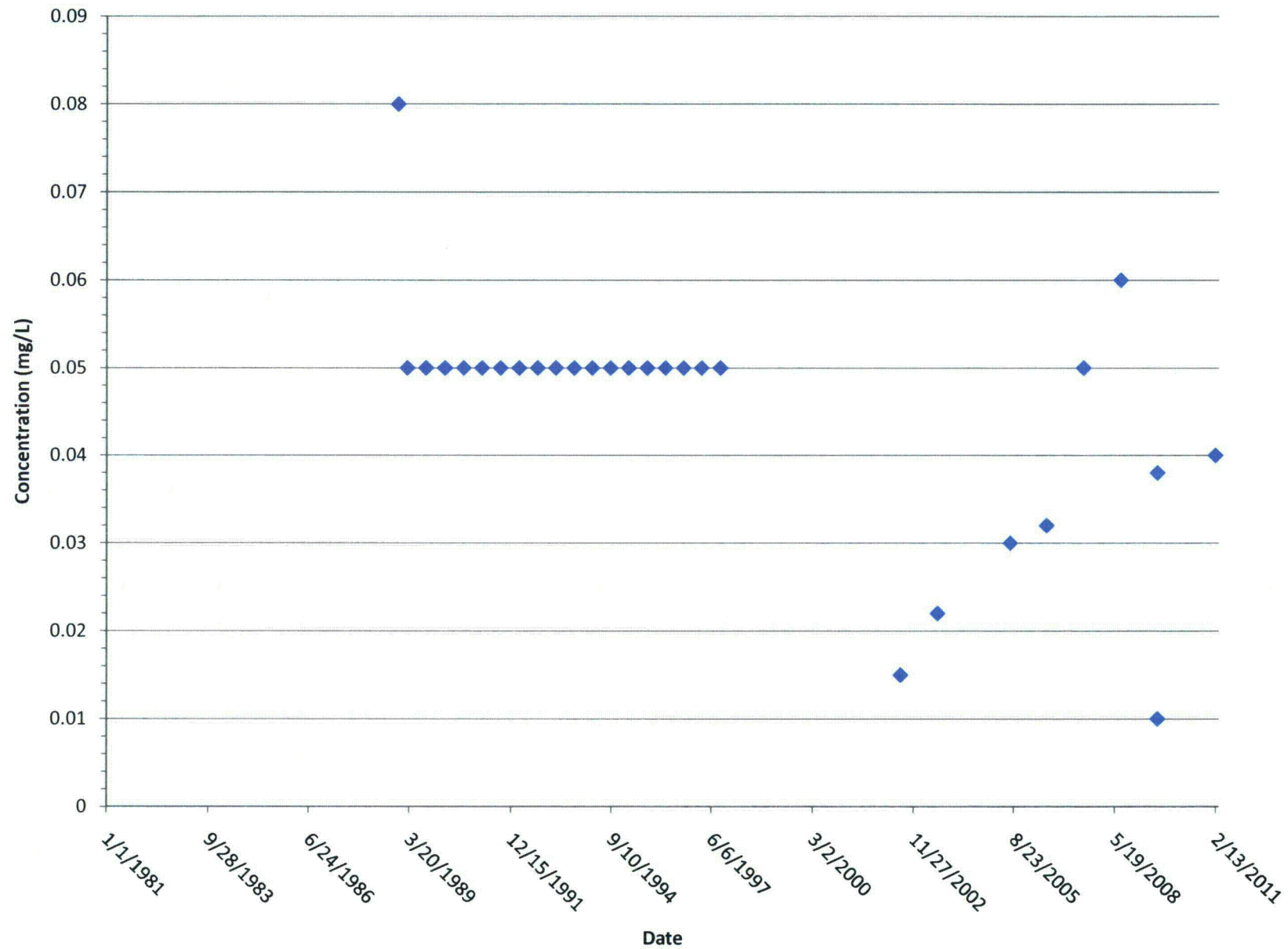
Date \_\_\_\_\_



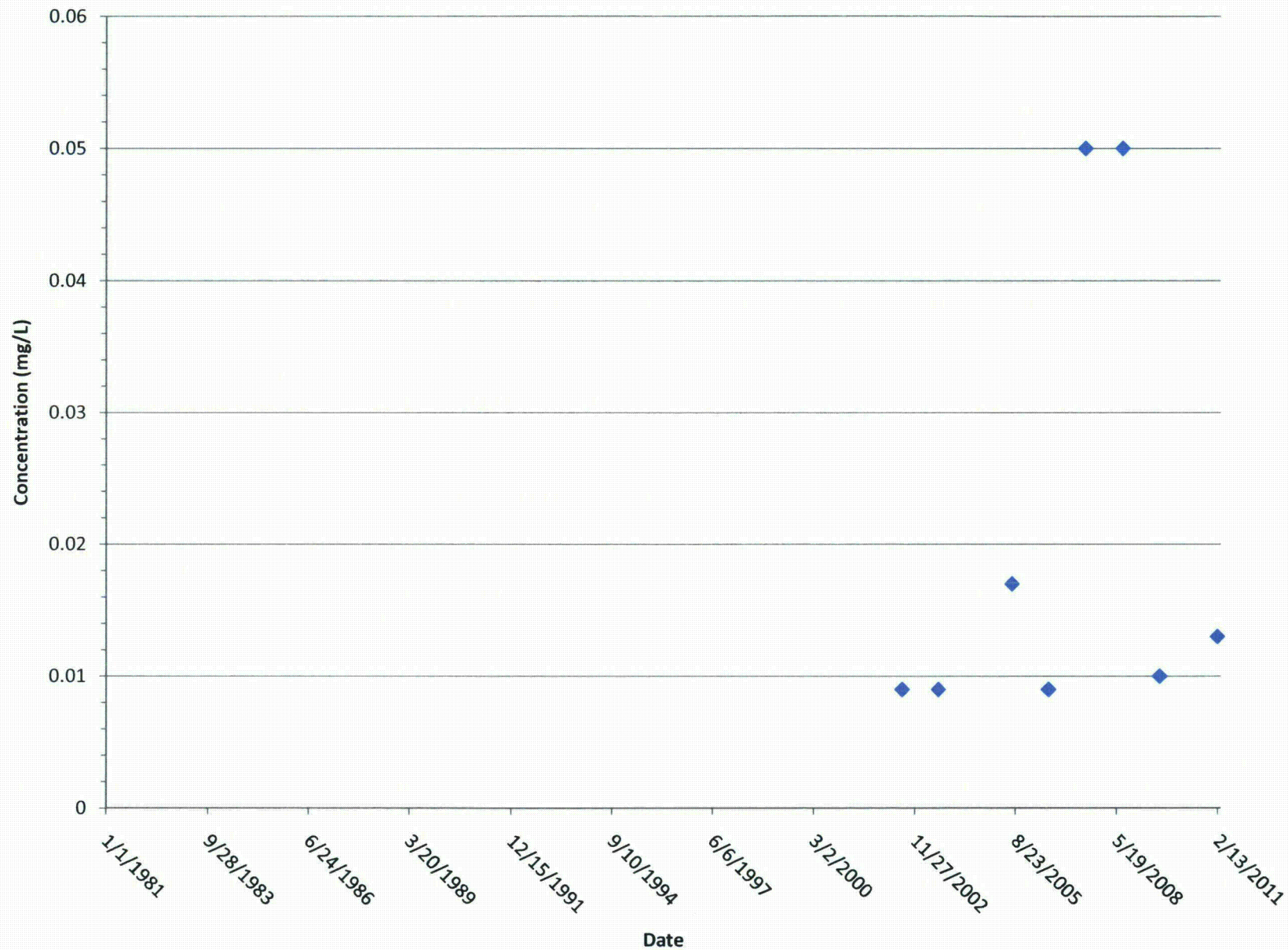
# MW-9 Nickel



## MW-14 Nickel

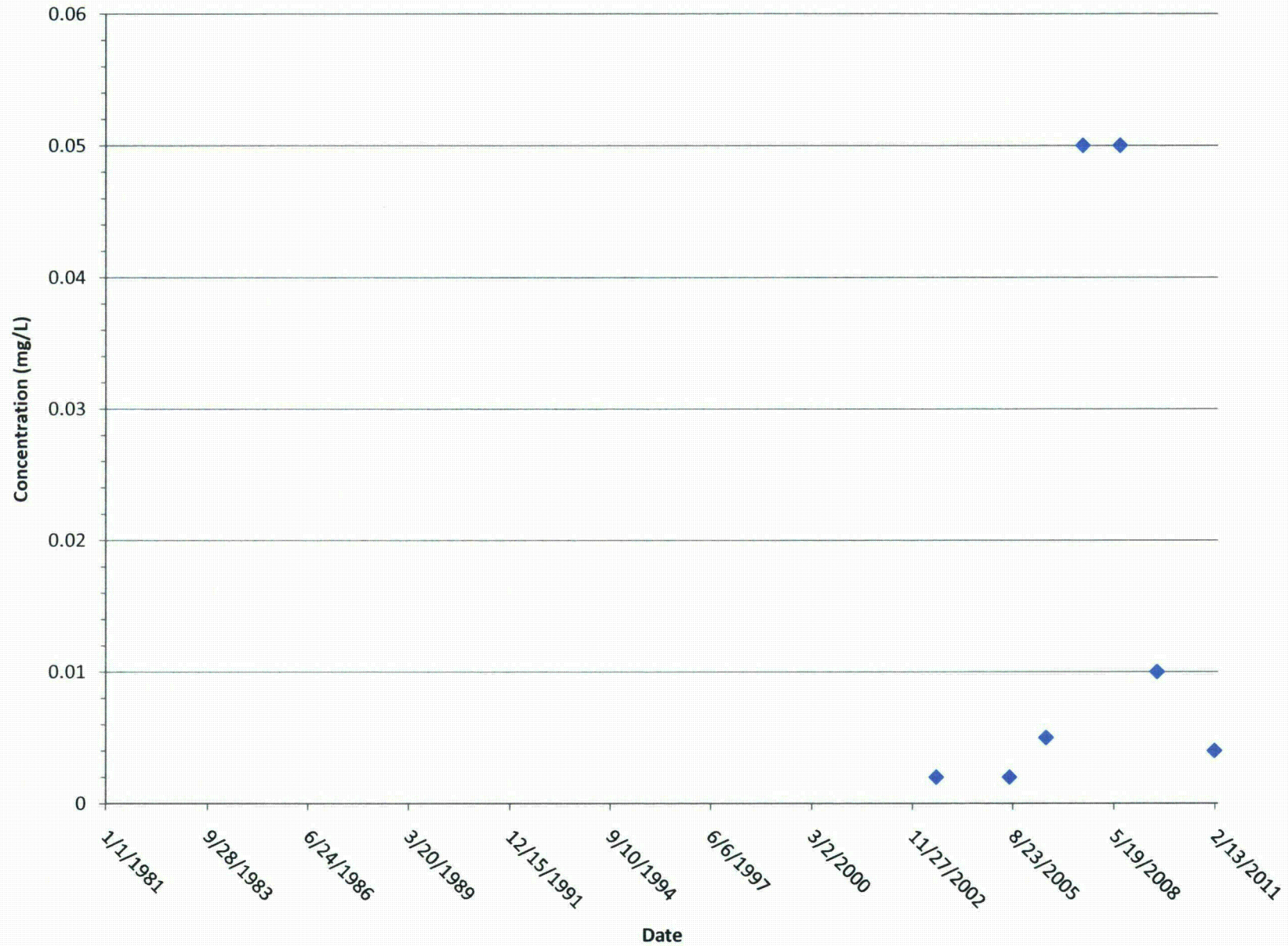


# MW-109 Nickel

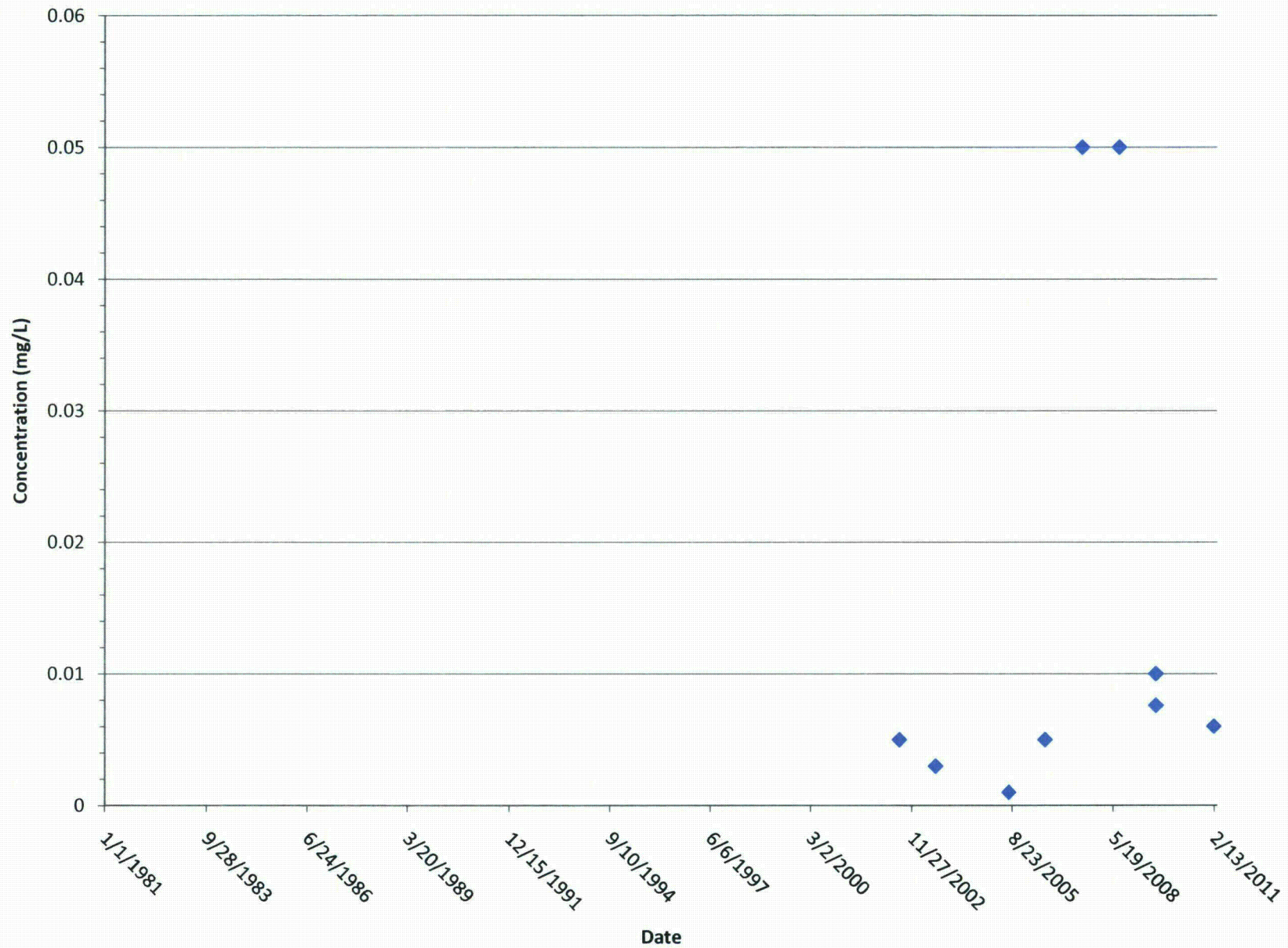




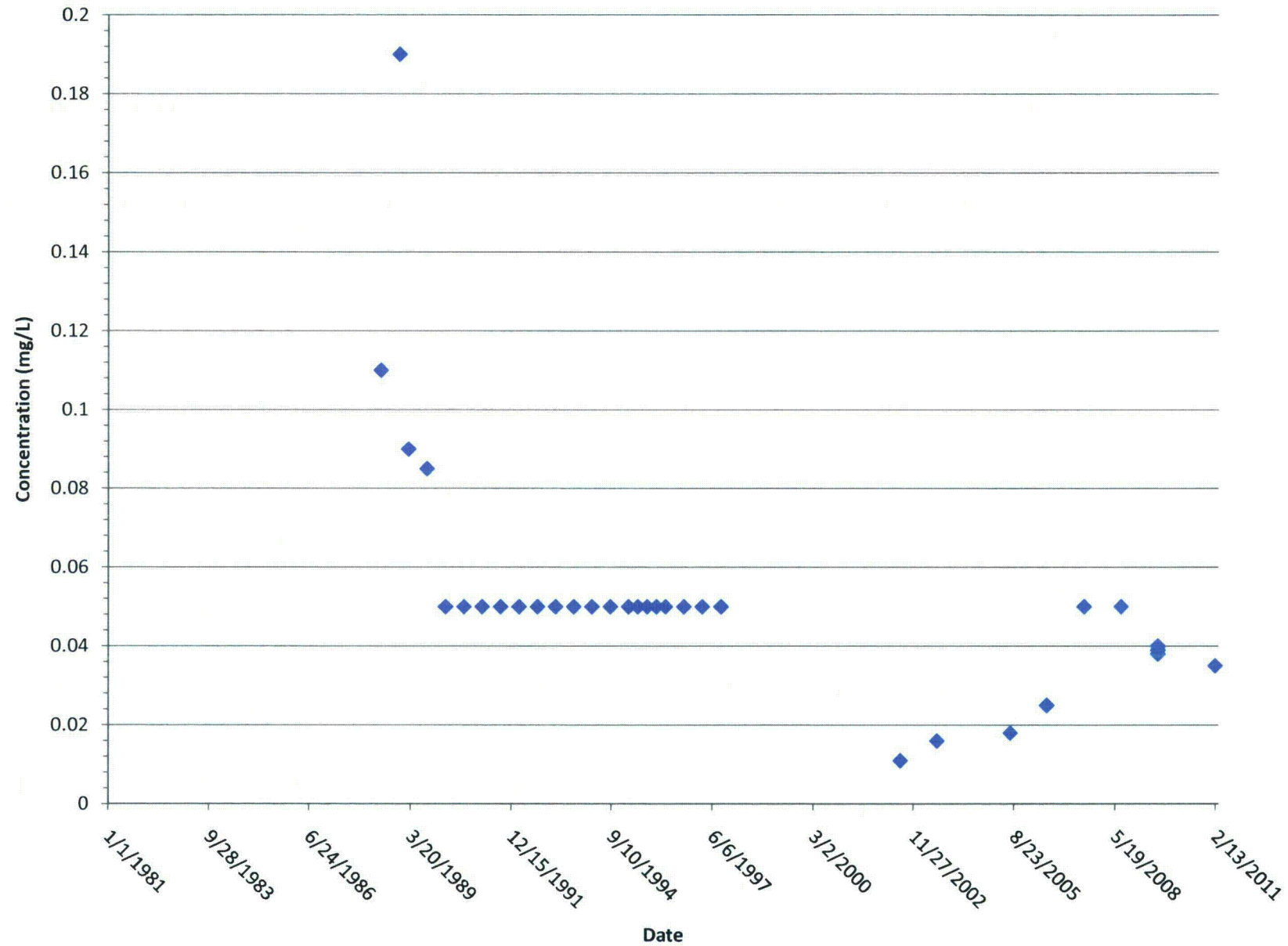
# MW-111 Nickel



# MW-110 Nickel



# MW-12 Nickel





## **ATTACHMENT II**

Input PHREEQC data set for  
Long Draw

DATABASE Phreeqc.dat

# Input dataset for Lang Draw model

USER PUNCH

```

-headings U pCi/L Radium pCi/L CELL DISTANCE m TIME YEARS DATE step
ALKALINITY U_ppm pH Ferri Cl_ppm S(6)_ppm Ra2(pCi/L) Ni_ppm
-start
5 USPECIES = MOL("Ca2UO2(CO3)3")+ MOL("CaUO2(CO3)3-2") + MOL("UO2+2")+
MOL("UO2CO3") + MOL("UO2Cl+") + MOL("UO2Cl2") + MOL("UO2(CO3)2-2")+
MOL("UO2(CO3)3-4") + MOL("UO2(OH)3-") + MOL("UO2(OH)2") + MOL("UO2OH+") +
MOL("UO2(OH)4-2")+MOL("UO2SO4")+ MOL("UO2(SO4)2-2") + MOL("(UO2)2(OH)2+2")
10 SURFCOMP = MOL("Hfo_wOUO2+") + MOL("Hfo_sOUO2+") + MOL("Hfo_wOUO2(CO3)2-3")
+ MOL("Hfo_wOUO2CO3-")
15 PUNCH USPECIES*238*1000*.67*1000
#Uranium in pCi/L
20 PUNCH (TOT("Ra")*226*1000)/(226*2.8E-15*1600)
#Radium in pCi/L
25 PUNCH CELL NO
30 PUNCH CELL NO*4
35 PUNCH TOTAL TIME/(3600*24*365)
40 PUNCH (TOTAL TIME/(3600*24)+34578) # you
can install an actual date by changing the 34578 value, WHICH is currently
set for Sept 1 1994.
45 PUNCH step no # puts
step number in column 7
50 PUNCH ALK*50000
55 PUNCH TOT("U")*238*1000
60 PUNCH -LA("H+")
65 PUNCH EQUI("Fe(OH)3(a)")
70 PUNCH TOT("CL")*1000*35.453
75 PUNCH TOT("S(6)")*1000*96.064
80 SURFCOMP = MOL("Hfo_wOUO2+") + MOL("Hfo_sOUO2+") + MOL("Hfo_wOUO2(CO3)2-3")
+ MOL("Hfo_wOUO2CO3-")
85 PUNCH TOT("Ra")*226*1.0E12 # Ra in pCi/L
90 PUNCH TOT("Ni")*1000*58.69

-end

```

TITLE Transport: Bear Creek Lang Draw Model Phreeqc 2.0

```

SOLUTION 1000 solution MW-86 # Solution to mix with upgradient
(MW-36) water for upgradient boundary condition
units mg/L
# Samplename MW-86
pH 4.5
pe 12
temp 25
Ca 420
Mg 700
Na 278 charge
K 42
Fe 926
Mn 35.9
Al 230
S(6) 9040
Cl 600
C(4)
F 0.1
P 0.01
Si 21.4 #as SiO2
Ni 0.08
U 3.303662 # U-natural (pCi/L) 2038
Ra 4.5e-09

```

END

SOLUTION 2000 MW-36 background groundwater  
clean water

#THIS IS WATER FROM MW-36

units mg/L  
# Samplename MW-36  
pH 7.8  
pe 12  
temp 25  
Ca 158  
Mg 21  
Na 61  
K 7  
Fe 0.1  
Mn 0.11  
Al 0.5  
S(6) 425  
Cl 25  
C(4) 153  
Ni 0.01  
U 0.003  
Ra 0.5E-09

END

SOLUTION 3000 MW-14  
units mg/L  
# Samplename MW-14  
pH 7.4  
pe 12  
temp 25  
Ca 440  
Mg 59  
Na 34 charge  
K 2  
Fe 0.1  
Mn 0.49  
Al 0.5  
S(6) 1053  
Cl 90  
C(4) 331  
Ni 0.01  
U 0.054  
# U-natural (pCi/L)  
Ra 1.2E-09

END

MIX  
1000 .594427  
2000 .405573  
SAVE SOLUTION 0-30  
END

# CELL SETUP STARTS HERE FIRST SIMULATION

EQUILIBRIUM PHASES 1-30  
Al(OH)3(a) -1.36 0.0  
Fe(OH)3(a) 1.69 1.000000E-4  
Calcite 0.0 0.0  
Gypsum 0.0 0.2  
SiO2(a) 0.0 0.0

SURFACE 1-30  
-equilibrate with solution 1-30



Hfo wOH Fe(OH)3(a) equilibrium phase 0.2 53400 #0.2 sites per mole of  
 Fe(OH)3(a) present; 53400=600x89 (89 is formula weight for goethite) is  
 surface area per mole of iron hydroxide  
 Hfo\_sOH Fe(OH)3(a) equilibrium\_phase 0.005

SAVE EQUILIBRIUM PHASES 1-30  
 SAVE SURFACE 1-30  
 SAVE Solution 1-30

END

SOLUTION 31-55 Initial solution for column THIS IS MW-15

	units	ppm
units mg/L		
# Samplename		MW-15
pH	6.0	
pe	12	
temp	25	
Ca	650	
Mg	250	
Na	212 charge	
K	18	
Fe	2.18	
Mn	0.35	
Al	1.33	
S(6)	2420	
Cl	375	
C(4)	1450	
F	0.3	
P	0.01	
Si	20.78	
Ba	#	
Ni	0.025	
U	1.20000000	
Ra	2.5312E-09	

#as SiO2

EQUILIBRIUM PHASES 31-55

Al(OH)3(a)	-1.36	0.1
Fe(OH)3(a)	1.69	1.000000E-4
Calcite	0.0	0.01
Gypsum	0.0	0.2
SiO2(a)	0.0	0.0

SURFACE 31-55

-equilibrate with solution 31-55

Hfo wOH Fe(OH)3(a) equilibrium phase 0.2 53400 #0.2 sites per mole of  
 Fe(OH)3(a) present; 53400=600x89 (89 is formula weight for goethite) is  
 surface area per mole of iron hydroxide  
 Hfo\_sOH Fe(OH)3(a) equilibrium\_phase 0.005

SAVE SURFACE 31-55  
 SAVE EQUILIBRIUM PHASES 31-55  
 SAVE Solution 31-55

END

SOLUTION 56-119 Initial solution for column MW-12

	units mg/L	
# Samplename		MW-12
pH	7.0	
pe	12	
temp	25	
Ca	450	
Mg	150	
Na	265 charge	
K	14	

Fe 0.69  
 Mn 0.07  
 Al 1.15  
 S(6) 2000  
 Cl 275  
 C(4) 878  
 F 0.3  
 P 0.01  
 Si 18  
 Ni 0.025  
 U 0.16  
 Ra 1.5E-09

#as SiO2

## EQUILIBRIUM PHASES 56-119

Al(OH)3(a)	-1.36	0.01
Fe(OH)3(a)	1.69	1.000000E-4
Calcite	0.0	0.4
Gypsum	0.0	0.0
SiO2(a)	0.0	0.0

## SURFACE 56-119

-equilibrate with solution 56-119

Hfo wOH Fe(OH)3(a) equilibrium phase 0.2 53400 #0.2 sites per mole of  
 Fe(OH)3(a) present; 53400=600x89 (89 is formula weight for goethite) is  
 surface area per mole of iron hydroxide  
 Hfo\_sOH Fe(OH)3(a) equilibrium\_phase 0.005

## SAVE EQUILIBRIUM PHASES 56-119

SAVE SURFACE 56-119

SAVE Solution 56-119

END

SOLUTION 120-162 Initial solution for column MW-14  
units mg/L

# Sample name MW-14

pH 7.7  
 pe 12  
 temp 25  
 Ca 350  
 Mg 59  
 Na 34 charge  
 K 2  
 Fe 0.1  
 Mn 0.49  
 Al 0.5  
 S(6) 800  
 Cl 70  
 C(4) 331  
 F  
 P  
 Si  
 Ni 0.01  
 U 0.054  
 Ra 1.2E-09

## EQUILIBRIUM PHASES 120-162

Al(OH)3(a)	-1.36	0.01
Fe(OH)3(a)	1.69	1.000000E-4
Calcite	0.0	0.4
Gypsum	0.0	0.0
SiO2(a)	0.0	0.0

```

SURFACE 120-162
  -equilibrate with solution 120-162
Hfo wOH Fe(OH)3(a) equilibrium phase 0.2 53400 #0.2 sites per mole of
Fe(OH)3(a) present; 53400=600x89 (89 is formula weight for goethite) is
surface area per mole of iron hydroxide
Hfo_sOH Fe(OH)3(a) equilibrium_phase 0.005

```

```

SAVE EQUILIBRIUM PHASES 120-162
SAVE SURFACE 120-162
SAVE Solution 120-162

```

END

```

MIX
2000 0.5
3000 0.5
SAVE SOLUTION 163-210
END

```

```

EQUILIBRIUM PHASES 163-210
  Al(OH)3(a) -1.36 0.01
  Fe(OH)3(a) 1.69 1.000000E-4
  Calcite 0.0 0.4
  Gypsum 0.0 0.0
  SiO2(a) 0.0 0.0

```

```

SURFACE 163-210
  -equilibrate with solution 163-210
Hfo wOH Fe(OH)3(a) equilibrium phase 0.2 53400 #0.2 sites per mole of
Fe(OH)3(a) present; 53400=600x89 (89 is formula weight for goethite) is
surface area per mole of iron hydroxide
Hfo_sOH Fe(OH)3(a) equilibrium_phase 0.005

```

```

SAVE SURFACE 163-210
SAVE Solution 163-210

```

END

```

MIX
2000 0.8
3000 0.2
SAVE SOLUTION 211-242
END

```

```

EQUILIBRIUM PHASES 211-242
  Al(OH)3(a) -1.36 0.01
  Fe(OH)3(a) 1.69 1.000000E-4
  Calcite 0.0 0.4
  Gypsum 0.0 0.0
  SiO2(a) 0.0 0.0

```

```

SURFACE 211-242
  -equilibrate with solution 211-242
Hfo wOH Fe(OH)3(a) equilibrium phase 0.2 53400 #0.2 sites per mole of
Fe(OH)3(a) present; 53400=600x89 (89 is formula weight for goethite) is
surface area per mole of iron hydroxide
Hfo_sOH Fe(OH)3(a) equilibrium_phase 0.005

```



SAVE EQUILIBRIUM PHASES 211-242  
 SAVE SURFACE 211-242  
 SAVE Solution 211-242

END  
 PRINT

-reset false  
 -surface true  
 SELECTED OUTPUT  
 -file BC\_mod02.sel #can  
 be SEL or XLS  
 -reset false  
 # -step true #this  
 prints the time step in the first column, set to "false" in order to eliminate  
 that column

#1995 through 1997 Plateau 2

MIX

1000 .594427

2000 .405573

SAVE SOLUTION 0

# 1994 through 1995

TRANSPORT

-cells 242 #235  
 is total cells  
 -length 4 #4  
 meter cells .10000000 40.000000  
 -shifts 9.00000 #6  
 yrs\*365\*24\*3600/2522880= 75 shifts; we start at the dam, John added a  
 year for the diffence in length for the first water  
 -time step 3155760.0 #This  
 is 29.2 days in seconds and essentially indicates hydraulic  
 conductivity  
 -punch cells 1 20 52 98 121 159 181 242  
 -punch frequency 1  
 -flow direction forward  
 -boundary conditions flux flux  
 -correct disp true  
 -dispersivity 235\*30.0000  
 -diffusion\_coef 0.0e-0 #No  
 diffusion  
 -tempr 1.0 #No  
 heat retardation

END

#1995 through 1997 Plateau 2

MIX

1000 .349935

2000 .650065

SAVE SOLUTION 0

write Solution 0

#Over-

TRANSPORT

-shifts 20.0000

END

#1997 through 2000 Plateau 3

MIX

1000 .087363

2000 .912637

SAVE SOLUTION 0

write Solution 0.

#Over-

TRANSPORT

-shifts 30.0000

END

#2000 through 2010          Plateau 4

MIX

1000          .004258

2000          .995742

SAVE SOLUTION 0

#Over-

write Solution 0.

TRANSPORT

-shifts          60.0000

END

#2006 through 2010          Plateau 5

MIX

1000          1.25E-5

2000          .999988

SAVE SOLUTION 0

#Over-

write Solution 0.

TRANSPORT

-shifts          109.000

END

END

**ATTACHMENT III**

Input PHREEQC data set for  
Northern Pathway



DATABASE C:\Phreeqcm.dat

## USER PUNCH

```

-headings U pCi/L Radium pCi/L CELL DISTANCE m TIME_YEARS DATE step
ALKALINITY U_ppm pH Ferri Cl_ppm S(6)_ppm RA_pCi/L NI_ppm
-start
3 USPECIES = MOL("Ca2UO2(CO3)3")+ MOL("CaUO2(CO3)3-2") + MOL("UO2+2")+
MOL("UO2CO3") + MOL("UO2Cl+") + MOL("UO2Cl2") + MOL("UO2(CO3)2-2")+
MOL("UO2(CO3)3-4") + MOL("UO2(OH)3-") + MOL("UO2(OH)2") + MOL("UO2OH+") +
MOL("UO2(OH)4-2")+MOL("UO2SO4")+ MOL("UO2(SO4)2-2") + MOL("UO2)2(OH)2+2")
4 SURFCOMP = MOL("Hfo_wOUO2+") + MOL("Hfo_sOUO2+") + MOL("Hfo_wOUO2(CO3)2-3")
+ MOL("Hfo_wOUO2CO3-")
5 PUNCH USPECIES*238*1000*.67*1000
#Uranium in pCi/L
7 PUNCH (TOT("Ra")*226*1000)/(226*2.8E-15*1600)
#Radium in pCi/L
11 PUNCH CELL NO #if
you want to eliminate a column, you remove it from the heading, then comment
out the line that applies to that column
13 PUNCH CELL NO*4
15 PUNCH TOTAL TIME/(3600*24*365)
17 PUNCH (TOTAL TIME/(3600*24)+34578) # you
can install an actual date by changing the 34578 value, WHICH is currently
set for Sept 1 1994.
19 PUNCH step no #puts
step number in column 7
21 PUNCH ALK*50000
23 PUNCH TOT("U")*238*1000
25 PUNCH -LA("H+")
26 PUNCH EQUI("Fe(OH)3(a)")
27 PUNCH TOT("CL")*1000*35.453
28 PUNCH TOT("S(6)")*1000*96.064
30 SURFCOMP = MOL("Hfo_wOUO2+") + MOL("Hfo_sOUO2+") + MOL("Hfo_wOUO2(CO3)2-3")
+ MOL("Hfo_wOUO2CO3-")

32 PUNCH TOT("Ra")*226*1.0E12 # Ra in pCi/L
33 PUNCH TOT("Ni")*1000*58.69

-end

```

TITLE Transport: Bear Creek North Path

SOLUTION 1000 solution MW-86

units mg/L

# Samplename MW-86

pH 4.5

pe 12

temp 25

Ca 420

Mg 700

Na 278 charge

K 42

Fe 926

Mn 35.9

Al 230

S(6) 9040

Cl 400

F 0.1

P 0.01

Si 21.4

Ni .1

U 0.6

Ra 1.51872E-08

END

#as SiO2

## SOLUTION 2000 MW-36 background groundwater

units mg/L  
# Samplename MW-36  
pH 7.4  
pe 12  
temp 25  
Ca 158  
Mg 21  
Na 61  
K 7  
Fe 0.1  
Mn 0.11  
Al 0.5  
S(6) 425  
Cl 25  
C(4) 153  
Ni 0.01  
U 0.003  
Ra 2.5312E-09

END

## SOLUTION 3000 MW-43

units mg/L  
# Samplename MW-43 11/10/94  
pH 7.7  
pe 12  
temp 25  
Ca 974.  
Mg 198.  
Na 71. charge  
K 17.  
Fe 7.91  
Mn 0.85  
Al 0.01  
S(6) 2080  
Cl 575.  
C(4) 854.  
F .2  
Si 5.4  
Ba #  
Ni 0.02  
U 0.0581  
Ra 5.164E-09

END

MIX

1000 .334046  
2000 .665954  
SAVE SOLUTION 0-54  
END

# CELL SETUP STARTS HERE FIRST SIMULATION

EQUILIBRIUM PHASES 1-54

Al(OH)3(a)	-1.36	0.0
Fe(OH)3(a)	1.69	1.000000E-4
Calcite	0.0	0.0
Gypsum	0.0	0.2
SiO2(a)	0.0	0.0

SURFACE 1-54

```

-equilibrate with solution 1-54
Hfo wOH Fe(OH)3(a) equilibrium phase 0.2 53400 #0.2 sites per mole of
Fe(OH)3(a) present; 53400=600x89 (89 is formula weight for goethite) is
surface area per mole of iron hydroxide
Hfo_sOH Fe(OH)3(a) equilibrium_phase 0.005

```

```

SAVE EQUILIBRIUM PHASES 1-54
SAVE SURFACE 1-54
SAVE Solution 1-54

```

END

```

MIX
1000 .334046
2000 .665954
SAVE SOLUTION 55-84
END

```

# CELL SETUP STARTS HERE FIRST SIMULATION

```

EQUILIBRIUM PHASES 55-84
Al(OH)3(a) -1.36 0.0
Fe(OH)3(a) 1.69 1.000000E-4
Calcite 0.0 0.1
Gypsum 0.0 0.2
SiO2(a) 0.0 0.0

```

SURFACE 55-84

```

-equilibrate with solution 55-84
Hfo wOH Fe(OH)3(a) equilibrium phase 0.2 53400 #0.2 sites per mole of
Fe(OH)3(a) present; 53400=600x89 (89 is formula weight for goethite) is
surface area per mole of iron hydroxide
Hfo_sOH Fe(OH)3(a) equilibrium_phase 0.005

```

```

SAVE EQUILIBRIUM PHASES 55-84
SAVE SURFACE 55-84
SAVE Solution 55-84

```

END

SOLUTION 85-125 Initial solution for column THIS IS MW-74

units mg/L ppm

# Sample name MW-74 9/94

```

pH 6.7
pe 12
temp 25
Ca 450.
Mg 116.
Na 67. charge
K 12.
Fe 0.66
Mn 0.48
Al 0.96
S(6) 1900.
Cl 200.
C(4) 708.
F 0.2
P 0.01
Si 15.83
Ba #
Ni 0.025
U 0.062

```

#as SiO2

#table 3-12



Ra 2.936E-09

## EQUILIBRIUM PHASES 85-125

Al(OH)3(a)	-1.36	0.1
Fe(OH)3(a)	1.69	1.000000E-4
Calcite	0.0	0.4
Gypsum	0.0	0.2
SiO2(a)	0.0	0.0

## SURFACE 85-125

-equilibrate with solution 85-125

Hfo wOH Fe(OH)3(a) equilibrium phase 0.2 53400 #0.2 sites per mole of  
Fe(OH)3(a) present; 53400=600x89 (89 is formula weight for goethite) is  
surface area per mole of iron hydroxide  
Hfo\_sOH Fe(OH)3(a) equilibrium\_phase 0.005

SAVE SURFACE 85-125

SAVE EQUILIBRIUM PHASES 85-125

SAVE Solution 85-125

END

SOLUTION 126-170 Initial solution for column MW-43  
units mg/L

# Samplename MW-43 11/10/94

pH	7.7
pe	12
temp	25
Ca	974.
Mg	198.
Na	71. charge
K	17.
Fe	7.91
Mn	0.85
Al	0.01
S(6)	2080
Cl	575.
C(4)	854.
F	.2
P	
Si	5.4
Ba	#
Ni	0.02
U	0.0581
# U-natural (pCi/L)	
Ra	2.5E-9

## EQUILIBRIUM PHASES 126-170

Al(OH)3(a)	-1.36	0.01
Fe(OH)3(a)	1.69	1.000000E-4
Calcite	0.0	0.4
Gypsum	0.0	0.0
SiO2(a)	0.0	0.0

## SURFACE 126-170

-equilibrate with solution 126-170

Hfo wOH Fe(OH)3(a) equilibrium phase 0.2 53400 # 0.2 sites per mole  
of Fe(OH)3(a) present; 53400=600x89 (89 is formula weight for goethite) is  
surface area per mole of iron hydroxide  
Hfo\_sOH Fe(OH)3(a) equilibrium\_phase 0.005

SAVE EQUILIBRIUM PHASES 126-170

SAVE SURFACE 126-170

SAVE Solution 126-170

END

MIX

2000 0.5

3000 0.5

SAVE SOLUTION 171-233

END

EQUILIBRIUM PHASES 171-233

Al(OH)3(a)	-1.36	0.01
Fe(OH)3(a)	1.69	1.000000E-4
Calcite	0.0	0.4
Gypsum	0.0	0.0
SiO2(a)	0.0	0.0

SURFACE 171-233

-equilibrate with solution 171-233

Hfo wOH Fe(OH)3(a) equilibrium phase 0.2 53400 #0.2 sites per mole of  
Fe(OH)3(a) present; 53400=600x89 (89 is formula weight for goethite) is  
surface area per mole of iron hydroxide

Hfo\_sOH Fe(OH)3(a) equilibrium\_phase 0.005

SAVE EQUILIBRIUM PHASES 171-233

SAVE SURFACE 171-233

SAVE Solution 171-233

END

MIX

2000 1.0

3000 0.0

SAVE SOLUTION 234-260

END

EQUILIBRIUM PHASES 234-260

Al(OH)3(a)	-1.36	0.01
Fe(OH)3(a)	1.69	1.000000E-4
Calcite	0.0	0.4
Gypsum	0.0	0.0
SiO2(a)	0.0	0.0

SURFACE 234-260

-equilibrate with solution 234-260

Hfo wOH Fe(OH)3(a) equilibrium phase 0.2 53400 #0.2 sites per mole of  
Fe(OH)3(a) present; 53400=600x89 (89 is formula weight for goethite) is  
surface area per mole of iron hydroxide

Hfo\_sOH Fe(OH)3(a) equilibrium\_phase 0.005

SAVE EQUILIBRIUM PHASES 234-260

SAVE SURFACE 234-260

SAVE Solution 234-260

END

END

PRINT

-reset false

-surface false

## SELECTED OUTPUT

```

-file BC_mod02.sel #can
    be SEL or XLS
-reset false
# -step true #this
prints the time step in the first column, set to "false" in order to eliminate
that column

```

#1995 through 1997 Plateau 2

## MIX

1000 .334046

2000 .665954

SAVE SOLUTION 0

# 1994 through 1995

## TRANSPORT

```

-cells 260 #235
is total cells
-length 4 #4
meter cells .20000000 20.000000
-shifts 4.00000 #6
yrs*365*24*3600/2522880= 75 shifts; we start at the dam, John added a
year for the diffence in length for the first water
-time step 6311520.0 #This
is 29.2 days in seconds and essentially indicates hydraulic
conductivity
-punch cells 10 40 70 85 110 142 203 260
-punch frequency 1
-flow direction forward
-boundary conditions flux flux
-correct disp true
-dispersivity 260*20.000000
-diffusion_coef 0.0e-0 #No
diffusion
-tempr 1.0 #No
heat retardation

```

## END

#1995 through 1997 Plateau 2

## MIX

1000 .262052

2000 .737948

SAVE SOLUTION 0

write Solution 0

#Over-

## TRANSPORT

-shifts 11.0000

## END

#1997 through 2000 Plateau 3

## MIX

1000 .166453

2000 .833547

SAVE SOLUTION 0

write Solution 0.

#Over-

## TRANSPORT

-shifts 14.0000

## END

#2000 through 2010 Plateau 4

## MIX

1000 .069069

2000 .930931

SAVE SOLUTION 0

write Solution 0.

#Over-



TRANSPORT  
-shifts 29.0000

END

#2006 through 2010 Plateau 5

MIX  
1000 .010855  
2000 .989145  
SAVE SOLUTION 0  
write Solution 0.

#Over-

TRANSPORT  
-shifts 10 #00

END

END

#### **ATTACHMENT IV**

Modifications to the Thermodynamic  
Database for Uranium and Radium

# **Modifications to the Thermodynamic Database for Uranium and Radium**

by

**John J. Mahoney**

**Mahoney Geochemical Consulting LLC**

## **DATABASE**

The thermodynamic database used for these calculations (summarized in Table 1) was a modified version of the WATEQ4F database provided with PHREEQC (Parkhurst and Appelo, 1999). Modifications were primarily based upon changes to the reactions in the SOLUTION\_SPECIES<sup>1</sup> portion of the database for the uranyl ( $\text{UO}_2^{+2}$ ) component. Additionally, reactions for radium were also added to the database; the solution reactions were originally taken from the MINTEQ.V4.dat database also provided with PHREEQC.

### **Uranium**

For uranium the revised data were from two sources. Reactions in solution were updated using the OECD NEA 2003 compilation (Guillaumont et al., 2003). This document is an update of an earlier compilation also done under the auspices of the NEA (Grenthe et al., 1992). The reactions that were updated primarily involved uranyl complexation reactions involving hydroxide and carbonate. Table 1 lists the NEA selected values along with the values in several of the unmodified databases included in the PHREEQC program package. The table also lists the values used in the revised database, called WATEQ\_NEA.dat in Table 1.

In addition to the NEA update reactions, three ternary uranyl complexes were also added to database. These complexes included  $\text{CaUO}_2(\text{CO}_3)_3^{-2}$ ,  $\text{Ca}_2\text{UO}_2(\text{CO}_3)_3^0$ , and  $\text{MgUO}_2(\text{CO}_3)_3^{-2}$ . The constants for these three reactions were reported in the literature after the 2003 NEA compilation was released. The values for these three complexation constants were taken from Dong and Brooks, (2006, 2008). The inclusion of these complexes will tend to increase

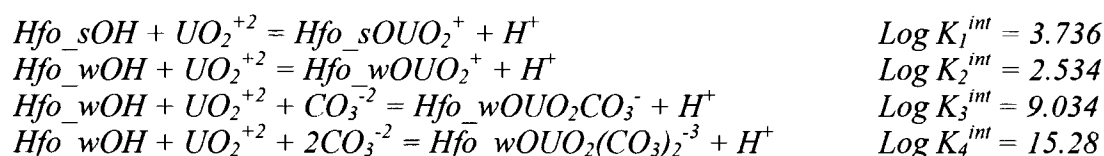
---

<sup>1</sup> The term SOLUTION\_SPECIES is the keyword used in PHREEQC to define these reactions.



solubility concentrations estimates for uranyl and decrease adsorption of uranyl onto HFO in geochemical models (Mahoney et al., 2009b). Inclusion of the complexes improves model estimates by providing a more realistic set of complexation reactions in solution. Their presence will also tend to increase the model determined concentration of uranium in solution, which produces a more conservative model estimate. As this study was primarily aimed at adsorption reactions onto hydrous ferric oxide (HFO), no attempt was made to update uranyl bearing mineral phases in the database.

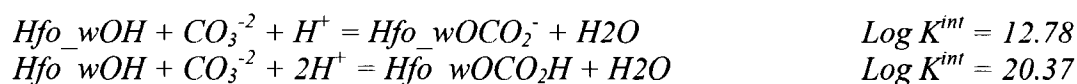
In addition to modifications to the SOLUTION\_SPECIES portion of the database, the reactions that defined the surface complexation of uranyl onto hydrous ferric oxide (HFO) were updated based upon the recently published results of Mahoney et al. (2009a). This set of four reactions replaced the estimated values for the two reactions that were originally presented in Dzombak and Morel, (1990). The following surface complexation reactions were used to describe uranium (as uranyl) adsorption onto hydrous ferric oxide:



These revised set of reactions correct the values reported by Dzombak and Morel for  $K_1^{int}$  and  $K_2^{int}$ , which were not based upon comparison to laboratory derived data. Rather Dzombak and Morel used a correlation between the log K for the first metal hydroxide complex and the log  $K_1^{int}$  and  $K_2^{int}$  values. When compared to experimental measurements the Dzombak and Morel estimated values for log  $K_1^{int}$  and  $K_2^{int}$  tended to significantly overestimate the amount of uranyl adsorption at low pH conditions and tended to underestimate uranium adsorption at high pH conditions particularly when carbonate was also present in solution. The newer values, published in Mahoney et al. (2009a), were based upon model based fits to laboratory measurements. Moreover, the revised data set included two surface complexation constants for uranyl carbonate complexes (the  $K_3^{int}$  and  $K_4^{int}$  reactions). Complexation constants for any type of uranyl carbonate surface complex were not included in the original Dzombak and Morel (1990) compilation that eventually became the basis for the surface complexation portion of the database included in the PHREEQC package. The existence of uranyl carbonate surface complexes has long been known, although various groups define them differently. The

Dzombak and Morel compilation was never meant to be a definitive treatise on surface complexation reactions involving uranium, and so this shortcoming can be excused. However, any detailed study involved with uranium adsorption must consider the reactions in some form or other. The revised database does consider these reactions.

In addition to the uranyl adsorption reactions, two additional surface complexation reactions were added to the database. These reactions are defined below:



These final two reactions were defined by Appelo et al. (2002), and will influence sorption at higher partial pressures of  $\text{CO}_2(\text{g})$ . Specifically, these two additional reactions will tend to occupy sites on the surface that could complex with uranium. This will produce a concomitant increase in uranium concentrations in the pore waters (Mahoney et al., 2009b).

## Radium

Speciation reaction constants for radium were also added to this database. Values were obtained from Langmuir and Riese (1985). The following reactions were added to the database.

Species	Reaction	Log K
$\text{RaOH}^+$	$\text{Ra}^{+2} + \text{H}_2\text{O} = \text{RaOH}^+ + \text{H}^+$	-13.5
$\text{RaSO}_4$	$\text{Ra}^{+2} + \text{SO}_4^{-2} = \text{RaSO}_4$	2.76
$\text{RaCO}_3$	$\text{Ra}^{+2} + \text{CO}_3^{-2} = \text{RaCO}_3$	2.5
$\text{RaCl}^+$	$\text{Ra}^{+2} + \text{Cl}^- = \text{RaCl}^+$	-0.1
$\text{RaCl}_2$	$\text{Ra}^{+2} + 2\text{Cl}^- = \text{RaCl}_2$	-0.05

Surface complexation reactions onto HFO for radium (as  $\text{Ra}^{+2}$ ) generally use the same values as  $\text{Ba}^{+2}$ . However, for this database values were recalculated and slight differences were noted. According to the model proposed by Dzombak and Morel, divalent cations form outer sphere complexes with the strong surface sites (designated as  $\text{Hfo\_sOH}$ ) and inner sphere complexes

with the weak sites (Hfo\_wOH). Using only Ca, Ba and Sr, the correlation between  $\log K_{\text{MOH}}$  the strong site surface complexes was

$$\log K_1^{\text{int}} = -0.6592 * \log K_{\text{MOH}} + 5.6719$$

a  $\log K_1^{\text{int}}$  of 5.3424 was noted for radium<sup>2</sup>. The  $\log K_1^{\text{int}}$  value for Ba<sup>+2</sup> was 5.46.

The value for the  $\log K_2^{\text{int}}$  Reaction ( $\text{Hfo\_wOH} + \text{Ra}^{+2} = \text{Hfo\_wORa}^{+} + \text{H}^{+}$ ) was based upon the overall regression equation defined in Dzombak and Morel. The calculated value for  $\log K_2^{\text{int}}$  was -7.333. The  $\log K_2^{\text{int}}$  value for Ba<sup>+2</sup> was -7.2.

---

<sup>2</sup> Langmuir and Riese (1985) write the radium hydrolysis reaction as  $\text{Ra}^{+2} + \text{H}_2\text{O} = \text{RaOH}^{+} + \text{H}^{+}$ , however Dzombak and Morel removed water from their equations and used equations of the form  $\text{Ra}^{+2} + \text{OH}^{-} = \text{RaOH}^{+}$ , for their correlations. Therefore, for radium the  $\log K_{\text{MOH}}$  becomes 0.5, and the corresponding  $\log K_{\text{MOH}}$  for barium is 0.53.

**Table 1. Continued. Surface complexation reactions for uranium adsorption onto HFO and solubility product constants for selected phases.**

DATABASE COMPARISON						
SPECIES	OECD NEA UPDATE	PHREEQC Databases				
	2003 Guillaumont et al.	WATEQ4F.dat	WATEQ_NEA.dat Version for this project	lnl.dat	minteq.v4.dat	minteq.dat
SURFACE COMPLEXES						
Hfo_sOUO2+	NEA does not discuss	5.2	3.736	We are using the Mahoney, Cadle and Jakubowski (2009) constants plus two reactions for carbonate surface complexation [Hfo_wOCO2-, and Hfo_wOCO2H]		
Hfo_wOUO2+		2.8	2.534			
Hfo_wOUO2CO3-			9.034			
Hfo_wOUO2(CO3)2-3			15.28			
PHASES (limited selection listed)						
UO2SO4	Free Energy provided no value for K given			1.9681		
UO2SO4:2.5H2O	1.589			-1.4912		
UO2SO4:3.5H2O	1.585			-1.4805		
UO2SO4:3H2O *	-0.831* 0.754 (recalculated)			-1.4028		
UO2SO4:H2O				-6.0233		
Schoepite (UO3:2H2O)	UO3 · 2H2O(cr) -> UO2 + 2 + 2 OH- + H2O(l) , 10 ,0 log s K = - (23.19 ± 0.43). Or 4.81 in proton form	5.404	5.404	4.8333	5.994	5.404



**Table 1. Comparison of uranium solution complexation reactions in various databases provided with PHREEQC and selected values included in the updated database.**

DATABASE COMPARISON							
SPECIES	OECD NEA UPDATE	PHREEQC Databases					
	2003 Guillaumont et al.	WATEQ4F.dat	WATEQ_NEA.dat Version for this project	lnf.dat		minteq.v4.dat	minteq.dat
all digits retained in table to facilitate traceability	Equation signs retained as in original; data is mainly from Table 3-2. To reduce error these values were mainly copied and pasted into cells	CO3-2 is component		HCO3- is component	using CO3-2 as component		
CO3-2 HCO3- reaction		10.329		-10.3288		10.329	10.33
UO2OH+	-5.250	-5.2	-5.250	-5.2073		-5.897	-5.09
UO2(OH)2(aq)	-12.150		-12.150	-10.3146			
UO2(OH)3-	-20.250	-19.2	-20.250	-19.2218			
UO2(OH)4--	-32.400	-33	-32.400	-33.0291			
UO2CO3(aq)	9.94	9.63	9.94	-0.6634	9.6654	9.6	10.071
UO2(CO3)2--	16.61	17.0	16.61	-3.7467	16.9109	16.9	17.008
UO2(CO3)3---	21.84	21.63	21.84	-9.4302	21.5562	21.6	21.384
UO2SO4(aq)	3.15	3.15	3.15	3.0703		3.18	2.709
UO2(SO4)2--	4.14	4.14	4.14	3.9806		4.3	4.183
UO2(SO4)34-	3.02						
(UO2)2OH+++	-2.700	-2.7	-2.700	-2.7072			
(UO2)2(OH)2++	-5.620	-5.62	-5.620	-5.6346		-5.574	-5.645
(UO2)3(OH)4++	-11.900	-11.9	-11.900	-11.929			
(UO2)3(OH)5+	-15.550	-15.55	-15.550	-15.5862		-15.585	-15.593
(UO2)3(OH)7-	-32.200	-31	-32.200	-31.0508			
(UO2)4(OH)7+	-21.900	-21.9	-21.900	-21.9508			
(UO2)3(CO3)6(6-)			54.00	-8.0601	53.9127	Not present	Not present
(UO2)2CO3(OH)3-	-19.010 CO2(gas) component		2UO2+2 + CO3-2 + 3H2O = (UO2)2CO3(OH)3- + 3H+ log_k -0.86	-11.2229			
(UO2)3CO3(OH)3+	NOT IN NEA 2003 nor Grenthe et al. 1992						
(UO2)3(OH)5CO2+	NOT IN NEA 2003 Same as (UO2)3O(OH)2(HCO3)+			-9.6194	42.0246		
(UO2)3O(OH)2(HCO3)+	-17.500 CO2(gas) component		3UO2+2 + CO3-2 + 3H2O = (UO2)3O(OH)2(HCO3)+ + 3H+ log_k 0.65	-9.7129			
(UO2)11(CO3)6(OH)12-	-72.500 CO2(gas) component		11UO2+2 + 6CO3-2 + 12H2O = (UO2)11(CO3)6(OH)12- + 12H+ log_k 36.40	NA			
Ca2UO2(CO3)3(aq)	NEA did not select value some discussion in NEA VS they cite a range of 26.5 to 30.55, Dong and Brooks 2006 report 30.70, this value was selected		30.7				
CaUO2(CO3)3-	Dong and Brooks 2006, report 27.18 this value was selected		27.18				
MgUO2(CO3)3-2	Dong and Brooks 2006, 25.8 This value was selected		25.8				

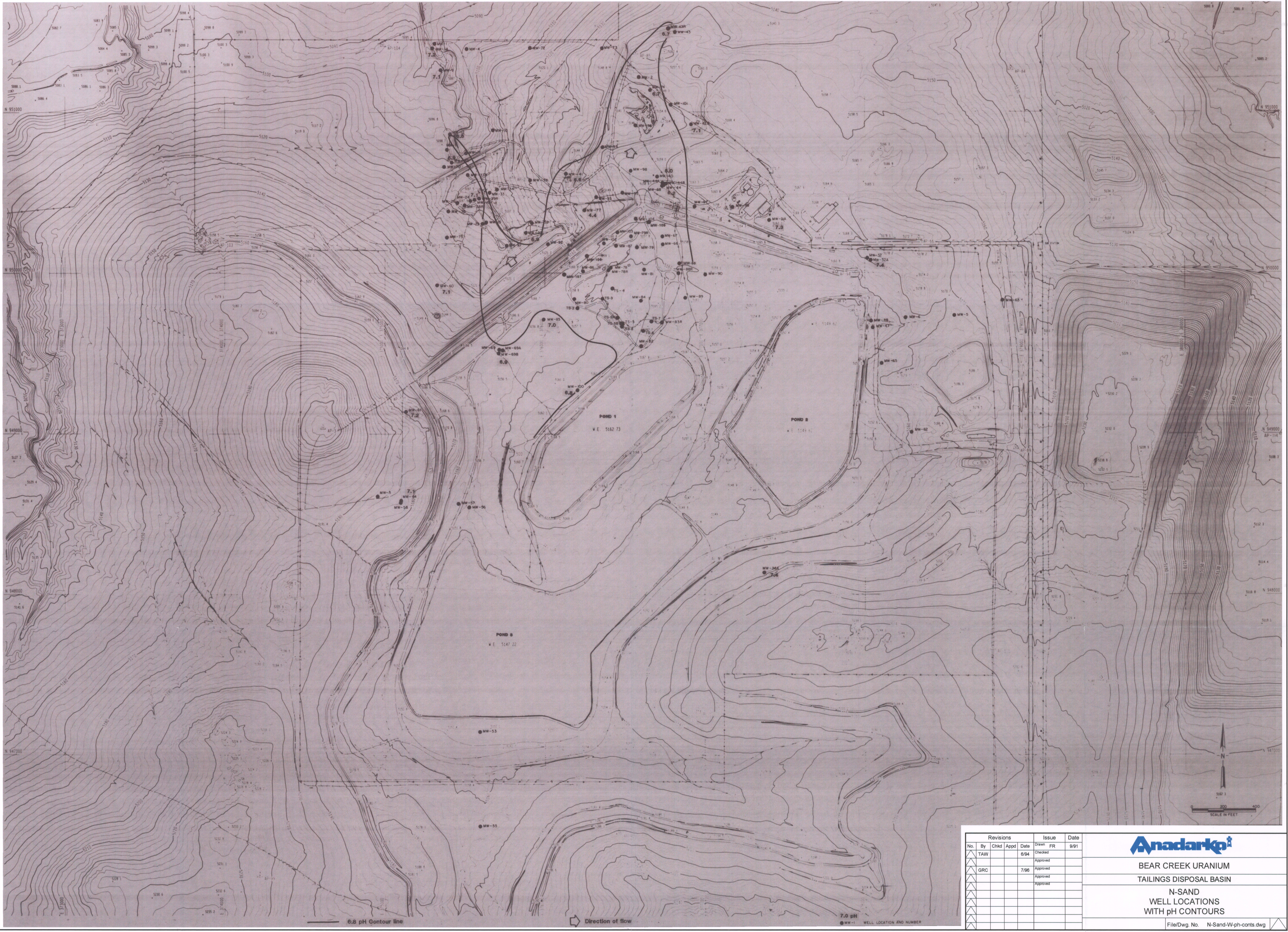
## REFERENCES

- Appelo, C. A. J.; Van der Weiden, M. J. J.; Tournassat, C.; Charlet, L., 2002. Surface complexation of ferrous iron and carbonate on ferrihydrite and the mobilization of arsenic. *Environ. Sci. Technol.* vol. 36, p. 3096–3103.
- Dong, W., and Brooks, S.C., 2006. Determination of the formation constants of ternary complexes of uranyl and carbonate with alkaline earth metals ( $\text{Mg}^{2+}$ ,  $\text{Ca}^{2+}$ ,  $\text{Sr}^{2+}$ , and  $\text{Ba}^{2+}$ ) using anion exchange method. *Environ. Sci. Technol.* vol. 40, p. 4689-4695.
- Dong, W., and Brooks, S.C., 2008. Formation of aqueous  $\text{MgUO}_2(\text{CO}_3)_3^{2-}$  complex and uranium anion exchange mechanism onto an exchange resin. *Environ. Sci. Technol.* vol. 42, p. 1979-1983.
- Dzombak, D.A., and Morel, F.M.M., 1990, Surface complexation modeling - hydrous ferric oxide: New York, John Wiley and Sons, 393 p.
- Grenthe, I., Fuger, J. Konings, R.J.M., Lemire, R.J., Muller, A.J., Nguyen-Trung, C. and Wanner, H., 1992. Chemical Thermodynamics of Uranium. 2004 reprint available from NEA OECD. 735 p.
- Guillaumont, R., Fanghanel, T., Neck, V., Fuger, J., Palmer, D., Grenthe, I., Rand, M. H., 2003. Update on the Chemical Thermodynamics of Uranium, Neptunium, Plutonium, Americium and Technetium; Elsevier B.V. Amsterdam. 960 p.
- Langmuir, D. and Riese, A.C., 1985. The thermodynamic properties of radium. *Geochimica et Cosmochimica Acta*, vol. 49, p. 1593 -1601.
- Mahoney, J.J., Cadle, S.A, and Jakubowski, R.T., 2009a, Uranyl adsorption onto hydrous ferric oxide – a re-evaluation for the diffuse layer model database. *Environ. Sci. and Technol.*, vol. 43, no. 24, p. 9260-9266. DOI 10.1021/es901586w.
- Mahoney, J.J., Jakubowski, R.T. and Cadle, S.A., 2009b, Corrections to the diffuse layer model database for uranyl adsorption onto hydrous ferric oxide - Ramifications for solute transport modeling. (Poster presented at U2009 Global Uranium Symposium, May 2009 Keystone, CO.)
- Parkhurst, D.L., and Appelo, C.A.J., 1999, User's guide to *PHREEQE* (version 2) - a computer program for speciation, batch-reaction, one-dimensional transport, and inverse geochemical calculations. U.S. Geological Survey Water Resources Investigation Report 99-4259, 312 p.

## REFERENCES

- Appelo, C. A. J.; Van der Weiden, M. J. J.; Tournassat, C.; Charlet, L., 2002. Surface complexation of ferrous iron and carbonate on ferrihydrite and the mobilization of arsenic. *Environ. Sci. Technol.* vol. 36, p. 3096–3103.
- Dong, W., and Brooks, S.C., 2006. Determination of the formation constants of ternary complexes of uranyl and carbonate with alkaline earth metals ( $\text{Mg}^{2+}$ ,  $\text{Ca}^{2+}$ ,  $\text{Sr}^{2+}$ , and  $\text{Ba}^{2+}$ ) using anion exchange method. *Environ. Sci. Technol.* vol. 40, p. 4689-4695.
- Dong, W., and Brooks, S.C., 2008. Formation of aqueous  $\text{MgUO}_2(\text{CO}_3)_3^{2-}$  complex and uranium anion exchange mechanism onto an exchange resin. *Environ. Sci. Technol.* vol. 42, p. 1979-1983.
- Dzombak, D.A., and Morel, F.M.M., 1990, Surface complexation modeling - hydrous ferric oxide: New York, John Wiley and Sons, 393 p.
- Grenthe, I., Fuger, J. Konings, R.J.M., Lemire, R.J., Muller, A.J., Nguyen-Trung, C. and Wanner, H., 1992. Chemical Thermodynamics of Uranium. 2004 reprint available from NEA OECD. 735 p.
- Guillaumont, R., Fanghanel, T., Neck, V., Fuger, J., Palmer, D., Grenthe, I., Rand, M. H., 2003. Update on the Chemical Thermodynamics of Uranium, Neptunium, Plutonium, Americium and Technetium; Elsevier B.V. Amsterdam. 960 p.
- Langmuir, D. and Riese, A.C., 1985. The thermodynamic properties of radium. *Geochimica et Cosmochimica Acta*, vol. 49, p. 1593 -1601.
- Mahoney, J.J., Cadle, S.A, and Jakubowski, R.T., 2009a, Uranyl adsorption onto hydrous ferric oxide – a re-evaluation for the diffuse layer model database. *Environ. Sci. and Technol.*, vol. 43, no. 24, p. 9260-9266. DOI 10.1021/es901586w.
- Mahoney, J.J., Jakubowski, R.T. and Cadle, S.A., 2009b, Corrections to the diffuse layer model database for uranyl adsorption onto hydrous ferric oxide - Ramifications for solute transport modeling. (Poster presented at U2009 Global Uranium Symposium, May 2009 Keystone, CO.)
- Parkhurst, D.L., and Appelo, C.A.J., 1999, User's guide to *PHREEQE* (version 2) - a computer program for speciation, batch-reaction, one-dimensional transport, and inverse geochemical calculations. U.S. Geological Survey Water Resources Investigation Report 99-4259, 312 p.





Revisions					Issue	Date
No.	By	Chkd	Appd	Date	Drawn	FR
1	TAW			6/94	Checked	9/91
2					Approved	
3	GRC			7/96	Approved	
4					Approved	
5					Approved	
6						
7						
8						
9						
10						
11						
12						
13						
14						
15						
16						
17						
18						
19						
20						

**Anadarko**

BEAR CREEK URANIUM  
TAILINGS DISPOSAL BASIN

N-SAND  
WELL LOCATIONS  
WITH pH CONTOURS

File/Dwg. No. N-Sand-W-ph-contrs.dwg